



National Library
of Canada

Acquisitions and
Bibliographic Services Branch

395 Wellington Street
Ottawa, Ontario
K1A 0N4

Bibliothèque nationale
du Canada

Direction des acquisitions et
des services bibliographiques

395, rue Wellington
Ottawa (Ontario)
K1A 0N4

Veuillez lire - Please read

Cher lecteur - Dear reader

NOTICE

The quality of this microform is heavily dependent upon the quality of the original thesis submitted for microfilming. Every effort has been made to ensure the highest quality of reproduction possible.

If pages are missing, contact the university which granted the degree.

Some pages may have indistinct print especially if the original pages were typed with a poor typewriter ribbon or if the university sent us an inferior photocopy.

Reproduction in full or in part of this microform is governed by the Canadian Copyright Act, R.S.C. 1970, c. C-30, and subsequent amendments.

AVIS

La qualité de cette microforme dépend grandement de la qualité de la thèse soumise au microfilmage. Nous avons tout fait pour assurer une qualité supérieure de reproduction.

S'il manque des pages, veuillez communiquer avec l'université qui a conféré le grade.

La qualité d'impression de certaines pages peut laisser à désirer, surtout si les pages originales ont été dactylographiées à l'aide d'un ruban usé ou si l'université nous a fait parvenir une photocopie de qualité inférieure.

La reproduction, même partielle, de cette microforme est soumise à la Loi canadienne sur le droit d'auteur, SRC 1970, c. C-30, et ses amendements subséquents.

UNIVERSITY OF ALBERTA

QUATERNARY SEDIMENTOLOGY AND STRATIGRAPHY OF THE MAYO REGION,
YUKON TERRITORY

by
TIMOTHY RICHARD GILES



A THESIS
SUBMITTED TO THE FACULTY OF GRADUATE STUDIES AND RESEARCH
IN PARTIAL FULFILLMENT OF THE REQUIREMENTS FOR THE DEGREE
OF MASTER OF SCIENCE

DEPARTMENT OF GEOLOGY

EDMONTON, ALBERTA
FALL 1993



National Library
of Canada

Acquisitions and
Bibliographic Services Branch

395 Wellington Street
Ottawa, Ontario
K1A 0N4

Bibliothèque nationale
du Canada

Direction des acquisitions et
des services bibliographiques

395, rue Wellington
Ottawa (Ontario)
K1A 0N4

Your file *Votre référence*

Our file *Notre référence*

The author has granted an irrevocable non-exclusive licence allowing the National Library of Canada to reproduce, loan, distribute or sell copies of his/her thesis by any means and in any form or format, making this thesis available to interested persons.

L'auteur a accordé une licence irrévocable et non exclusive permettant à la Bibliothèque nationale du Canada de reproduire, prêter, distribuer ou vendre des copies de sa thèse de quelque manière et sous quelque forme que ce soit pour mettre des exemplaires de cette thèse à la disposition des personnes intéressées.

The author retains ownership of the copyright in his/her thesis. Neither the thesis nor substantial extracts from it may be printed or otherwise reproduced without his/her permission.

L'auteur conserve la propriété du droit d'auteur qui protège sa thèse. Ni la thèse ni des extraits substantiels de celle-ci ne doivent être imprimés ou autrement reproduits sans son autorisation.

ISBN 0-315-88135-6

Canada

UNIVERSITY OF ALBERTA

RELEASE FORM

NAME OF AUTHOR: TIMOTHY RICHARD GILES

TITLE OF THESIS: QUATERNARY SEDIMENTOLOGY AND STRATIGRAPHY OF
THE MAYO REGION, YUKON TERRITORY

DEGREE: MASTER OF SCIENCE

YEAR THIS DEGREE GRANTED: 1993

Permission is hereby granted to the UNIVERSITY OF ALBERTA LIBRARY to
reproduce single copies of this thesis and to lend or sell such copies for private,
scholarly or scientific research purposes only.

The author reserves all publication and other rights in association with the
copyright in this thesis, and except as hereinbefore provided neither the thesis nor any
substantial portion thereof may be printed or otherwise reproduced in any material form
whatever without the author's prior written permission.

(SIGNED)

T. Giles

PERMANENT ADDRESS:

1017 Chamberlain St.

Victoria, B.C.

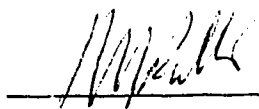
V8S 4C1

DATED

May 18 1993

UNIVERSITY OF ALBERTA
FACULTY OF GRADUATE STUDIES AND RESEARCH

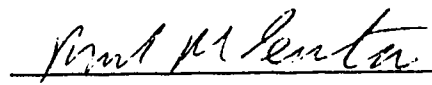
The undersigned certify that they have read, and recommend to the Faculty of Graduate Studies and Research for acceptance, a thesis entitled QUATERNARY SEDIMENTOLOGY AND STRATIGRAPHY OF THE MAYO REGION, YUKON TERRITORY submitted by TIMOTHY RICHARD GILES in partial fulfillment of the requirements for the degree of MASTER OF SCIENCE in GEOLOGY



Dr. Nathaniel W. Rutter (Supervisor)



Dr. Thomas F. Moslow



Dr. Mark M. Fenton



Dr. Ian A. Campbell

Date: May 18, 1973

Abstract

Sedimentological analysis of Quaternary sediments along the Stewart River near Mayo, central Yukon Territory, is used to determine the environmental history of the region. Thirteen sedimentary facies are defined and interpreted as: lodgement till (Facies 1), meltout till (Facies 2), mass-movement diamictons (Facies 3), longitudinal bar deposits (Facies 4, 6 and 8), transverse bar deposits (Facies 5, 7 and 8), planar and ripple laminated sand deposits (Facies 9, 10 and 11), organic deposits (Facies 12), and loess (Facies 13). Seven stratigraphic units (Units A to G) are interpreted from these facies and they form five informal chronostratigraphic intervals: interglacial, proglacial, glacial, immediate postglacial and Holocene.

Results of this study indicate that during the Mid-Wisconsinan a wandering gravel bed river occupied the Mayo River valley and the Stewart River valley downstream of Mayo. Interglacial river sediments consist of coarse gravels and sands (Unit A) with abundant wood fragments which have yielded several radiocarbon dates (38.1 to 35.4 ka). Environmental reconstructions from pollen and macrofossil data indicate a willow dominated, low arctic tundra around 29.6 ka. Deposits of only one glaciation, the Late Wisconsinan McConnell advance, are recognized. A poorly sorted and highly disrupted sand, gravel and diamicton sequence (Unit B) was deposited proglacially in the Mayo Indian Village Section. As topographically controlled ice advanced from the east along the Stewart valley, the Mayo River was deflected to the northwest. Glacial deposits (Unit C) include mass-movement diamictons overlain by a thin layer of lodgement till, a thicker and more laterally extensive bed of meltout till, and a discontinuous cap of mass-movement diamicton. Postglacially, the region was dominated by an ice-contact lake dammed by stagnating ice in the Stewart valley and a second, higher lake formed behind a lateral moraine across the mouth of the Mayo valley. When the upper lake breached the moraine it deposited a sequence of deltaic sediments (Unit D) in the lower ice-dammed lake. Melting of the ice dam caused instability and debris flows deposited lobes of diamicton (Unit E) as the lake drained. After the lake level dropped gravels of the incipient Mayo River were deposited in channels on top of the delta (Unit F). During the Holocene, loess with multiple paleosols (Unit G) developed on top of the sections as the Stewart and Mayo Rivers incised into the unconsolidated proglacial and deltaic sediments.

Prior to the McConnell glaciation, the Stewart River flowed to the southwest from the Fraser Falls area, rather than following its present course to the west past Mayo. During deglaciation morainal sediment southwest of Fraser Falls deflected the Stewart River into its

present channel. This is evidenced by the absence of interglacial gravel in the Stewart River valley between Fraser Falls and Mayo. In addition, pre-McConnell glaciation fluvial deposits in the Mayo area are characterized by clasts of northern provenance and are distinct from the modern Stewart River gravels

Acknowledgments

Financial aid for this thesis was contributed by the Boreal Institute for Northern Studies through a research grant. Logistical support in the study area was provided by the Geological Survey of Canada. My committee members Dr. Nat Rutter, Dr. Tom Moslow, Dr. Mark Fenton and Dr. Ian Campbell are to be thanked for contributing their expertise and time and bringing this thesis to conclusion.

In the field I was assisted by, and sometimes overwhelmed by, Vic Levson, Dr. Alejandra Duk-Rodkin, Dr. Norm Catto, Steve Morison, and Ryan and Lana Cooper. I am grateful to Dr. Chris Burn for his help in the field and the use of his boat. Gordon and Stephney Hind are thanked for providing lodging and along with Bernard and Sylvie Menelon and the Cooper family for their hospitality during the summers I spent in Mayo.

Dr. Owen Hughes supervised the fieldwork and I only wish he could have lived to see this final product. I missed my chances to let him review this work and it lacks his special knowledge of the Quaternary of central Yukon. I hope he would have approved of the results. Dr. Nat Rutter guided the study, providing advice and assistance throughout, and he finally gets to see the fruits of his labour.

I would like to thank my parents, Robin and Ruth, for unleashing me on this unsuspecting world and for their continuing encouragement in this effort. Brad and Allyson Hamilton and Clark and Shari Logan are to be congratulated on getting married during my tenure as a student (funny, just after living with me?). James MacEachern is thanked for his skill in sedimentology and soccer. Michelle Woytenko, Heather Blyth and Gaileen Lyons are to be praised for their lust for life and men. John Kulig spent many tedious, but no doubt enjoyable, hours ripping and shredding this thesis to make it, you know, whadyamacallit, readable. Numerous insightful comments on central Yukon Quaternary geology were provided by the honourable Dr. Brent Ward. To the future Drs. Vic Levson and Dan Kerr, I believe that the end is mercifully near for you two as well. To Mel Reasoner and Norm Catto, I can only say cheers.

Aileen receives a big hug for her patience as this all came together. Her encouragement and support were appreciated despite my reactions, thanks.

And now, for something completely different.....

Table of Contents

Chapter	Page
I Introduction.....	1
A Objectives.....	1
B Study Area.....	2
1 Setting.....	2
2 Bedrock Geology.....	6
3 Glacial Geology.....	9
II Methods of Investigation.....	16
A Field Methods.....	16
B Field Descriptions.....	16
C Pebble fabrics in diamicton and gravel.....	17
D Laboratory Studies.....	18
1 Grain Size Analysis.....	18
2 Pebble Lithologies.....	18
3 Wood Analysis.....	19
4 Bond.....	19
III Stratigraphic Framework.....	20
Mayo Section.....	20
MIV Section.....	27
Third Section.....	27
McIntyre Park Section.....	32
IV Facies Descriptions and Interpretations.....	33
Introduction: The Concept of "Facies".....	33
Facies 1 Diamicton with well developed sub-horizontal partings and striated clasts	33
Description.....	33
Interpretation.....	38
Facies 2 Massive and layered diamicton with sorted sediment lenses.....	43
Description.....	43
Interpretation.....	54
Facies 3 Massive and stratified diamicton interbedded with sand and gravel.....	58
Subfacies 3A Isolated clasts and massive diamicton lenses.....	58
Description.....	58
Interpretation.....	58

Subfacies 3B Massive or stratified diamicton interbedded with sand and gravel ...	60
Description.....	60
Interpretation.....	65
Subfacies 3C Massive diamicton interbedded with sand and gravel	69
Description.....	69
Interpretation.....	70
Facies 4 Massive and stratified matrix-filled pebbly gravel	71
Description.....	71
Interpretation.....	75
Facies 5 Planar cross-stratified matrix-filled pebbly gravel	77
Description.....	77
Interpretation.....	78
Facies 6 Massive and stratified openwork pebbly gravel	79
Description.....	79
Interpretation.....	80
Facies 7 Planar cross-stratified openwork pebbly gravel	81
Description.....	81
Interpretation.....	81
Facies 8 Massive, stratified and cross-stratified pebbly sand, sand, silt and clay.....	83
Subfacies 8A Massive, stratified and cross-stratified pebbly sand, sand, silt and clay.....	83
Description.....	83
Interpretation.....	84
Subfacies 8B Planar cross-stratified pebbly sand and sand	85
Description.....	85
Interpretation.....	86
Subfacies 8C Planar cross-stratified sand.....	87
Description.....	87
Interpretation.....	87
Facies 9 Planar, wavy and massive bedded or laminated sand, silt and clay	89
Description.....	89
Interpretation.....	91
Facies 10 Trough and planar tabular cross- stratified sand	94
Description.....	94
Interpretation.....	97

Facies 11 Climbing ripple cross-laminated sand.....	99
Description.....	99
Interpretation.....	102
Facies 12 Sands, silt and clay with organic detritus.....	103
Description.....	103
Interpretation.....	105
Facies 13 Silts and organics.....	106
Description.....	106
Interpretation.....	107
V Lithostratigraphic Units.....	108
Unit A: Lower gravel and sand	108
Unit B: Lower sand and gravel	111
Unit C: Diamicton.....	112
Unit D: Upper sand and silt	114
Unit E: Upper diamicton	117
Unit F: Upper gravel.....	119
Unit G: Silt and organics	119
VI Chronology.....	120
VII Quaternary History.....	122
Interglacial.....	122
Proglacial	124
Glacial	124
Postglacial.....	128
Holocene	130
VIII Conclusions.....	134
Bibliography	136
Appendix 1A: Pebble fabric data	147
Appendix 1B: Rose diagrams.....	149
Appendix 1C: Cumulative primary eigenvalue against mean lineation plots.....	159
Appendix 2A: Grain size data	161
Appendix 2B: Grain size ternary plots	163
Appendix 3A: Raw pebble data	164
Appendix 3B: Pebble lithology percentages.....	167
Appendix 3C: Pebble lithology ternary diagrams.	170
Appendix 4A: Lithostratigraphic logs and detailed section diagrams for the Mayo Section...	173
Appendix 4B: Lithostratigraphic logs and detailed section diagrams for the Mayo Indian Village Section.	188
Appendix 4C: Lithostratigraphic logs and detailed section diagrams for the Third Section...	200
Appendix 5: Wood Identification Reports	205
Appendix 6: Radiocarbon Dates	206

List of Tables

Table 1: Radiocarbon dates from the Mayo Region	13
Table 2: Summary of the sedimentary features and environments of deposition of the facies in the Mayo region	34

List of Figures

Figure 1: Map of the Yukon Territory and location of the study area.....	3
Figure 2: Physiography of the Yukon Territory. The Eastern Yukon Plateau is subdivided into the Stewart, Macmillan, and Pelly Plateaus. (Modified after Bostock 1970).....	4
Figure 3: Permafrost limits and mean annual temperature isotherms of the Yukon Territory. (Modified after Brown 1978).....	5
Figure 4: Bedrock geology map of the central Yukon. (Modified after Gabrielese et al. 1977).....	8
Figure 5: Quaternary Cordilleran and Laurentide ice sheet limits in Yukon Territory. (Modified after Tarnocai and Schweger 1991).....	10
Figure 6: Subdivisions of Quaternary events and deposits in Yukon Territory. (Modified after Hughes et al. 1989).....	11
Figure 7: Late Wisconsinan McConnell ice limits in central Yukon Territory. (Modified after Hughes 1983b, c).....	14
Figure 8: Location map of the main sections in the Mayo region. Surficial geology is modified from Hughes 1983c.	22
Figure 9: Air photograph of the Mayo region. Air photograph A19604-25.	23
Figure 10: Schematic cross-section of the stratigraphic units in the Mayo Section.	24
Figure 11: Representative sections of the units and sedimentology present in the Mayo Section.	26
Figure 12: Schematic cross-section of the stratigraphic units in the MIV Section.....	28
Figure 13: Representative sections of the units and sedimentology present in the MIV Section.....	29
Figure 14: Schematic cross-section of the stratigraphic units in the Third Section.....	30
Figure 15: Representative section of the units and sedimentology present in the Third Section.....	31
Figure 16: Schematic diagram of the embedded clasts at the base of Unit C.....	37
Figure 17: Ternary plot of primary, secondary and tertiary eigenvalues (S1, S2, and S3) from lodgement till fabrics.	40
Figure 18: Primary eigenvectors (S1) plotted against the trend of the mean axis (mean lineation) of lodgement till fabrics.	41
Figure 19: Ternary plot of primary, secondary and tertiary eigenvalues (S1, S2, and S3) from meltout till fabrics.	48
Figure 20: Primary eigenvectors (S1) plotted against the trend of the mean axis (mean lineation) of meltout till fabrics.	49

Figure 21: Cross-section of the englacial tunnel located near the base of Unit C at 490 metres in the Mayo Section. Folding and faulting in the sand is common. Note the stratification in the sand paralleling the form of clasts held within till of Unit C.	50
Figure 22: Schematic cross-section through diamicton flows. These may be noses or margins of a debris flow. Plate 9 is a photograph of the left half of this diagram.	64
Figure 23: Ternary plot of primary, secondary and tertiary eigenvalues (S1, S2, and S3) from mass-movement diamicton fabrics.	66
Figure 24: Primary eigenvectors (S1) plotted against the trend of the mean axis (mean lineation) of mass-movement diamicton fabrics.....	67
Figure 25: Unidirectional rose diagrams representing two dimensional pebble orientations in pebble and cobble gravel of facies 4. Sample statistics are the mean lineation, average pebble dip, and the primary, secondary and tertiary eigenvalues of each sample.	74
Figure 26: Paleogeographic reconstruction of the Mayo Region during Mid Wisconsinan time.	123
Figure 27: Paleogeographic reconstruction as Late Wisconsinan Cordilleran McConnell ice advanced into the Mayo Region.....	125
Figure 28: Paleogeographic reconstruction during full glacial times.....	126
Figure 29: Immediate postglacial paleogeographic reconstruction of the Mayo region.	129
Figure 30: Surficial geology map of the Mayo region (modified from Hughes 1983c). The morainal ridge (stippled) is the lateral moraine deposited on the north side of the Stewart valley glacial lobe. The glacial limit of the McConnell glaciation can be seen on the north and south sides of the Stewart valley. The letters I, M, P and T are located at the Mayo Indian Village, Mayo, McIntyre Park and Third Sections respectively.....	132

List of Plates

Plate 1: Embedded boulders along the basal contact of facies 1 diamicton. (Unit A gravel below and Unit C diamicton above.).....	36
Plate 2: Flutings on the base of facies 1 in Unit C, eroded into gravel and sand of Unit A. Orientation of the flutings was measured at 241°-061°. Diamicton exposed is facies 1 at the base and grades into facies 2 higher.	39
Plate 3: This is a typical exposure of the Mayo Section. Unit A gravel is exposed at the base and is covered by a thick sequence of Unit C diamicton. The section is capped by a thin veneer of Units D and G. Note the layering in the diamicton which is a reflection of variations in matrix grain size, clast percentage and mineralogic content.....	45
Plate 4: This boulder is at the contact between two layers of facies 2 diamicton. The layer contact is interpreted as a reactivation surface where glacial erosion occurred but there was little or no deposition of lodgement till. Diamicton below clast is deformed, sand lenses and clasts are oriented parallel to the surface of the boulder.....	46
Plate 5: Pebbles within facies 2 diamicton project down into the large sand and gravel lense. Beds underneath the pebbles are deformed for about 2 centimetres, forming shallow scours as a result of increased turbulent flow in the constricted tunnel space.	52
Plate 6: Diamicton lense within the large sand and gravel lense. Diamicton exposed above and below the sand is of facies 2. Diamicton lense parallels the bedding in the lense and the tunnel roof. Pick is 75 centimetres long.....	53
Plate 7: Isolated clast with drape structure, pierces and disrupts underlying beds.....	59
Plate 8: Thin lenses or beds of well sorted sand give this subfacies 3B diamicton a stratified appearance. This structure is located around 420 metres in the Mayo Indian Village Section.....	61
Plate 9: Possible flow stratification in a sediment gravity flow diamicton. Strata are defined by color, pebble content. Figure 22 is an expanded diagram of this feature.....	63
Plate 10: Facies 4, massive and stratified clast supported, matrix-filled moderately to poorly sorted small to large pebble gravel. Note the crude imbrication of clasts and the wide variation in grain size.....	72
Plate 11: Units A, B, D, and G exposed near the upstream terminus of the Mayo Section. The lower grey gravel of Unit A has broad trough shaped deposits dominantly of facies 4 and 6. The brown gravel of Unit B consists of facies 4, 5, 6, 7 and 8. Planar bedded sand, silt and clay of Unit D overlies the distinct contact eroded by the advancing ice. Soil of Unit G caps the section	73
Plate 12: Openwork pebble gravel beds of facies 7. Strong oxidation is common in these beds as they are permeable and groundwater flows through them freely.	82
Plate 13: Large migrating dune or megaripple on a channel floor. Towards the upstream (left) and downstream ends this structure is interbedded with gravelly beds. Flow was towards the right of plate to the southwest. Pick is 75 centimetres long.	88

Plate 14: Planar bedded sand and silt at the base overlain by a deformed layer of sand and silt. This bed is overlain by in-phase climbing ripples deposited under lower flow regime conditions.	90
Plate 15: Ball and pillow loading structures, original stratification appears to have been planar bedded sand. Note the finer nature of the darker colored sand at the base of photo overlain by lighter colored coarser sand.....	92
Plate 16: Depositional-stoss climbing ripples grading vertically into a thin discontinuous layer of erosional-stoss climbing ripples and rapidly into trough cross-stratified sand. The climbing ripples have slightly finer sand than the troughs. Note the accentuation of internal laminae and bounding surfaces by oxidation. Note also the mud intraclasts which are present in troughs and rarely in climbing ripples. Most mud clasts look like pock marks in the sand.....	96
Plate 17: Depositional and erosional stoss climbing ripples with some mud intraclasts at the base of the sequence overlain by well developed depositional-stoss climbing ripples lacking intraclasts. Erosively overlain by trough cross-stratified or erosional-stoss climbing ripples. Note the coarse grained nature of these upper beds.....	100
Plate 18: DSCR at the base grading vertically into ESCR covered by the thickest continuous silt drape, a subsequent drape of fine sand, and a second thin, discontinuous drape of silt. These are erosively overlain by an ESCR bed which is again draped by silt. This is overlain by finely laminated, wide crested DSCR with thin silt drapes.	101
Plate 19: A thick bank collapse deposit. The lower contact is erosional. Side contacts are visible and illustrate a dip angle of 10-20°. Note the distorted laminated beds. Deposit is 80 to 100 centimetres thick and 3 to 4 metres wide.....	104
Plate 20: Ten metres of Unit B sand and gravel are present at the base of this part of the MIV Section. Unit C diamicton is the prominent layer which appears to pinch out toward the right (east) of this plate. In the horizontally stratified sand of Unit D, which is up to 45 metres thick, one of the large erosional disconformities formed by channel incision can be seen truncating bedding. Unit F gravel and Unit G loess and soil cap the section. The view is 55 metres high and 125 metres wide.....	116
Plate 21: Upper diamicton (Unit E) in the Third Section. Sand at the base and separating the diamicton are part of the underlying sand and gravel of Unit D. The two diamicton lenses are different in color, texture and pebble content. Lower diamicton lense pinches out near the right of plate and thickens off plate to the left. The intervening sand layer pinches out to the left of plate.....	118

I INTRODUCTION

Since prospectors first discovered placer gold in the Stewart River gravel bars there has been an interest in the geology of the Mayo region. Exploration rapidly moved northwards to silver prospects around Elsa and Keno Hill as the gold reserves in the bars were exhausted. Quaternary glacial limits and features in central Yukon Territory were defined by Bostock (1943, 1948, 1966) and Hughes (1969, 1983a, b, c, d). On the basis of moraine morphology, glaciofluvial surface elevations, soil distribution, and permafrost feature development three ages of glaciation have been established (Bostock 1966, Hughes 1969, Tarnocai et al. 1985). The youngest of these, the Late Wisconsinan McConnell glaciation, formed a terminal moraine 18 kilometres down the Stewart River valley from the town of Mayo. The extent of the McConnell glaciation in the Mayo region is well defined by correlative lateral moraines. Previous studies have established a basic stratigraphic framework for the Mayo region but a detailed sedimentologic study is required to better understand the glacial dynamics and environmental history of the area. Recent cutbank erosion and exposure of sediments along the Stewart River near Mayo has allowed investigation of the stratigraphy, pollen, macrofossils and permafrost features of the region (Hughes et al. 1987; Matthews et al. 1990). This study focuses on the sedimentology of the exposed sequences, which is used to infer depositional environments, and combined with stratigraphic data, to reconstruct the Quaternary history of the Mayo region.

A Objectives

The objectives of this study are to:

1. investigate the sedimentology of the Quaternary deposits in the Mayo region and identify sedimentary facies;
2. determine the depositional environments of each facies by comparison to modern sedimentary environments; and
3. incorporate sedimentologic data with stratigraphic and geomorphic information to determine the glacial dynamics of the region, refine the stratigraphy and chronology of the deposits, and develop a late-Pleistocene geologic and geographic history.

B Study Area

1 Setting

The study area is located on the Stewart Plateau in central Yukon Territory near the town of Mayo (63°36'N, 135°35'W; Figure 1). Central Yukon is dominated physiographically by the Yukon Plateau which is divided into the Western and Eastern Yukon Plateaus and the Tintina Valley (Bostock 1970; Figure 2). The Stewart Plateau is most northerly portion of the Eastern Yukon Plateau which also includes the Pelly and Macmillan Plateaus. The Stewart Plateau is a tableland dissected by a network of deep, broad valleys (Bostock 1948). The elevation varies between 770-1400 metres (2500-4600 ft) above sea level and it lies between the Tintina Valley on the southwest, the Macmillan Plateau on the south, the Selwyn mountains on the east and the Wernecke and Ogilvie Mountains on the north and northwest. The Stewart and Mayo Rivers are incised into the Stewart Plateau to a depth of 490 metres (1600 ft) above sea level. The broad, fault-induced Tintina Valley has portions of the Pelly, Stewart and Yukon rivers flowing along it towards the northwest. The Tintina Valley is a broad, fault-induced valley trending southeast to northwest along which the Pelly River flows for over 150 kilometres, the Yukon River at least 100 kilometres, and the Stewart River for 50 kilometres.

Mayo lies within the Central Yukon Basin Climate Division which is characterized by a sub-arctic continental climate (Wahl et al. 1987). The mean annual air temperature for Mayo is -4°C (Environment Canada 1982). This climate division has extreme temperature ranges and has the record Yukon winter lows (Snag, -62.3°C; Mayo, -62.2°C) and the record summer high (Mayo, 36.1°C). Maximum lows are usually recorded in February and maximum highs are in June and July. Precipitation is low to moderate at 300-400 mm annually (average 335 mm), over half of which occurs as summer showers. Relative humidity is around 50 to 80% (Wahl et al. 1987).

Mayo is located in the widespread permafrost zone close to the -5°C isotherm (Brown 1978; Figure 3). Upland regions and mountain peaks have tundra covers with numerous permafrost features: polygons, stone lines, stone nets, bare-centre circles, felsenmeer and solifluction lobes. Lacustrine sediments upstream from Mayo in the Stewart River valley contain thaw lakes, thaw slumps and ice wedges (Burn et al. 1986, Burn and Michel 1988, Burn 1987, Burn and Friele 1989, Burn 1990). Active layer thickness in these sediments is between 35 and 100 centimetres (Burn and Friele 1989).

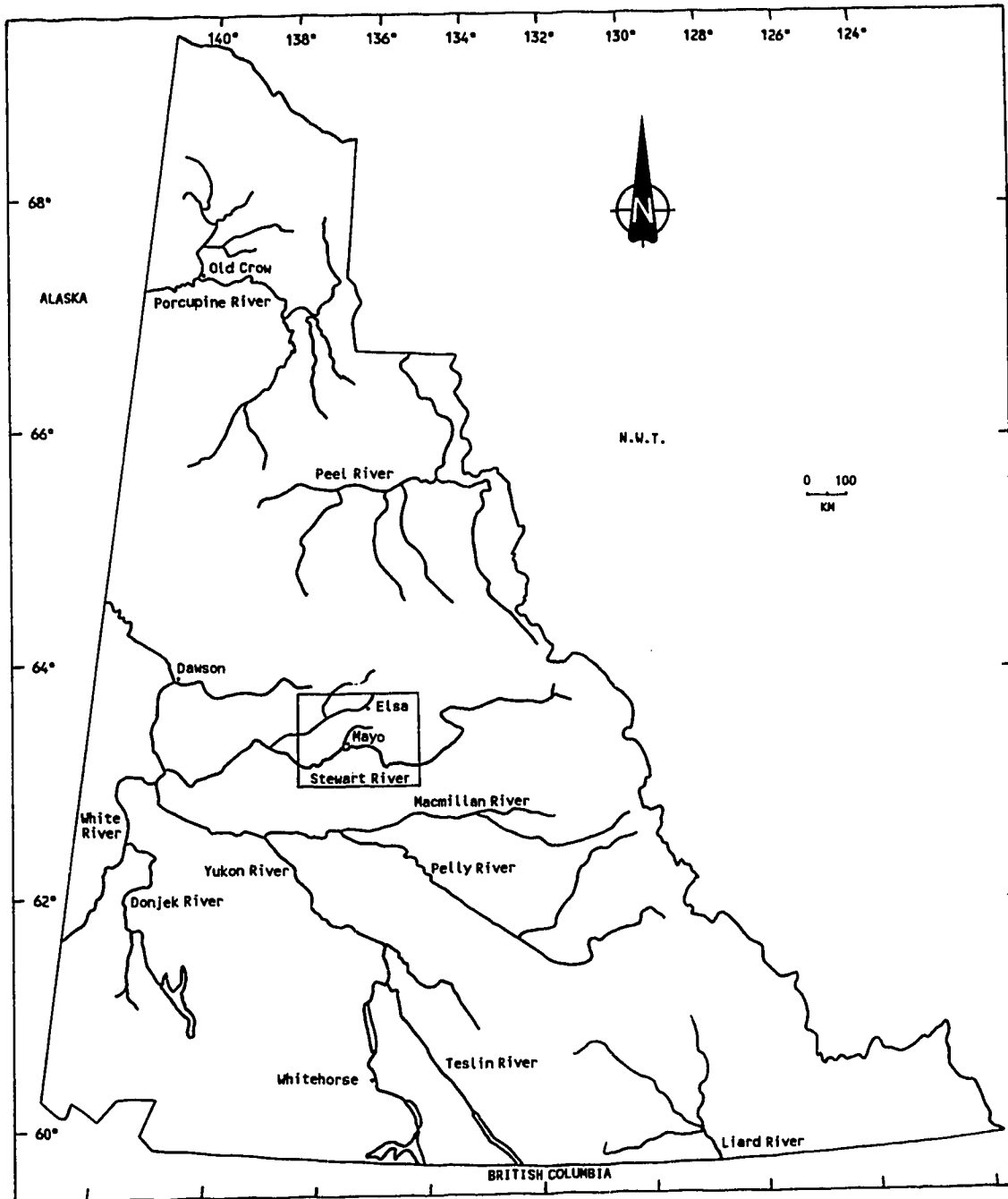


Figure 1: Map of the Yukon Territory and location of the study area.

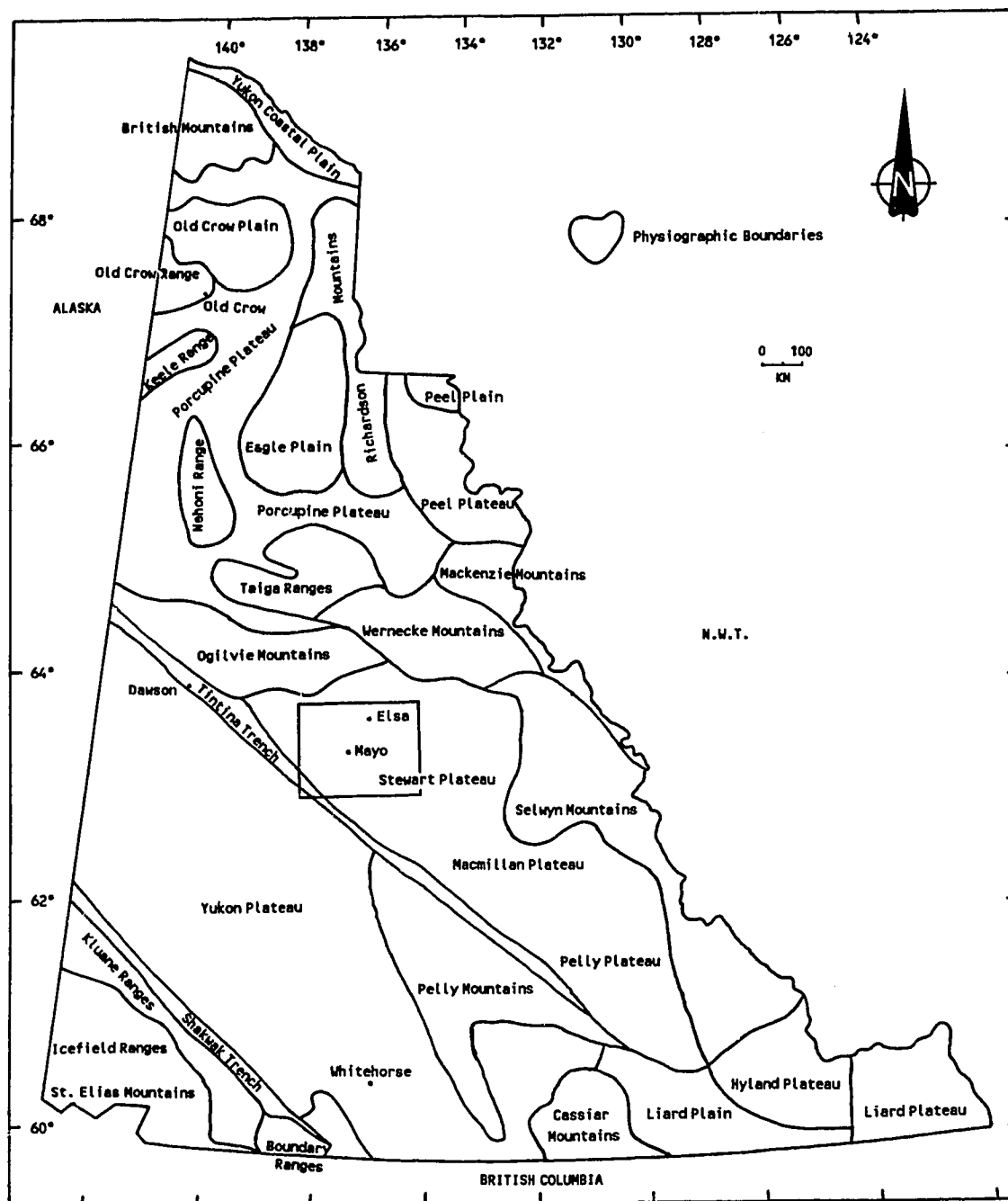


Figure 2: Physiography of the Yukon Territory. The Eastern Yukon Plateau is subdivided into the Stewart, Macmillan, and Pelly Plateaus. (Modified after Bostock 1970).

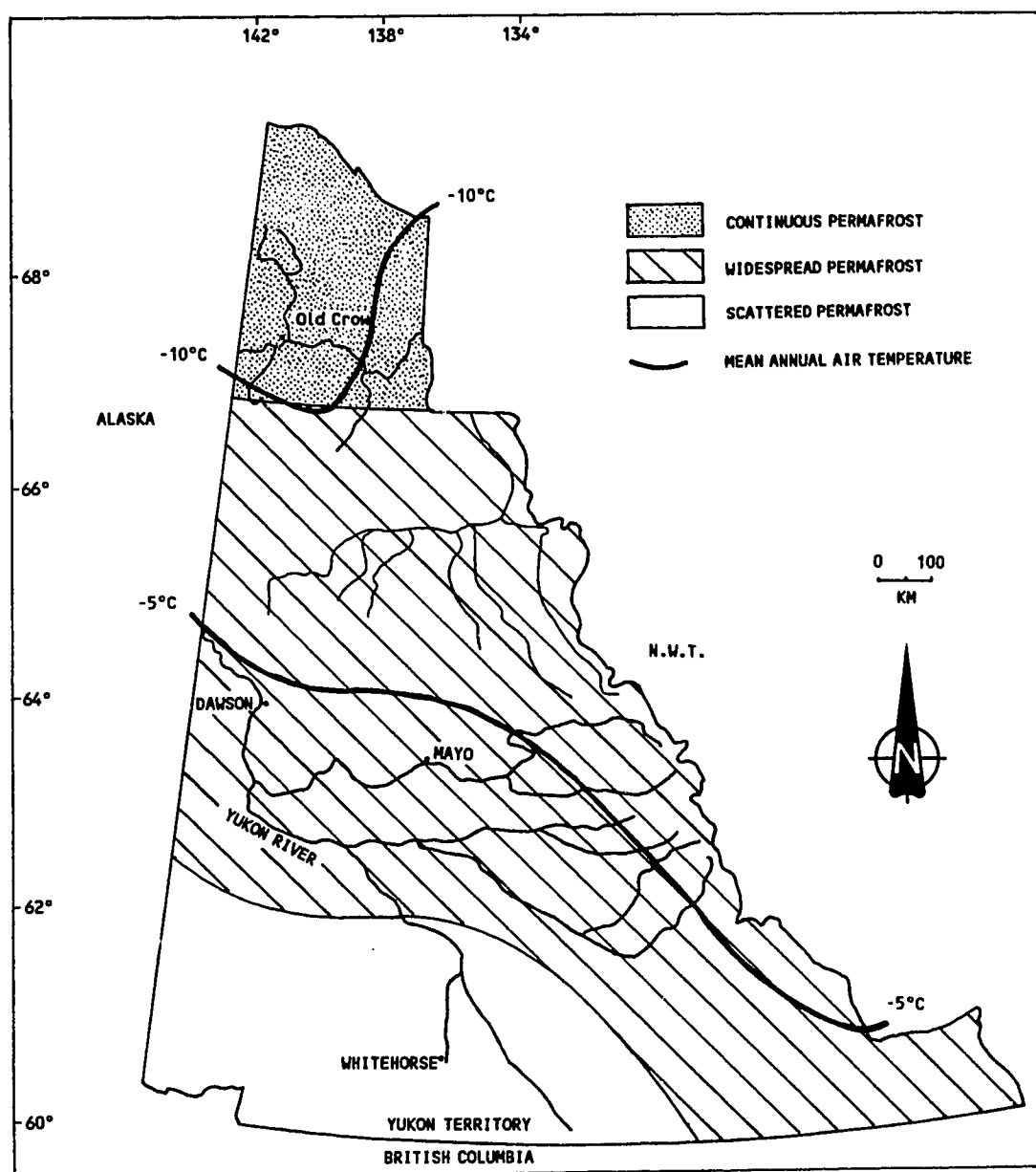


Figure 3: Permafrost limits and mean annual temperature isotherms of the Yukon Territory.
(Modified after Brown 1978).

Mayo is in the Pelly River Ecoregion 12 of Oswald and Senyk (1977). Ecoregions are defined on the basis of vegetation, regional landscape, bedrock and surficial geology, climate, and soils. Vegetation in the region is dominantly a northern mixed deciduous and coniferous forest (boreal forest), consisting predominantly of white spruce (*Picea glauca*) with minor amounts of black spruce (*Picea mariana*) and paper birch (*Betula papyrifera*). Aspen (*Populus tremuloides*), balsam (*Populus balsamifera*) and poplar (*Populus*) are common and the lodgepole pine (*Picea contorta*) northern limit is located southwest of Mayo (Burn 1987). South-facing slopes commonly have *artemesia* grasslands or steppe vegetation (Cwynar et al. 1987). The understory consists of feathermoss, willows, sagewort and ericaceous shrubs, with sphagnum mosses common in wetter terrain. Alpine firs (*Abies lasiocarpa*) are found at higher elevations, commonly along treeline which is at 1370 to 1400 metres (4500 to 4600 feet; Oswald and Senyk 1977). Shrub birch and willow together with ericaceous shrubs occur at higher elevations and extend above treeline.

2 Bedrock Geology

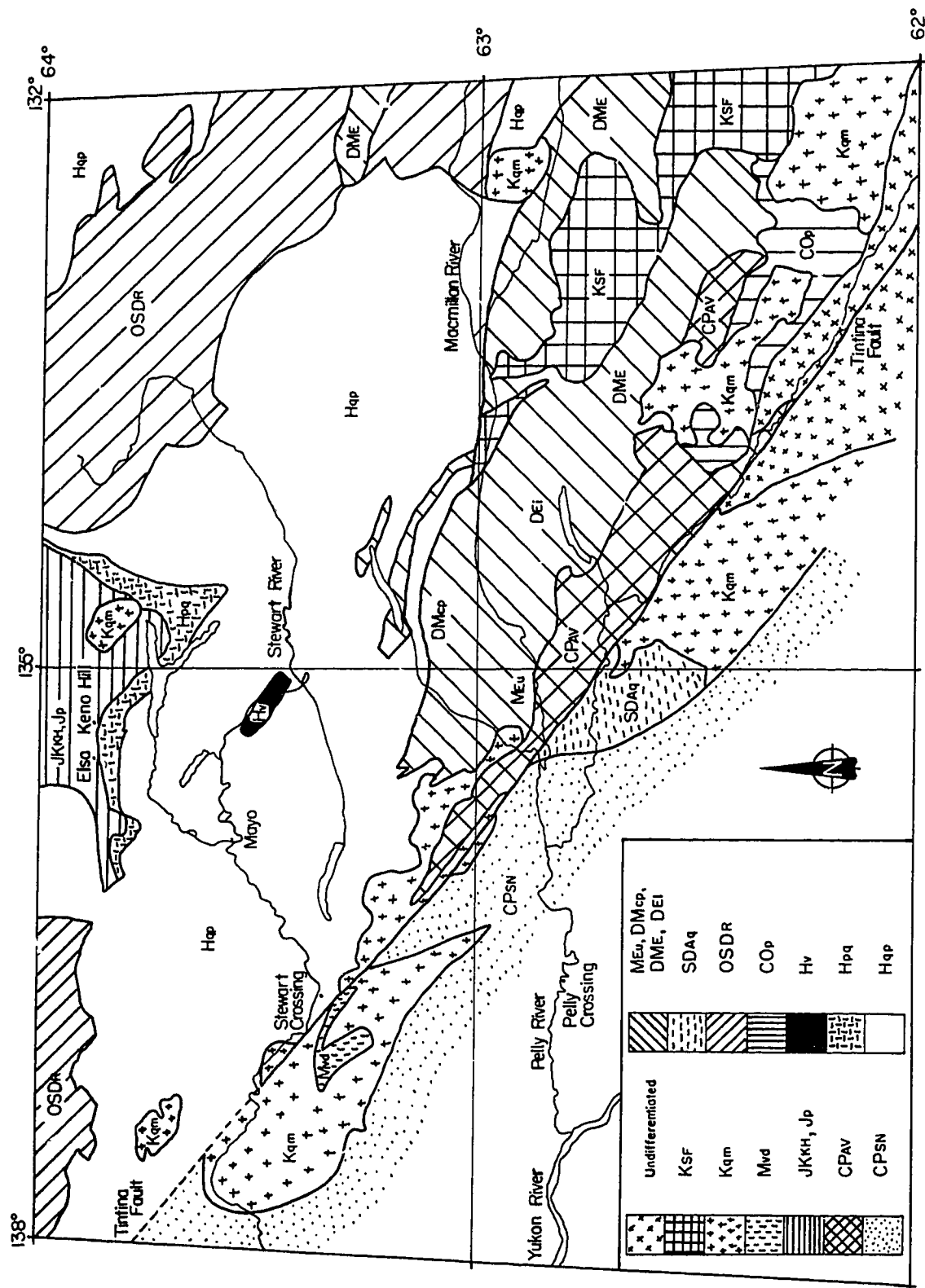
The Central Yukon region has been the site of numerous investigations since the end of the 19th century. Initial geological interest, circa 1883, was concerned with gold placer deposits along the Stewart River and its tributaries. McConnell (1901) and Keele (1905, 1906) conducted the first reconnaissance surveys of the region and described some of the first mineral occurrences.

Economic geology in the Mayo region has concentrated on the Keno-Galena Hill silver-lead deposit and placer gold and tungsten in Dublin Gulch, Duncan Creek, Highet Creek and around Keno Hill (Cairnes 1916; Cockfield 1919, 1920, 1921, 1924). The first comprehensive bedrock maps are from north of Mayo and were completed by Bostock (1943, 1948, 1964), McTaggart (1950, 1960), Boyle (1956, 1957a, 1957b), Green (1958), Green and McTaggart (1960) and Green and Roddick (1962). A collection of Geological Survey of Canada reports from the early 1900's, accompanied by a partial bedrock geology map of the Yukon, was produced by Bostock (1957). A 1:2 000 000 scale geologic map of the Southern Yukon, including the Mayo region, was produced by Gabriele et al. (1977; Figure 4).

The Tintina Fault is the dominant geological boundary in central Yukon. It is a Late Tertiary (Pliocene) graben occurring along an early Tertiary strike-slip fault (Tempelman-Kluit 1980). Geologic units have been transcurrently displaced up to 450 kilometres (Tempelman-Kluit 1980).

Symbol	Age	Lithology
Kqm	Cretaceous	quartz monzonite, granodiorite.
KSF	Cretaceous	SOUTH FORK: andesite, dacite, basalt.
JKKH	Jurassic-Cretaceous	KENO HILL: quartzite.
Jp	Jurassic	graphitic phyllite, quartzite, greenstone.
Mvd	Mesozoic	andesite, trachyte.
CPAV	Carboniferous-Pennsylvanian	ANVIL RANGE: andesite, basalt, slate, chert, limestone.
CPSN	Carboniferous-Pennsylvanian	schist, gneiss.
MEu	Mississippian	EARN GROUP: chert, argillite, quartzite, limestone.
DME	Devonian-Mississippian	EARN GROUP: shale, chert arenite, conglomerate.
DMcp	Devonian-Mississippian	CRYSTAL PEAKS: chert pebble conglomerate.
DEi	Devonian	EARN GROUP: slate, quartzite, limestone.
SDAq	Silurian-Devonian	ASKIN GROUP: quartzite, shale.
OSDR	Ordovician-Silurian-Devonian	ROAD RIVER: black graptolitic shale, chert.
COp	Cambrian-Ordovician	shale, limestone.
Hqp	Hadrynian	gritty quartzite, argillite, shale, phyllite.
Hpq	Hadrynian	graphitic phyllite, quartzite.
Hv	Hadrynian	greenstone.

Figure 4: Bedrock geology map of the central Yukon. (Modified after Gabrielese et al. 1977).



Basement rocks in central Yukon are the Pre-Cambrian and Palaeozoic Yukon Group metasediments. These are massive, blue-grey and grey quartzites, phyllitic quartzites, phyllites, schists, pebbly quartzites and limestones (Green 1958; Hpq, Hqp and COp on Figure 4). These are overlain by Palaeozoic shales, cherts, quartzites, conglomerates and limestones (Gabrielese 1977; OSDR, SDAq, DEI, DMcp, DME, and MEu on Figure 4). Jurassic and Cretaceous quartzites and phyllites are present to the north of the study area (Jp and JKKH on Figure 4). Mesozoic intrusions are common throughout the area as sills of diorites and gabbros, stocks of granodiorites or monzonites, and quartz porphyry (Green 1958; Green and Roddick 1962; Kqm on Figure 4).

3 Glacial Geology

Glacial limits on the Central Yukon Plateau were established by Bostock (1966), who recognized four advances of the Cordilleran ice sheet, from oldest to youngest, Nansen, Klaza, Reid, and McConnell. Landform soil associations were used to help define the age and extent of the glacial advances (Bostock 1966, Tamocai et al. 1985). Unglaciaded regions of west central Yukon have thicker and better developed soils than those formed on glacial surfaces. The Nansen and Klaza (Bostock 1966) advances were the most extensive and are the least recognizable. Some researchers (Tamocai et al. 1985, Smith et al. 1986, Tamocai and Schweger 1991) have since termed them as the undifferentiated pre-Reid glacial advances (Figure 5). Others (Hughes et al. 1969, Jackson et al. 1990) still recognize two advances, the Klaza and Nansen (also referred to as the younger pre-Reid and older pre-Reid, respectively), which are separated by intertill sediments containing the Fort Selkirk tephra dated at 1.48 ± 0.19 Ma (Westgate 1989; Figure 6). Basalts occurring between the two tills in the Fort Selkirk region yielded ages around 1.4 Ma (Westgate 1989) and firmly establishes the Nansen glaciation as Early Pleistocene. Pre-Reid soils are well-developed luvisols and brunisols with clay skins, cryogenic features, sand wedges and involutions (Rutter et al. 1978, Smith et al. 1986).

Reid ice-marginal features are moderately preserved and can be traced across most of the Central Yukon Plateau (Hughes et al. 1969). The Reid glaciation is postulated as Illinoisan (Oxygen isotope stage 6, 8, 10 or 12; Hughes et al. 1969), although an Early Wisconsinan age (Oxygen isotope stage 5b or 5d) is a possibility (Hughes et al. 1987). The Old Crow tephra overlies Reid age deposits and has been dated at 86 ± 8 ka (Wintle and Westgate 1986; Figure 6), 109 ± 14 ka (Berger 1987) and most recently at 140 ± 10 ka (Westgate et al. 1990). The Sheep Creek tephra has been found underlying the Old Crow tephra in the Fairbanks region which suggests an age >150 ka for the Reid deposits (Ward 1993).

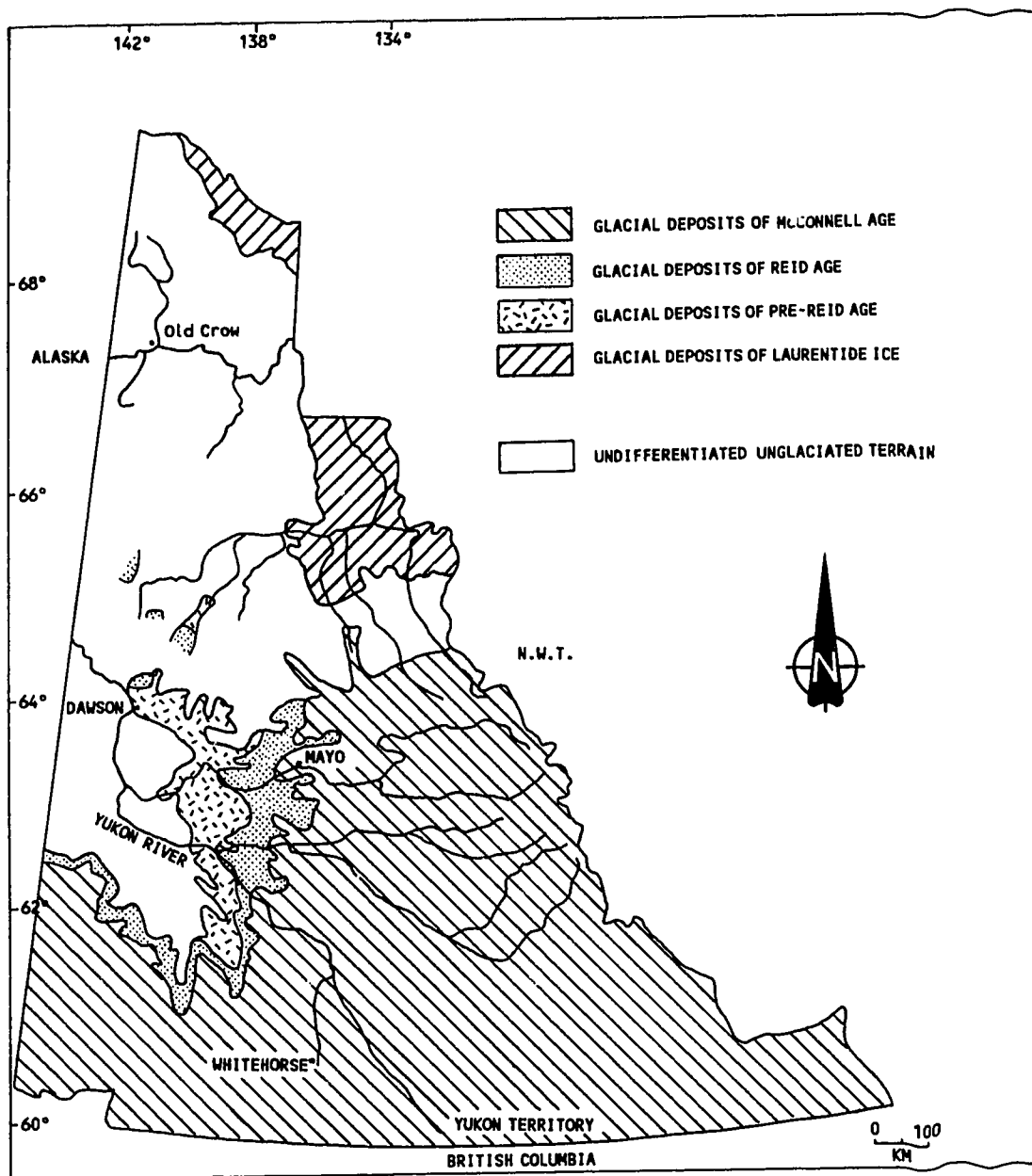


Figure 5: Quaternary Cordilleran and Laurentide ice sheet limits in Yukon Territory. (Modified after Tarnocai and Schweger 1991).

	Yukon Plateaus Bostock 1966; Hughes et al. 1969	Snag-Klutan area Rampton 1971	Silver Creek Denton and Stuiver 1967	Liard Lowland Klassen 1978, 1987	Southern Ogilvie Mountains Vernon and Hughes 1966	Old Crow Flats Morian 1980
Holocene	Postglacial 8.5, 8.6, 8.9 ka	Neoglacialation	Neoglacialation	Postglacial		
P L E I S T O C E N E	McConnell Glaciation 29.6, 35.4, 35.9 36.7, 38.1 ka	13.7 ka	Slims Nonglacial Interval 12.5 ka		13.7 ka	12.5 ka
	Field Soil		Kluane Glaciation 29.6 ka	Till D 23.9 ka	Last Glaciation	Glacial-Lacustrine Clay 25.2 ka
	Sheep Creek Tephra (> 80 ka) >46.6 ka	Old Crow Tephra (86-140 ka) >49 ka	Boutellier Nonglacial Interval > 37.7 ka	Intertill Unit C-D		Alluvium "Disconformity A" Old Crow Tephra (86-140 ka)
	Field Glaciation -----	Minor Creek Glaciation -----	Icefield Glaciation	Till C	>53.9 ka	
	Pre-Field Soil ----- Klaiza Glaciation <1.08 Ma ----- Fl Selkirk tephra 0.84-1.48 Ma Fl Selkirk basalt 1.4 Ma -----	?	Silver Nonglacial Interval Shakwak Glaciation? ----- ----- Shakwak Glaciation?	Intertill Unit B-C? >0.23 Ma Till B? Intertill Unit A-B? >0.76 Ma Till A?	Intermediate Glaciation Old Glaciation? Mosquito Gulch Tephra (1.22 Ma) Old Glaciation	Alluvium Little Timber Tephra (> 1.2 Ma) Lacustrine Clay

Figure 6: Subdivisions of Quaternary events and deposits in Yukon Territory. (Modified after Hughes et al. 1989).

The Reid-McConnell interglacial was cool and subhumid, allowing moderate development of brunisols with thin clay skins and rare cryogenic features or sand wedges on Reid age deposits (Foscolos et al. 1977; Rutter et al. 1978). Finite dates from the Reid-McConnell interglacial in the Mayo region are listed in Table 1. The 35 400 year old date is from a small willow branch taken from near the middle of gravels in the Mayo Section. The 35 900 and 36 700 year old ages were obtained on willow branches from near the upstream end of the Mayo Section. The 29 600 year old date was an accelerator mass spectrometry (AMS) date on *corispermum* seeds from the base of the Mayo Indian Village Section (Matthews et al. 1990). The 38 100 year old age was on an in situ willow stump near the base of the Mayo Section (Matthews et al. 1990). There are also nine infinite dates from wood taken from below the diamicton in the Mayo Indian Village and Mayo Sections (Table 1).

Cordilleran McConnell age ice advanced from two major source areas: the Selwyn Mountains and the Cassiar Mountains (Hughes et al. 1969; Figure 2). The Selwyn Lobe (Campbell 1967) affected the Mayo region, advancing from the east. Margins become digitate and topographically controlled with ice moving preferentially through valleys, most of which are oriented east-west. Late Wisconsinan McConnell age glacial deposits are the most readily recognizable and are well preserved (Bostock 1966). McConnell equivalent glacial deposits have been identified and dated throughout the Yukon Territory (Figure 6). This advance was accompanied by severe cold, but was relatively short as indicated by narrower and shallower ice wedges than Reid age ice wedges (Foscolos et al. 1977, Rutter et al. 1978). The northwestern extension or Selwyn Lobe of the Cordilleran ice sheet was mapped by Bostock (1966) and Hughes et al. (1969). More recent detailed work in the Mayo-Big Kalzas Lake regions was completed by Hughes (1983a, b, c, and d; Figure 7).

Soils inside the McConnell end moraine are a result of up to 14 000 years of exposure following retreat of the McConnell ice (Tarnocai et al. 1985). McConnell or Stewart Neosol (Smith et al. 1986) solum thicknesses are relatively thin, averaging 20 centimetres, as compared to Reid (45-56 centimetres) or pre-Reid (91-109 centimetres) soils (Tarnocai et al. 1985). McConnell soils are characterized as eutric or dystic brunisols with a weakly developed Bm horizon, a well developed calcium carbonate rich Cca horizon and rarely a leached argillic Ae horizon above the Bm. These soils develop under a forest cover and are usually light brown (10 YR), lack clay skins, cryogenic features, sand wedges or involutions (Smith et al. 1986). Loess averages 22 centimetres in thickness and is deposited on all ages of deposits (Tarnocai et al. 1985).

AGE	SECTION	MATERIAL	STRATIGRAPHIC UNIT	ANALYSIS	LAB NUMBER	REFERENCE
HOLOCENE						
8520±120	Upstream	Wood	Unit D?	Conventional	-	Burn et al. 1986
8560±130	from	Wood	Unit D?	Conventional	-	Burn et al. 1986
8870±200	Mayo	Organic material	Unit D?	Conventional	-	Burn et al. 1986
PRE LATE WISCONSINAN (REID-McCONNELL INTERGLACIAL)						
29 600±300	MIV	Corispermum seeds	Unit A	AMS	TO-292	Mathews et al. 1990
35 400±320	Mayo	Salix wood	Unit A	High Pressure	GSC-4927(HP)	This report
35 900±380	Mayo	Salix wood	Unit A	High Pressure	GSC-5142(HP)	This report
36 700±400	Mayo	Salix wood	Unit A	High Pressure	GSC-5139(HP)	This report
38 100±1330	Mayo	Salix wood	Unit A	Conventional	GSC-4554	Mathews et al. 1990
>35 000	Mayo	Wood	Unit C	Conventional	I(GSC)-180	Trautman and Walton 1962
>46 580	MIV	Wood	Unit B	Conventional	GSC-331	Dyck et al. 1966
>42 000	MIV	Picea wood	Unit B	Conventional	GSC-3931	Unpublished
>51 000	MIV	Picea wood	Unit B	Conventional	GSC-4436	Unpublished
>47 000	MIV	Picea wood	Unit B	Conventional	GSC-4472	Unpublished
>52 000	MIV	Picea wood	Unit B	High Pressure	GSC-5123(HP)	This report
>51 000	Mayo	Picea wood	Unit A	High Pressure	GSC-4920(HP)	This report
>51 000	Mayo	Picea wood	Unit A	High Pressure	GSC-4924(HP)	This report
>51 000	Mayo	Picea wood	Unit A	High Pressure	GSC-5152(HP)	This report

Table 1: Radiocarbon dates from the Mayo Region.

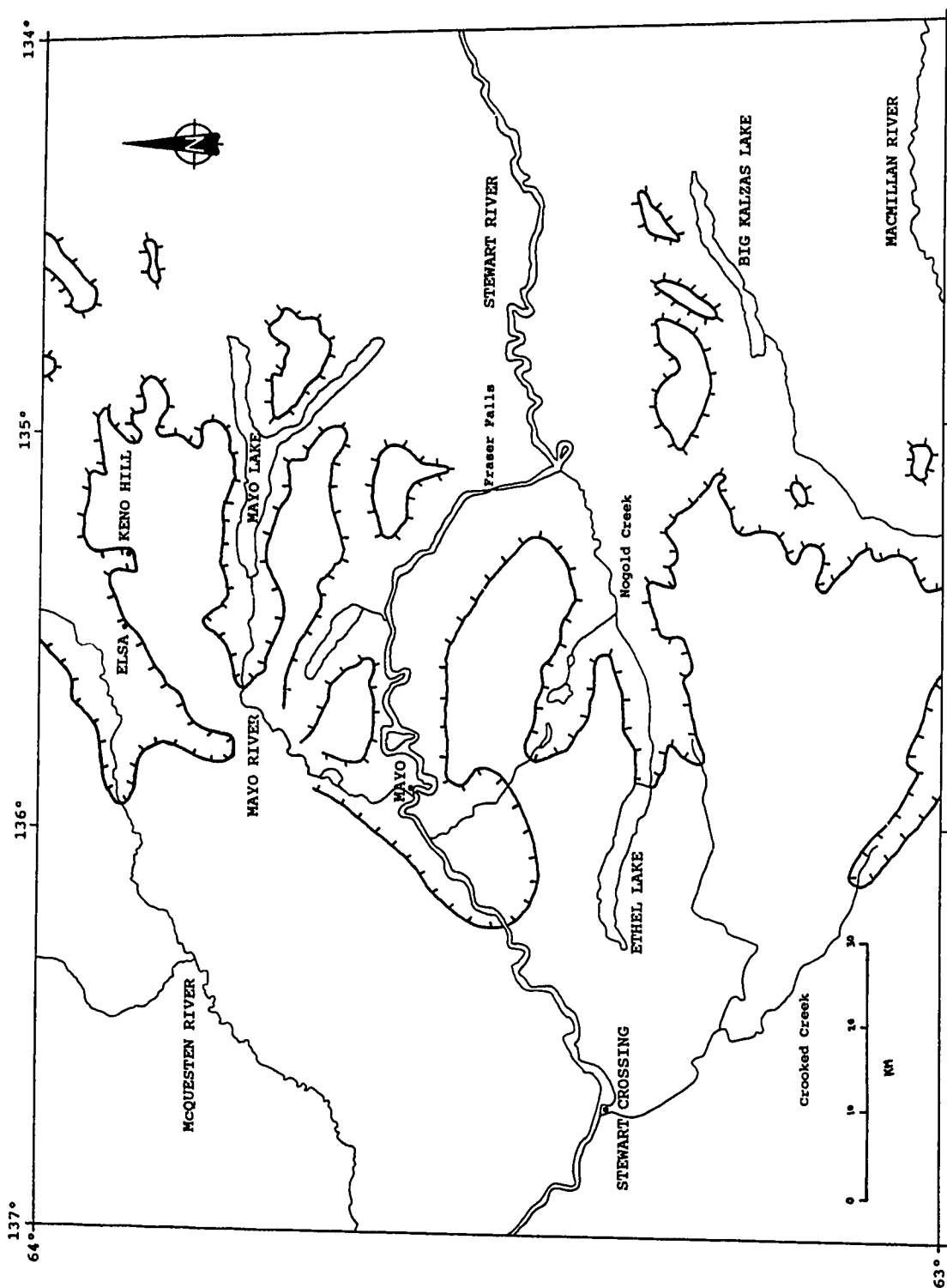


Figure 7: Late Wisconsinan McConnell ice limits in central Yukon Territory. (Modified after Hughes 1983b, c).

Postglacially the Stewart valley in the Mayo region was dammed by ice and a large proglacial lake formed. Hughes (1983c) mapped the limits of the lake from about 5 kilometres west of Mayo, up the Stewart valley, to as far east as Fraser Falls. Wood pieces taken from within these lake sediments have been dated at 8560 ± 130 and 8520 ± 120 (Burn et al. 1986; Table 1). An age of 8870 ± 200 (Burn et al. 1986) was obtained from organic material thought to have been buried underneath the active permafrost layer by cryoturbation.

II METHODS OF INVESTIGATION

A Field Methods

Three river cut bluffs exposed on the Stewart River downstream of the town of Mayo as well as roadcut sections in the area were investigated. Air photo analysis was completed prior to fieldwork. Distinctive morphologic features were noted and sections available for study were identified. Fieldwork was undertaken from June to August 1988 and in May and June of 1989. During the first season a comprehensive overview of the three main sections was completed and sedimentologic and stratigraphic data were accumulated on individual units. In the second field season, areas previously not described and problem areas, especially the gravel sections, were examined. Detailed descriptions were made where the sediments were accessible. The diamictons were most difficult to study owing to their cohesive, cliff-forming nature and location higher in the sections.

B Field Descriptions

The sections were initially subdivided into stratigraphic units on the basis of gross features and sediment type. Detailed examination through numerous vertical and horizontal logs permitted analysis of the sedimentology of individual beds and the lateral variation within units. Horizontal logs were less detailed than vertical logs, used mostly to note obvious variations and to describe the gravel deposits in the Mayo Section. Photographic panoramas were constructed in order to indicate location of stratigraphic correlations, faults, samples, fabrics, logged sections and basic units. Stratigraphic units were determined by visual approximation giving a rough outline which could then be further subdivided into beds within units. A variety of samples from the units were obtained for bulk textural analysis, pebble lithologies, wood and bone identification, radiocarbon dating, amino acid dating and pollen and macrofossil identification. Elevations were measured with a metre tape and altimeter.

Sedimentary descriptions were recorded in order to obtain characteristics of individual beds, facies, and units. Clasts are defined as sedimentary fragments of all sizes from clay to boulders. In this thesis the term clast refers to all sediment greater than 2 millimetres in diameter. On the Wentworth-Udden size classification scheme this would be small pebbles and coarser. Data collected for sand, gravel and diamicton beds included:

1. matrix or clast supported sediments
2. openwork or matrix-filled framework

3. sorting and grading of the sediments
4. grain size of sediments, clasts and matrix
5. imbrication, shape, rounding and percentages of clasts
6. striations, faceting or fracturing of clasts
7. primary sedimentary structures such as stratification, banding and inclusions.
8. secondary sedimentary structures such as water escape, loading, deformation and convoluted structures, compacted and cemented sediments
9. organic content such as wood, organic fragments and bones and their size, shape, condition and location
10. oxidation or discoloration
11. geometry, nature and distinctiveness of contacts
12. bed geometry, thickness and lateral continuity
13. matrix color
14. vertical jointings and horizontal partings
15. shape, size and abundance of sand and gravel lenses.
16. paleocurrent orientations

C Pebble fabrics in diamicton and gravel

Three dimensional analysis of pebble orientations in diamicton were completed to ascertain the flow direction of the transporting medium. Following the method of Harrison (1957) 42 fabrics were measured within the three sections. Although 25 pebbles is considered sufficient to establish whether a preferred fabric orientation is present or not (Domack and Lawson 1985), many samples had 50 pebbles measured for a more significant evaluation. Individual fabrics were taken in as small an area as possible, less than 50 centimetres wide by 50 centimetres high by 30 centimetres deep and commonly only 20 x 20 x 10 centimetres. Harrison (1957) suggests that spatial restrictions of 250 metres horizontally and one metre vertically are the maximum distances to which a fabric can be held significant in till.

Drake (1974) established that pebble shape directly affects fabric strength in diamictons. Of Zingg's (1935) four shape classes a-axis parallel orientations were strongest with prolates, good with blades and poor with discs and spheres (Drake 1974). Measurements of trend and plunge of long axes of prolate and blade shaped pebbles, with a:b axial ratios of at least 3:2, were taken. Clasts measured were mostly medium pebbles (16 millimetres to 32 millimetres), although small, large and very large pebbles (2 millimetres to 64 millimetres) were also sampled.

Analysis of the fabric data was completed with the use of two fabric statistics programs. The ROSY (Version 1.3 1988; D.B. McEachern 1988) program produces two dimensional vector analysis where only the orientation (trend) and not the dip (plunge) is used. Appendix 1B contains the rose diagrams produced from the fabrics. The fabrics have been separated according to the sedimentary facies in which they were located.

STEREO (Version 3.4 1987; D.B. McEachern 1988) produces an equal area projection contoured stereoplot. Normalized eigenvalues (S1, S2, S3) were calculated for the three mutually orthogonal eigenvectors (V1, V2, V3). Eigenvector V1 is parallel to the maximum clustering of the pebble axes and is the representation on a plane of the main axis or primary mode of the fabric (Mark 1974). Significance levels of the primary eigenvector are reached at 0.575 for 20 measurements and 0.484 for 50 or more measurements (Mark 1973, 1974).

D Laboratory Studies

1 Grain Size Analysis

Grain size analyses were performed in order to obtain sand, silt and clay percentages for comparison of various diamictons (Appendix 2A and 2B). They provide a quantitative textural description of the sediment that may reflect the transport history, depositional mechanisms and environmental conditions of deposition. The Geological Survey of Canada laboratory in Ottawa analyzed thirty-one samples that provided percentages of sand, silt and clay. The remaining 40 diamicton samples were analyzed by the author using the hydrometer and sieving methods described in ASTM D422 (1990). The information from hydrometer and sieve analysis was plotted on 3 cycle log paper from which percentages of sand, silt and clay could be obtained.

2 Pebble Lithologies

Pebble samples were taken of gravel and diamicton units throughout the Mayo region and were identified to determine their provenance. Clasts selected for analysis are coarser than 10 mesh, usually medium to large pebble size (16 millimetres to 64 millimetres). Clasts were identified and then were grouped into:

1. Quartzites, banded and massive.
2. Gneisses and quartz gneisses.
3. Schists.
4. Cherts, massive or layered, cherty argillite and argillite.

5. Sandstones, quartz eye sandstones, and chert and quartz pebble conglomerates.
6. Vein quartz.
7. All types of igneous rocks.

Samples were divided into stratigraphic units and raw numbers for each lithology are listed in tables in Appendix 3A. Provenance studies require that rocks are identifiable in hand specimen and located in one specific region to be assured of their origin. Lithologies were combined into three categories: Quartzite, Chert, and Sandstone (QCS) as listed in Appendix 3B. These categories were based on bedrock geology of central Yukon (see Figure 4). The Quartzite category contains quartzites, gneisses and schists which are locally derived from the Mayo and Keno Hill regions (JKKH, Jp, Hqp and Hpq). Cherts (OSDR) occur both to the northwest of Mayo and to the northeast. The sandstones originate from the southeast of Mayo (DME, DMcp). Vein quartz and igneous intrusions are deemed ubiquitous as they occur throughout the area and are not specifically from one region. Cumulative QCS percentages are listed in Appendix 3B for stratigraphic units and plotted on ternary diagrams (Appendix 3C).

3 Wood Analysis

Wood samples were generally well preserved, occurring in sand, gravel and diamicton beds. Wood fragments were identified by R.J. Mott (Geological Survey of Canada; Appendix 5). Three species of wood were identified: *Picea* (spruce), *Salix* (willow), and *Larix* (larch). The Mayo Section contained many wood fragments of both spruce and willow. Fewer pieces were recovered from the MIV Section but they contained larch as well as spruce and willow. Seven samples of wood were submitted to the Geological Survey of Canada for high pressure radiocarbon dating (Table 1; Appendix 6). Samples were dated relative to a standard of 1950 A.D. with a half life of ^{14}C of 5568 years.

4 Bone

Two bone samples were found in talus deposits at the base of the Mayo Section at 707 and 878 metres. They were identified by C.D. Harington (National Museum of Canada) as a thoracic vertebra fragment and the right radius of a small horse such as *Equus lambei* (Harington, personal communication to O.L. Hughes, 1988). These bones were derived from the gravel underlying the diamicton. A third bone was found on a gravelly point bar of the Stewart River opposite the MIV Section. It was dirty grey, deeply checked and heavily eroded. This bone was identified by C.D. Harington as a left femur fragment from a *Mammuthus* sp. (mammoth).

III STRATIGRAPHIC FRAMEWORK

In the Mayo region the Stewart River changes from an unconfined meandering river to an incised river. Downstream of Mayo this incision has exposed three large sections of gravel, sand and diamicton (Figures 8 and 9). The Mayo Section (63°35'N, 135°54'W) is 1700 metres long and up to 30 metres high, forming a steep cliff with several gullies dissecting it. The Mayo Indian Village Section (MIV Section; 63°36'N, 135°56'W) is over 1800 metres long and up to 57 metres high. A broad talus slope provides access to various parts of the section. The Third Section (63°35'N, 135°57'W) is over 1000 metres long and about 60 metres high. It is partially vegetated, poorly exposed and, except for the upper diamicton, easily accessible. A fourth section, the McIntyre Park Section, is located near where the Mayo-Stewart Crossing road crosses the Mayo River (63°36'N, 135°54'W).

Deposits in the sections can be divided into seven stratigraphic units. These units are:

- G. Soil and loess,
- F. Upper gravel,
- E. Upper diamicton,
- D. Upper sand,
- C. Diamicton,
- B. Lower sand and gravel,
- A. Lower gravel and sand.

Mayo Section

The lowest exposed sediments in the Mayo Section are well stratified, coarse gravels with minor sandy interbeds (Unit A, Figures 10 and 11). The gravels are exceptionally well exposed and beds are laterally continuous for hundreds of metres. The base of the section is covered by a talus slope down to the Stewart River. Throughout the exposure are widely spaced normal faults which usually extend to the upper contact of the unit but not beyond.

A small, 130 metres wide and up to 6 metres thick, deposit of Unit B is preserved at the upstream end of the section. It occurs as a broad shallow trough-shaped deposit of sandy gravel conformably overlying Unit A. These sediments are unconformably overlain by matrix-supported diamictons (Unit C). The diamicton extends along most of the section but pinches out towards the eastern or upstream end. The lower contact is sharp and planar along the entire section, truncating sedimentary structures and faults in the underlying gravel.

Explanation of Map Unit Designations

A simple map unit designation consists of a genetic symbol (upper case letter) followed by the morphological descriptor(s) (lower case letter). The textural modifier(s) is applied as a prefix where texture is known from field observations. Compound map units, consisting of two simple designations separated by an oblique (/), are used where mixtures cannot be separated because of either limitations of map scale or inability to differentiate the units by airphoto interpretation. In the case of combinations of morainic (M) or colluvial (C) deposits, the combination is shown by use of the two genetic symbols, separated by a comma.

Textural Modifiers

f	fen
---	-----

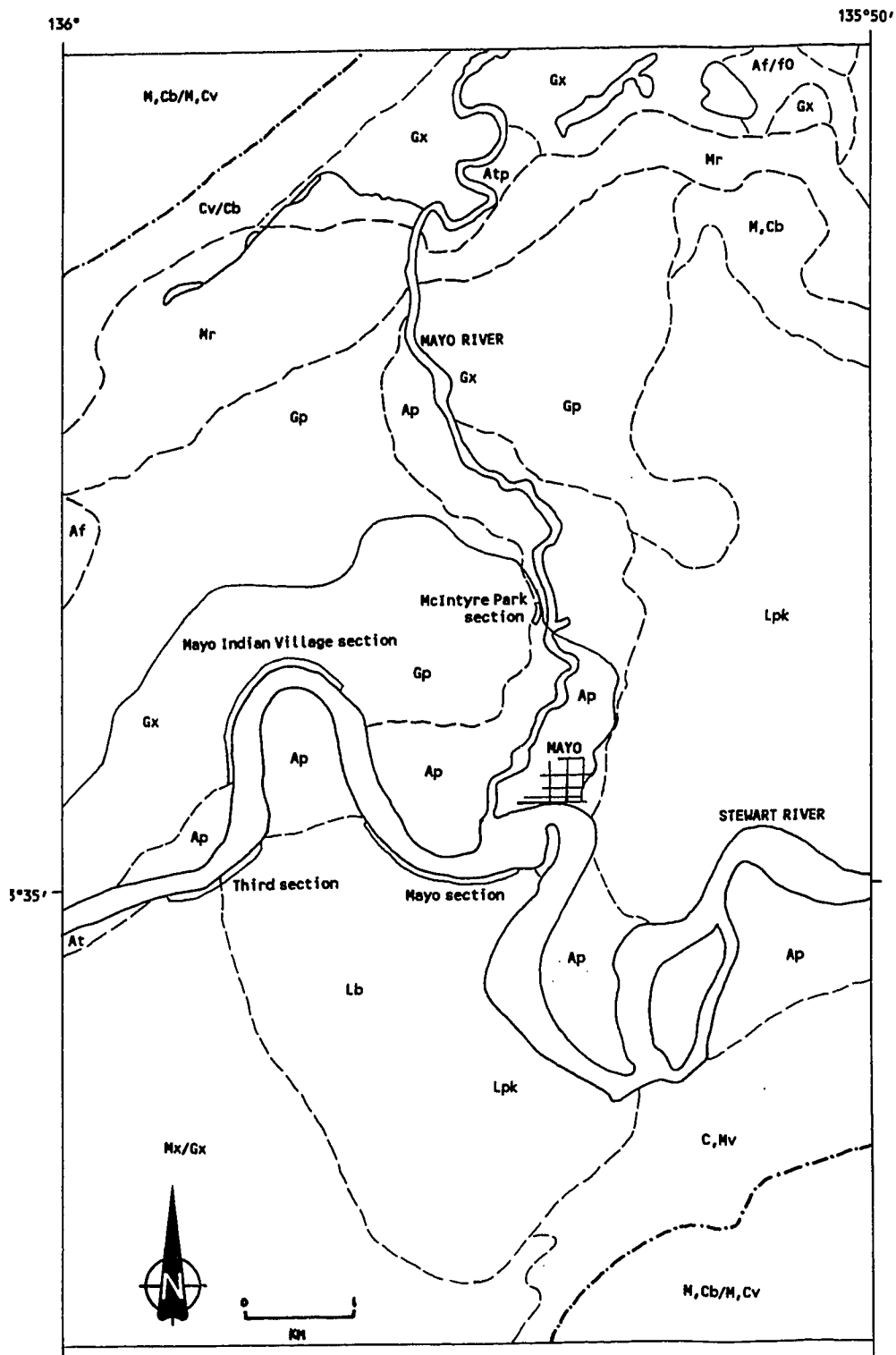
Genetic Categories

A	Alluvial deposits
C	Colluvial deposits
G	Glaciofluvial deposits
L	Glaciolacustrine deposits
M	Morainic deposits
O	Organic deposits

Morphologic Modifiers

b	blanket
f	fan
k	thermokarst
p	plain
r	ridged
t	terrace
v	veneer (generally <2 metres thick)
x	complex (combinations of modifiers)

Figure 8: Location map of the main sections in the Mayo region. Surficial geology is modified from Hughes 1983c.



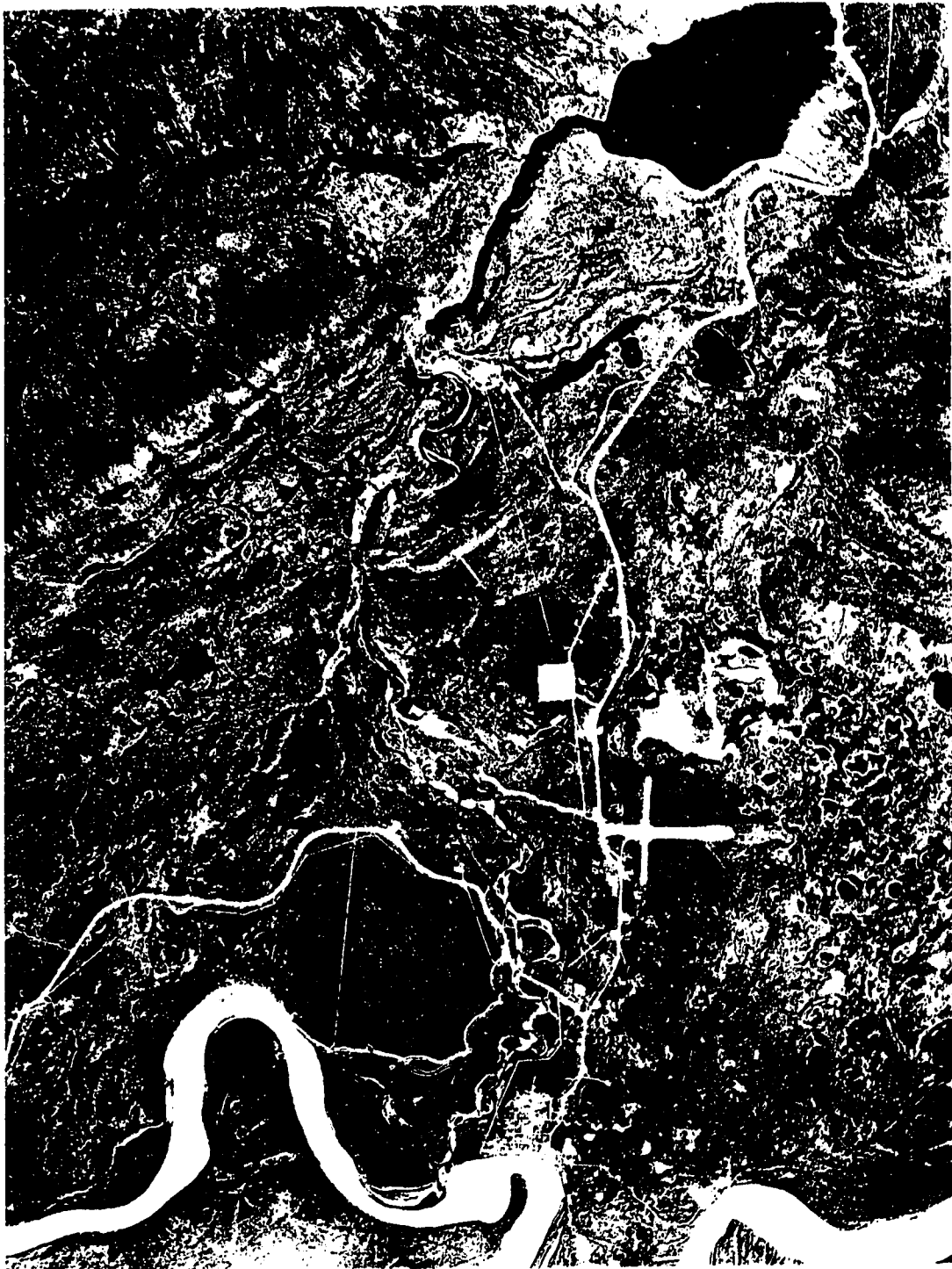


Figure 9: Air photograph of the Mayo region. Air photograph A19604-25.

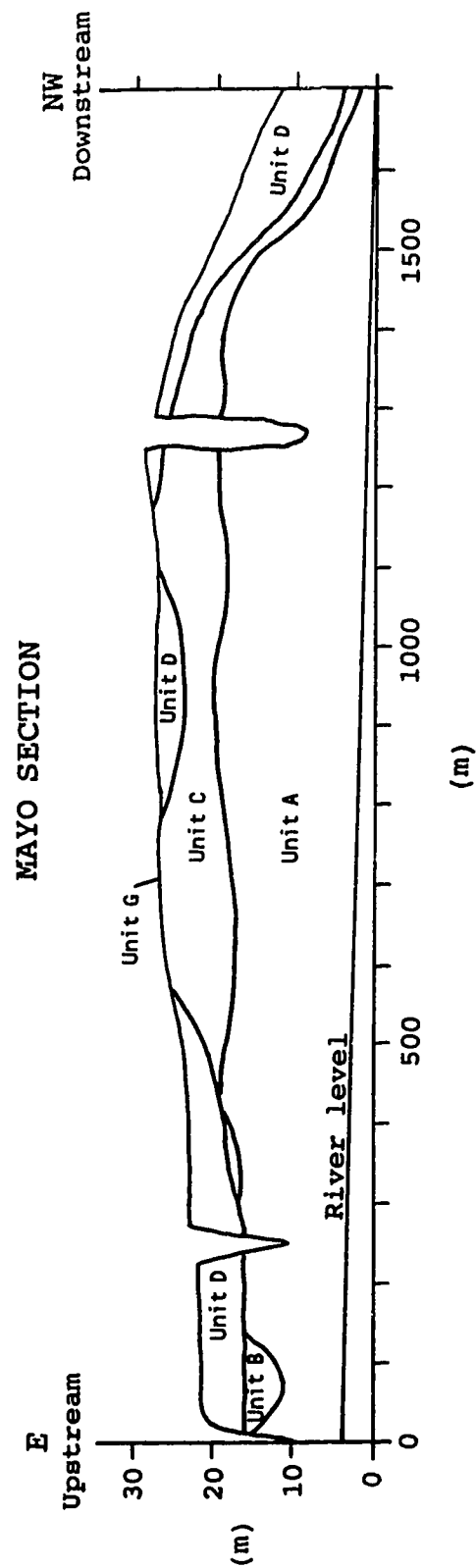


















Figure 10: Schematic cross-section of the stratigraphic units in the Mayo Section.

LEGEND FOR VERTICAL LITHOSTRATIGRAPHIC LOGS

Vertical logs are labelled according to the distance in metres from the upstream end of the section. Vertical scale is in metres. Average grain size is indicated across the base of the log. Dashed lines for average grain size indicate that only the approximate grain size of the sediment was obtained and/or the section was covered or inaccessible.

	Clays and silts		Planar stratification
	Sands		Trough cross-stratification
	Pebbly sands		Planar cross-stratification
	Matrix-filled gravels		Erosional stoss climbing ripples
	Openwork gravels		Depositional stoss climbing ripples
	Diamicton		Sediment gravity flow margin
	Lenses		Organics
	Frost wedge		Fault

x Radiocarbon date

M-01 Pebble fabric

Cl Clay

P Pebbles

Si Silt

C Cobbles

Sa Sand

B Boulders

G Granules

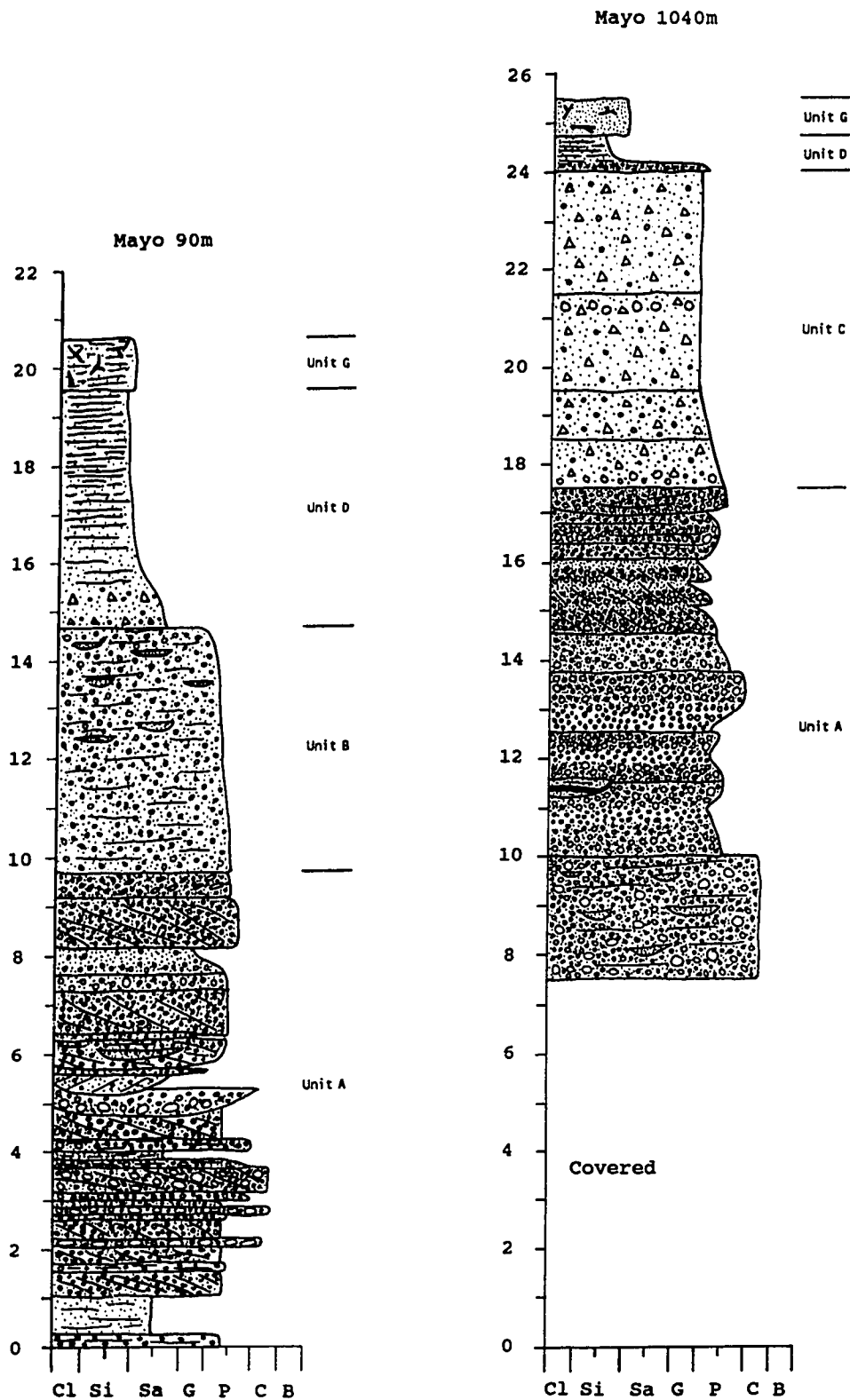


Figure 11: Representative sections of units and sedimentology present in the Mayo Section.

Conformably overlying the diamictons is a sequence of interbedded sand, silt and clay with rare pebbly lenses (Unit D). This unit is thickest at the upstream end where there is little or no diamicton preserved. Capping the section is a 50 to 100 centimetre thick soil and loess layer (Unit G) developed from the sediments directly beneath.

MIV Section

The basal unit at the MIV Section is an intermittently exposed sand and silt deposit (Unit A, Figure 12). This unit only occurs in the central portion of the section and is unconformably overlain by a thick sequence of sand and gravel (Unit B, Figure 13). The sand and gravel is exposed for 10 metres at the upstream end but thickens to greater than 50 metres and extends to the surface towards the downstream terminus. It consists predominantly of well-stratified but commonly highly distorted sand and gravel with rare diamicton lenses.

The sand and gravel is unconformably overlain a 1-10 metre thick, matrix-supported diamicton (Unit C). The diamicton is continuous for 1300 metres rising towards the downstream end. Near the upstream end of the section the diamicton forms pods or lenses in the overlying sediments. At the downstream end the unit thickens to up to 10 metres in a broad trough shape. A gradational upper contact is consistent along the entire section into the overlying sand (Unit D). Unit D consists of a fining up sequence of sand which has broad trough shaped, gravel based erosional disconformities cut into it. The sand is well stratified and individual beds are readily traceable for 100's of metres. The unit is thickest toward the upstream end and pinches out where Unit B extends to the top of the section.

Unconformably overlying Unit D is a 950 metre wide exposure of coarse gravel (Unit F). This is dominantly strongly-oxidized, clast-supported, poorly stratified gravel forming a 1-2 metre thick layer near the top of the section. They typically grade upward into fine gravel and sand. Capping the entire section is a 1-2 metre thick soil and loess deposit (Unit G). This is conformably deposited onto the gravelly unit (F), the sandy unit (D) and the lower sand and gravel unit (B) along the section. This unit also contains a thin, poorly preserved but identifiable ash layer at 970 and 1550 metres.

Third Section

Poorly exposed gravel (Unit A, Figures 14 and 15) is present at the base of the Third Section. This is a well stratified, small to medium pebble gravel exposed to a maximum of 3

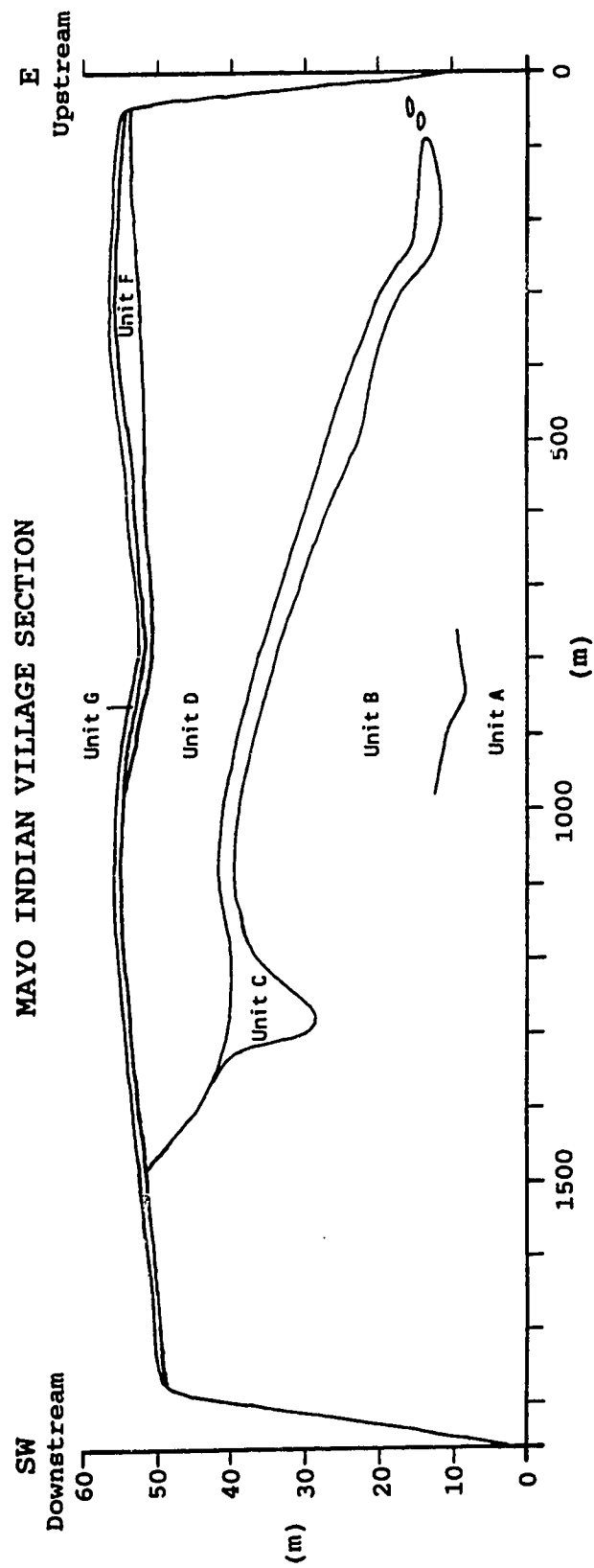


Figure 12: Schematic cross-section of the stratigraphic units in the MIV Section.

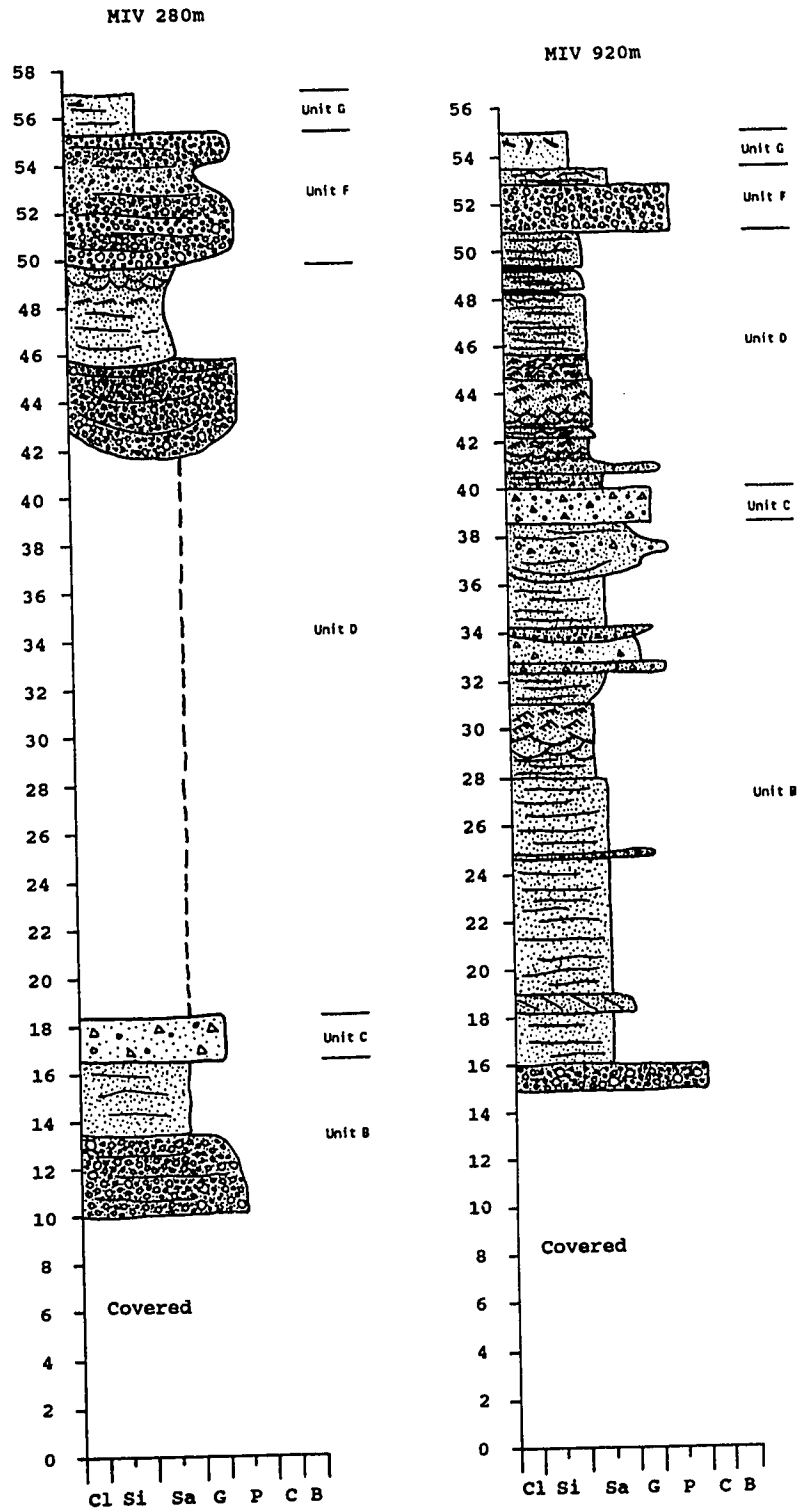


Figure 13: Representative sections of the units and sedimentology present in the MIV Section.

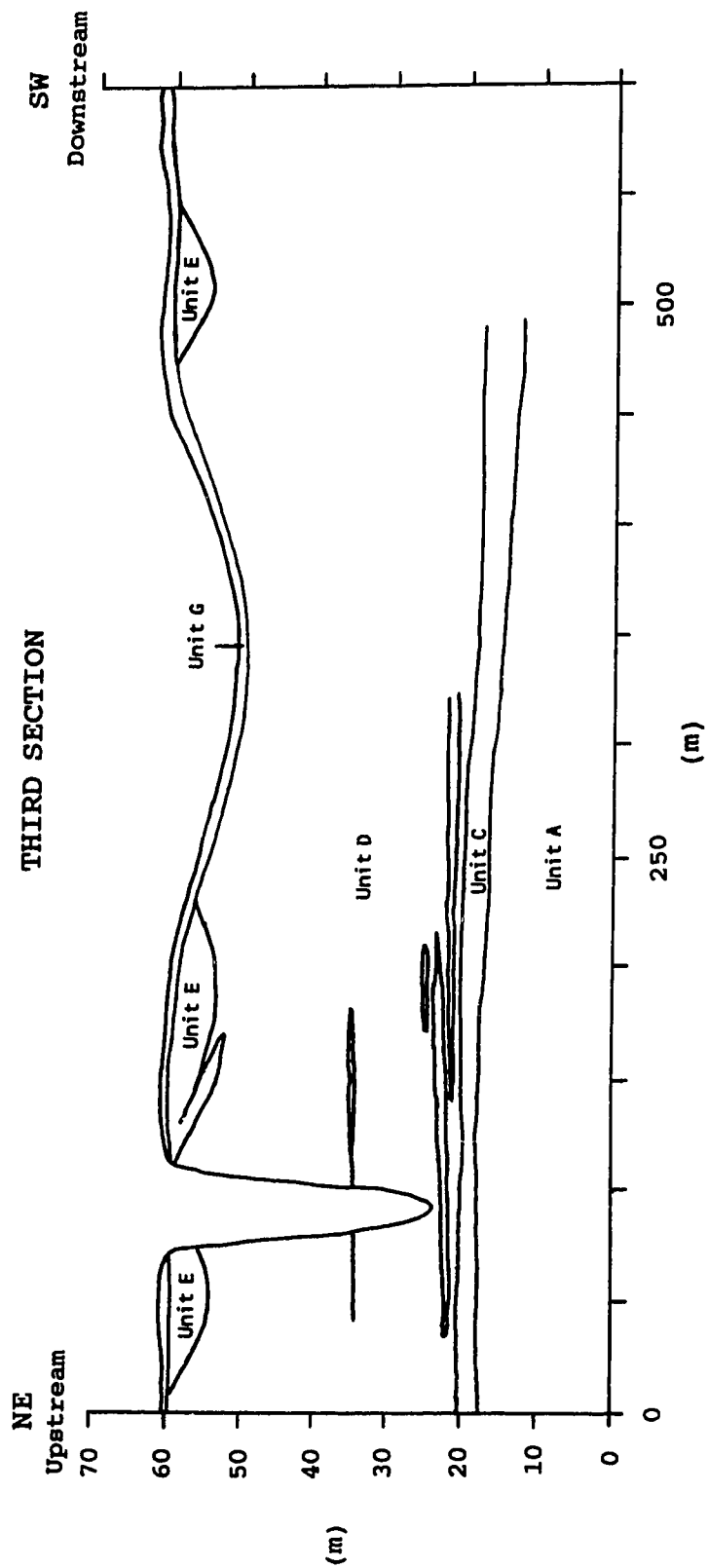


Figure 14: Schematic cross-section of the stratigraphic units in the Third Section.

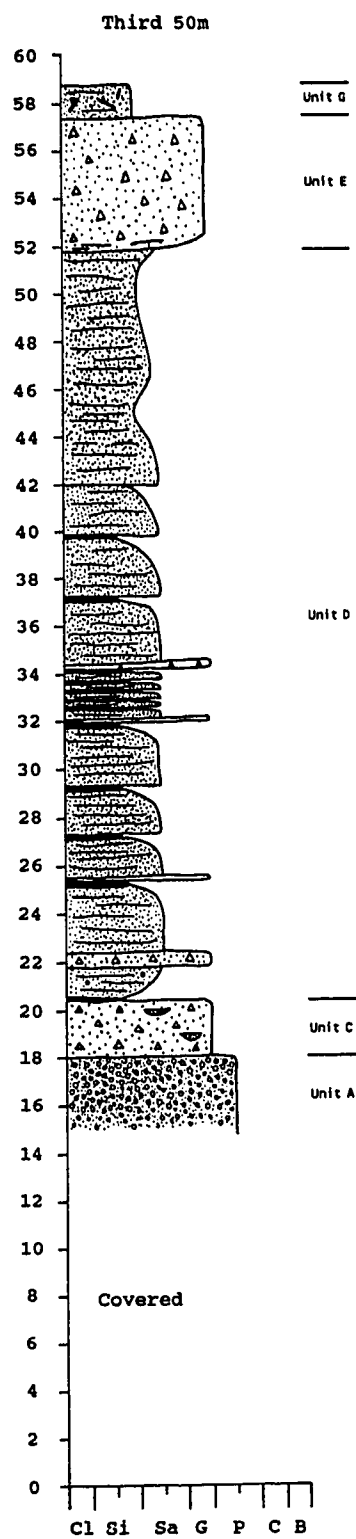


Figure 15: Representative sections of units and sedimentology present in the Third Section.

metres. Unit A unconformably underlies an intercalated sequence of matrix-supported diamicton (Unit C) and sand, silt and clay (Unit D). The diamicton is continuous across the face at 1-4 metres thick and dips slightly to the southwest. Diamicton is confined to the lowest 5 metres above the unconformity except for thin discontinuous lenses. The sand, silt and clay unit extends across the face and is up to 30 metres thick. This unit is well stratified in repetitive fining upward sequences. Near the top there are some contorted and distorted sand units. The unit can extend to the surface but is more commonly truncated by broad trough-shaped diamicton bodies (Unit E) with sharp to interbedded lower contacts. The matrix-supported diamicton occurs in lenses stacked upon each other. Capping the section is a 1-2 metre thick soil and loess deposit (Unit G) which has a conformable lower contact with both Units D and E.

McIntyre Park Section

The McIntyre Park Section is located to the northeast of the MIV Section along a bluff cut by the Mayo River (Figure 8 and 9). It is a scree covered face in a gravel pit and only Units D and G are exposed. Large scale, coarse gravelly beds of Unit D are poorly exposed with no clear upper or lower contact. The gravel beds form tangential foresets across much of the face and individual foresets can be traced for over 5 metres laterally. Unit G is an organic layer which is poorly exposed and covers the top of the section.

IV FACIES DESCRIPTIONS AND INTERPRETATIONS

Introduction: The Concept of "Facies".

Facies descriptions and interpretations have become the building blocks of sedimentary geological work. Facies can be described to be the external appearance, look, aspect or condition of a body of rock or sediment (Teichert 1958; Walker 1984). The facies concept was introduced to geology by Nicolas Steno in 1669 to represent the entire aspect of a part of the earth's surface during a certain interval of geological time (Teichert 1958). The first application of the facies concept in a stratigraphical context was by Amand Gressly in 1838 (Walker 1984).

The facies concept is the most frequently used and misused concept in sedimentary geology. As it is applied today in sedimentology, facies represent the collective lithologic and palaeontological characteristics of a sedimentary unit. This is a purely descriptive expression of the primary observable properties of a sedimentary unit. Genetic interpretations are not included in the description of the facies as they are subjective and allow preconceived concepts to enter into the description. The description alone should enable the worker to interpret the hydrodynamic or ecological conditions present during deposition. One facies interpretation is not diagnostic of one depositional environment as a facies may be deposited in many different environments. Genetically related facies of environmental significance may be grouped as a facies association similar to Collinson (1970) or as an architectural element (Miall 1985). The strength of facies is noted when several facies interpretations are used together to arrive at an overall depositional environment which is the sum of the individual parts.

Thirteen lithofacies are recognized in the unconsolidated sediments in the Mayo region. Major features and environments of deposition are summarized in Table 2.

Facies 1: Diamicton with well developed subhorizontal partings and striated clasts.

Description

Facies 1 is a dense, massive, silty-sand diamicton with well developed subhorizontal partings and striated clasts. The diamicton is dark olive grey (5Y 3/2 dry), less than 50 centimetres thick and only found in Unit C between 800 and 1050 metres in the Mayo Section

Facies	Lithology	Sedimentary Structures	Interpretation
1	Diamicton with well developed subhorizontal partings and striated clasts	Massive, subhorizontal partings, abundant striated clasts, dense, embedded clasts, flutings, strong unimodal pebble fabrics, sharp basal contact	Lodgement till
2	Massive and layered diamicton with sorted sediment lenses	Massive to layered, dense, abundant sorted sediment beds, striated clasts, unimodal pebble fabrics	Meltout till
3A	Isolated clasts and massive diamicton lenses	Isolated clasts, massive beds of diamicton, piercement and drape structures	Dropstones and dump mounds
3B	Massive or stratified diamicton interbedded with sand or gravel	Massive to stratified, loosely consolidated, abundant sorted sediment beds	Sediment gravity flows
3C	Massive diamicton interbedded with sand and gravel	Massive, thin and discontinuous, loosely consolidated, wisps of sorted sediments	Colluvium
4	Massive and stratified matrix-filled pebbly gravel	Massive and planar matrix-filled laterally continuous beds	Longitudinal bars and channels
5	Planar cross-stratified matrix-filled pebbly gravel	Matrix-filled foresets, forms couplets with facies 7	Transverse bars
6	Massive and stratified openwork pebbly gravel	Massive and planar openwork beds, well sorted	Longitudinal bars and channels
7	Planar cross-stratified openwork pebbly gravel	Openwork foresets, well sorted, forms couplets with facies 5	Transverse bars
8A	Massive, stratified and cross-stratified pebbly sand, silt and clay	Fining upward beds, complex planar and ripple stratification	Bar top and channel sands
8B	Planar cross-stratified pebbly sand	Fine grained foresets	Transverse bars
8C	Planar cross-stratified sand	Asymmetrical inclined planar strata, flexed at crest	Channel floor duneform
9	Planar, wavy and massive bedded or laminated sand, silt and clay	Planar, wavy and massive stratification	Low relief sand sheets or ripples, shallow lacustrine or fluvial
10	Trough and planar cross-stratified sand	Trough and planar cross-stratification	Migrating large ripples, shallow lacustrine or fluvial
11	Climbing ripple cross-laminated sand	Erosional stoss and depositional stoss climbing ripples	High sedimentation, low migration rates, shallow lacustrine or fluvial
12	Sand, silt and clay with organic detritus	Distorted stratification, high organic content	Bar and bank deposits
13	Silt and organics	Horizontal laminations	Loess and soil

Table 2: Summary of the sedimentary features and environments of deposition of the facies in the Mayo region.

and between 700 and 920 metres in the MIV Section. The matrix coarsens upward from silt near the base to silty-sand at the top.

The diamicton breaks easily along well developed subhorizontal to horizontal partings which are 1 to 2 centimetres apart. Partings gradually become wider spaced, up to 4 centimetres apart, and less well developed upwards through the unit. They are frequently oxidized and infilled with silt, especially lower in the unit. Vertical joints, spaced 1 to 3 centimetres apart, are present but are less well developed than the partings and commonly lack the oxidation typical of the partings. When dessicated this unit has a blocky appearance and the vertical jointing is more evident.

This diamicton consists of 30 to 40% clasts, ranging in size from small pebbles to boulders, dominantly small to large pebbles. Clasts are subrounded to well rounded with bullet shaped clasts (rollers and blades) occurring frequently. Striated clasts with the striations mostly parallel to the a-axis are present. Many clasts are broken or shattered, usually along foliation. A thin silty oxidation coating is commonly found on clasts.

At the base of this facies in the Mayo Section there are two boulders embedded into underlying sediments (Plate 1; Figure 16). The a-axes of these boulders plunge at 10 to 25° toward the east at 082°. Both boulders are striated and faceted, with the striations closely paralleling the a-axes. Deformed diamicton is present to the southwest of the boulders, and also pushed up and around on top of the boulders. A gravel lense infills a cavity in the lee of the boulders. This wedge-shaped lense, 25 centimetres thick by 75 centimetres long, is derived from the underlying gravel deposits. Diamicton stringers encase the smaller clast and extend from between the two boulders, pass below the rear boulder and extend horizontally into sand. The stringer is 10 centimetres below the contact between the gravel and diamicton. Sand below this stringer is not disturbed but the sand above is deformed and distorted. Poorly defined elongate undulations associated with these boulders are oriented at 235°.

A few sand beds are present in facies 1. These are up to 10 centimetres thick, but usually 1 to 3 centimetres, and up to 50 centimetres wide. The lenses are subhorizontal and irregular or trough-shaped and usually possess weak horizontal stratification that tapers off into diffuse stringers in the diamicton. The lower contacts of these beds are usually indistinct but the upper contacts tend to be clear and defined by a well developed horizontal parting. Small horizontal pebble gravel lenses, 1 to 3 centimetres thick by 5 to 15 centimetres long, with sharp irregular boundaries are also present.

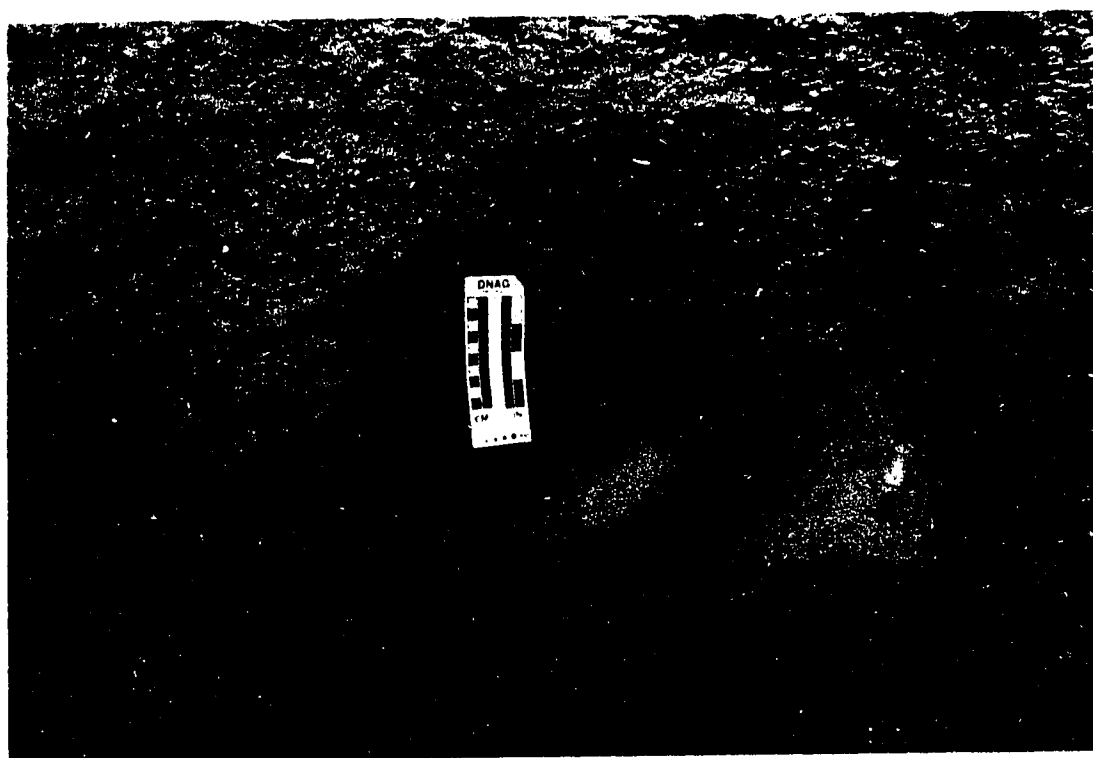


Plate 1: Embedded boulders along the basal contact of facies 1 diamicton. (Unit A gravel below and Unit C diamicton above.) See figure 16 and text for further explanation.

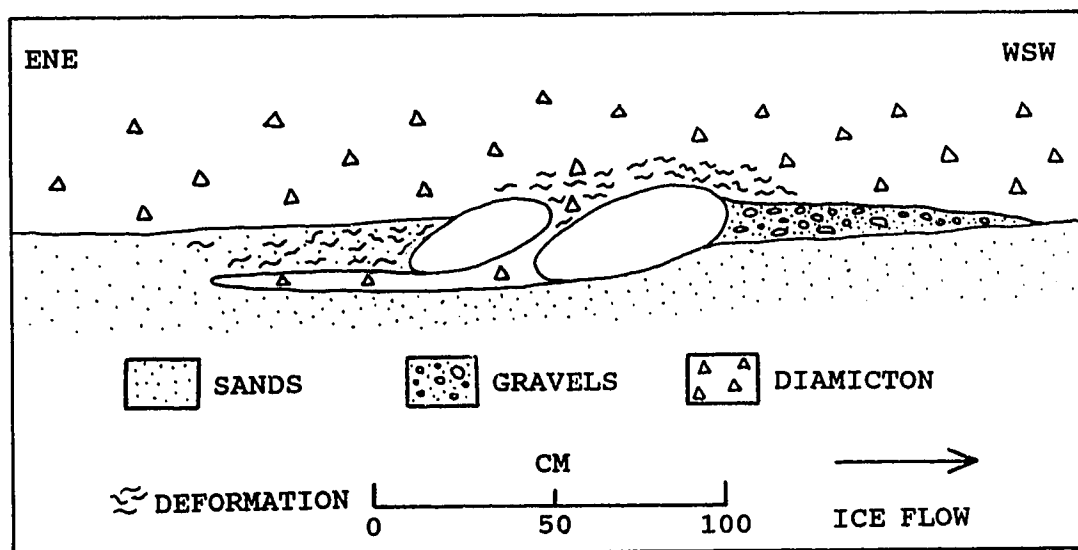


Figure 16: Schematic diagram of the embedded boulders at the base of Unit C.
See text for further explanation.

The lower contact of the diamicton is sharp and erosively cross-cuts bedding in the sand and gravel below. Distortion in the upper 5 to 10 centimetres of the underlying sediments is common. Well developed elongate ridges and undulations, oriented toward 61° (241°) are present at the basal contact (Plate 2). These undulations are 20 to 30 centimetres apart crest to crest (wavelength) and have a depth of up to 5 centimetres (amplitude). Clasts may occur at the terminus of these undulations. Compressive deformation of sediment in front of clasts embedded into the underlying sediments is common. Sand stringers squeezed or pulled up from the underlying deposits reach up into the diamicton. Diamicton lenses infill topographic irregularities and rarely intrude into the underlying sand or gravel.

Pebble fabrics were completed at thirteen locations in diamicton of this facies (Appendix 1A and 1B) and have eigenvector (V1) orientations towards the west-southwest (233° to 260°), with a mean eigenvector of 246° . Dip (plunge) measurements for these fabrics average 12° and vary from 08° to 24° . Primary eigenvalues (S1) are strongly unimodal and range from 0.69 to 0.88 and average 0.79. Plotting of the S1, S2 and S3 values on a ternary diagram (Figure 17) illustrates the strong preferred primary eigenvalue and weak secondary and tertiary values. A plot of the primary eigenvalue against the trend of the mean axis (Figure 18) shows the strong preferred orientation and tight clustering of the primary eigenvalue. The fabrics all suggest glacier ice flow direction was parallel to the Stewart valley.

Interpretation

This diamicton is interpreted to be subglacial lodgement till formed under confining conditions at the base of a sliding glacier. The sediments are characterized by well developed subhorizontal partings, striated clasts, dense and compact texture, a strong unimodal pebble fabric, embedded clasts, compressively deformed lenses, flutings, and a sharp, erosional basal contact. Lodgement till "is deposited by plastering of glacial debris from the sliding base of a moving glacier by pressure melting and/or other mechanical processes" (Dreimanis, 1988). When the tractive force of the sliding glacier exerted on the particle is equal to the frictional resistance between the glacier bed and the particle which is in traction, then that particle becomes lodged. Shearing and pressure melting at points of contact with subglacial obstructions are important secondary mechanisms (Boulton 1970a). Features of lodgement tills have been noted by numerous authors (Boulton 1970a, 1971, 1972, 1974, 1975, 1976, 1978, 1979; Goldthwait 1971; Marcussen 1975; Dreimanis 1976, 1982, 1988; Kruger 1979, 1984; Haldorsen 1981, 1982; Hallet 1981; Eyles et al. 1983; Muller 1983a and b; Eyles and Miall 1984; Levson and Rutter 1986, 1988; Elson 1988).

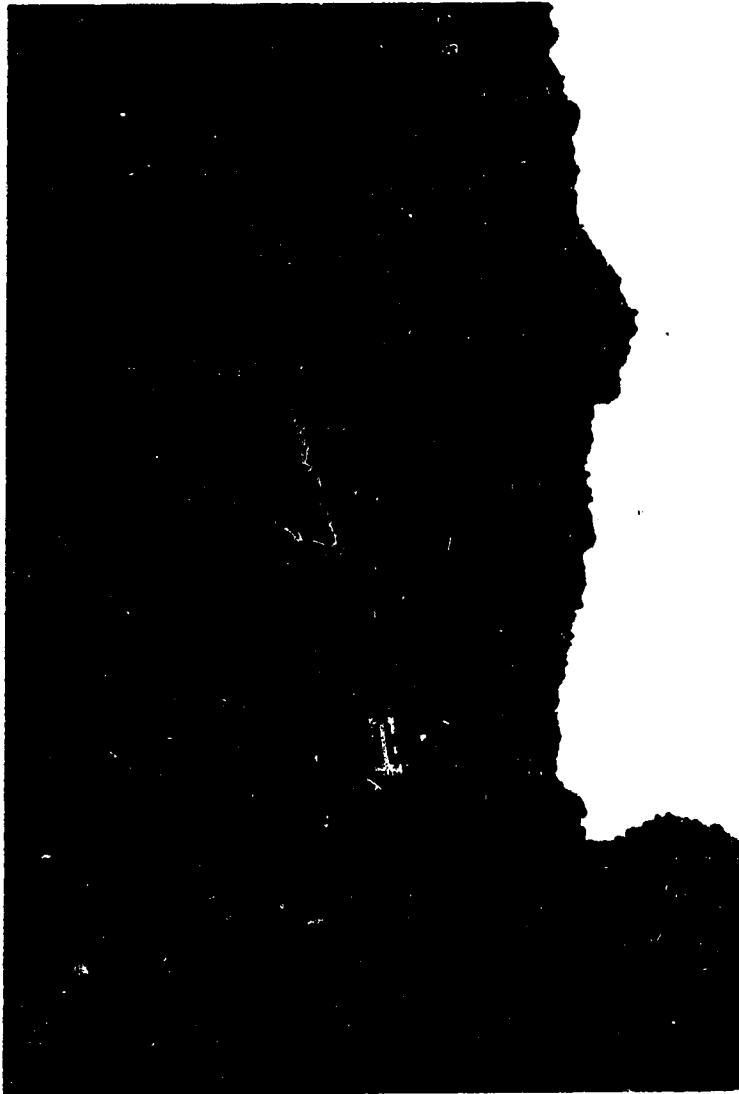


Plate 2: Flutings on the base of facies 1 in Unit C, eroded into gravels and sands of Unit A.
Orientation of the flutings was measured at 241° - 061° . Diamicton exposed is facies 1 at the base and grades into facies 2 higher.

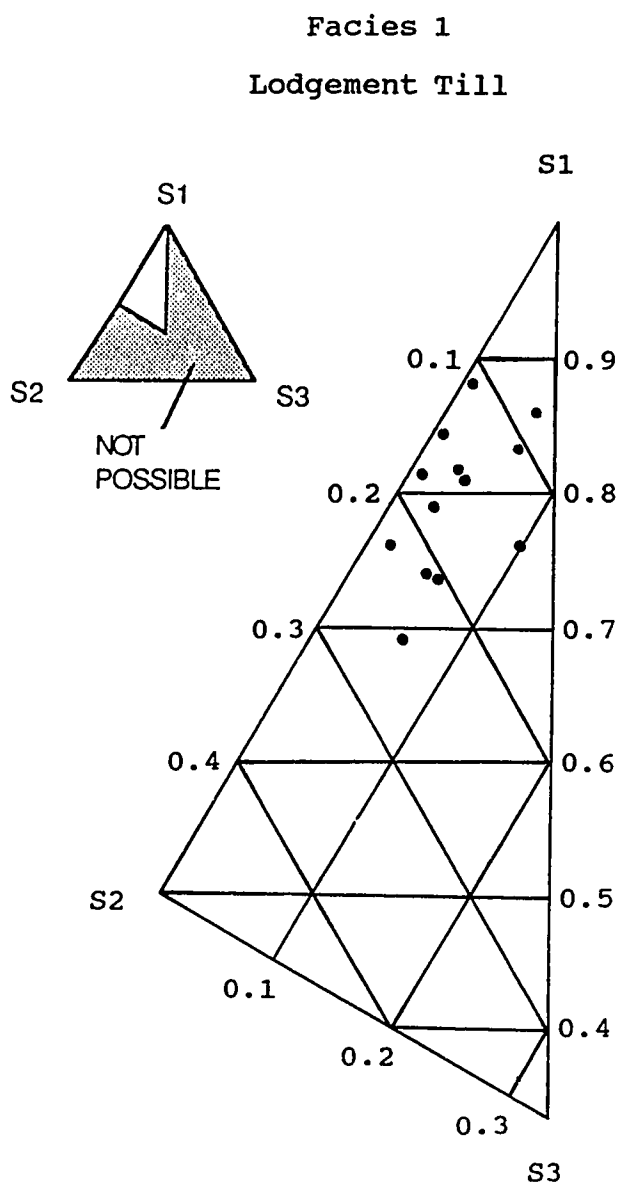


Figure 17: Ternary plot of primary, secondary and tertiary eigenvalues (S1, S2, and S3) from lodgement till fabrics.

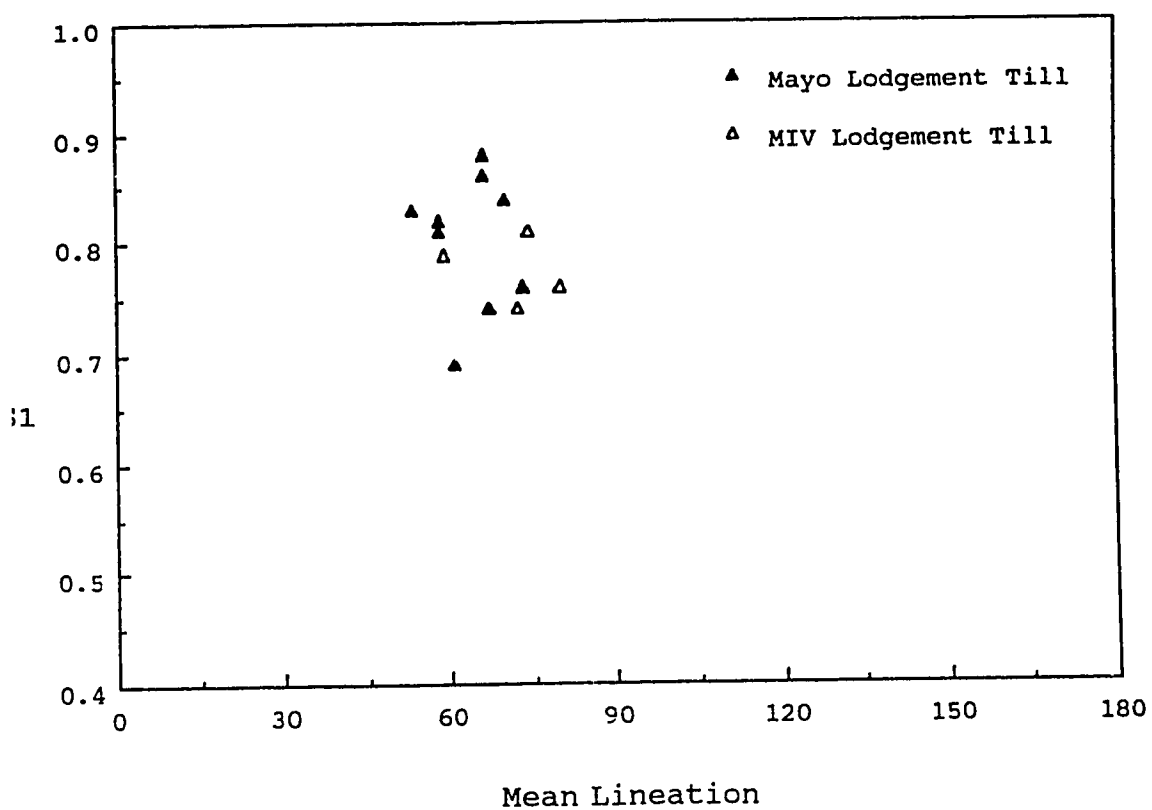


Figure 18: Primary eigenvectors (S1) plotted against the trend of the mean axis (mean lineation) of lodgement till fabrics.

The lodgement process is not continuous and the episodic nature allows erosion to occur within what is considered as one till and lenses of sorted sediment may form (Eyles et al. 1983; Dreimanis 1988). During stoppages in ice-flow, subglacial and englacial meltwaters pass through tunnels which develop and close rapidly within ice (Kruger 1979). Rapid constriction of passageways is typical owing to the internal plastic nature of the ice or reactivation of the glacier. Water contacting debris-rich ice eroded and transported sediment and redeposited it as sorted sediment lenses at the base of the ice on top of lodgement till. In the Mayo and MIV Sections these lenses are commonly stratified and have plano-convex shapes, the lower contact in underlying till sometimes being erosive. They frequently have sheared tops as a result of continued advance and deposition of the till (Shaw 1982; Levson and Rutter 1988). Differential compaction owing to post-depositional dewatering may cause silt and clay laminations to drape clasts in till (Muller 1983).

Lodgement tills have a fine sandy silt matrix (Appendix 2) and are characteristically thin and overconsolidated, properties which are derived from the process of deposition and the confining pressures of overlying ice (Kruger 1979; Dreimanis 1976). Abrasive particle interactions in debris-rich basal ice, eroding previously deposited sediment, bedrock, and clasts within the ice, promotes comminution of sediment (Elson 1961, 1988; Boulton 1975, 1978; Boulton and Eyles 1979) and production of fine-grained material for lodgement till. Haldorsen (1982) suggests that matrix grain size depends greatly upon the initial grain size characteristics of the original material.

Well developed subhorizontal partings, common to lodgement tills, form as small wedges of sediment are sheared under pressure and are later accentuated by expansion owing to pressure removal of overlying ice (Dreimanis 1976; Haldorsen 1982; Muller 1983). Slickensides may form on the individual wedges as they slide over one another during deposition. Joints develop perpendicular to the surface as pressure of overlying ice is released upon melting and differential upward expansion causes vertical cracking in the diamicton. Lithologically dissimilar intraclasts of soft sediment incorporated into lodgement till are sheared and smeared parallel to ice flow (Kruger 1979). Several crushed intraclasts can form shear bands which impart a crude stratification (Boulton 1976). Glaciotectonism associated with lodgement commonly distorts the underlying sediments (Kruger 1979). Folding and faulting are caused by pressures developed at the base of the ice (Boulton 1976).

Striated clasts are relatively rare in the Mayo region owing to the hardness of the regional bedrock. Most striated clasts in the Mayo region occur in this facies reflecting their transport in

basal ice. Clasts are striated as they are dragged across bedrock, by collisions with other clasts, and when they become lodged and are abraded by passing debris-rich ice. Embedded clasts occur when the tractive force of the ice is unable to overcome the substrate friction and the clasts become lodged (Boulton 1976, 1978; Kruger 1979; Shaw 1985). In the Mayo Section two bullet-shaped boulders have come to rest in an imbricate position with striations on the exposed long axis (stoss) surface. These clasts have a prow of sediment in the down-ice direction as they were dragged through underlying unconsolidated sediments. Rapidly buried clasts show little abrasive modification while low deposition rates allow clasts to become heavily abraded. Faceting results when a clast becomes lodged and overriding debris-rich ice abrades and smooths the exposed surface for a long period. Clasts do not survive long periods of basal zone transport before being abraded or deposited. Clasts which undergo long distance transport are rapidly moved to englacial positions and are not usually deposited by lodgement. Pebble lithologies are thus dominantly local in lodgement tills because of the rapid rate of abrasion (Dreimanis 1976). Strong unimodal clast fabrics reflect transport, orientation and deposition by glacial ice (Boulton 1976; Dreimanis 1976; Kruger 1979). Unimodal orientations are best developed in tills that have not undergone subsequent reworking by water or gravity.

The lower contact of lodgement tills are sharp and erosional reflecting the abrasive processes that occurred at the sole of the glacier. Flutings developed in the wake of embedded clasts are later infilled and appear as an inverted ridges on the base of the diamicton. In the Mayo Section flutings were oriented towards the southwest-northeast and indicate ice flow downvalley to the southwest. The embedded clasts reflect on the high pressure and shearing nature of the lodgement process. The sharp and distinct lower contact results from debris-rich basal ice eroding the unconsolidated gravel and sand (Unit A). Higher concentrations of clasts in the lodgement tills reflects local incorporation of clasts from this gravelly substrate.

Facies 2: Massive and layered diamicton with sorted sediment lenses.

Description

Massive and layered, olive to dark olive grey (5Y 5/4, 5/2, 4/3, 4/2 and 3/2 dry) diamicton is the most common diamicton in the Mayo region. It is the dominant diamicton present in the Mayo and MIV Sections and occurs only in Unit C. The layered nature and numerous lenses give it a stratified appearance, especially higher in the section. This deposit is less consolidated, less clast rich and has fewer striated clasts than facies 1. The silty sand matrix in

the basal regions coarsens upward into a fine and medium sand matrix. This diamicton has a maximum thickness of 8 metres in the Mayo Section and 2 metres in the MIV Section.

Horizontal layers are visible throughout this diamicton and represent tabular bodies in three dimensions (Plate 3). Lighter and darker layers are observable in the better exposed and dried exposures and reflect variations in matrix grain size, pebble content and mineralogic content. Light diamicton layers, up to 50 centimetres thick, are widely spaced throughout the dominant finer matrixed darker layers that are up to 2 metres thick. Layers are laterally continuous for hundreds of metres and have gradational, commonly interfingering, to distinct contacts. Occasional stone lines occurring at layer contacts are laterally continuous for up to 50 metres. A large bullet shaped boulder along an internal layer contact is embedded into and deforms the diamicton in the layer beneath it (Plate 4). A distinct sediment wedge infills a space on the stoss side of the boulder. Sand lenses and clasts in close proximity to the boulder are aligned parallel its surface.

Subhorizontal partings, spaced 0.5 to 5 centimetres apart, are better developed and closer spaced towards the base of the facies and enhance the stratified appearance. Partings may be open or can be filled with clay, silt or sand. They are commonly oxidized with the degree of oxidation decreasing upward. Very fine scale fissility, 0.1 to 1 centimetre apart, is developed locally. These frequently have silt particles along them and may have clay coatings. Vertical jointing is rare and relatively widely spaced, 5 to 10 centimetres apart.

Silt, sand and gravel lenses or stringers occur throughout facies 2, but are more abundant towards the top. Gravel lenses are 3 to 15 centimetres thick and laterally continuous for up to 5 metres. They consist of up to 70% small to large pebbles in a medium to coarse sand matrix. Horizontally stratified fine to medium sand lenses, 1 to 20 centimetres thick and 20 centimetres to 10 metres long, contain some folded or irregular laminations. Widely spaced silt lenses, 0.5 to 5 centimetres thick and continuous for up to 2 metres, are common toward the top of the unit. All lenses are planar, convex, plano-convex and most commonly biconvex. They may also be irregularly shaped. Wisps and stringers of fine sand and silt, continuous for up to 2 metres, are scattered throughout this facies.

Striated clasts are occasionally observed among the small pebbles to cobbles and rare boulders of this facies. Clasts, which comprise 5 to 40% of the diamicton, are more concentrated towards the base of the deposit but do not form clast clusters. They are

subrounded to rounded and rarely angular, and towards the base they are better rounded. Blade shaped clasts in the diamicton are common while those occurring in sediment lenses tend to be discose or bladed and better rounded. Clast rich areas containing 30% large pebbles and small cobbles are continuous for at least 10 metres in beds up to 25 centimetres thick. These clasts may have one or two grain thick sand and silt shadows, some of which are oxidized. Rare, undistorted clasts of friable sediment are present. These may be angular and sometimes retain their original sedimentary structures.

The lower contact of the facies is usually distinct when overlying the sand and gravel of Unit A. Clast concentrations in the basal regions are commonly found over sharp and planar contacts. Inclined stringers of clasts sometimes extend up to 5 metres from the underlying gravel into the diamicton. The lower contact is commonly gradational over 5 to 10 centimetres when overlying facies 1. Darker, angular inclusions of facies 1 diamicton are incorporated into this facies and lie subhorizontally near the base. They are 1 to 2 centimetres thick and 30 to 40 centimetres wide, are smeared and distorted, and usually dip at shallow angles upvalley. Where these inclusions are present the lower contact is clear and sharp. Flame structures are sometimes present when overlying facies 3 (Massive and stratified diamicton interbedded with sand and gravel). The upper contact of facies 2 commonly interfingers or is gradational into facies 3 and is difficult to define accurately. The upper zone of this facies is frequently interbedded with the overlying gravel, sand and silt deposits.

The fourteen pebble fabrics from this facies have well developed a-axis orientations (Appendix 1A) suggesting flow toward the west-southwest to southwest parallel to the valley. The mean eigenvector (V1) for the 14 samples was 062°, ranging from 048° to 095° with one reading of 013°. The dip angles average 14° and range from 09° to 23°. The primary eigenvalue (S1) averages 0.77 and ranges from 0.66 to 0.90 (Figure 19). Mean axis versus primary eigenvalue plots of facies 2 diamicton fabrics (Figure 20) illustrate relatively high eigenvalues and a slightly more diverse mean trend of the mean axis than for facies 1.

Situated 490 metres from the upstream end of the Mayo Section is a large deposit of well bedded sand and gravel located within facies 2 (Figure 21). It has an irregular concave base and a smooth convex top. Sand occupies the northern side of the lense and coarsens upward from predominantly fine grained at the base into a mix of fine to coarse sand. The finer sand is horizontally bedded or planar cross-stratified. Medium and coarse sand beds tend to have more erosional-stoss climbing ripples (ESCR; Type A of Harms et al. 1982) than depositional-stoss climbing ripples (DSCR; Type B of Harms et al. 1982). Rarely, transitional sigmoidal stoss and

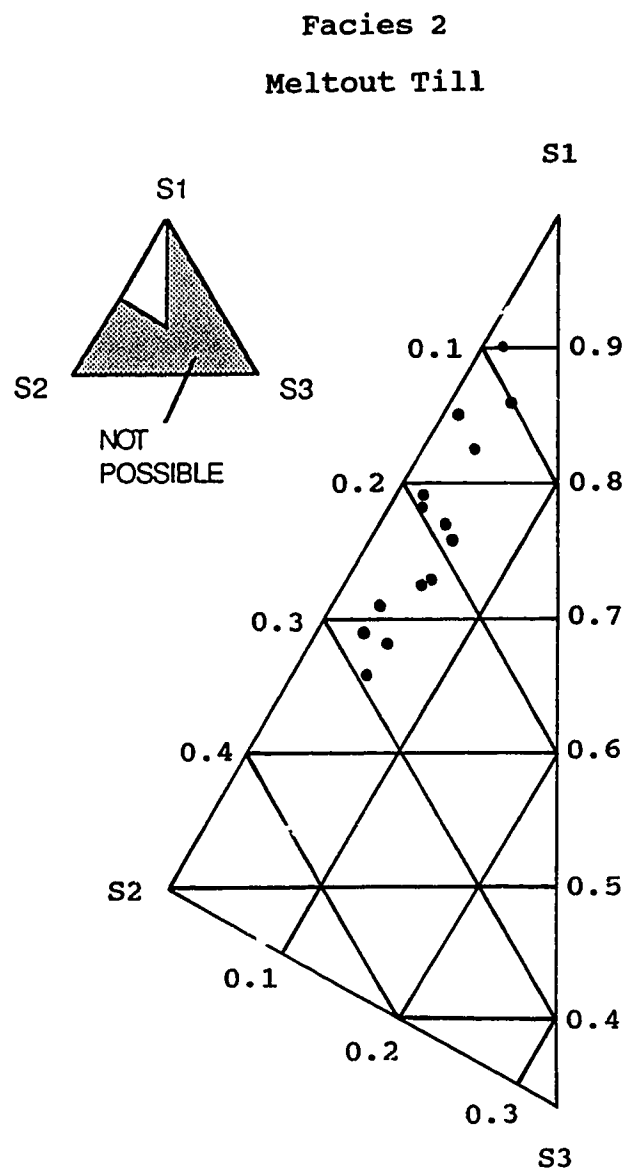


Figure 19: Ternary plot of primary, secondary and tertiary eigenvalues (S1, S2, and S3) from meltout till fabrics.

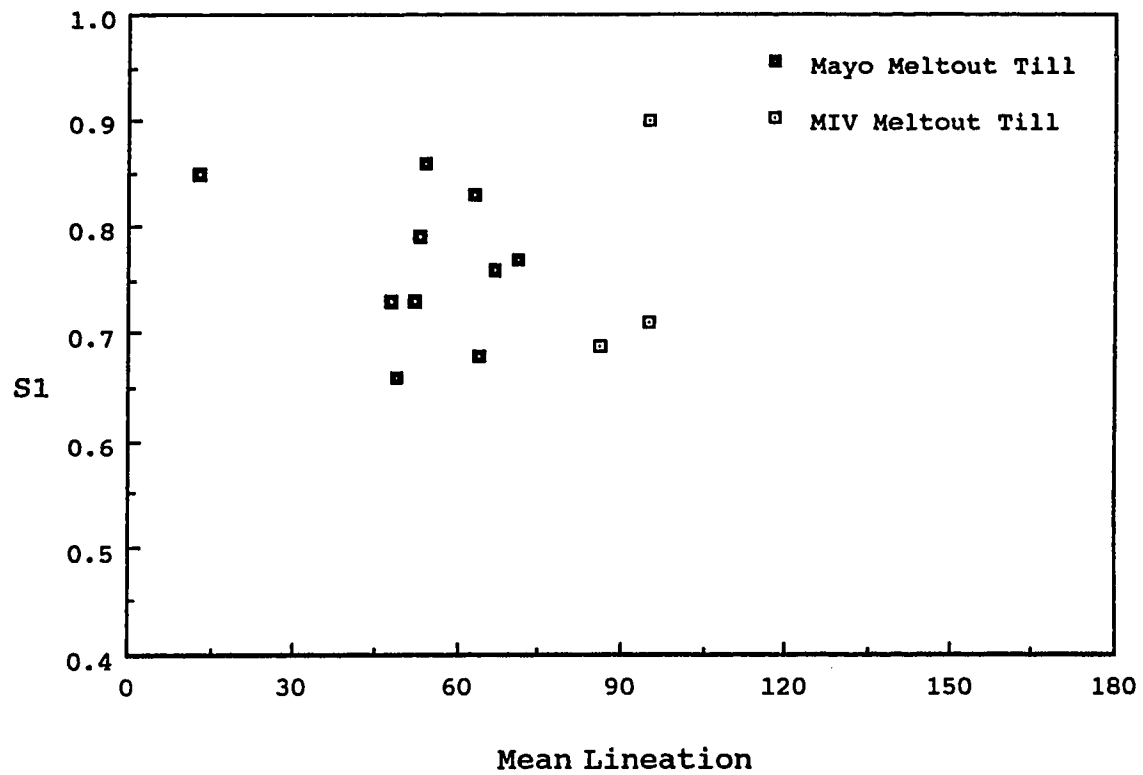


Figure 20: Primary eigenvectors (S1) plotted against the trend of the mean axis (mean lineation) of meltout till fabrics.

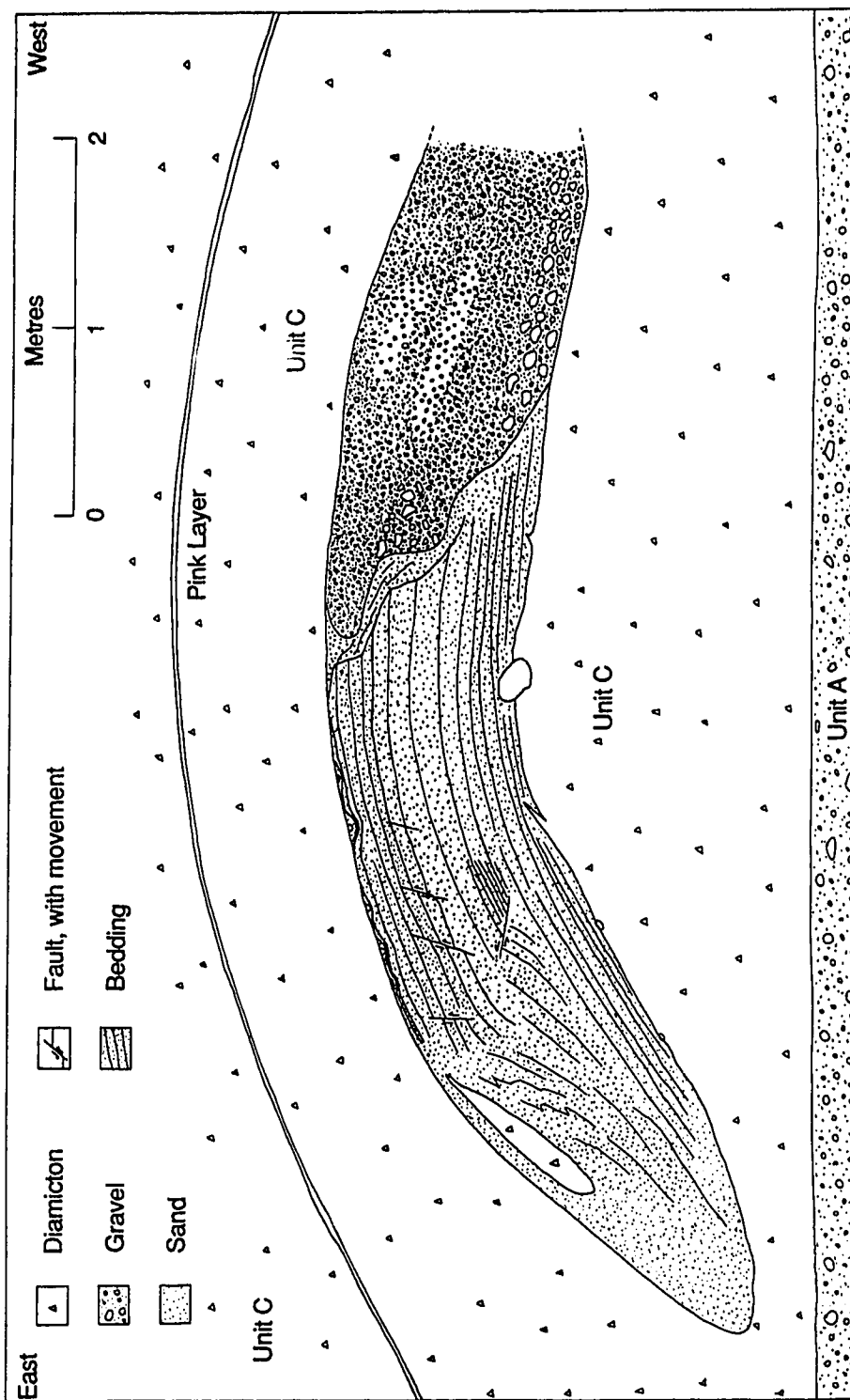


Figure 21: Cross-section of the englacial tunnel located near the base of Unit C at 490 metres in the Mayo Section. Folding and faulting in the sand are common. Note the stratification in the sand at the top of the lense paralleling the form of the clasts held within till of Unit C.

leeside climbing ripples are preserved. Paleocurrent measurements on beds and ripples indicate flow toward the west and northwest (279 to 330°). Sand foresets have dips usually between 10° and 20° but many also that measure as high as 30° to 35°. Small, 1 to 2 centimetres thick and 10 to 40 centimetres wide, beds of small pebbly granular gravel are common in the upper half of the sand and possess clear, well defined basal contacts that sometimes crosscut bedding. The lenses fine upwards from a discontinuous one pebble thick lag to a granule and sand cap. Structurally the sand is complexly faulted, folded and distorted. Some beds are vertical and others are offset vertically downwards. Small scale normal faults have displacements of 2 to 6 centimetres and reverse faults have displacements of 2 to 12 centimetres. Folding is common and highly distorted, convoluted and rare overturned beds are present. The basal contact of the sand is clear but irregular and generally concave. Numerous clasts from the underlying diamicton protrude up into the sand. The upper contact of the lense is sharp and convex. In places, clasts held in the overlying diamicton project into the sand below (Plate 5). Shallow scours in the sand beds conform to the clast shape for up to 3 centimetres below the clast. Sand beds infilling the scours also mirror the shape of the clasts.

Gravel occupies the downstream (southern) half of the lense and has irregular and clear lower contacts over diamicton. They have irregular and transitional to clear and erosive contacts over sand and commonly distort bedding in the sand. The basal 20 centimetres of the gravel consists of 60 to 70% large pebbles with a fine to medium sandy matrix which fines upward into 10 to 20 centimetres of small to medium pebble openwork gravel. Overlying this is 50 centimetres of mixed clast supported and openwork small and medium pebble gravel with rare lenses of cobbles and large pebbles. Bedding throughout the gravel is crudely horizontal or dips at low angles to the northwest (316° to 320°). Cobbles and large pebbles form clast clusters with a poorly sorted sand matrix. Small sand shadows in the lee of clast clusters indicate northwesterly flow.

Diamicton is also found in the lense, near the base and close to the top. The lower diamictons are intermixed with sand and have tendrils extending into the diamicton below. The upper diamicton lense (Plate 6), which is 15 centimetres thick and over one metre long, parallels the sand bedding and geometry of the upper contact. It consists of 15% small to medium pebbles in a massive fine sand and silt matrix.

A pinkish layer, 3 centimetres thick at its maximum, is present in the diamicton approximately one metre above the large sand and gravel lense (Figure 21). This layer generally parallels the geometry of the upper surface of the lense and is laterally continuous for at least 10

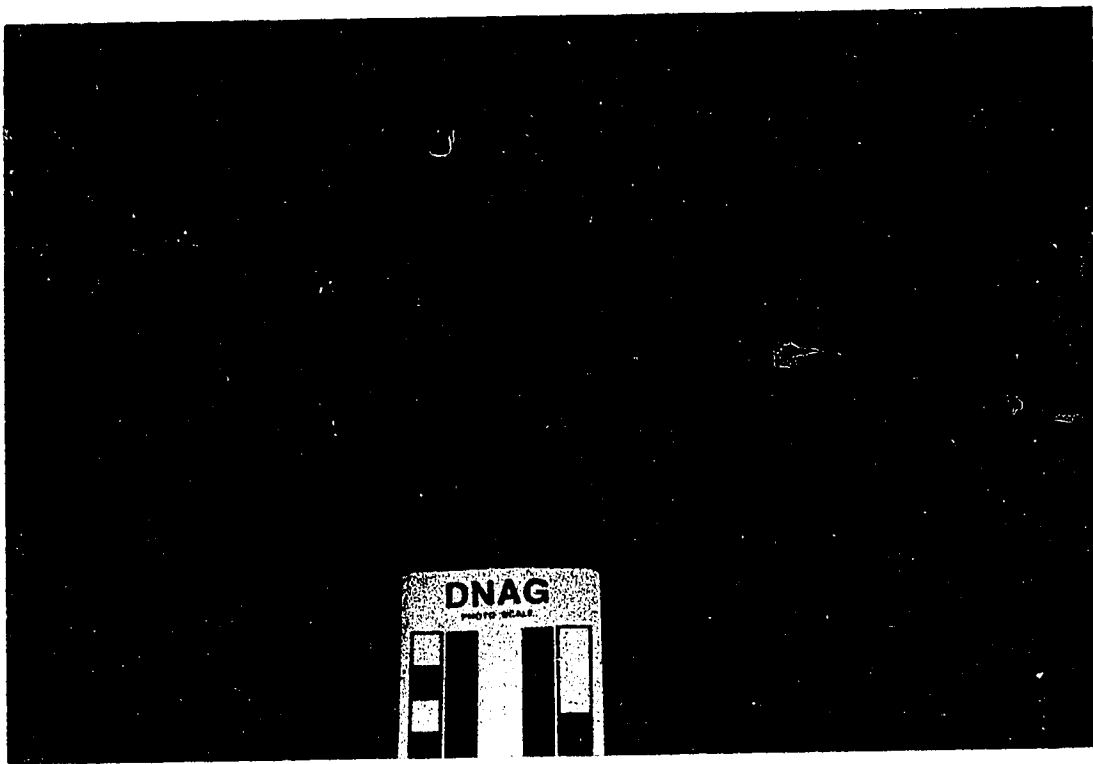


Plate 5: Pebbles within facies 2 diamicton project down into the large sand and gravel lense. Beds underneath the pebbles are deformed for about 2 centimetres, forming shallow scours as a result of increased turbulent flow in the constricted tunnel space.

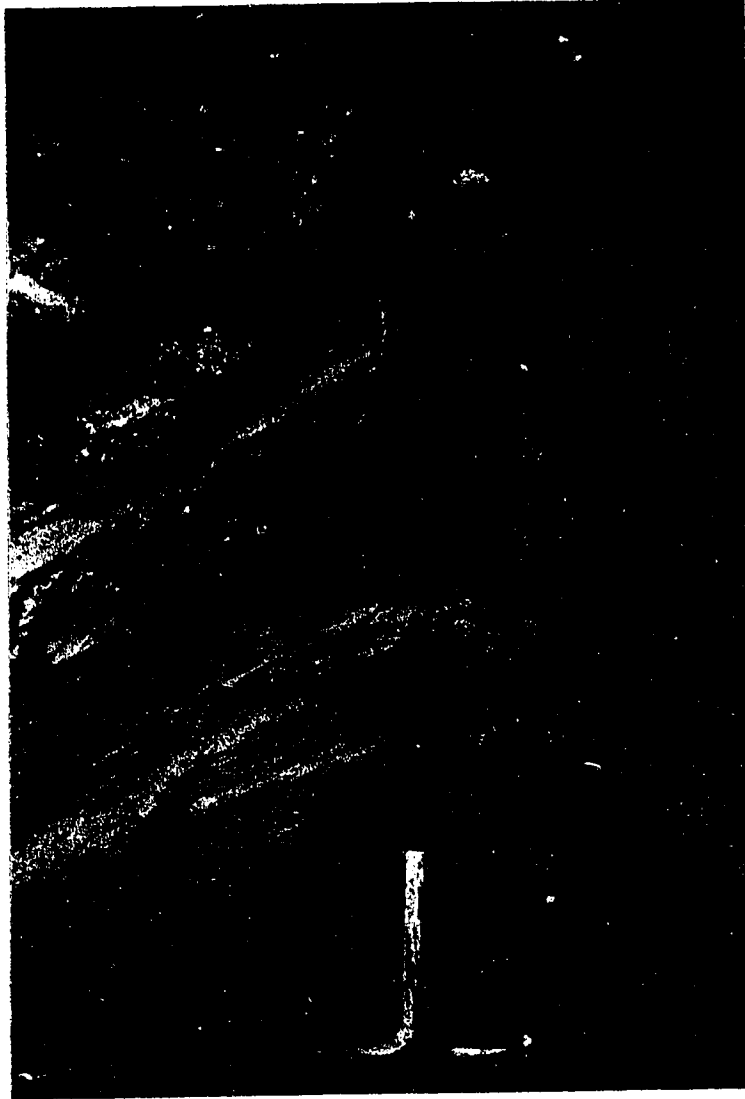


Plate 6: Diamicton lense within the large sand and gravel lense. Diamicton exposed above and below the sands is of facies 2. Diamicton lense parallels the bedding in the lense and the tunnel roof. Pick is 75 centimetres long.

metres either side of the lense. The pink-purple color is only well developed on the weathered external surface of the diamicton. Internally it is a grey-pink color. Some of the fine-grained argillite clasts in the layer are also a pink-purple color. During hydrometer analysis pink sediment of fine clay size separated out indicating that the pink material is a fine-grained component of the total layer.

Interpretation

Facies 2 diamicton is interpreted to be a meltout till based on its massive and layered appearance, dense nature, abundant lenses of sorted sediment, the presence of striated clasts and strong unimodal pebble fabrics. Meltout till is defined as "till deposited by a slow release of glacial debris from ice that is not sliding or deforming internally" (Dreimanis 1988). The genesis and properties of meltout tills have been well documented (Boulton 1968, 1970a and b, 1972, 1976; Dreimanis 1976, 1988; Shaw 1977, 1979, 1982, 1983, 1985, 1987, 1988; Eyles 1979; Lawson 1979a and b, 1981a and b; Haldorsen 1984, 1982; Haldorsen and Shaw 1982; Eyles et al. 1983).

Meltout tills form in the accumulation zone beneath thick temperate glaciers where there is basal stagnation and localized pressure melting occurring in debris-rich subglacial ice (Boulton 1970a; Haldorsen 1982) or from buried debris-rich basal ice remnants in ice stagnation deposits (Haldorsen 1982). Ablation of ice is concentrated at the upper and lower surfaces of debris rich ice masses. Meltout tills tend to be tabular deposits resulting from massive ice block stagnation and can be of variable thickness depending on debris content and ice thickness. Melting of ice under confining conditions results in restricted movement of sediment permitting the meltout till to retain some of the englacial features of the debris-rich ice from which it is derived (Lawson 1979a; Shaw 1985; Dreimanis 1988). Basally transported and deposited meltout tills are massive and occur stratigraphically lower in section (Shaw 1977). Englacially transported and basally deposited meltout tills tend to have more abundant sediment lenses in the diamicton giving them a more stratified appearance. Meltout tills, confined by the weight of overlying ice and debris, are relatively compact and cohesive, although not as dense as lodgement tills which have additional movement-induced compaction.

The layers in meltout tills in the Mayo Section may be indicative of different transport zones, debris banding in the ice or varying debris sources or the reactivation of ice (Lawson 1979a; Dreimanis 1988; Levson and Rutter 1988). Sediments carried in basal transport zones will tend to be more abraded and have a higher concentration of fines (Dreimanis 1988).

Sediment rich and poor bands existing in the ice may be deposited intact as layers (Lawson 1981a). If debris was derived from a specific source and remained coherent during transport and deposition it may form a distinct layer in the deposit. Ice reactivation may occur after a period of ablation and deposition of basal meltout till. This creates an erosional surface and the tills deposited may be different in texture, color and clast content. Some layer contacts are marked by stone lines or clast pavements representing flushing at the base of the ice which can remove finer sediment. The basal contact of layers sometimes represent surfaces upon which lodgement and erosion has been active. Reactivation has formed localized lodgement tills which are indicated by embedded boulders (isolated clast pavements) and furrows (Plate 4). These boulders are commonly flat-iron shaped reflecting their transport in the debris-rich basal zone. Deformation of the underlying diamicton is a result of the clast being dragged through it.

The stratified appearance of the meltout tills is enhanced by subhorizontal partings. Partings reflect the unloading of the deposit after the weight of overlying ice is removed by melting. These are variable in development, at the base of the facies the basal meltout tills having stronger partings than the upper, less constricted englacially deposited meltout till. The matrix is slightly coarser than lodgement till (Facies 1; Appendix 2) and suggests decreased debris comminution occurred during transport and deposition and increased removal of fines by percolating waters during meltdown (Lawson 1979a; Dreimanis 1988).

Lenses of sorted sediment are representative of meltwater reworking sediment within the ice mass. Water from melting of glacial ice initially flows along ice crystal boundaries and clast-ice crystal contacts. The dendritic pattern of flow enlarges these pathways leading to development of substantial cavities in the ice. Prolonged tunnel use causes vertical and horizontal erosion owing to the thermal energy and abrasive nature of sediment-laden waters. Constriction or closure of passageways, the result of decreasing meltwater discharge or internal ice deformation, occurs relatively quickly (Haldorsen and Shaw 1982). Isolated sediment accumulations are deposited in the tunnels and appear as in situ lenses surrounded by unworked meltout till. Lenses with convex bases result when water moving along the ice-substrate boundary incises small troughs into the substrate. Biconvex lenses, the most common type in the sections, form when one of these tunnels infills with sediment and maintains its shape during subsequent melting. Planar based lenses form englacially from initially circular tunnels that, as supporting ice is removed, settle differentially onto the substrate and lose the basal trough shape. As there is greater thickness of sediment in the initial trough-shaped centre of the lense a convex upper surface may develop. As debris laden ice melts significant distortion can occur producing irregular shaped lenses (Elson 1961; Lawson 1979a,

1981a; Haldorsen and Shaw 1982; Dreimanis 1988). Debris-poor layers may become better sorted owing to increased meltwater activity and appear as thin wispy laminae of sand and silt (Dreimanis 1976).

Clasts in this facies in the sections are rarely striated because of their lithologic hardness and the decreased abrasion of debris carried above the basal region. Clast shapes in the sediment lenses and diamictons reflect their different transport mechanisms. Glacially transported clasts tend to retain their angularity and bladed shape, whereas pebbles carried by water are frequently better rounded as a result of more abrasive transport. Sand and silt shadows around clasts represent the increased flushing that occurs around clasts during meltout. Friable clasts of sediment, incorporated when frozen, that are not crushed or smeared are suggestive of passive deposition (Boulton 1976; Shaw 1982, 1985). Preservation of angularity and the original internal sedimentary structure in some of these friable clasts is common in the meltout tills in the Mayo region. These features preclude lodgement, which by its dynamic and abrasive plastering-on process would smear and destroy the friable clasts (Shaw 1985).

The lower contact is usually gradational with the underlying lodgement till and appears to be a continuum in deposition from active to stagnant ice retaining englacial features owing to the passive deposition by meltout. Inclusions of lodgement till in the meltout till are blocks incorporated during ice movement and erosion but not deposited until ice movement stopped. The sharp planar contacts, solemarks, and other submill deformations between the gravel and meltout till in the Mayo Section were formed through erosion by active ice. Flutings formed by the lodgement process are preserved beneath stagnant ice and subsequently infilled by debris released from passive meltout. Occasional stringers of gravel extending upwards into the meltout till are sediment rafts incorporated during compressive flow as active ice overrode lodged ice masses. Fingers or flames of facies 3 projecting into this facies represent loading by the ice during deposition.

The large sand and gravel lense located within meltout till in the Mayo Section is an englacial tunnel deposit that was located near the base of the glacier and was completely enclosed in debris-rich ice (Figure 21). The concave base and convex top of the lense, internal structures, protruding clasts and position within meltout till all support this interpretation. Tunnel deposits which occur within lodgement tills have truncated, flat tops (Eyles et al. 1982), while those associated with meltout tills have sharp, convex upper surfaces (Haldorsen and Shaw 1982; Shaw 1982, 1985). Subglacial tunnels have solid bases and settling of debris during

meltout affects only the edges of the deposit. Internal folding and faulting is caused by instability at the base of the englacial tunnel as it settles during meltout, and the core as well as the margins will settle and be disturbed (Boulton 1972; Shaw 1982). During use the tunnel was probably ovoid but the resulting deposit is concavo-convex. Sediments at the base of the tunnel underwent relatively little deformation during settling because the zone underneath them was debris-rich and little ice was removed. Sediments higher in the lense settle further and are progressively more deformed. Normal (extensional) faulting visible throughout the deposit is more intense towards the edges indicating increased settling. Beds originally horizontally deposited are folded and faulted and some have become almost vertical. The reddish purple layer in the meltout till above the tunnel represents an englacial debris band. It was deposited from stagnant ice onto the underlying topography and reflects the irregular thickening over the tunnel sediments.

The tunnel deposit exhibits horizontal beds, cross-beds and cross-laminations. Diamicton lenses within the sand were deposited by spalling of frozen debris from the wall or the roof into the tunnel (Plate 6). These lenses indicate that the top of the tunnel was still within the debris-rich basal zone of the glacier. Clasts occurring at the interface between the top of the tunnel and the surrounding ice produce scours in the tunnel deposits (Plate 5). Clasts are held within overlying ice and project into the tunnel (similar to type 2 boulder scours of Shaw 1983). Water flowing past this constriction will increase in velocity and turbulence, creating local erosion around and below the obstruction (Shaw 1983). Bedding in tunnel sand surrounding the pebble exhibit truncation of original strata and subsequent deposits are conformable to the scour base and clast surface. Stratification is convex down around the clast and forms a broad bowl-shaped depression. A large clast protrudes from the till up into the sand and suggests that underlying debris-rich ice held the boulder in place while meltwaters incised into the ice.

Pebble fabrics in meltout tills tend to have strong preferred orientations consistently parallel to ice flow (Dreimanis 1983). Release of debris from ice is passive and generally preserves the englacial orientation of the clasts. Meltout till fabric orientation varies between the Mayo and MIV Sections. In the Mayo Section the average mean lineation was 054°, in comparison, the MIV Section average mean lineation was 092°. Differences in the fabric orientations between the sections reflect changes in flow by the ice mass and variations in topography. The valley thalweg lies between the two sections as suggested by the dip of respective diamicton bodies. The valley walls are oriented parallel to 060° to 070° opposite the Mayo Section and 050° to 060° near the MIV Section. The Mayo tills were deposited on a relatively low gravelly terrace by ice near the valley centre and indicate more closely the actual

flow direction of the ice mass. Ice moving over the MIV Section is topographically higher and less confined by the river channel. It may also be a reflection of when the ice was at its maximum and would be able to override basal topography and flow parallel to the valley sides.

Facies 3: Massive and stratified diamicton interbedded with sand and gravel.

This facies consists of three types of diamictons interbedded with varying amounts of sorted sediments. Subfacies 3A, a rare deposit, consists primarily of isolated clasts or massive diamicton. Subfacies 3B is the most abundant and is composed of diamicton interbedded with large quantities of sand and gravel. Subfacies 3C has a significant quantity of sorted sediments in massive diamicton but is rarely present.

Subfacies 3A: Isolated clasts and massive diamicton lenses.

Description

Isolated clasts and small beds of diamicton are infrequently observed within the sand of Unit D. Clasts are subangular to rounded, small to large pebbles with rare cobbles. Diamicton lenses are irregular to flat plano-convex shaped and range in width from 20 centimetres to 2 metres. Both clasts and diamictons pierce the sediments below them and are draped by stratified sediments (Plate 7). The clasts are beyond the competence level of the currents which deposited the enclosing sediments. These deposits are located well above the diamicton unit (Unit C) and are not associated with it.

Interpretation

These sediments are interpreted to be subaqueously deposited ice-rafted dropstone and dump diamictons (Thomas and Connell 1985) primarily because of the isolated nature of these deposits. Dropstones are a result of vertical deposition of individual clasts from floating icebergs. Clast sizes range from sand grains to boulders, while the materials may be rock or soft sediments (till pellets of Owenshine 1970; till clots of Edwards 1986). Piercement structures under the clasts are the result of their impacting and penetrating the soft sediment. Symmetrical draping of sediment on top produces a low mound centred on the dropstone.

Dumping occurs when sediment-laden icebergs break up or overturn and debris is deposited chaotically on the bed as massive diamicton mounds, sometimes called bergmounds

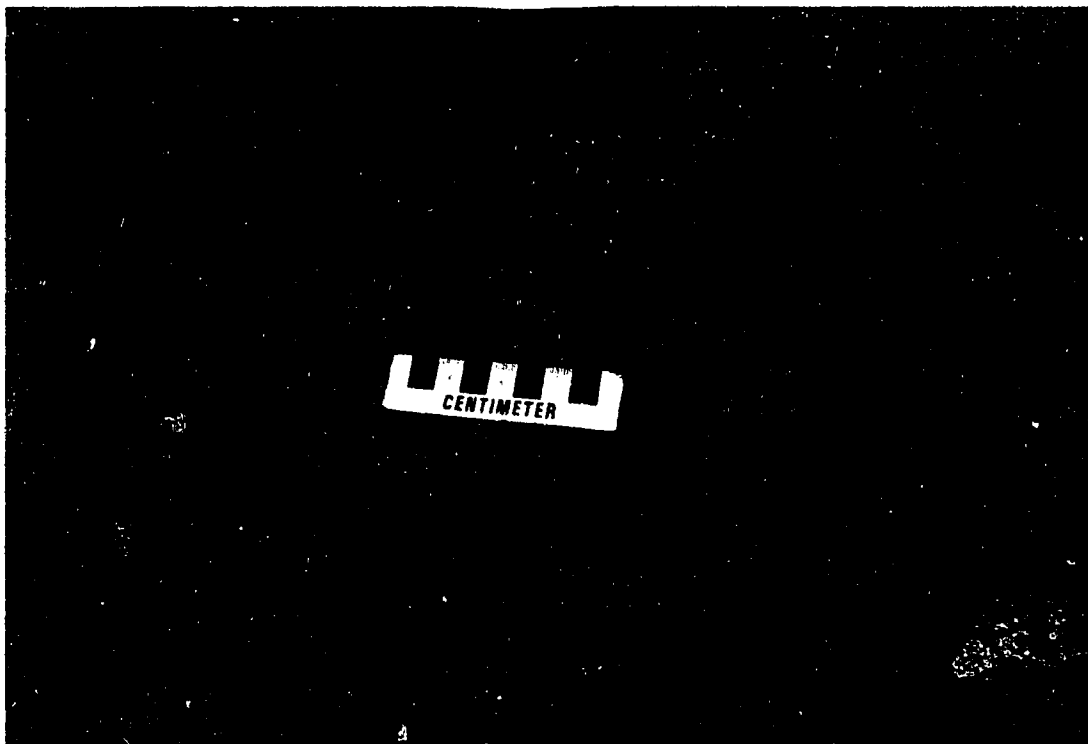


Plate 7: Isolated clast with drape structure, pierces and disrupts underlying beds.

(Fecht and Tallman 1977). The basal clasts, similar to individual dropstones, frequently pierce and buckle the underlying sediment. Subsequent rhythmic sedimentation emplaces symmetrical drapes which mirror the form of the underlying dump mound (Thomas and Connell 1985).

Subfacies 3B: Massive or stratified diamicton interbedded with sand and gravel.

Description

This subfacies consists of interbedded diamicton, sand and gravel. It is highly variable in texture, structure, morphology and location. It occurs as discontinuous beds with complex to distinct lower contacts and gradational or interbedded upper contacts. The diamictons are usually 10 centimetres to 1 metre thick with a maximum thickness of 10 metres. Internally the deposits consist of thin beds of diamicton, 2 to 50 centimetres thick, with intercalated sorted sediment beds. The number and thickness of sorted interbeds increases upward through thicker diamicton deposits. Thinner deposits of this subfacies are less stratified and have less internal variation.

Matrix-supported diamicton dominates these deposits with the matrix varying from sandy-silt to fine and medium sand. The diamictons are dark olive grey to olive grey (5Y 3/2 to 4/2 dry), dark greyish brown to dark olive brown (2.5Y 4/2 to 4/4 dry) and brown yellow (10Y 6/6 dry). The color varies with exposure and oxidation. Color and grain size are at least partially related, the lighter diamictons tending to be coarser. There are 5 to 30% small to medium pebbles with rare cobbles and boulders that are subangular to rounded, mostly subrounded, of mixed grain shapes, and very rarely striated. Rare wood pieces are found near the base of the beds, usually small twigs which are poorly to moderately preserved.

Generally, 10 to 30% of the deposits volume is composed of clean well sorted gravel, sand, silt, and clay beds and lenses, although locally this may be up to 60%. These interbeds give the unit a stratified appearance (Plate 8). Gravel beds are usually poorly sorted, matrix and clast supported, and consist of small to large pebbles with some cobbles within a fine to medium sand matrix. Fining upward, massive and crudely stratified deposits dominate, but there are also inversely graded planar cross-stratified and massive beds. Gravel bed lower contacts can be either distinct or gradational, and may be loaded onto sand forming balls or pillows of pebbles. Very fine to coarse sand beds, 10 to 100 centimetres thick and extending laterally for 1 to 20



Plate 8: Thin beds of well sorted sand give this subfacies 3B diamicton a stratified appearance.
This structure is located around 420 metres in the Mayo Indian Village Section.

metres, are usually horizontally stratified or planar cross-bedded and rarely massive. Individual beds are 0.5 to 20 centimetres thick and may be continuous up to 10 metres laterally. Small gravel and diamicton lenses occur in the sand and isolated clasts are present sporadically.

Thin, convexo-planar gravel lenses with poorly sorted granules to medium pebbles in a fine sandy matrix are common. Small sand lenses, 0.5 to 10 centimetres thick by 10 centimetres to 3 metres wide, are weakly horizontally laminated or bedded. These lenses are convexo-planar or irregularly shaped and commonly are folded, squeezed, and distorted. Lower contacts of the gravel and sand lenses are distinct and upper contacts are commonly eroded by overlying deposits. Thin stringers of sand, silt, and clay, 0.1 to 0.5 centimetres thick and traceable for up to 1 metre, have clear to indistinct irregular contacts.

Subhorizontal partings are found in some of the diamictons, ranging from 0.2 to 5 centimetres apart, and can be crudely to well developed. They are best exposed in thicker beds which have been weathered but commonly indistinct in recently exposed deposits. The diamicton breaks into small blocks along moderately developed subvertical to vertical jointings and subhorizontal partings. Oxidation is common along partings but less so in the vertical joints.

Lower contacts are both distinct and gradational, and may be complexly interbedded with the underlying deposits. Iron stained upper and lower contacts are frequent. Load structures at basal contacts, where slabs of diamicton settle into underlying deposits are common. Some diamicton lenses have been injected down into the underlying sand. Where sand and gravel are loaded onto their upper surfaces squeeze up or injection structures occur. Folding and faulting which disrupt bedding are best exposed at the contacts between sand, gravel and diamictons. Sediments are also internally convoluted, folded and faulted by post-depositional soft-sediment deformation.

One diamicton layer consists of beds of diamicton, sand, and sand, silt, and clay (Plate 9, Figure 22). Stratification is generally parallel to the base, but at the margins they are folded up and back on each other. Bedding is accentuated by color variations from dark brown silt to light brown sand. Inclusions of sandy-silt diamicton are common and are preserved as angular blocks. Three distinct diamicton flows are preserved, to the left, a lower well stratified flow and an upper more massive bed, and to the right a massive deposit occurs. The lower flow thickens to the east and pinches up and out to the west and its eastern margin is convoluted. The upper bed also pinches out to the west and has a broadly folded margin with massive diamicton to the east. The diamicton to the right is massive, overlies the lower bed and abuts the upper bed.

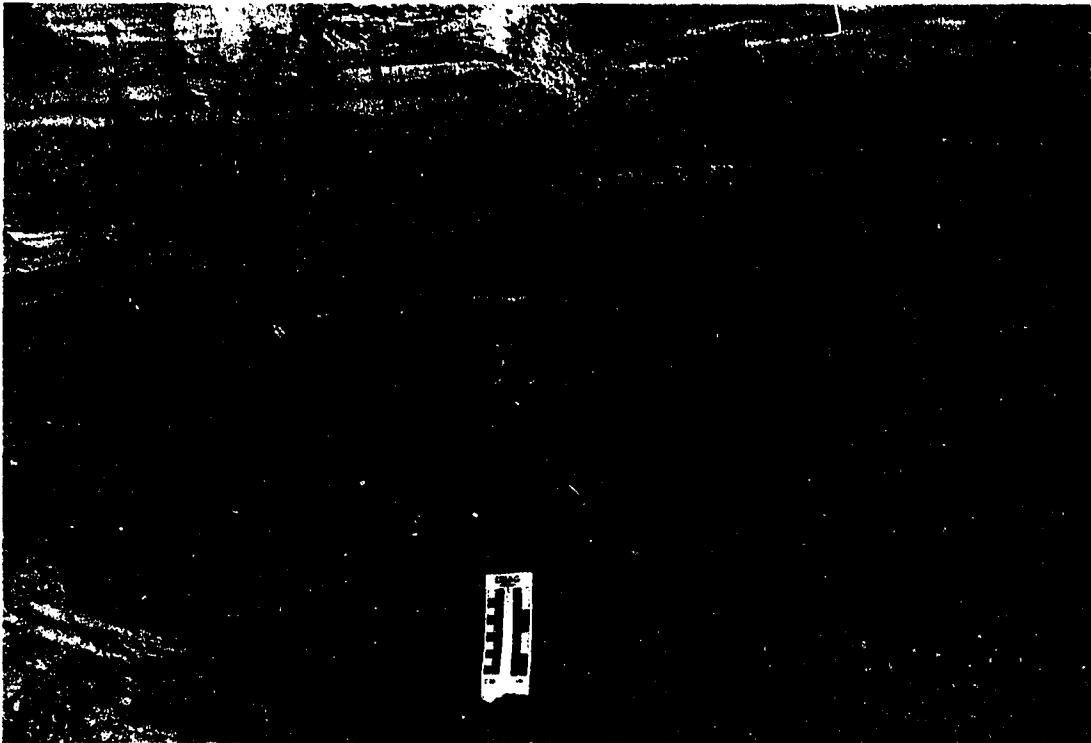


Plate 9: Photograph illustrating the possible flow stratification in a debris flow diamicton. Strata are defined by color, pebble content. Figure 22 is a diagram of this same feature.

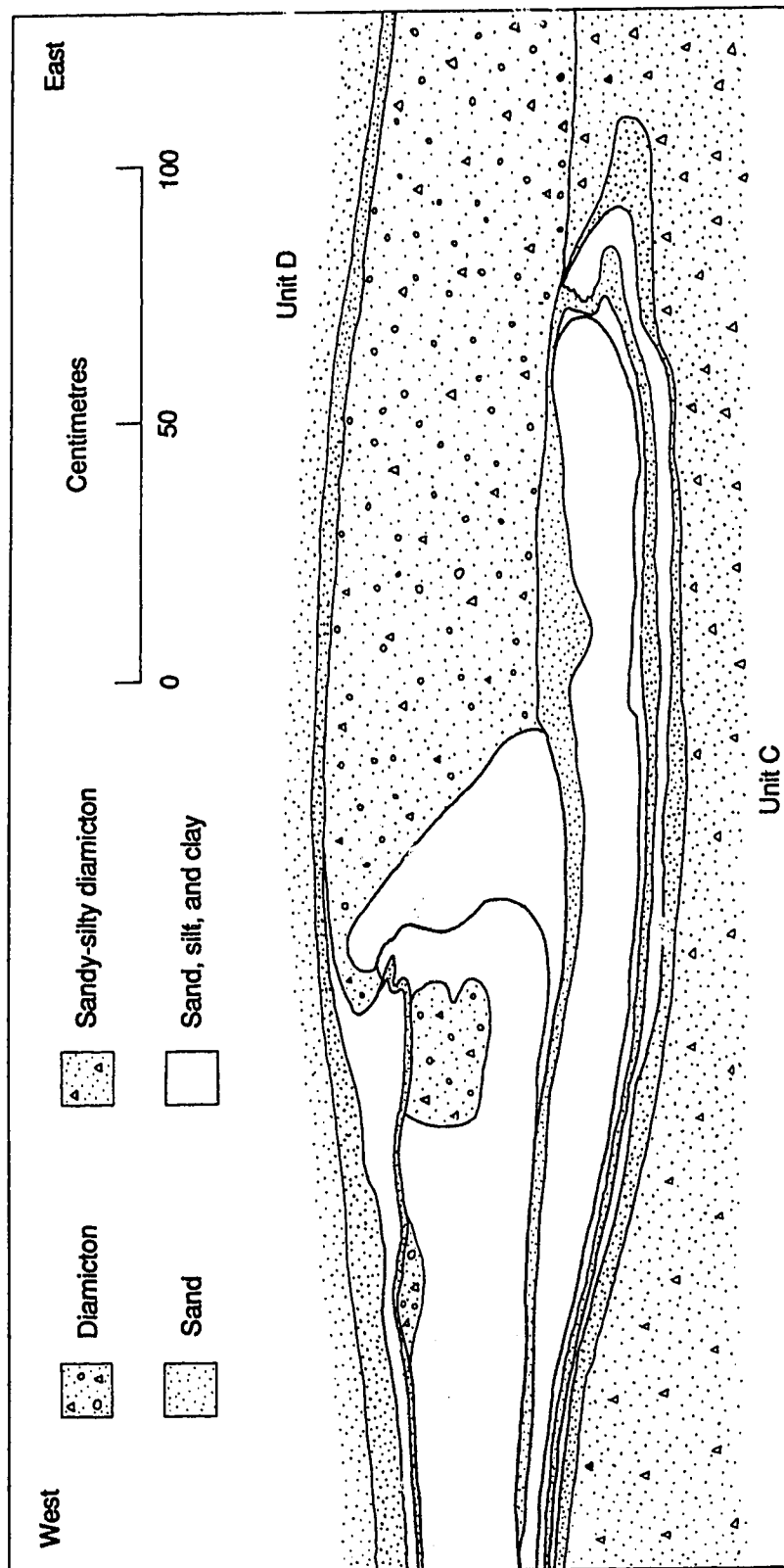


Figure 22: Schematic cross-section through diamicton flows. These may be noses or margins of a debris flow. Plate 9 is a photograph of the left half of this diagram.

Fabrics in this subfacies have highly variable primary eigenvalues and diverse orientations (Figures 23 and 24; Appendix 1). Primary eigenvalues from this subfacies average 0.65 and range from 0.49 to 0.85. Three fabrics were completed on subfacies 3B in the MIV Section and these indicate a preferred orientation toward the east (reverse of updip direction of 277°). Fabrics I-45 and I-46 are suggestive of flows originating from the valley walls and moving toward the valley centre. Fabric I-44 was taken in a confined channel and indicates flow along the base of the channel was towards the east (113°). A fabric in the lower diamicton at the Third Section has an orientation parallel to the valley (reverse of 065°). The upper diamicton in the Third Section has 8 fabrics with flow orientations toward the east (233° to 291°) and two with orientations toward the west (106° and 116°).

Interpretation

Sediments of subfacies 3B are interpreted to be sediment gravity flow deposits on the basis of the internal stratification, the number of sorted sediment lenses, the poorly consolidated nature and their proximity to lodgement and meltout tills. This subfacies occurs under and on top of lodgement till, meltout till and colluvium (Subfacies 3C). Sediment gravity flows are gravity driven flows of water and sediment controlled by water content, slope and velocity (Lawson 1982, 1988), and range from massive and poorly sorted to well sorted and stratified (Lowe 1982). Sediment gravity flows have been intensely studied and have been classified by the nature of the dominant sediment support mechanism and rheology (Middleton and Hampton 1973, 1976; Lowe 1979; Nardin et al 1979). Five flow types are defined: turbidity currents, fluidized flow, liquefied flow, grain flow and debris flow (Lowe 1979). These range from sediment support through fluid turbulence in the turbidity current to matrix support in a debris flow.

Flows initiate when water content increases as buried ice melts or water infiltrates into the disaggregated sediment. They range rheologically from plastic to viscous to semi-fluid and vary in velocity according to rheology. As water content increases so does sorting, velocity, erosiveness and channelization while grain-size, matrix density and flow thickness decrease. Lawson (1988) describes six zones or horizons each with varying transport mechanisms within flow deposits. These are the basal traction zone, shear zone, plug zone, liquefied zone, meltwater horizon and the dewatered horizon.

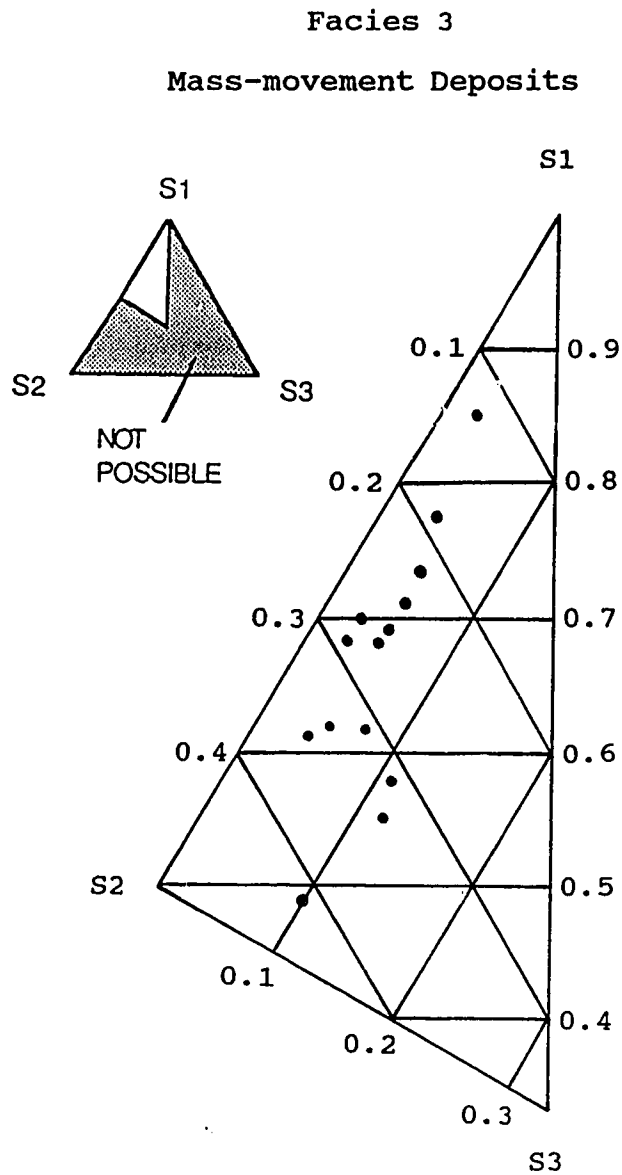


Figure 23: Ternary plot of primary, secondary and tertiary eigenvalues (S1, S2, and S3) from mass-movement diamicton fabrics.

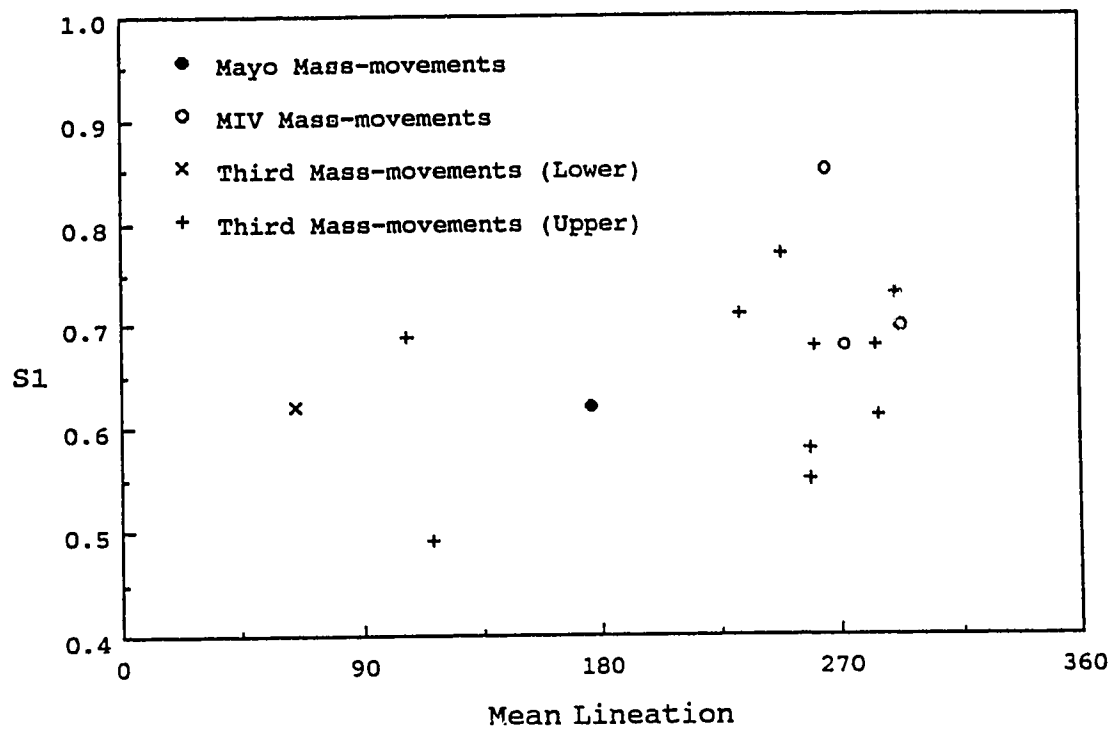


Figure 24: Primary eigenvectors (S1) plotted against the trend of the mean axis (mean lineation) of mass-movement diamicton fabrics.

When water content is lowest the sediment flow is slow and viscous with a lower shear zone overlain by a thick undeforming rafted plug of sediment. In the shear zone dispersive pressures and clast interactions may cause clasts to migrate upward to the zone of least shear (low pressure areas, Lawson 1988). There is internal cohesiveness and the original properties of the sediment are sometimes preserved because of the lack of deformation. These flows form lobate deposits with distinct noses and raised marginal ridges. Basal stratification paralleling underlying topography is not a feature of till and is consistent with deposition in a fluid medium. Deposits become less lobate as the water content rises, flow velocities increase and the shear zone expands into the rafted plug. Flow remains laminar until, with increasing water content, the velocity is too high and turbulence starts. At this point dispersive pressures are relaxed and clasts are unable to be maintained in dispersion. They are transported by saltation or traction in the basal zone and settle out of the flow as a lag deposit. At the highest water content flows appear fluid and readily erode the channels in which they flow. They are turbulent, having no internal strength, and transport finer materials in suspension and coarser sediment by traction. They deposit in depressions or unconfined flats as sheet-like deposits.

The interbedded nature of the diamictons with sand or gravel lenses and beds is indicative of the episodic deposition. Individual sediment gravity flows show numerous changes from laminar to turbulent flow and the nature of the deposits reflects upon their flow histories. Depending on when the flow stops, clasts can be normally or inversely graded or found as a basal lag. Less viscous varieties develop internal stratification and may have raised marginal ridges. Sorted sediments between terrestrial flows are discontinuous lenses or stringers of sand and gravel, that develop from small channelized flows or ponding of meltwaters. Flow marginal stratification (Figure 22; Plate 9) may be parallel to the lobate edge of the flow. The exposed face is a cross-section through three flows and the two stratified bodies to the left show marginal or maybe frontal ridges. The lower diamicton was a relatively fluid flow depositing well bedded layers of sand, silt, clay and diamicton. The upper flow was more viscous, possibly having a plug of stony diamicton riding on the finer sand, silt and clay which forms the body of the flow. The diamicton to the right was the most viscous, forming a massive unsorted body.

Subaqueous sediment gravity flow deposits are commonly well stratified internally, tend to be more areally extensive than subglacial or subaerial deposits and are associated with rhythmically deposited sand, silt, and clay. In water the resistance to movement is reduced allowing flows to initiate on lower angle slopes and continue to move longer. The sediments may become better sorted during the extended period of flow and are commonly finer as they

incorporate lacustrine sediments. In shallow lakes coarse sorted sediment lenses and beds from channelized meltwater inflow are frequent. Suspended sediment rainout deposition may form thin layers of silt and clay between flow events in distal or inactive portions of the lakes. These are not always preserved owing to the erosive nature of the flows.

Distortion along the basal contacts occurs when flows erode and load onto underlying water saturated sediments. In terrestrial flows there are slabs of diamicton which settle down and displace the sediments underneath. In subaqueous flows the sediments below are more frequently incorporated into the flow. Upper contacts of flows are also distorted by loading of coarse better sorted sediments which squeezes out the water in the diamicton. Folding is common as stratification in the more viscous flows becomes convoluted. Post-depositional folding may also occur by loading and colluviation of the flow deposit. Faulting also occurs post-depositionally and may be the result of ice blocks melting out, loading, and other movements.

Subfacies 3C: Massive diamicton interbedded with sand and gravel.

Description

This subfacies consists of massive diamicton with thin wisps, stringers and lenses of silt, sand and gravel. The matrix-supported diamicton has 5 to 30% clasts and a matrix which varies from sandy-silt to medium sand. Clasts are subangular to rounded small to large pebbles, with rare cobbles and boulders. The diamicton forms discontinuous bodies with complex to distinct lower contacts and gradational or interbedded upper contacts. The deposits, usually 50 centimetres to 2 metres thick, have a maximum thickness of 4 metres. Subfacies 3C occurs in Unit C in both the Mayo and MIV Sections.

Infrequent beds of gravel, sand, and silt give the deposits a weakly stratified appearance. Poorly sorted granular to medium pebble gravel, with a fine sandy matrix, are found in thin convexo-planar lenses. Sand occurs as small, 0.5 to 10 centimetres thick by 10 centimetres to 3 metres wide, convexo-planar, biconvex or irregular shaped lenses. Very fine to coarse sand beds are usually horizontally stratified or planar cross-bedded and rarely massive. Lower contacts of the lenses are distinct and upper contacts are commonly truncated by overlying deposits. Stringers or laminations of sand, silt and clay are common and traceable for up to 1 metre. These are 0.1 to 0.5 centimetres thick and have clear to indistinct irregular contacts.

The diamicton is frequently faulted, folded, and convoluted. Distortion is best observed at the contacts between stringers or lenses and the massive diamictons. Lower contacts are usually gradational or interbedded. The diamicton may interfinger with underlying sand, gravel or other diamictons. Slabs of diamicton are commonly loaded onto underlying deposits. Squeeze up or injection structures occur where sand or gravel is loaded onto the upper surface of the diamicton. A single fabric in subfacies 3C gives a north-south orientation and is bimodal (M-15; Appendix 1A and 1B).

Interpretation

These diamictons are interpreted as colluvial deposits occurring in ice-marginal or supraglacial positions, and more rarely subglacially. This interpretation is based on the thin and discontinuous nature of the deposits, massive and unsorted appearance, lack of consolidation and thin wisps of washed sediment. Colluviation includes fall, spall, topple or collapse, slide or slump, and lateral spreads or retrogressive slumps (Lawson 1988; Varnes 1978). Subglacial colluvium occurs in cavities under the glacier where sediment slides or falls into cavities.

Subaerial colluvial diamictons are ice slope colluvium and slope colluvium occurring supraglacially and ice-marginally. Ice slope colluvium collects along active or stagnant ice margins (Lawson 1988). These deposits consist of thin wedges, lenses or ridges extending parallel to the ice margin. Deposits can be matrix to clast supported and are usually massive and structureless with small sediment lenses from meltwater flow and ponding. Slope colluvium deposits form where buried ice melts out and the overlying sediments are reworked by gravity. This deposit is distinct from ice slope colluvium because it has not been reworked by meltwaters and is internally structureless. Clasts are common throughout the deposit and pebble fabrics are essentially random.

The massive nature of these deposits distinguishes them from the better stratified sediment gravity flows. The lenses and stringers that are present are thin and discontinuous. Slumping, sliding and falling debris will form unsorted masses and there is little opportunity for further reworking by meltwater. Complex internal distortion occurs during slumping and sliding of the sediment. As ice melts out beneath the diamicton it may cause uneven settling and faults and/or folds may develop. The basal contacts of supraglacial colluvium are frequently gradational into meltout tills. Ice-marginal lower contacts are more complex, they can be interbedded, depositional, or erosional. The underlying sand and gravel is commonly reworked and may be injected or incorporated into the colluvium by loading.

Facies 4: Massive and stratified matrix-filled pebble gravel.

Description

Facies 4 is the dominant gravel facies in the Mayo region, occurring in Units A, B and F. It consists of a clast-supported, matrix-filled, moderately to poorly sorted small to large pebble gravel (Plate 10) containing all sizes of sediment from clay to boulders. Clast percentages range from 30 to 90%, but are usually 60 to 80%. They are subangular to well rounded with larger clasts usually more rounded. Clasts are mostly blade or roller shaped although there are discose cobbles. Some shattered schistose and quartzite cobbles are found. The matrix consists of fine to coarse sand in the pebbly beds and granules with small pebbles in cobbly beds.

Stratified and massive beds and chaotic structures are common in this facies. Massive beds may be laterally connected to stratified beds. Beds are 2 to 20 centimetres thick in repetitive sequences that can reach thicknesses of 2 metres. Beds may be continuous for up to 200 metres and are commonly stacked in broad trough shaped deposits, each bed a mirror image of the underlying trough form (Plate 11). Imbrication is crudely to well developed and dominated by a-axis transverse to flow and b-axis imbricated [a(t) b(i)]. Measurements of imbrication on cobble beds indicate flow towards west at 272° (Figure 25) with a b-axis dip of 08° .

Normal grading is common with cobbles or large and medium pebbles at the base fining up into medium and small pebble and granule gravel. The matrix concurrently decreases in grain size up through the bed. Rare inverse grading displays small to medium pebble gravel coarsening up over 10 to 15 centimetres to large pebble gravel. Occasionally there are medium and large pebble caps, one or two pebbles thick, on top of small pebble gravel beds. Towards the top of Unit A in the Mayo Section the clasts are smaller (small pebbles and granules) and the beds better sorted. Beds are 2 to 10 centimetres thick and stacked repetitively for 1 to 2 metres. Rare cobbly zones are deposited lower in the unit towards the upstream end of the Mayo Section (0 to 250 metres) and can be traced for over 100 metres laterally. Large pebble and cobble clusters are occasionally present.

Facies 4 is horizontally and vertically associated with massive and stratified openwork pebble gravel (Facies 6) and massive, stratified and cross-stratified pebbly sand, sand, silt and clay (Subfacies 8A). Small beds of openwork gravel, commonly heavily oxidized, are quite common. These are 10 to 20 centimetres thick and 50 to 100 centimetres long and are



Plate 10: Fa
sorte
varia



Plate 11: Ur
lowe
and
sarn
adv:

Fabric 8930 Facies 4.

Mean Lin. 095°

Dip 08°

S1 0.97

S2 0.02

S3 0.01

25 clasts



Fabric 8931 Facies 4.

Mean Lin. 092°

Dip 07°

S1 0.97

S2 0.03

S3 0.00

25 clasts



Figure 25: Unidirectional rose diagrams representing two dimensional pebble orientations in pebble and cobble gravel of facies 4. Sample statistics are the mean lineation, average pebble dip, and the primary, secondary and tertiary eigenvalues of each sample.

dominated by small and medium pebbles. Fine sand, silt, clay and organic detritus (Facies 12), branches, tree trunks and stumps, up to 3 metres length and 20 centimetres diameter, are common along the upper contact and may project into overlying deposits. Massive, stratified and cross-stratified pebbly sand, sand silt and clay (Subfacies 8A) are found deposited gradationally on top of the gravel beds. There is a continuum from medium to small gravel to granules and sand. Oxidation is pervasive throughout the facies but is more obvious in the matrix of the coarser fractions.

The lower contact is usually distinct and planar. Broad shallow trough shaped contacts occur commonly, mostly in the coarser beds. Beds are gradationally deposited onto thin openwork beds of facies 6. The upper contacts are usually distinct when overlain by gravelly facies (Facies 4 to 7) but mostly gradational when overlain by finer deposits (Facies 8, 9 and 12). Load structures are common where these gravels are deposited on finer sediments.

Interpretation

Facies 4 is interpreted to be channel and longitudinal bar deposits of a wandering gravel-bed river. A wandering gravel-bed river exhibits an irregular sinuous channel, sometimes split about islands and in some places braided (Desloges and Church 1987). Wide shallow channels flanked and locally divided by expanses of bare gravel are common, but channel diversion is not as frequent as in braided rivers (Ferguson and Werritty 1983). They have a well defined pool and riffle sequence with meander-like alternation of bed orientation (Ferguson and Werritty 1983). Massive to poorly stratified gravel is the most commonly observed deposit, finer grained sand and organic deposits are much more easily erodible during flood events. Migration is irregular with abrupt changes in direction, channel avulsion and reoccupation of seasonal or perennial side channels (Desloges and Church 1983; Smith 1983).

Longitudinal bars are initiated when diffuse gravel sheets (Hein and Walker 1977) or bedload sheets (Whiting et al. 1988) deposit a coarse bedload lag in the centre of a channel. Subsequent accretion takes place by addition of fine material on top of and downstream of bar core until the bar is exposed (Leopold and Wolman 1957). Channel sediments are incipient bars that form when the gravel sheets do not accrete and instead produce a thin laterally continuous deposit mirroring the channel form. Deposits of this type are common in shallow, high discharge flows in paraglacial settings (Rust and Koster 1984).

Coarser beds, composed dominantly of cobbles, are found mostly in the base of broad laterally continuous channel deposits and not as part of the accreting longitudinal bars. This reflects the domination of transport in gravelly sheets through topographic lows. Stratification indicates episodic deposition of sediment or fluctuations in flow velocity. Gravelly sheets migrating downstream will be deposited as stacked horizontal beds. Massive and chaotic beds are suggestive of high rates of sedimentation during high flow. Lateral extent and consistency in thickness of beds illustrates the high rates of flow and sedimentation. Clast b-axis imbrication [a(t), b(i)] indicates gravelly bedload sedimentation by rolling of clasts along the bed (Hein 1984). The well developed unimodal cobble clast fabric (Figure 25; S1 values of 0.97 and 0.96) supports channelized flow of coarser cobbles and pebbles. Clast imbrication indicates flow to the west (092° to 272°) consistent with flow from the Mayo River valley into the Stewart River valley. The coarse nature of the deposit reflects the local source of material (Appendix 3; Figure 4). Matrix sediments fill the pore spaces between clasts indicating that matrix infilling was synchronous with clast deposition (Frostick et al. 1984).

Normal grading is the result of reducing flow velocities which releases larger clasts from transport earlier. Inverse grading occurs as finer gravel was deposited first and then covered by coarser clasts as flow velocities increase. Clast clusters form around large obstacle clasts which divert flow and reduce flow velocity (Brayshaw 1984, 1985). Large clast were commonly surrounded by numerous smaller clasts in both stoss and wake positions. These clast clusters may be two-dimensional representations of three-dimensional transverse rib structures. Towards the top of Unit A the gravel is finer and has higher matrix content reflecting lower flow velocities. Organic debris collected on the bar surface and was rapidly buried by continued sedimentation. This suggests that some of the bedforms were part of intermittently subaerially exposed bars.

Distinct lower contacts indicate that there has been selective erosion of finer sediments along the underlying bed surface. Basal contacts of channels are erosive and concave down although stacked channel fill beds usually have depositional contacts mirroring the broad channel morphology (Plate 10). Coarser channel fill beds sometimes have erosive contacts reflecting the increased turbulence during higher flow events. The gravel sheets that constitute bars usually have relatively flat, depositional lower contacts. Thin matrix-filled beds are commonly depositional onto openwork beds as a result of matrix infiltration (Frostick, Lucas and Reid 1984). Coarser beds tend to have loaded and erosional contacts whereas the finer deposits were more commonly depositional.

Facies 5: Trough and planar cross-stratified matrix-filled pebble gravel.

Description

Facies 5 consists of relatively abundant, clast-supported, matrix-filled, moderately to well sorted, small to large pebble gravel. Internal stratification is dominated by planar cross-beds with trough shaped bases. This facies is found in Units A and B, most frequently in the Mayo Section. Clasts are subangular to well rounded small pebbles to cobbles which are dominantly bladed and discose. Larger clasts tend to be better rounded. Clasts can occur as 30 to 90% of the deposit, but usually between 70 and 85%. Shattered clasts, mostly quartzite and schist cobbles, are frequent. The matrix is a mix of fine to coarse sand with granules and small pebbles occurring in coarser beds.

Beds are 5 to 100 centimetres thick and up to 10 metres wide. Internal cross-stratification is 3 to 20 centimetres thick and there are interbedded coarser and finer gravelly cross-strata. Openwork cross-strata are sometimes interbedded with matrix-filled cross-strata. Cross-strata have well preserved concave bases but the upper contacts are commonly eroded. Cross-strata dip between 2° and 20° and occasionally up to 35°. Imbrication [a(t) b(i)] may be well developed but usually is crude with coarser clasts having better imbrication.

Normal grading is common with small pebbles to cobbles occurring at the base of individual cross-strata and fining upward into medium and small pebbles. Similarly the matrix fines upward with coarse and medium sand grading up into medium and fine sand. Well sorted medium and coarse grained sand are deposited as interbedded lenses. Rare large pebble and cobble clast clusters are present. Silty sand shadows develop in the lee of large clasts.

This facies occurs primarily in association with trough and planar cross-stratified openwork pebble gravel (Facies 7) and planar cross-stratified pebbly sand and sand (Subfacies 8B). Organic detritus is common near the base of cross-strata, and where the crests are present along the upper surface. Red and yellow oxidation may be strong, but is more commonly sporadic and associated mostly with the matrix.

The lower contact is clear, commonly a shallow, scoured trough that cross-cuts bedding in underlying units. Rarely the lower contact is flat and gradational, tending to occur where the facies is 40% or more matrix and clasts are mostly small pebbles. The upper contacts of cross-

strata are usually truncated by overlying gravel beds, but can be preserved when overlain by sand lenses.

Interpretation

Trough and planar cross-stratified beds in gravel are interpreted to be foreset accretions on margins of transverse bars (Hein 1984; Morison and Hein 1987; Smith 1990). Evidence to support this interpretation includes the inclination of bedding, less laterally continuous nature of the beds, the trough shaped basal contacts, and the generally finer grain size of the clasts. In shallower flows, transverse bars may develop from a diffuse gravel sheet (Hein and Walker 1977; Gustavson 1978). These sheets move by bedload transport, rolling and sliding clasts along the channel floor. When the sheets eventually stall they commonly have inclined margins which following clasts will roll down and form foresets. Foresets are dependent on the rate of sediment aggradation being greater than progradation allowing vertical bar growth to continue. This frequently occurs because the stalled gravel sheet acts to divert and slow the flow. When a bar progrades faster than it aggrades low relief longitudinal bars may form consisting of horizontally bedded sand and gravel.

Shallow flows are required for foresets to develop, the ratio of flow depth to grain size indicates depths of less than 1 metre for this facies. Clasts collect on the foresets and the bar progrades downstream. Cascading of clasts down the foreset and preferentially collecting at the base creates asymptotic foresets with wider and coarser bases. Oversteepened foresets, at an angle greater than the angle of repose, are indicative of ice deposited in the sediments and later melted out creating a higher angle than original. Better developed b-axis imbrication of larger clasts infers high flow velocities have better abilities to orient or reorient clasts (Bluck 1974).

Bar-form sediments are generally finer than nearby channel deposits as a result of lower flow velocities. Clast size typically fines downstream and upwards through the bar as the migrating bar stalls during lower flow. This is common in the Mayo Section gravel where individual gravelly foresets fine upwards into sand and gravel. Foresets commonly exhibit interbedding of finer and coarser beds with a general decrease in grain size downstream in an individual bar. Interbedded openwork foresets indicate fluctuating flow velocities which can periodically maintain finer sediment in suspension (Rust 1984). Clast clusters form around large clasts deposited near the base of foresets (Brayshaw 1984). Large clasts have several smaller clasts in both stoss and wake positions. The foreset form is sometimes elongated downstream

and is thicker than usual around the cluster. Silt and sand shadows form around clasts as a result of reduction in flow velocity around clasts in a finer grained flow.

Lower contacts of this deposit are frequently concave and represent turbulence at the base of the migrating foresets. When two flows converge around a bar the result is a highly turbulent and erosional flow which creates a deep scour. Planar contacts are the result of continuous migration and erosion at the front margin of the bar with less turbulence, likely occurring in slightly deeper flows. Depositional contacts occur as the rate of bar migration slows when flow velocity is low, sediment is finer, and turbulence is minimal. Organic debris may be deposited on the surface of the gravel sheet or bar as flow slackens. These are rarely preserved because increased flow velocities will rapidly erode the surface sediments. At the base of stalled foresets there is a low velocity back eddy which permits deposition and preservation of organic detritus.

Facies 6: Massive and stratified openwork pebble gravel.

Description

Facies 6 occurs as thin beds of moderately to well sorted gravel consisting of small to medium pebbles with rare large pebbles or small cobbles. This facies is rare and occurs predominantly in basal portions of Unit A in the Mayo Section. Beds are 5 to 20 centimetres thick and may be laterally continuous for up to 5 metres. Clasts make up over 80% of the beds and are dominantly subrounded to well rounded, blade and disc shaped. There are numerous shattered and fractured pebbles of mostly metamorphic lithologies. A medium to coarse sand and granule matrix may infill between the clast-supported pebbles in the upper 5 centimetres, making up 10% of the bed.

Stratification is usually poorly developed, crudely horizontal bedding changing to massive or imbricated gravel. Imbrication usually is well developed with a-axis transverse and b-axis parallel to flow [a(t), b(i)]. Normal grading occurs in many beds, large and medium pebbles fining upwards to small pebbles. The matrix content commonly increases upwards as clast size decreases. Occasional pebble clusters occur but are small and indistinct. Oxidation is common throughout and most strongly developed in the coarser, matrix poorer portions.

Facies 6 is frequently gradational or interbedded with massive and stratified matrix-filled pebble gravel (Facies 4) and massive, stratified and cross-stratified pebbly sand, sand, silt and

clay (Subfacies 8A). Organic detritus is rare and only appears in the upper few centimetres of the bed. Lower contacts tend to be distinct and flat, especially when overlying finer deposits. Gradational or interbedded contacts are common and tend to occur when this facies overlies a coarser bed.

Interpretation

This facies is interpreted to be channel or long-run deposits similar to facies 4 but occurring during fluctuating flow conditions. Openwork beds are indicative of fluctuations in flow strength (Smith 1974; Harms et al. 1982) or post-depositional winnowing of the matrix (Bluck 1976). All sizes of sediment are in transport in a gravelly sheet but the flow deposits only the coarser fractions of bedload. Providing that finer sediments are available, current velocities are high enough to maintain them in suspension (Smith 1985) or remove them post-depositionally as flow rate increases again. A consistent deceleration in flow velocity will produce a bed of moderately to well-sorted, normally graded, openwork or matrix-poor, clast-supported gravel. Any matrix is a result of sporadic discharge or clogging of gravel during aggradation as flow wanes (Frostick et al. 1984). Matrix deposited on these openwork beds clogs the pore spaces between clasts and restricts further infiltration of later fines.

Flow cannot maintain matrix in suspension and synchronously deposit small to medium pebbles for long periods. Thus, the beds in this facies are thin and of limited lateral extent. They are commonly overlain by a matrix-filled bed (Facies 4) forming an openwork and matrix-filled couplet. The matrix-filled bed may form as fines infiltrate into the openwork gravel or be normal sedimentation. The fines will infiltrate until the pores become clogged, flow ceases or a new bed is deposited. This will produce an openwork and a matrix-filled bed which has a gradational boundary formed by a two-stage depositional process. Couplets may represent regular diurnal discharge fluctuations where increased flow occurs by melting of ice masses during the day and decreased flow during nights (Smith 1974).

Flat and erosional lower contacts reflect the higher velocities of flow prior to and during clast deposition. In many cases the basal contacts are irregular onto clast surfaces as much of the interstitial matrix is removed from the underlying deposit. Depositional contacts occur when the grain size of the substrate is coarser than the bed being deposited and flow is insufficient to move the coarser clasts.

Facies 7: Trough and planar cross-stratified openwork pebble gravel.

Description

Facies 7 was deposited mostly in the basal regions of Unit A in the Mayo Section. Well sorted small to medium, subrounded to well rounded pebbles dominate this deposit (Plate 12). Clasts are predominantly bladed or discose, commonly shattered and frequently have oxidized coatings. Clast contents are up to 85% and the matrix of medium and coarse sand is rarely above 5%. Only the top few centimetres of the foresets have any matrix. Coarser clasts tend to form thicker foresets and have a higher percentage of matrix than finer deposits.

Beds are 20 to 60 centimetres thick with internal planar cross-strata 2 to 10 centimetres thick. Cross-strata are up to 50 centimetres high and can be 1 to 2 metres long. These generally dip towards the south and west at angles from 5° to 30°, averaging 15° to 20°. Asymptotic foresets are quite common although only the bases are well preserved, the tops having been eroded or reworked. Grading is normal, medium pebbles fining upwards to small pebbles and granules. There are also alternating beds of medium and small pebbles. Imbrication, dominantly a(t) b(i) may occur in the medium pebble beds when clasts are bladed or discose. Smaller pebble beds have better rounded clasts and are usually not well imbricated.

Lower contacts are both distinct and gradational, the latter occurring when cross-strata are asymptotic at the base. Wood is occasionally found along interbedded contacts. Facies 7 is commonly interbedded with clast-supported, trough and planar cross-stratified, matrix-filled pebble gravel (Facies 5) and planar cross-stratified pebbly sand and sand (Subfacies 8B).

Interpretation

Beds of facies 7 are interpreted to have been deposited on the foreset margins of migrating transverse bars during high flow events (Hein 1984). Evidence for this includes the matrix-free beds, inclination of bedding and the less laterally continuous nature of beds. The hydrodynamics of deposition of openwork beds on foresets is similar to that in massive or planar beds. Diffuse bedload gravel sheets migrate across a transverse bar core and deposit on the lee margin of the bar. This may be a result of rapid change in flow conditions over a bar (Harms et al. 1982). Flow velocities increase across shallow bars but as flow moves off the edge of the bar the water depth increases and the flow slackens rapidly. Saltating clasts moved on bar surfaces are released as the flow passes into the deeper and slower water collecting on the foresets.

Section. Clasts are subangular to well rounded small pebbles to cobbles which are dominantly bladed and discose. Larger clasts tend to be better rounded. Clasts can occur as 30 to 90% of the deposit, but usually between 70 and 85%. Shattered clasts, mostly quartzite and schist cobbles, are frequent. The matrix is a mix of fine to coarse sand with granules and small pebbles occurring in coarser beds.

Beds are 5 to 100 centimetres thick and up to 10 metres wide. Internal cross-stratification is 3 to 20 centimetres thick and there are interbedded coarser and finer gravelly cross-strata. Openwork cross-strata are sometimes interbedded with matrix-filled cross-strata. Cross-strata have well preserved concave bases but the upper contacts are commonly eroded. Cross-strata dip between 2° and 20° and occasionally up to 35°. Imbrication [a(t) b(i)] may be well developed but usually is crude with coarser clasts having better imbrication.

Normal grading is common with small pebbles to cobbles occurring at the base of individual cross-strata and fining upward into medium and small pebbles. Similarly the matrix fines upward with coarse and medium sand grading up into medium and fine sand. Well sorted medium and coarse grained sand are deposited as interbedded lenses. Rare large pebble and cobble clast clusters are present. Silty sand shadows develop in the lee of large clasts.

This facies occurs primarily in association with trough and planar cross-stratified openwork pebble gravel (Facies 7) and planar cross-stratified pebbly sand and sand (Subfacies 8B). Organic detritus is common near the base of cross-strata, and where the crests are present along the upper surface. Red and yellow oxidation mottling is strong, but is more commonly sporadic and associated mostly with the matrix.

The lower contact is clear, commonly a shallow, scoured trough that cross-cuts bedding in underlying units. Rarely the lower contact is flat and gradational, tending to occur where the facies is 40% or more matrix and clasts are mostly small pebbles. The upper contacts of cross-

support this interpretation includes the inclination of bedding, less laterally continuous nature of the beds, the trough shaped basal contacts, and the generally finer grain size of the clasts. In shallower flows, transverse bars may develop from a diffuse gravel sheet (Hein and Walker 1977; Gustavson 1978). These sheets move by bedload transport, rolling and sliding clasts along the channel floor. When the sheets eventually stall they commonly have inclined margins which following clasts will roll down and form foresets. Foresets are dependent on the rate of sediment aggradation being greater than progradation allowing vertical bar growth to continue. This frequently occurs because the stalled gravel sheet acts to divert and slow the flow. When a bar progrades faster than it aggrades low relief longitudinal bars may form consisting of horizontally bedded sand and gravel.

Shallow flows are required for foresets to develop, the ratio of flow depth to grain size indicates depths of less than 1 metre for this facies. Clasts collected on the foresets and the bar progrades downstream. Cascading of clasts down the foreset and preferentially collecting at the base creates asymptotic foresets with wider and coarser bases. Oversteepened foresets, at an angle greater than the angle of repose, are indicative of ice deposited in the sediments and later melted out creating a higher angle than original. Better developed b-axis imbrication of larger clasts infers high flow velocities have better abilities to orient or reorient clasts (Bluck 1974).

Bar-form sediments are generally finer than nearby channel deposits as a result of lower flow velocities. Clast size typically fines downstream and upwards through the bar as the migrating bar stalls during lower flow. This is common in the Mayo Section gravel where individual gravelly foresets fine upwards into sand and gravel. Foresets commonly exhibit interbedding of finer and coarser beds with a general decrease in grain size downstream in an individual bar. Interbedded openwork foresets indicate fluctuating flow velocities which can periodically maintain finer sediment in suspension (Rust 1984). Clast clusters form around large clasts deposited near the base of foresets (Brayshaw 1984). Large clasts have several smaller clasts in both stoss and wake positions. The foreset form is sometimes elongated downstream

occurring in slightly deeper flows. Depositional contacts occur as the rate of bar migration slows when flow velocity is low, sediment is finer, and turbulence is minimal. Organic debris may be deposited on the surface of the gravel sheet or bar as flow slackens. These are rarely preserved because increased flow velocities will rapidly erode the surface sediments. At the base of stalled foresets there is a low velocity back eddy which permits deposition and preservation of organic detritus.

Facies 6: Massive and stratified openwork pebble gravel.

Description

Facies 6 occurs as thin beds of moderately to well sorted gravel consisting of small to medium pebbles with rare large pebbles or small cobbles. This facies is rare and occurs predominantly in basal portions of Unit A in the Mayo Section. Beds are 5 to 20 centimetres thick and may be laterally continuous for up to 5 metres. Clasts make up over 80% of the beds and are dominantly subrounded to well rounded, blade and disc shaped. There are numerous shattered and fractured pebbles of mostly metamorphic lithologies. A medium to coarse sand and granule matrix may infill between the clast-supported pebbles in the upper 5 centimetres, making up 10% of the bed.

Stratification is usually poorly developed, crudely horizontal bedding changing to massive or imbricated gravel. Imbrication usually is well developed with a-axis transverse and b-axis parallel to flow [a(t), b(i)]. Normal grading occurs in many beds, large and medium pebbles fining upwards to small pebbles. The matrix content commonly increases upwards as clast size decreases. Occasional pebble clusters occur but are small and indistinct. Oxidation is common throughout and most strongly developed in the coarser, matrix poorer portions.

Facies 6 is frequently gradational or interbedded with massive and stratified matrix-filled pebble gravel (Facies 4) and massive, stratified and cross-stratified pebbly sand, sand, silt and

This facies is interpreted to be channel or long-run deposits similar to facies 4 but occurring during fluctuating flow conditions. Openwork beds are indicative of fluctuations in flow strength (Smith 1974; Harms et al. 1982) or post-depositional winnowing of the matrix (Bluck 1976). All sizes of sediment are in transport in a gravelly sheet but the flow deposits only the coarser fractions of bedload. Providing that finer sediments are available, current velocities are high enough to maintain them in suspension (Smith 1985) or remove them post-depositionally as flow rate increases again. A consistent deceleration in flow velocity will produce a bed of moderately to well-sorted, normally graded, openwork or matrix-poor, clast-supported gravel. Any matrix is a result of sporadic discharge or clogging of gravel during aggradation as flow wanes (Frostick et al. 1984). Matrix deposited on these openwork beds clogs the pore spaces between clasts and restricts further infiltration of later fines.

cannot maintain matrix in suspension and synchronously deposit small to medium pebbles for long periods. Thus, the beds in this facies are thin and of limited lateral extent. They are commonly overlain by a matrix-filled bed (Facies 4) forming an openwork and matrix-filled couplet. The matrix-filled bed may form as fines infiltrate into the openwork gravel or be normal sedimentation. The fines will infiltrate until the pores become clogged, flow ceases or a new bed is deposited. This will produce an openwork and a matrix-filled bed which has a gradational boundary formed by a two-stage depositional process. Couplets may represent regular diurnal discharge fluctuations where increased flow occurs by melting of ice masses during the day and decreased flow during nights (Smith 1974).

Flat and erosional lower contacts reflect the higher velocities of flow prior to and during clast deposition. In many cases the basal contacts are irregular onto clast surfaces as much of the interstitial matrix is removed from the underlying deposit. Depositional contacts occur when the grain size of the substrate is coarser than the bed being deposited and flow is insufficient to move the coarser clasts.

above 5%. Only the top few centimetres of the foresets have any matrix. Coarser clasts tend to form thicker foresets and have a higher percentage of matrix than finer deposits.

Beds are 20 to 60 centimetres thick with internal planar cross-strata 2 to 10 centimetres thick. Cross-strata are up to 50 centimetres high and can be 1 to 2 metres long. These generally dip towards the south and west at angles from 5° to 30°, averaging 15° to 20°. Asymptotic foresets are quite common although only the bases are well preserved, the tops having been eroded or reworked. Grading is normal, medium pebbles fining upwards to small pebbles and granules. There are also alternating beds of medium and small pebbles. Imbrication, dominantly a(t) b(i) may occur in the medium pebble beds when clasts are bladed or discose. Smaller pebble beds have better rounded clasts and are usually not well imbricated.

Lower contacts are both distinct and gradational, the latter occurring when cross-strata are asymptotic at the base. Wood is occasionally found along interbedded contacts. Facies 7 is commonly interbedded with clast-supported, trough and planar cross-stratified, matrix-filled pebble gravel (Facies 5) and planar cross-stratified pebbly sand and sand (Subfacies 8B).

Interpretation

Beds of facies 7 are interpreted to have been deposited on the foreset margins of migrating transverse bars during high flow events (Hein 1984). Evidence for this includes the matrix-free beds, inclination of bedding and the less laterally continuous nature of beds. The hydrodynamics of deposition of openwork beds on foresets is similar to that in massive or planar beds. Diffuse bedload gravel sheets migrate across a transverse bar core and deposit on the lee margin of the bar. This may be a result of rapid change in flow conditions over a bar (Harms et al. 1982). Flow velocities increase across shallow bars but as flow moves off the edge of the bar the water depth increases and the flow slackens rapidly. Saltating clasts moved on bar surfaces are released as the flow passes into the deeper and slower water collecting on the foresets.



Plate 12: Openwork gravel beds of facies 7. Strong oxidation is common in these beds as they are permeable and groundwater flows through them freely.

Interbedding of matrix-filled and openwork foresets occurs when the flow is sporadic (Frostick et al. 1984; Rust 1984). Synchronous deposition of fines with the clasts occurs when flow is slower and forms matrix-filled beds. Rapid flow will produce well sorted matrix-free foresets. The paucity of matrix may reflect the lack of fine sediments in the flow. More probable is that larger clasts are deposited on bar foresets while accompanying finer sediments remains in transport. Matrix only occurring in the upper portions of foresets is a product of restricted infiltration, partially due to the smaller clast size with smaller interclast pore spaces which leads to clogging of the surficial pore spaces. High flow velocities are typical for this facies and do not allow for secondary infiltration of matrix materials.

Facies 8: Massive, stratified and cross-stratified pebbly sand, sand, silt and clay.

This facies consists dominantly of well sorted fine to coarse sand, with up to 30% pebbles, granules, silt and clay. It is essentially a finer-grained equivalent of the gravel facies with varying hydrodynamic properties forming relatively similar sedimentary structures. Based on internal stratification, basal contacts and morphology, this facies is broken into three subfacies. Subfacies 8A and 8B are common whereas subfacies 8C is rare.

Subfacies 8A: Massive, stratified and cross-stratified pebbly sand, sand, silt and clay.

Description

This subfacies occurs as thin, concavo-planar, fining upward stratified sandy sheets or lenses with gradational bases. Beds are thin and discontinuous, ranging from 1 centimetre to 1 metre thick, averaging 3 to 30 centimetres, and up to 10 metres wide. Lenses are typically normally graded from coarse sand to silt and clay with well sorted internal strata. Inverse grading where basal sand coarsens up to granules and small pebbles is infrequent. These beds are laterally continuous into gravelly beds, usually massive and stratified matrix-filled pebble gravel (Facies 4). Occasionally it passes transitionally into planar cross-stratified pebbly sand and sand (Subfacies 8B). This subfacies occurs in Unit A, B and D.

Internal stratification which characterizes these beds is complex and varied. Planar stratified beds form the basal deposit in the coarse and medium sand, with strata as thin as 0.3 centimetres and continuous for 5 metres. The horizontal beds or laminae are differentiated by

slight variations in grain size. Rare massive sand beds are present in the sequence and may occur in the coarse basal region and in the finer upper areas. In the horizontal and massive beds normal grading accentuates contacts. Openwork granule layers or trough cross-stratified medium and coarse sand beds rarely form the basal deposit. Planar cross-stratified beds are sometimes deposited above the troughs and have cross-strata dipping at 10° to 20° . Small scale erosional-stoss climbing ripples occur in medium and fine sand near the top of the beds. Silt and clay may be preserved at the top of the bed as a thin, finely laminated drape.

Other characteristics of subfacies 8A include dominantly rounded, small to medium pebbles forming imbricated, one or two clast thick basal lags. They also form in bases of trough cross-beds, as imbricated stringers along bedding planes, as pebble clusters, and rarely as the capping deposit of an inversely graded bed. Iron staining is weak and diffuse and is concentrated in the upper zones of the sandy beds. Organic debris is commonly preserved in the upper finer strata of these deposits and consist of all sizes from large branches to fine organic detritus.

Undulatory or slightly convex gradational lower contacts are prevalent and frequently cross-cut underlying strata. Fine sediments commonly drape pebbles of, and infiltrate into, underlying gravels. At the base of troughs sharp contacts sometimes occur, but these change to gradational contacts along the margins. Upper contacts are usually sharp and clasts from above may be embedded into the sand.

Interpretation

Sediments of this subfacies represent deposition of bedload and suspended sediment on bar tops, in channels on bars, and in main channels during waning flow conditions (Rust 1972; Eynon and Walker 1974). This interpretation is based on the location proximal to the bar gravel facies, in the bases of channels, and finer nature of the sediments. Pebble lags and clusters, openwork granule beds and coarser sand beds occur at the base of beds. The fining upward sequence of sediments reflects the reduction in flow velocity as flow slackens. This is a finer bar tail deposit equivalent to the massive and stratified gravel bar core and channel facies (Facies 4 and 6). Bar and channel deposits fine downstream as flow velocity is dissipated across the bar surface and through channels on top of the bars.

Repetitive planar strata are the result of numerous pulses of fine to coarse sand and granules moving under upper flow regime conditions across bar surfaces or in channels. Sediment is released from transport as successive thin sand sheets migrate across the surface

forming upper plane bed planar laminations (Bridge and Best 1988). Massive beds form as sand is rapidly deposited from saltation and suspension. These may form in upper flow regime plane bed conditions when aggradation is sufficiently rapid and formation of laminae is suppressed (Arnott and Hand 1989). Trough and planar cross-stratification occurs during lower flow regime conditions. These represent migration of sand-dominated two and three dimensional large ripple forms over the bar top during turbulent flow (Harms et al. 1982; Morison and Hein 1987). Continuing flow decrease allows development of erosional-stoss climbing ripples representative of rapidly migrating small ripples with high sediment input (Jopling and Walker 1968; Harms et al. 1982). Draped laminations of silt and clay may be preserved on top of these deposits but commonly are eroded by subsequent coarser sedimentation. Silt can collect as water slowly moves over the bed, but clay requires vertical suspension settling in still water (Ashley et al. 1982). Inverse grading is infrequent but indicates a reversed sequence as flow velocity rises. Pebble lags or stringers in this dominantly sandy subfacies represent higher flow velocities.

Infiltration of sand into underlying gravel may occur when the gravel is matrix deficient. Sand penetrates for a couple of centimetres into the gravels before clogging the pore spaces and preventing further infiltration (Frostick et al. 1984). Draping of fine sediments over clasts is a result of erosion of the matrix previously deposited with the clasts. A moderate velocity flow removes fines from between the clasts but is unable to move clasts. At a later time, sand is deposited onto the exposed gravelly surface and drapes the clasts.

Commonly these deposits infill depressions forming a concave basal contact. Flow velocity drops as water ponds and sediments are passively released from transport onto the bar surface or channel base. Erosional contacts usually represent the previous base of a shallow channel cutting over the bar which becomes infilled. These deposits are not commonly associated with the formation of the channel but are late-stage infilling of fine sediments. Upper contacts are usually eroded into by coarser overlying sediments which are loaded onto these beds. Convolute strata may occur at the tops of these beds as subsequent gravel is deposited onto the bar top. Organic debris is abundant in this unit, indicating quiet water or subaerial exposure of the bar during slack water or channel migration.

Facies 8B: Planar cross-stratified pebbly sand and sand.

Description

This subfacies consists of large planar cross-stratified pebbly sand beds which can be 2 metres long by 30 centimetres high. Internal cross-strata are 2 to 10 centimetres thick and dip at angles between 10° and 25°. Cross-strata are commonly sigmoidal at the base and crest, although crests are rarely preserved. This deposit is dominantly sand which is moderately sorted and normally graded. Grading is visible both vertically and horizontally. These beds can contain up to 30% clasts, mostly small and medium pebbles. These are deposited along bedding planes as lag deposits and preferentially collect at the bases of cross-strata. They also fine vertically and laterally with pebbles commonly imbricated [a(t) b(i)].

Subfacies 8B is present in Unit A and B, most frequently near the base of the Mayo Section. It is laterally associated with trough and planar cross-stratified matrix-filled pebble gravel (Facies 5) and trough and planar cross-stratified openwork pebble gravel (Facies 7). Organic debris is common in these deposits and collects at the base and along upper internal cross-strata contacts. Iron staining is rare and mostly present only on the finer sand fractions.

Lower contacts of the beds are usually morphologically similar to the internal foreset geometry. These deposits tend to be gradationally deposited onto the coarser gravelly facies of the bars. Scoop-shaped contacts are less common and frequently a coarse pebbly lag overlies the contact.

Interpretation

Subfacies 8B is interpreted to be fine-grained bar marginal foresets based on the internal stratification and lateral continuity with facies 5 and 7. These deposits are finer-grained sedimentological equivalents of facies 5 and 7 (Boothroyd and Ashley 1975; Rust 1984). Sandy foresets develop during declining flow stages around the margins of gravel bars (Jopling 1965). Pebbles indicate slightly higher flow velocities moving coarser sediments. Lags form as pebbles are released from saltation or suspension and cascade down the foreset, coming to rest in the lee of the bar form. Sigmoidal foreset crests illustrate vertical aggradation during progradation. Trough shaped bases are a result of grains rolling down the angle-of-repose foreset before coming to rest in the lee or shadow of the bar as toesets.

The lower contact is frequently depositional because clasts drop out of saltation as water deepens and are not actively eroding the bed. Where there is an erosional basal contact it may indicate flow convergence of two channels around a bar during higher flow conditions. This

creates turbulence and scours the bed surface upon which the finer sediments may be deposited during slack flow.

Subfacies 8C: Planar cross-stratified sand.

Description

This subfacies was noted only twice, occurring in Unit A in the Mayo Section. Broad hummocks with flat bases and asymmetrical convex tops are preserved (Plate 13). These units can be up to 1 metre thick and 2 to 5 metres wide. They are associated laterally and vertically with massive and stratified matrix-filled pebble gravel (Facies 4) and massive, stratified and cross-stratified pebbly sand, sand, silt and clay (Subfacies 8A).

Internal stratification is asymmetrical inclined planar laminae flexed at the crest. A large stoss and smaller lee slope of a large dune is preserved. The laminations are 0.5 to 1 centimetre apart and get coarser and thicker downslope. Rare clasts occur as thin beds or stringers along bedding contacts at the base of the stoss and lee slopes. The basal contact is gradational onto underlying gravel. Laterally it lenses into coarser stratified gravel. A second duneform is partially developed on the upper surface but rapidly grades into gravel.

Interpretation

This subfacies is a dune or megaripple deposited on a channel floor (Harms and Fahnestock 1965). The internal lamination and morphology of the sand body support this interpretation. The exposed deposit is a cross-sectional view parallel to flow (Plate 13). High suspended sediment flows passing through a broad channel experienced a decrease in flow velocity, possibly as a reaction to increasing water depth. Sedimentation occurred on both stoss and lee slopes which suggests progradation was slow relative to aggradation and allowed vertical buildup instead of lateral migration. The stoss slope developed as sediment was carried upslope by traction. The lee slopes represents deposition of grains reaching the crest and cascading down the slope. Orientation of the foresets indicates flow was towards the southwest. The overlying gravel appears to have been deposited quietly without much erosion of the sand body.

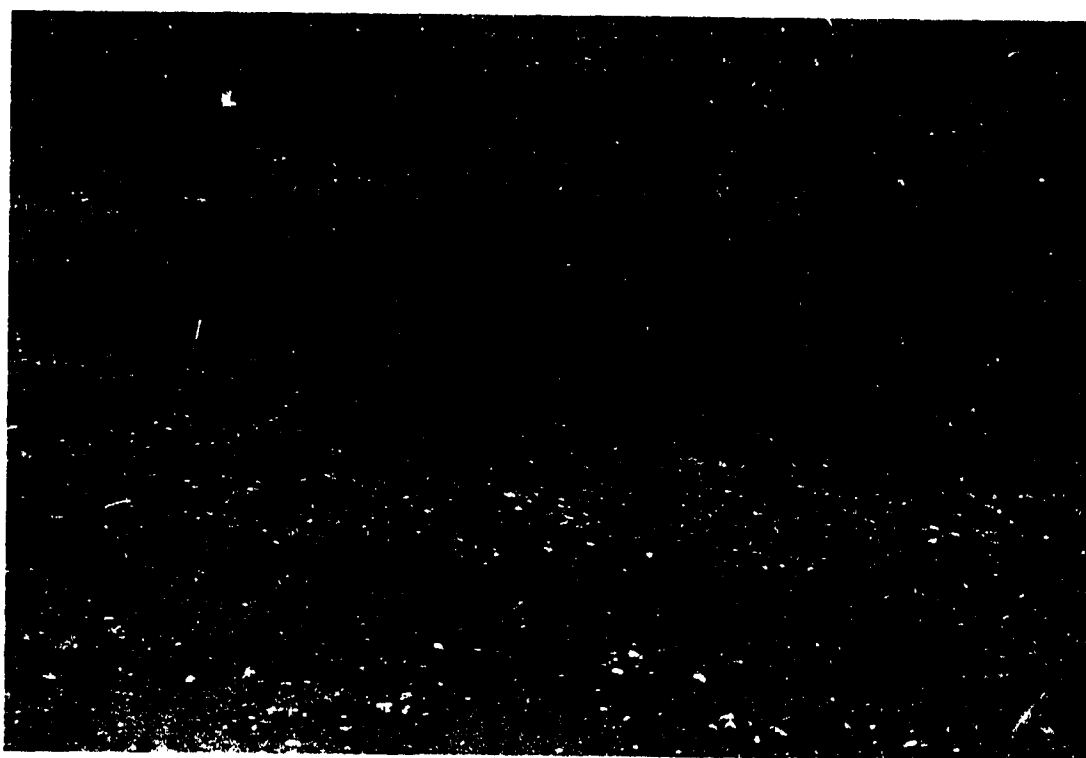


Plate 13: Large migrating dune or megaripple on a channel floor. Towards the upstream (left) and downstream ends this structure is interbedded with gravelly beds. Flow was to the right of the plate. Pick is 75 centimetres long.

Facies 9: Planar, wavy and massive bedded or laminated sand, silt and clay.

Description

Planar, wavy and massive bedded sand is the most common sand facies, occurring in all three sections in Units A, B, D or F. The deposits consist of sand, silt and clay with rare pebbles and mud intraclasts. Beds are planar to wavy stratified or massive and are 1 to 30 centimetres thick (Plate 14). Coarser beds are frequently broad trough shaped and have an erosional base with sand thickest in the centre of the trough. Normal grading is common, mixed sands grading up into fine and very fine sand, silt and clay. Some reverse grading occurs as clay, silt, and sand coarsens upward into silt, fine and medium sand, and pebbly coarse sand. The dominant deposit in this facies is a normally graded, planar stratified, medium to fine sand bed with a flat, erosional basal contact, that is capped by silt and clay laminations.

Planar laminations in this study are considered equivalent to parallel (Paola et al. 1989) or horizontal (Cheel 1990). Planar and wavy beds commonly occur together with planar strata near the base changing to wavy or incipient ripple bedding. Beds consist dominantly of fine and medium sand. Internally the sand forms laminae or beds 0.1 to 5 centimetres thick with thinner laminae 0.1 to 0.5 centimetres dominant. Rare well sorted coarse sand and granule beds form beds 1 to 10 centimetres thick with 0.3 to 3 centimetre thick crude internal strata. The coarser beds tend to form broad, shallow trough shaped lenses with scoured bases, up to 20 metres wide.

Massive beds are 2 to 30 centimetres thick, usually of moderately sorted sand extending laterally for up to 20 metres. One 5 to 8 centimetre thick, horizontal, massive sand bed is notable. It consists of distinctive pale white fine and very fine sand which are massive with rare crude horizontal beds. The scoured basal contact is oxidized red-orange.

Silt and clay form horizontal laminations or draped laminations. The draped laminae are slightly thicker in the depressions than over crests. Silt laminae are internally laminated 0.1 to 2 centimetres thick and form beds that are 0.1 to 8 centimetres thick. Clay beds are very finely laminated and vary from 0.1 to 3 centimetres thick and form beds 0.1 to 10 centimetres thick. Silt and clay occurs in beds over 100 metres long or as small lenses or beds, about 1 metre wide.

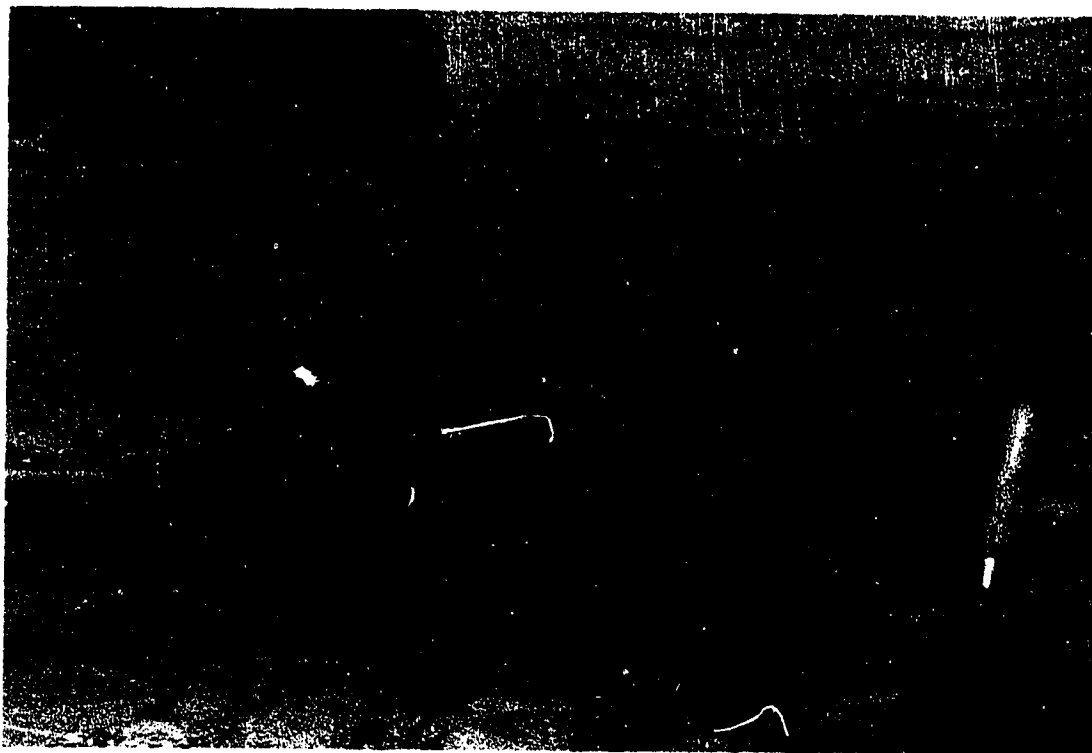


Plate 14: Planar bedded sand and silt at the base overlain by a deformed layer of sand and silt.
This bed is overlain by in-phase climbing ripples deposited under lower flow regime conditions.

Mud intraclasts, granules or pebbles are rare, and finer sand is common only in small quantities. Pebbles occur as thin lags in coarser sand beds and also as isolated clasts with piercement and drape structures that disrupt underlying beds (Plate 7). Lag pebbles are small, whereas the isolated clasts can be up to cobble size. Mud intraclasts are dark brown, irregular to spherical shaped and consist of silt and clay, 0.1 to 3 centimetres in size. Beds are 1 to 20 centimetres thick and have 5 to 80% intraclasts, concentrated towards the base, in fine and medium sand. They form crude layers, interbedded with sand, which fine upward in both thickness and intraclast size. Intraclast clusters are not usually associated with clay or silt beds and only rarely appear as rip-ups from local sediments. Up to 10% small pebbles are included in some of the intraclast lenses.

Loading and deformation structures are common in silt and clay. Sand deposited onto silt and clay beds with high water content produce flames, folds, faults, and ball and pillow structures (Plate 15). Silt and clay are sometimes squeezed and folded by overlying sediments but remain as a cohesive boudinaged unit. Normal faulting is visible throughout the unit with displacements of 1 to 5 centimetres common. Red-orange staining tends to occur in the upper, finer sediments of a bed. Small, 0.5 to 3 centimetre, irregular or disc shaped carbonate concretions appear along bedding contacts. Concretions in an oxidized bed are themselves strongly oxidized. Organic detritus is common along bedding contacts and collects in small bundles, 1 to 3 centimetres thick by 3 to 15 centimetres long, or disseminated throughout the sediments.

Lower contacts of sand beds are usually abrupt and may be broad, shallow trough-shaped or flat. Lower contacts of silt and clay beds are gradational into sand beds. The upper contacts of silt and clay beds are frequently eroded by subsequent coarser sand deposition. A complete sequence of this facies has a sharp base with planar bedded sand changing to wavy bedded sand and then fining up into horizontally laminated silt and clay. Planar bedded sand is laterally equivalent to, and quite commonly overlain and partially eroded by, trough cross-stratified or climbing ripple cross-laminated sand (Facies 10 and 11).

Interpretation

Sediments in this facies are interpreted to be deposited in shallow lacustrine or fluvial environments. The lateral continuity of the beds, fine-grained nature of the deposits and well developed, normally graded sand, silt and clay beds support a lacustrine origin. A fluvial environment is indicated by the less laterally extensive beds, the lack of the finer grained silt and



Plate 15: Ball and pillow loading structures, original stratification appears to have been planar bedded sands. Note the finer nature of the darker colored sands at the base of photo overlain by lighter colored coarser sands.

clay component and association with coarser fluvial deposits. Planar sand laminations can be deposited under upper flow regime or lower flow regime conditions (Harms et al. 1982). Wavy or incipient ripple beds form as the flow regime changes from upper to lower in response to a change in velocity or a change in flow depth. Massive sand beds form under upper flow regime conditions (Arnott and Hand 1989). Silt and clay deposited in horizontal laminations are a product of quiet water suspension settling.

Upper plane beds produce horizontally laminated very fine to coarse sand beds under upper flow regime conditions (Cheel 1990). The upper plane bed bedforms that produce planar laminations are described differently by numerous authors. Thin sand sheets or elongate, very low amplitude bedforms (Smith 1971; Paola et al. 1989), sinusoidal very low bed forms in-phase with the water surface (Cheel 1990) or low relief, straight crested rhomboid ripples (Langford and Bracken 1987) all may produce planar laminations. The consensus reached is a low relief sandy bedform that migrates under upper flow regime conditions. Upper flow regime in-phase waves (downstream-migrating, standing waves or antidunes) can also produce low angle inclined or horizontal laminations (Cheel 1990). Upper flow regime conditions are attained in high velocity deep water flows or in relatively shallow water depths. Coarse to fine sand is carried by bedload transport in the lowest 1 centimetre above the bed while very fine sand and silt are transported in suspension dispersed throughout the whole flow (Bridge 1978). Horizontal laminations are described by Cheel and Middleton (1986) as less than 1 millimetre thick textural laminae, fining up or coarsening up, and heavy mineral sheets.

Horizontal laminations grading up into wavy or incipient ripple bedding is a product of declining flow. Ripples may be developed but are not stable in continued upper flow regime conditions (Cheel 1990). Preservation of the waves or ripples requires sedimentation to continue in the lower flow regime. Horizontal to wavy laminations are frequently preserved in the section and indicate that this was a common occurrence.

Coarse sand (>0.7 millimetres) planar laminations may also form in the lower flow regime (Harms et al. 1982). There is a small range of flow velocities under which the lower flow regime plane beds are stable, and thick or laterally extensive accumulations would not be expected to have a lower flow regime origin. If flow velocity decreases small ripples will develop and if flow increases large ripples will form (Harms et al. 1982). Conditions for their formation are difficult to maintain and these deposits rarely occur in the sections.

Massive sand beds may form under upper flow regime plane bed conditions when aggradation is sufficiently rapid (Arnott and Hand 1989). Formation of laminae is suppressed by rapid deposition without subsequent tractional transport. The interbedded nature of the massive and planar laminated sand supports the origin in upper flow regime conditions. Higher sediment concentrations produce massive beds and reduced fallout and aggradation allows formation of planar laminae.

Horizontally laminated or draped silt and clay beds are formed by vertical accretion (Ashley et al. 1982). The underlying topography controls the shape of the laminations. Individual clay-silt laminae may be traced up to 100 metres suggesting a lacustrine environment. The thick bedded nature of these deposits suggest relatively long periods of quiet allowing extended deposition.

Conditions required for planar, wavy and massive stratification development occur in shallow lacustrine or fluvial environments (Harms et al. 1982; Walker and Cant 1984). The broad, laterally unrestricted beds in Unit B and D support a lacustrine or deltaic origin. Thin and extensive internal laminations forming thick beds are consistent with unconfined flow across a wide area. Flat basal contacts of many of the beds suggest an erosive bedform eroding and smoothing the underlying sediments. Mud intraclasts indicate localized erosion of fine grained suspension deposits by renewed current flow. Dropstones which pierce the sediments are indicative of icebergs floating in lakes depositing clasts onto the lake floor. Pebbly lags are suggestive of increased channelized flow across the lake floor or delta. Organic detritus occurring in the silt and clay beds infers quiet shallow waters. Oxidized beds indicate subaerial exposure of the sediments, such as in a shallow lake, or groundwater percolation.

A fluvial origin is interpreted for the planar stratified sand in Units A, B and F, but this facies occurs infrequently in these units. Beds are laterally discontinuous, overlying beds erosively cross-cut planar laminated deposits. There is very little silt and clay associated with the fluvial deposits because the flow is too rapid to allow suspension deposition. These beds are associated with other fluvial gravel and sand deposits.

Facies 10: Trough and planar tabular cross-stratified sand.

Description

Cross-stratified beds are abundant and consist of fine to coarse sand. This facies is common in Units B and D and occurs in small quantities in Units A and F. Trough cross-stratified beds occur more frequently than planar tabular cross-stratified deposits.

Planar tabular cross-stratified sand occurs in 1 to 15 centimetre thick deposits consisting of individual beds up to 5 centimetres thick. Thin internal cross-laminae are 0.1 to 1 centimetre thick and have oxidized basal contacts. Medium and coarse sand beds dominate in this bedform. Foresets are frequently composed of alternating coarse and fine-grained laminations. Cross-strata dip angles range from 5° to 40°, but are most commonly between 10° and 20°. The angle of the foresets increases upwards through individual beds.

Planar tabular cross-beds develop transitionally into or from trough cross-beds. They are usually gradational to slightly erosional on top of planar beds. The lower contact of planar tabular cross-stratified beds are flat and horizontal or low angle inclined. These beds are commonly associated laterally with planar beds or trough cross-stratified beds and rarely with climbing ripples.

Trough cross-beds are deposited in sequences up to 50 centimetres thick. Troughs are 1 to 5 centimetres deep by 5 to 40 centimetres wide and have fine internal laminations, 0.1 to 0.5 centimetres thick (Plate 15). Sediments in troughs range from very fine sand to granules, but are predominantly medium to coarse sand. Troughs are defined by oxidation of heavy minerals along bedding planes. Laminations are defined by oxidation and slight color variations which indicate grain size changes. Sand in individual troughs fines upward and bed sets are also normally graded. Silt beds drape and conform to underlying trough cross-stratified beds, thinning over crests and as thick as 10 centimetres in lows.

Small pebbles are frequently found scattered in bases of troughs. Subrounded to rounded dark brown clay and silt, 0.1 to 1 centimetre size, mud intraclasts occur sporadically throughout these deposits. Oxidation is common surrounding intraclasts and pebbles. Organic detritus collects in small bundles, 1 to 3 centimetres thick by 3 to 15 centimetres wide, along bedding contacts or disseminated throughout the sediments. Small scale normal faults with displacements of 1 to 5 centimetres are seen occasionally.

Trough cross-beds develop transitionally from planar tabular cross-beds or erosional-stoss climbing ripples beds. When overlying depositional-stoss climbing ripples there is usually a thin transitional deposit of erosional-stoss climbing ripples (Plate 16) or the contact is



Plate 16: Depositional-stoss climbing ripples grading vertically into a thin discontinuous layer of erosional-stoss climbing ripples and rapidly into ripple trough cross-stratified sands. The climbing ripples have slightly finer sands than the troughs. Note the accentuation of internal laminae and bounding surfaces by oxidation. Note also the mud intraclasts which are present in ripple troughs and rarely in climbing ripples. Most mud clasts look like pock marks in the sands.

erosional. Troughs have distinct basal contacts when overlying planar beds. Load structures are common when these deposits form over silt or clay beds and troughs nearby may have intraclasts in them. Upper contacts are gradational into planar cross-stratified or erosional-stoss climbing ripples. Overlying deposits of planar stratified or depositional-stoss climbing ripples have distinct boundaries.

Interpretation

This facies is interpreted to be deposits of unidirectional shallow flows based on internal stratification and facies associations. Typically these occur in shallow lacustrine or fluvial environments. Planar tabular and trough cross-stratification develop under lower flow regime conditions in sand-bed flows (Harms et al. 1982). They may form as the product of individual migrating large ripples or as transverse sand bars in shallow flows (Smith 1972). The small scale of these deposits suggests that they were deposits of individual large ripples. Planar tabular beds are preserved from the movement of two-dimensional large ripples that advance by foreset accretion (Cant and Walker 1978). Trough cross-beds are formed by migrating three-dimensional large ripples (Harms et al. 1982). Two and three-dimensional large ripples are commonly found in shallow lacustrine or fluvial environments.

Two-dimensional large ripples are low, straight crested bedforms with well defined planar avalanche faces (Harms et al. 1982). They commonly migrate across sand flats in shallow waters or through channels. This bedform preserves only the leeside foresets as stoss slopes are eroded by subsequent ripple migration. The angle of climb of the stoss slope controls the preservation of underlying ripple sets, a high angle preserves more of the underlying ripple and a low angle will erode most of the previous ripple. This angle is

dependent on rates of flow and sediment aggradation (Harms et al. 1982). The increasing angle noted in Unit D in the MIV Section illustrates the reduction in flow velocity allowing greater aggradation. The migration and erosion by each ripple forms a flat and erosional lower contact.

Planar tabular cross-strata develop transitionally from erosional-stoss climbing ripples as flow velocity increases and the angle of climb is reduced. In coarse sand beds planar tabular cross-beds may also succeed lower plane beds. As velocity increases and the flow becomes more turbulent the straight crested nature of these bedforms changes gradually to sinuous. This signifies the change from two to three-dimensional ripples and the gradation in deposition from planar tabular to trough cross-stratified beds. A distinct change from lower flow regime

planar tabular cross-beds to upper flow regime plane beds is sometimes noted in these deposits. This is a reaction to a rapid change in flow velocity, and probably occurs without a significant increase in the sedimentation rate.

Three-dimensional large ripples have strongly irregular plan geometry with sinuous crests formed by turbulent flow (Harms et al. 1982). They have gentle stoss sides, lee sides that are at the angle of repose, rounded crests, and smooth transitions from foresets to toesets. The lower contact of each trough is scoured by the turbulent action of water at the base of advancing foresets. Infilling of sediment into the trough is parallel to the trough-shaped basal contact producing internal trough-shaped laminae. Each set represents preservation of foresets or toesets in scours maintained downstream of the migrating ripple. Preservation of troughs requires net aggradation of sediment or each advancing ripple trough will erode and rework the entire deposit of the previous ripple. Ripples have a low angle of climb, the larger this angle is the greater the portion of the previously deposited foreset laminations escape erosion. The angle of climb is a response to the rate of sediment aggradation and flow velocity. The decrease in grain size up through the trough reflects decreasing flow velocity and increasing angle of climb allowing deposition instead of erosion to occur.

Troughs are developed during low flow on bar surfaces, on channel floors and on sand flats. The size of the ripple increases with depth of flow, especially in finer sediments as a result of higher rates of suspension deposition. Height and spacing of ripples increase with rising flow velocity and then decrease as they approach the transition from lower to upper flow regime where they gradually change to upper plane beds or low amplitude antidunes. A similar sequence can be followed as flow decreases in velocity.

Coarser or heavier sediments are deposited basally in troughs. These include small pebbles, mud intraclasts and heavy minerals. Heavy mineral sheets are readily oxidized and these frequently outline internal laminae and trough bases in the MIV Section. Sediment is moved and deposited rapidly in this bedform and when deposited on silt and clay beds commonly forms load structures. Slowing of the flow will allow development of small climbing ripples on the backs of the large ripples. Erosional and depositional-stoss climbing ripples are frequently deposited gradationally from troughs. Silt drapes may cap the troughs if flow is rapidly slowed or diverted and mirrors the form of the trough.

Facies 11: Climbing ripple cross-laminated sand.

Description

Facies 11 occurs commonly in Unit D and less frequently in Units A and B. There are two variations of climbing ripples: erosional-stoss (ESCR, Type A) and depositional-stoss (DSCR, Type B) (Harms et al. 1982). They consist predominantly of well sorted fine and medium sand.

Depositional-stoss climbing ripples form 1 to 70 centimetre thick beds with fine internal laminations 0.1 to 0.5 centimetres thick. Complete preservation of the ripple is common, 2 to 10 centimetres high by 5 to 30 centimetres long and continuous ripple sets can be traced for over 2 metres. The stoss slopes are longer, have lower angles and are thinner than lee slopes (Plates 17 and 18). Foresets have interbedded thin fine sand laminae and thicker coarse sand laminae. Bases of laminae are marked by oxidation and heavy mineral concentrations. Small pebbles are sometimes found at the base of DSCR beds. Subangular to subrounded mud intraclasts, up to 1 centimetre diameter occur infrequently. Dish and pillar water escape structures, minor load structures and convolutions are visible when the ripples are associated with silt and clay beds. Organic detritus collects in small bundles, 1 to 3 centimetres thick by 3 to 15 centimetres long, on bedding contacts or is disseminated throughout the beds. Normal faulting is present with displacements of 1 to 5 centimetres.

Fine sand, silt and clay may form in thinly laminated beds up into 5 centimetres thick transitionally on top of DSCR beds. The fines mirror the morphology of the last ripple train. DSCR can develop transitionally from or into flat beds or ESCR. They also change to trough cross-beds across distinct contacts and gradationally through a thin ESCR sequence.

Erosional-stoss climbing ripple deposits are usually thin, 3 to 15 centimetres thick, and restricted laterally. They have 1 to 5 centimetre thick medium and fine sand sets with internal laminae 0.1 to 0.3 centimetres thick. Bounding surfaces of sets climb at angles from 5 to 20°. Only lee side foreset laminations are preserved in these sets. Coarse and fine grained internal laminae are frequently interbedded. Lower contacts of the beds, bounding surfaces and internal laminae are distinct. Stratification is accentuated by heavy mineral oxidation along bed contacts. Small and medium pebbles occur at the base of ESCR beds. Small mud balls, 0.1 to 1 centimetre, are abundant and occur up to 15% in the bases of ripple troughs. Organic detritus collects in small bundles, 1 to 2 centimetres thick by 3 to 10 centimetres long, at the base of foresets.



Plate 17: Depositional and erosional-stoss climbing ripples with some mud intraclasts at the base of the sequence overlain by well developed depositional-stoss climbing ripples lacking intraclasts. Erosively overlain by trough cross-stratified or erosional-stoss climbing ripples. Note the coarse grained nature of these upper beds.

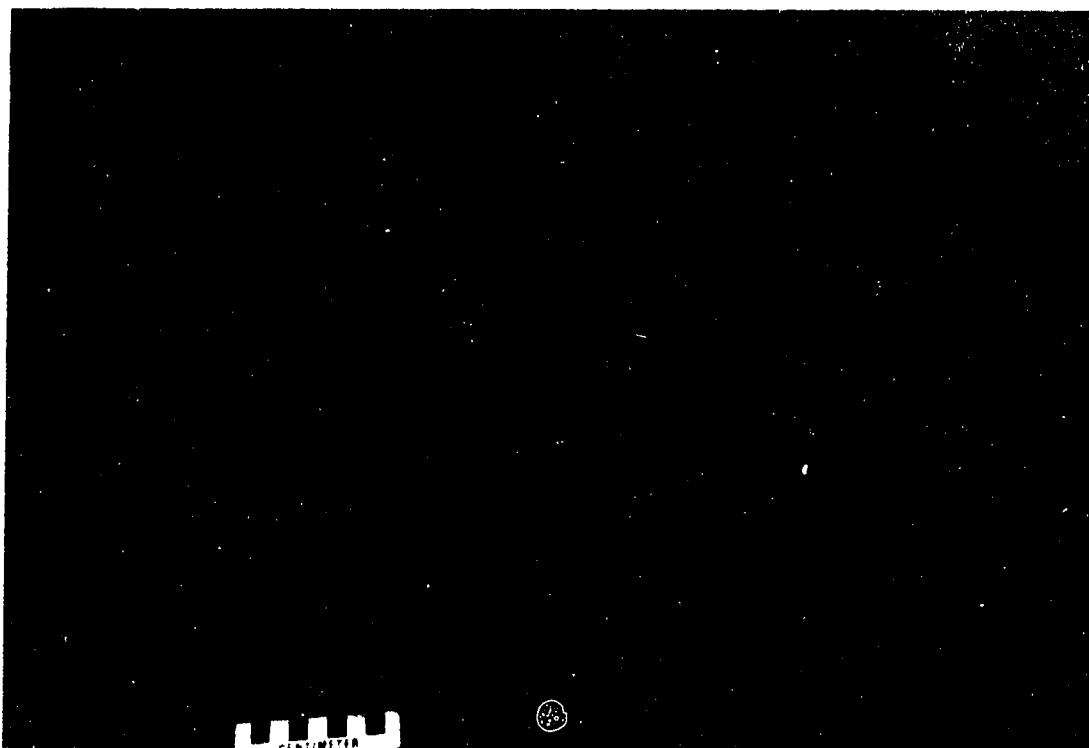


Plate 18: DSCR at the base grading vertically into ESCR covered by the thickest continuous silt drape, a subsequent drape of fine sand, and a second thin, discontinuous drape of silt. These are erosively overlain by an ESCR bed which is again draped by silt. This is overlain by finely laminated, wide crested DSCR with thin silt drapes.

The upper and lower contacts of ESCR tend to be gradational into DSCR with which these ripples frequently occur. Planar beds can develop gradationally from this deposit as the height of the ripples and the angle of climb of the bounding surfaces decrease. The change to planar tabular cross-strata is also gradual as foresets increase in height and the angle of climb is reduced. This bedform sometimes acts as a transitional stage between DSCR and trough cross-beds (Plate 16). Laminated silt and clay beds can be deposited as a drape up to 2 centimetres thick which follows the contours of the last ripples moving across the bed (Plate 18).

Interpretation

Depositional-stoss and erosional-stoss climbing ripple beds are interpreted to be sediments of migrating current ripples developed under unidirectional lower flow regime conditions (Harms et al. 1982). Current ripples are composed of very fine to coarse sand, have irregular plan geometry, are short crested and tend to occur in shallow flows (Harms et al. 1982). These bedforms develop in lacustrine environments and low velocity, shallow fluvial settings (McKee 1965; Jopling and Walker 1968; Ashley et al. 1982)

DSCR preserve both stoss and lee side laminations as one continuous laminae. The deposition of sediment on stoss slopes requires a rate of deposition that approaches or exceeds the rate of bedform migration (Rubin 1987). This requires either a high rate of deposition implying high transport rates and fallout from suspension (Ashley et al. 1982) or a low rate of migration indicating low transport rates. These conditions are met where a high sediment inflow meets standing or slow moving waters, such as in a delta. A low rate of migration is inferred where these deposits are overlain by silt and clay which require slow or still water to accumulate.

DSCR may develop from a bed of no movement as flow increases. Sediments collect in lee side troughs, producing thicker lee side than stoss side laminae. In a steady flow an increase in sediment supply will cause an increase in the angle of climb and thicker laminae. With an even sediment supply, the slower a ripple migrates the greater the angle of climb will be. Laminae are superimposed in rhythm such that they are stacked vertically or subvertically. Accelerated flow transitionally produces ESCR, the stoss side gets thinner and eventually disappears as the angle of climb gradually gets lower than the stoss slope. As flow wanes from DSCR deposition the transition is into draped laminations which mirror the form of the last deposited ripple.

ESCR form under higher flow velocities than DSCR and are the result of increased bedload transport and decreased suspended load (Harms et al. 1982). They preserve only the lee side laminae of the migrating ripple form. Erosion on the stoss slope produces bounding surfaces that climb in the direction of flow as the migrating bedform troughs aggrade downcurrent. The rate of deposition is below the rate of bedform migration so the resulting angle of climb is stoss-erosional and only the lee side laminae remain. Laminae are usually planar but may be concave up or sigmoidal as a result of being deposited in lee side troughs. These ripples form in shallow lacustrine or deltaic sequences where there is a high rate of sedimentation combined with higher flow. They are common in more channelized situations on the delta top where flow is faster and sediment is being brought in by rivers. The presence of mud intraclasts and small pebbles shows that ESCR are the product of faster flows than DSCR. ESCR are rarely continuous beyond a couple of metres because they require maintenance of moderate sediment input and flow.

ESCR may be developed from DSCR or a no movement bed as flow velocity increases. The transition from DSCR to ESCR involves slight thickening of lee side laminae and synchronous thinning and disappearance of stoss slopes. Continued flow increase produces various bedforms based on sediment size. Fine sand beds develop into upper plane beds, medium sand beds form three dimensional large ripples, medium and coarse sand beds forms two dimensional large ripples, and coarse sand beds develop into lower plane beds.

Facies 12: Sand, silt, and clay with organic detritus.

Description

Facies 12 consists of 80% fine sand, silt, and clay with up to 20% organic detritus, coarse and medium sand, granules, and pebbles (Plate 19). Deposits are 5 to 150 centimetres thick and 20 centimetres to 10 metres long and occur sporadically in the lower gravel in the Mayo Section.

The sediments are moderately to well sorted and beds are frequently normally graded. Sand beds are up to 20 centimetres thick and silt or clay beds are 1 to 5 centimetres thick. These deposits have massive or crudely to well stratified beds with internal planar laminations. Laminations are commonly distorted and broken by loading or reworking and are better preserved towards the base of deposits. There are rare occurrences of small ripples in fine sand beds up to 3 centimetres thick. Beds are frequently discontinuous owing to distortion and

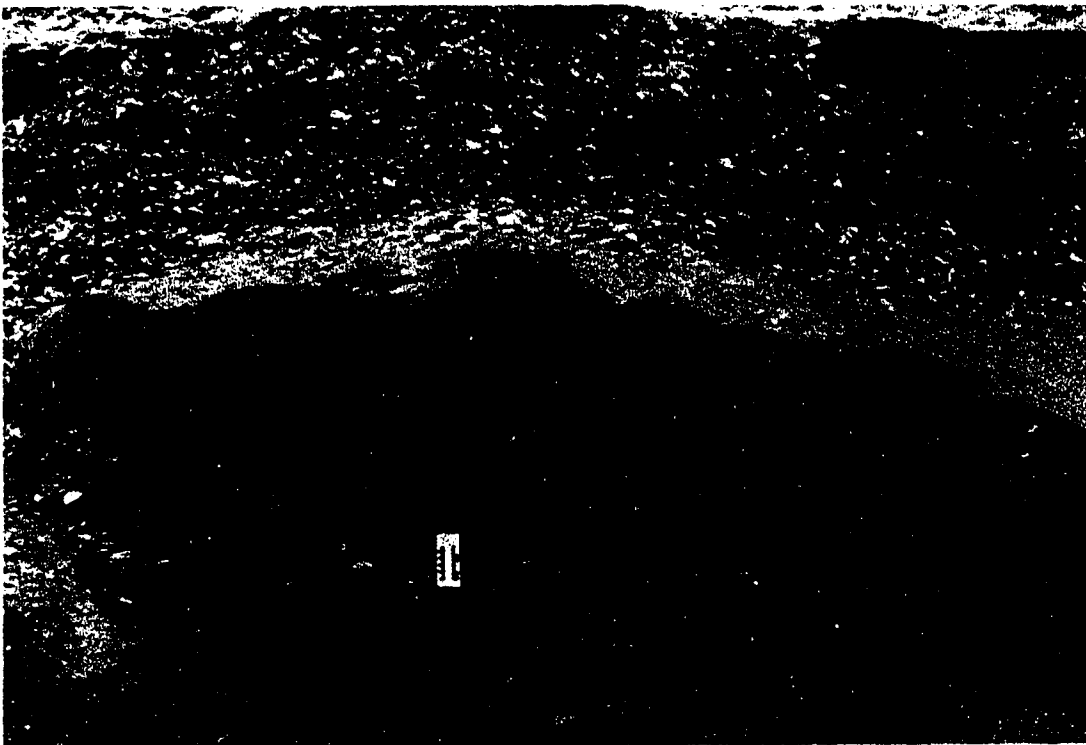


Plate 19: A thick bank collapse deposit. The lower contact is erosional. Side contacts are visible and illustrate a dip angle of 10-20°. Note the distorted laminated beds. Deposit is 80 to 100 centimetres thick and 3 to 4 metres wide.

convolution. Pebbles are deposited as discontinuous lags near the base or as individual clasts scattered throughout these deposits.

Sticks of wood, broken wood fragments, organic mats or detritus are commonly deposited along bedding surfaces. Wood can be 15 to 25 centimetres long by 1 to 2 centimetres diameter but are usually smaller. Many sticks are deposited long axis transverse to flow [a(t), b(i)] in layers continuous for 10 to 30 centimetres. There are some large tree trunks, up to 2 metres long by 30 centimetres diameter, and stumps with roots, 1 metre high and 1 to 2 metres around. Organic mats occur throughout these deposits. They consist of finely disseminated wood and rootlets with a fine silty-clay matrix and are usually less than 1 centimetre thick and from 3 to 20 centimetres wide. In some cases a large fragment of organic debris or a large clast forms an obstacle behind which finer debris has accumulated.

The lower contacts are usually irregular and broadly convex down and can be gradational or distinct. Gradational contacts have sand and silt draped onto underlying gravel with some loading structures. Distinct lower contacts are less common but occur where this facies is deposited on a previously eroded contact. These contacts can occur at angles up to 60°. The upper contacts are sharp, and frequently are truncated by overlying coarser deposits. Load structures are common with pebbles from above beds pushed into the unit and sand and silt squeezed up into the gravel.

Interpretation

The sediments of Facies 12 are interpreted to have accumulated in one of two ways, as a bank or bank collapse deposits or as bar top debris deposits. The deposits of are very similar but the process of formation is different. This facies occurs in gravelly braided stream environments in the Mayo Section.

Bar top debris deposits tend to be thin and laterally continuous lenses that collect on bars during high to waning flow. Bars usually subaerially exposed are submerged in the river during higher flow events and accumulate abundant organic debris and sediment. These deposits can contain large mats or blocks of organics and sediments that have been transported downstream after bank collapse. The mats may be bound together by vegetation and roots and the whole mass may have floated onto the bar. Original stratification is usually preserved but is commonly distorted owing to movement during rafting and emplacement. Deposits may be formed by one flow, as a product of numerous flows, or as a long term exposed bar.

Accumulation may be centred around vegetation, large clasts, other debris, within depressions, or deposited by decreased water competence. Beds of organic sand, silt and clay are deposited rapidly with a mix of pebbles and granules. The thin planar laminae are products of upper plane bed and suspension deposition. Wood pieces can range in size from small twigs to large logs. A large in situ stump was located at 90 metres in the Mayo Section and suggests tree growth during long periods of subaerial exposure. Bar top deposits have flat, trough shaped or irregular basal contacts which are always depositional. The basal deposits commonly infill between exposed clasts on the bar. Preservation potential for these deposits is low, but when preserved they tend to maintain their primary depositional characteristics.

Original bank deposits are well stratified, fine-grained sand and silt with abundant fine organic debris. They can form lenses of which are inclined along the side of a channel or be elevated deposits of overbank deposition during flood events. Organic debris collects throughout the beds and vegetation may grow in and stabilize the sediments. Bank collapse deposits occur where a stable bank is undercut by rising water level or channel migration. Overhanging bank sediments may remain coherent due to root binding and fall as a mass onto the eroded surface below. Internally, the sediments may retain the well stratified nature or may be distorted by resedimentation. Faulting and folding are common throughout. Organics occur as detrital wood and roots and less frequently as larger wood pieces. The lower contacts are distorted and frequently occur at high angles. These sediments are depositional but occur unconformably on erosional contacts which they are not responsible for eroding.

Facies 13: Silt and organics.

Description

This facies consists of a layer of organics overlain by a horizontally laminated silt. In the Mayo Section the organic layer dominates with very little silt. For the MIV and Third Sections the silt is predominant with a thin organic layer at the base. The deposit forms a low, vertical cliff capping the sections, but is unconsolidated and easily broken. This facies forms Unit G and it varies in thickness from 20 centimetres to 2 metres. An organic layer up to 30 centimetres thick is usually developed at the base of this facies. At the top of the layer is a 3 to 10 centimetre thick organic horizon consisting of >80% wood fragments with very little sediment. A 10 to 20 centimetre thick, oxidized, carbonate poor horizon underlies this and has up to 50% organics. Underlying this is silt and sand, with <10% organics, which have been enriched in carbonates.

Horizontally laminated silt is deposited transitionally on top of the organic horizon. Sediments include small quantities of clay, sand, granules and pebbles in the dominant silty deposits. Beds are massive to horizontally stratified with thin internal laminations. Laminations are 0.1 to 0.5 centimetres thick in 1 to 5 centimetre thick beds that may be laterally continuous for up to 3 metres. The sediments are yellow-buff colored, but change to purple, red, orange, tan and brown with oxidation and increasing organic content. Stratification is imparted from thin woody and organic horizons. Wood pieces are well preserved in most cases with bark, branches and roots attached, although they are sometimes partially or totally burnt. Large wood branches or trunks may be horizontally deposited or may remain in vertical growth positions. Roots extend throughout the silty deposits in quantities up to 30% and are both horizontally and vertically oriented.

The lower contact is undulatory and indistinct, commonly interbedded or gradational onto underlying sediments. The upper contact is undulatory and exposed to the weather. Presently there are trees and small plants growing on the upper surface into the silt. Convolutions are common throughout the deposit but are more concentrated in organic rich layers.

Interpretation

This facies consists of an organic horizon interpreted to be a soil and a silt deposit interpreted as loess formed by wind deposition. The soil is an orthic eutric brunisol similar to other soils found on Holocene surfaces in central Yukon (Rutter et al. 1978; Smith et al. 1986). The soil is characterized by a thin, partially decomposed organic F horizon, a well developed Bm horizon and a basal Cca horizon (Agriculture Canada Expert Committee on Soil Survey 1987).

The soil horizon is buried by windblown loess. Thin, laterally discontinuous, horizontal laminations of silt are the result of varying wind velocity. Most of the silt in the deposit is derived from the section below. The Mayo Section has no loess layer reflecting the coarseness of the underlying sediments. The MIV and Third Sections both have thick deposits as a result of wind blowing up the section and reworking the fine lacustrine sediments. Vegetation stabilizes and receives nutrients from the silt and continued sedimentation buries them as layers. Burnt wood in the loess indicates fires have occurred in the region reflecting the dryness of the climate. Coloration of the silt reflects oxidation by groundwater percolation and organic content. In some places the silt and organics have been folded and faulted in response to permafrost.

V LITHOSTRATIGRAPHIC UNITS

Deposits in the three main measured sections are divided into seven lithostratigraphic units based on texture, grain size, sorting and gross lithology:

- G Soil and loess.
- F Upper gravel.
- E Upper diamicton.
- D Upper sand and silt.
- C Diamicton.
- B Lower sand and gravel.
- A Lower gravel and sand.

Unit A: Lower gravel and sand.

The lower gravel and sand unit is the basally exposed deposit in all three sections and is equivalent to Unit 1 of Hughes et al. (1987; Figures 10, 12 and 14). The Mayo Section has the best exposure of these oldest sediments and is dominated by gravel. Coarse pebble and cobble gravels with sandy and silty-organic interbeds are deposits of channel sedimentation as gravelly sheets or low relief longitudinal bars in a wandering gravel-bed river (Neill 1973; Church 1983; Desloges and Church 1987). Towards the base of Unit A gravel forms coarse grained, trough shaped, laterally extensive beds which were deposited by gravel sheets moving through broad shallow channels. Longitudinal bars form as gravel sheets stall, inhibiting the movement of following sheets, and causing an accumulation of sediment. Gravelly sheets may be matrix-filled or openwork depending on flow velocity and content of fines in the flow. Massive or planar stratified beds (Facies 4 and 6) are deposits of gravelly sheets. Sand (Subfacies 8A) was deposited on the bar surface or in small channels crossing the bar when flow was reduced and mostly confined to main channels. Channels were relatively stable, maintaining their position for long periods permitting sedimentation of fines and allowing vegetation to grow on subaerial barforms and banks. Stabilized barforms were reworked by gradual channel migration and redeposited as bar top debris or bank collapse deposits (Facies 12).

Ice wedge casts in the lower portion of Unit A in the Mayo Section are evidence of permafrost present during gravel deposition and indicates that temperatures were below freezing. Ice wedge development in gravel requires longer periods of continued cold than in finer sediments as better drainage of gravel prevents ice buildup and subsequent distortion. Normal faults sometimes propagate from ice wedge casts in the Mayo Section and have

decreasing displacements in an upward direction implying that they may be synchronous with gravel deposition. No faults extend into diamicton of Unit C but some do cross the contact into brown gravel in Unit B.

Stratigraphically higher in the Mayo Section the nature of the fluvial deposits change. Clasts are smaller and beds become less laterally extensive. Massive and planar stratified pebble gravels (Facies 4 and 6) still dominate, but a greater number of trough and planar cross-stratified pebble gravels (Facies 5 and 7) and pebbly sands (Subfacies 8A and B) are present. These bedforms are associated with transverse bars which migrate by foreset accretion, typical in wandering to braided gravelly rivers. Transverse bars, migrating and breaking up faster than longitudinal bars, are smaller, finer grained and preserve less laterally extensive beds. An inclined face develops on the downstream margin of the bars and sediments deposited on this face are cross-stratified at the angle of repose (Facies 5, 7 and 8B). Bar top gravelly deposits are thin and infrequently preserved because clasts rarely settle on the bar surface, instead they move rapidly across the top, cascading down and collecting on the foresets. Variation in grain size and matrix content of the foreset reflects flow velocity and matrix content of the flow. Fewer organic-rich bar top, or bank deposits (Facies 12) are present. This may be an indication of the onset of glaciation reducing the vegetation production and diversity. No ice wedge casts were observed in the upper part of Unit A in the Mayo Section which suggests that the gravel was able to drain and maintain a low groundwater table although conditions for permafrost formation probably existed. Gravel in Unit A at the Third Section is similar in nature to this portion of the Mayo Section but is poorly exposed.

At the MIV Section, Unit A consists of planar laminated, trough cross-laminated and climbing ripple cross-laminated sand and silt (Facies 9, 10 and 11). Silt is the basal deposit and coarsens up into sand that has been extensively contorted and faulted. The sand has abundant fine organic detritus collected in ripple troughs. These sediments are interpreted not to be of the main river channel, but instead shallow water overbank flows or secondary channel fill deposits. The main channel of the river at this time existed between the Mayo and MIV Sections as illustrated by the general dip of the overlying diamicton deposit (Unit C) (Figures 10 and 12).

The climate when the overbank sand and silt was being deposited has been reconstructed using pollen and macrofossil records from the MIV Section (Hughes et al. 1987; Matthews et al. 1990). Pollen from the base of the MIV Section has high percentages of *Artemisia*, *Graminae* and *Cyperaceae*, significant quantities of *Picea* and *Betula* and traces of

Pinus, *Alnus* and *Salix*. This pollen record implies open treeless vegetation typical of a dry, low arctic tundra environment (Matthews et al. 1990) and specifically from a river floodplain environment. Spruce (*picea*) pollen is present but radiocarbon wood date evidence suggests that they are actually older and the dominant tree in the region was willow (*salix*). Spruce was confined to small groves and treeline was depressed to about 850 m (2760 feet). Willow and spruce specimens from similar strata have been dated (Table 1) and, whereas willow was dated finitely, spruce wood provides infinite dates. A wide variety of plant and arthropod macrofossils were recovered from Unit A in the MIV Section by Matthews et al. (1990). Plant fossils are consistent with a river floodplain environment and again spruce is almost nonexistent. This supports pollen evidence and radiocarbon dates which suggest the tundra had little spruce and was dominated by willow. Arthropod fossils indicate a dry, low arctic environment similar to the present northern Yukon and Northwest Territories mainland (Matthews et al. 1990). Matthews et al. (1990) conclude that the climate was drier and colder than present and that the temperature in July was lowered by as much as 5°C.

Evidence to support a major gravel-bed river in the Mayo valley includes the nature of the present day Stewart River, the orientation of bedforms in the gravel, and clast lithologies. McConnell (1901) first noticed that the nature of the Stewart River changes at Mayo townsite. The first gravel encountered is at the mouth of the Mayo River valley. There is no evidence of gravel as far upstream as Fraser Falls (Figure 7) and the river is a sand, silt and clay dominated, rapidly migrating, meandering river. Downstream of Mayo, the Stewart becomes a gravel-bed wandering river with gravelly barforms in an incised channel. Tempelman-Kluit (1980) hypothesized that the Stewart River flowed southwest through Nogold and Ethel Creeks in the Miocene and Pliocene (Figure 7). It did not flow into the present Stewart valley across Fraser Falls until postglacially dammed in Ethel Creek valley by a Late Wisconsinan moraine (Hughes 1983b). The Mayo River at this time was the principal drainage from north of Mayo and may have included present drainage into the McQuesten River. The preglacial Stewart and Mayo Rivers joined together in the Tintina Trench and eventually drained to the south into the Gulf of Alaska through the Alsek and Dezadeash Rivers (Tempelman-Kluit 1980).

Clast lithologies (Appendix 3; Figure 4) indicate provenance of the pebbles from quartzite, gneiss and schist bedrock (JKKh, Jp, HpQ and Hqp) and chert bedrock (OSDr) (Figure 4) to the northwest, north and northeast. The quartzites were identified as coming dominantly from the Keno Hill quartzite (JKKh) approximately 30 kilometres north. Clast imbrication and channel forms, gravel foresets and sand ripple orientations indicate flow was from the north

(Appendix 1, Fabrics 30 and 31). This supports the presence of a large river flowing south through the Mayo valley into the present day Stewart valley.

Unit B: Lower sand and gravel.

The lower sand and gravel unit dominates the MIV Section (Figures 12 and 13; Hughes et al. 1987, Unit 2) and there is a small exposure in the Mayo Section (Figures 10 and 11; Plate 9). These sediments are considered to be proglacial outwash deposits of a glacier advancing from the east. There is no preserved deposit of Unit B in the Third Section.

Brown gravel in the Mayo Section is a deposit of an aggrading, distal proglacial, sandy-gravelly braided Mayo River. This river was fed by melting ice in the McQuesten River valley, the Mayo Lake valley and the Janet Lake valley (Figure 7). The main channel of the river flowed between the Mayo and MIV Sections and the brown gravel is a deposit of a high-level, marginal channel which forms a broad, shallow, trough-shaped deposit mirroring the underlying topography in Unit A. Sediments are finer grained than in Unit A and are the result of gravelly sheets moving through rapidly aggrading and migrating channels. They have a high matrix content, are thin and laterally restricted, and are commonly truncated by other beds. Clast provenance data (Appendix 3) suggests that these sediments have a different source than Unit A. A distinct increase in Road River chert (OSDr) and Earn Group clastics (MEu, DMe and DEi) reflects onset of glaciation and influx of distally derived eastern lithologies (Figure 4). The absence of organic detritus in these sediments is a indication of rapid channel migration and of decreasing vegetation growth as the region cooled in response to the presence of ice.

In the MIV Section, Unit B is a thick sequence of sand, gravel and diamicton (Facies 3, 4, 5, 8, 9, 10, and 11) that is interpreted as ice-proximal fluvial, lacustrine and mass-movement sedimentation. The unit is continuous along the section, but there is no representative vertical stratigraphic sequence (Figure 10; Appendix 4). Ice-proximally, high sedimentation rates and sporadic discharge create a depositional environment with rapid lateral and vertical facies variations. The increase in chert and sandstone pebbles of an eastern provenance substantiates the proglacial nature of these sediments. Clasts with piercement and drape structures are found in the sand, indicating ice-rafting of debris from the ice and release in a glaciolacustrine or glaciofluvial environment.

Well-bedded and normally graded planar laminated to massive, very fine to coarse sand (Facies 9) is common in this unit. This sand was deposited from high velocity, high sediment

density flows. Beds have been extensively folded, faulted and convoluted, typical of high water content beds resulting from rapid deposition. Trough and planar cross-beds (Facies 10) and climbing ripple beds (Facies 11) are common in medium and coarse sand. Cross-beds have oversteepened dips suggesting post-depositional distortion occurred as a result of ice removal. Near the basal contact, massive, stratified and planar cross-stratified, matrix-filled sandy pebble and cobble beds (Facies 4, 5, 8A and 8B) deposited as gravelly sheets and bar foresets are common. Massive or crudely stratified diamictos (Facies 3) deposited by mass-movement are also found close to the base. There is little detrital organic material such as is found in Unit A and the large logs or branches appear to have been reworked from older deposits. Two broad channel forms have been scoured into the proglacial sediments by water from the high-level ice-marginal Mayo River. One (at 750 metres) has been infilled by stratified coarse gravel and its upper contact is truncated by sediments of Unit C. The second (at 1250 metres) is preserved as the form of a channel and is infilled with diamicton from Unit C.

Unit C: Diamicton.

The diamicton unit can be correlated between the three sections and is equivalent to Unit 3 of Hughes et al. (1987; Figures 9, 10 and 20). Diamicton was deposited as a sequence of ice-marginal mass-movements, lodgement till and meltout till, followed by supraglacial and ice-marginal mass-movements. Deposits in the Mayo and MIV Sections are of all three diamicton facies while the Third Section consists of only mass-movement diamicton. Diamicton types can be distinguished on the basis of fabric analyses (Appendix 1), textural variations (Appendix 2), and different sedimentary structures. The basal contact of this unit is mostly erosive and distinct onto the underlying sediments, however, sediments on top of the contact were not always responsible for the erosion.

The diamicton in the Mayo and MIV Sections has discontinuous sediment gravity flow and colluvial deposits (Subfacies 3B and 3C) at the base. As ice advanced along the Stewart valley sediment was deposited ice-frontally and ice-marginally. Overriding and incorporation of these deposits by the glacier sheared and disrupted bedding, and in some areas eroded them, leaving a discontinuous, well-bedded, massive or chaotic deposit. A broad trough cut into the underlying sand and gravel (Unit B) in the MIV Section is a high level channel which drained meltwaters from the Mayo valley during the early stages of glaciation. It is up to 10 metres deep and 70 metres wide (Figure 10; Appendix 4) and is infilled with massive sediment gravity flow deposits.

Overlying the mass-movement sediments for much of the Mayo and MIV Sections is a thin (20 to 50 centimetres thick), continuous, dense lodgement till (Facies 1). Lodgement tills form in ice-marginal areas when the glacier is sliding and depositing sediment. Underlying gravel and sand (Units A and B) is compressively deformed reflecting the shear produced by the glacier. Embedded boulders and flutings along the basal contact, and strong, unidirectional pebble fabrics (Appendix 1) indicate a lodgement genesis. Clast lithology data (Appendix 3) suggests the sediment source is a mix of locally sourced clasts and distal eastern rocks transported by ice.

Meltout till (Facies 2), deposited on top of and flanking the lodgement till, is thicker and more extensive across the sections. Meltout till is not as thick in the MIV Section as in the Mayo Section suggesting less debris-rich ice stagnated higher on the valley sides or that there was substantial reworking after deposition. The change from lodgement to meltout till is indistinct in the Mayo Section, but may be identified by changes in grain size, pebble fabric eigenvalues, or variations in the sedimentary structures. In the MIV Section variation between lodgement and meltout tills is visible in color and textural variations. The depositional environment of the two tills is different, lodgement forming as a result of plastering on of sediment at the base of a sliding glacier and meltout tills being produced from stagnating ice masses. Meltout tills have a slightly wider range in trends of the mean axis of pebble fabrics (Appendix 1) as a result of less confined conditions during deposition. Lodgement tills tend to have lower sand contents representing higher comminution in basal transport positions than englacially or supraglacially derived and deposited meltout tills.

Overlying the tills are mass-movement diamictos formed in ice-marginal environments. Interbedded colluvial diamicton, gravel, sand and silt are supraglacially deposited as ice stagnates. In the Mayo Section these are frequently overlain by diamicton interbedded with laterally continuous fine sand, silt and clay beds formed in an ice-contact lake. Ice-marginal deposits at the MIV Section occur contiguously on top of the meltout till as thin sediment gravity flows (Subfacies 3B) and colluvial deposits (Subfacies 3C) interbedded with sand and gravel. Towards the upstream end of the MIV Section (Figure 10) the inclined form of the diamicton deposit follows the preglacial valley wall. Here Unit C consists dominantly of sediment gravity flow and colluvial deposits exhibiting stratification and distortion typical of subaqueously deposited sediment. Fabrics 45 and 46 (Appendix 1) are from these sediments and illustrate an up-flow orientation of 265° and 272° respectively, indicating flow towards the east (085° and 092°) off the walls into the valley centre. These are reactivated sediments derived from diamicton of Unit C at higher elevations.

In the Third Section, Unit C is a 1 to 4 metre thick diamicton extending the length of the exposed section (Figures 20 and 24; Appendix 4C). The basal contact onto pebble gravel of Unit A is sharp and scoured. The diamicton thickens to the west with the basal contact dipping and the upper contact remaining almost level. The upper contact is distorted and frequently interbedded with the overlying gravel and sand (Unit D). A unidirectional pebble fabric, indicating sediment flow to the southwest, parallel to the Stewart valley, was measured in this unit (Appendix 1A, Fabric 24). From this evidence the diamicton is interpreted to be an ice-marginal, subaerial or shallow subaqueous, mass-movement deposit occurring immediately postglacially. The scoured basal contact is a result of abrasion by the advancing glacier. During advance and retreat, this ice mass deposited no sediment directly onto the gravelly substrate. Sedimentation after retreat was a series of sediment gravity flow deposits, originating from the ice mass to the east, infilling a shallow depression. The environment of deposition was initially subaerial to shallow subaqueous, however, the interbedded and distorted nature of the upper contact suggests a higher energy subaqueous environment occurred later.

Pebble lithology analysis for Unit C indicates a high percentage of distally derived clasts (Appendix 3). Equal numbers of local quartzites, likely incorporated from the underlying gravel of Units A and B, and eastern provenance cherts and sandstones are present. These distal clasts were glacially transported and illustrate the different origins of the fluvial and glacial deposits.

Unit D: Upper sand and silt.

The upper sand and silt unit (Unit 4 of Hughes et al. 1987; Figures 9, 10 and 20) is gradationally deposited onto diamicton (Unit C) in all three sections. After ice ablation and retreat, the Stewart River valley was dominated by an ice-contact or ice-proximal lake dammed by ice near the Third Section (Hughes 1983c). A large delta was building out of the Mayo valley into the lake in the Stewart valley (Figure 7). The delta body is thickest in the preglacial Mayo River valley, the form of which was maintained immediately postglacially. Unit D deposits in the McIntyre Park Section, likely located in or near the thalweg of the Mayo River, (Figure 8) represent proximal gravelly sedimentation of the delta. Large planar cross-stratified, pebbly-cobbly beds with a coarse sandy matrix dominate the exposure. The coarseness and size of the foresets indicates rapid deposition from high velocity flows. The foresets developed on the downstream margins of large bars or were deposited on the inclined prograding delta plain.

The MIV Section cuts across the mid to distal, marginal portions of the delta and Unit D is up to 40 metres thick at the upstream terminus (Appendix 4B), but pinches out at the downstream end and deposition appears to have been topographically controlled (Figures 10 and 23). The basal deposits are large sediment gravity flow lobes interbedded with massive to crudely stratified sand beds (Appendix 4B) occurring near the upstream end of the MIV Section. These are derived from till and diamicton (Unit C) higher on the valley sides which became unstable when submerged by rising waters. They grade upward over 1-2 metres into well sorted and well stratified sand. Massive, upper plane bed planar, and trough cross-stratified sand beds dominate above this but are gradually replaced by climbing ripples or lower plane bed planar and wavy beds. The top half of the unit is predominantly lower plane bed planar and wavy sand beds with laminae gradually becoming finer grained until they form thick sets of silt and clay near the top of the unit.

Four broad erosional disconformities cut into the sand throughout Unit D (Plate 20; Figure 10). These are broad channel forms, up to 12 metres deep and over 100 metres wide, which are sequentially laterally stacked as the channel migrated to the east (Appendix 4B). At the base of these channels there are gravelly sheets and small bar form deposits which grade upward into well stratified sand and silt beds. Initial downcutting and lateral erosion deposited a coarse gravelly lag and as the channels migrated they infilled with finer sand, silt and clay. These are interpreted to be distributary channels of the delta on the basis of the fining upward succession (Bhattacharya and Walker 1992) and trough shaped unconformable lower contacts. Clast lithology data from this unit suggests an increased influx of local quartzite clasts from the Keno Hill area while maintaining a significant quantity of distally derived clasts.

Planar laminated sand beds dominate Unit D in the Third Section (Figure 24). Gravel and diamicton facies occur sporadically in the lower 15 metres of the unit (Figure 20; Appendix 4C) and indicate the probable proximity of an ice mass. Near the base, sand beds are up to 3 metres thick with silt and clay caps up to 60 centimetres thick. Higher up the sand forms thinner beds, 15 to 75 centimetres thick, before again forming thicker beds. These fining upward sequences of planar laminated sand, silt and clay are representative of episodic fluvio-lacustrine sedimentation. Planar laminae developed under upper plane bed conditions in the upper flow regime imply high flow velocities, high sediment capacity, and rapid sedimentation. Near the top of this unit the beds are contorted and distorted with well developed ball and pillow structures (Plate 15), faults and folds. These structures are a reflection of pore water content and sedimentation rate as well as post-depositional loading by the overlying diamicton (Unit E).



Plate 20: Ten metres of Unit B sand and gravel are present at the base of this part of the MIV Section. Unit C diamicton is the prominent layer which appears to pinch out toward the right (east) of this plate. In the horizontally stratified sand of Unit D, which is up to 45 metres thick, one of the large erosional disconformities formed by channel incision can be seen truncating bedding. Unit F gravel and Unit G loess and soil cap the section. The view is 55 metres high and 125 metres wide.

The source of the thick sequence of sand in Unit D at the Third Section appears to have been the ice dam blocking the valley. Sediment released from an ice dam would be thickest close to the source and thin away. Unit D is thickest toward the downstream end of the section and gets thinner upstream (Appendix 4C). Diamicton bodies in the sand are coarsest and thickest toward the downstream end and fine and pinch out upstream. These features indicate the main source was the ice dam, but there could have been significant input by the delta building out of the Mayo valley or the valley sides to the north and south.

In the Mayo Section Unit D deposits are 1-2 metres thick but thicken to up to 8 metres towards the topographically lower ends of the exposure (Figures 10 and 11). Towards the upstream end of the section thin lenses of diamicton are interbedded with sand beds near the base of the unit. These are distal sediment gravity flow deposits from the delta aggrading to the northwest, the retreating Stewart River ice mass to the east, and topographically higher points in the lake basin. Higher up in the sequence these sediments fine up into tractional fine sand beds and vertically accreted silt and clay beds. Gravelly lags may be present at the base of fining upward sandy beds. Sand beds thin upward and occur less frequently synchronously with silt, and especially clay beds, becoming thicker and more common. Silt and clay beds are laterally continuous and represent suspension deposition in a standing body of water. The upper portion of this unit is fine-grained sand deposited from tractional current flow and, increasingly towards the top, silt and clay suspension deposits of a lake.

Unit E: Upper diamicton.

Unit E is only present in the Third Section and consists of diamicton (Subfacies 3B) in discrete plano-convex lobes up to 200 metres wide and 8 metres deep (Plate 21; Figures 14 and 15). These are sediment gravity flows deposited into standing water. Sand lenses visible throughout the diamicton suggest that there were numerous flows and resedimentation occurred on the upper surfaces between events.

Pebble fabrics in these deposits indicates that the source of these flows was the ice dam to the west (pebble orientations of 053° to 121°) and valley walls to the south and southwest of the Third Section (286° and 296°; Appendix 1A). It is likely that these flows occurred just prior to or during the collapse of the ice dam. Instability caused by breakup of the dam initiated sediment gravity flows along the margins of the lake and from the ablating ice mass. This unit may have distally equivalent but unrecognizable deposits in the Mayo and MIV Sections resulting from the drainage of the lake. Unit E is considered to be approximately time equivalent

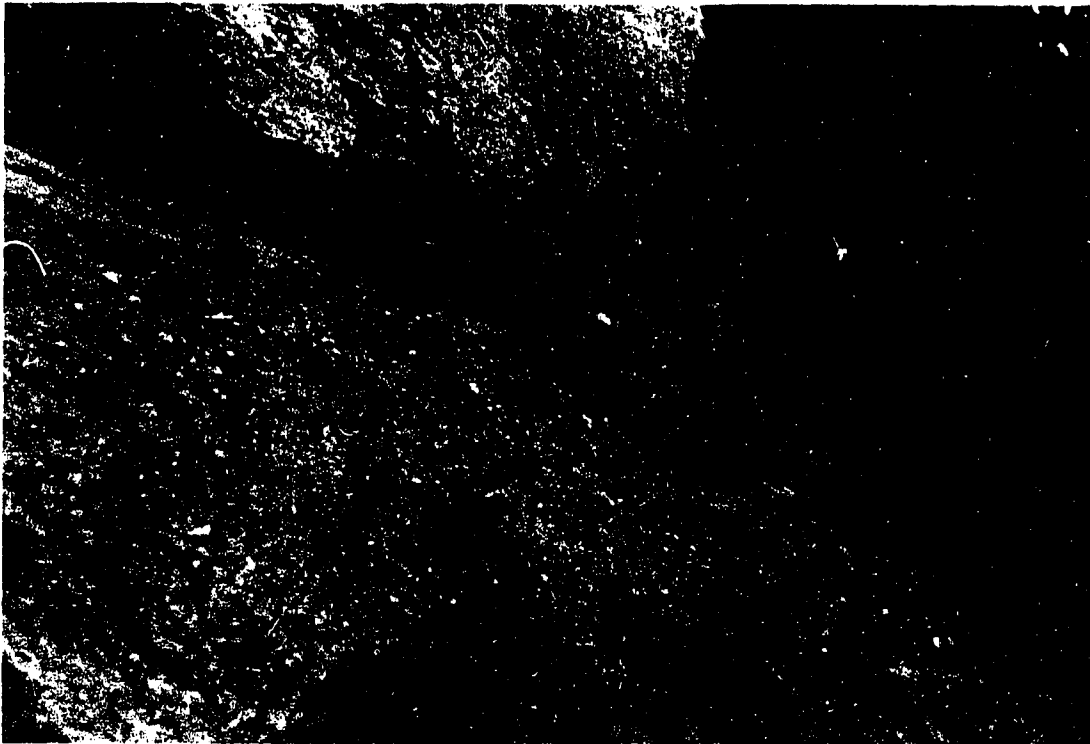


Plate 21: Upper diamicton (Unit E) in the Third section. Sand at the base and separating the diamicton is part of Unit D. The two diamictons lenses are different in color, texture and pebble content. Lower diamicton lense pinches out near the right of plate and thickens off plate to the left. The intervening sand layer pinches out to the left of plate.

to the late stages of lacustrine deposition in the Mayo Section and deltaic sedimentation in the MIV Section as the lake drained.

Unit F: Upper gravel.

Unit F is a thin and continuous, fining upward gravelly deposit across much of the top of the MIV Section (Unit 5 of Hughes et al. 1987; Figures 12 and 13). Gravel occurs along the basal contact for 1 to 4 metres and is overlain by up to a metre of medium and coarse sand. Gravelly sheets, low relief bars and foresetted beds with bar top and channel sand (Facies 4, 6, 8A and 8B) are indicative of a rapidly migrating braided stream. Beds of planar and planar cross-stratified sand (Facies 9 and 10) are common, with a few occurrences of climbing ripple and trough cross-stratified beds (Facies 10 and 11). The initial coarse gravelly sedimentation followed by finer sandy deposition is typical of a maturing braided stream.

These sediments were deposited by the Mayo River which flowed out of the Mayo valley after the lake in the Stewart valley drained. Reworking of coarse proximal delta sediments produced a thin sheet-like deposit of gravel and sand common to braided rivers or alluvial plains with numerous channels. Clasts are dominantly local quartzites, although distal chert and sandstone clasts derived from the moraine are present.

Unit G: Silt and organics.

Thick silt deposits, interpreted as loess, cover the MIV and Third Sections (Unit 6 of Hughes et al. 1987; Figures 13 and 15). The silt is derived from the thick fine-grained lacustrine sequence (Unit D) in the sections. Winds passing through the Stewart River valley erode and carry sediment upward forming cliff top deposits. Loess deposition is accompanied by soil development on the post-McConnell surface. The climate at present is conducive to vegetation growth and, combined with renewed exposure of the sediment cliffs by river undercutting, is promoting continued sedimentation of this unit.

All three sections are capped by a soil horizon. The Mayo Section has a thin mature soil developed on the lake sediments of Unit D and is quite heavily forested (Figure 11). The MIV and Third Sections are more open forested and receive a steady rain of fine silt from the underlying section.

VI CHRONOLOGY

Radiocarbon and accelerator mass spectrometry absolute age dating techniques have been used to date Quaternary sediments in the Mayo region (Table 1). The oldest finite date, $38\,100 \pm 1330$, was obtained by Matthews et al. (1990) from an in situ willow (*salix*) stump in Unit A in the Mayo Section. The stump was located in a silty-sand deposit (Facies 12) just above the basal stratigraphic exposure. It was reportedly in life position on a gravel bar and had been surrounded and submerged by sediment in the aggrading fluvial system (Matthews et al. 1990). Two willow samples (GSC-5139(HP), HHT-88032 and GSC-5142(HP), HHT-88227, Table 1, Appendix 5 and 6) were collected in this study from similar stratigraphic horizons in the Mayo Section (Figure 8) and were dated at $36\,700 \pm 400$ and $35\,900 \pm 320$ respectively. A third piece of willow was recovered at a slightly higher stratigraphic interval about 1300 metres distant. The age of $35\,400 \pm 300$ (GSC-4927(HP), HHT-88098) was obtained and this is correlative and suggests sand and gravel moving in broad channels across a broad alluvial plain. The four corresponding dates from this unit imply that the ages are correct and that the river was actively aggrading between 38.1 and 35.4 ka.

In the MIV Section Matthews et al (1990) dated *Corispermum* seeds from the sand and silt of Unit A at $29\,600 \pm 300$. This date establishes the minimum age of the Reid-McConnell interglacial in the Mayo region and provides a maximum age for the onset of the McConnell glaciation. Willow from the Mayo Section has provided the only finite dates while spruce (*Picea*) samples from the MIV and Mayo Sections (Table 1; Appendix 6) have yielded infinite dates. Some of the spruce has been taken from the interglacial gravel and sand (Unit A), some from the preglacial sand and gravel (Unit B), and some from the glacial diamicton and till (Unit C). These facts suggest that willow was the prevailing tree vegetation in the region and spruce has been resedimented from older deposits. There remain several samples of willow (Appendix 5) which may provide further information towards a younger finite age for the onset of glaciation than the 29.6 ka date of Matthews et al. (1990). Some samples contain both spruce and willow which if dated might provide excellent comparative ages of the different types of wood.

Sediments interpreted to be of a glacial origin have very little organic material incorporated. Postglacial sediments in the three sections provide very few wood samples and none were selected for dating. Close to the top of the MIV Section is a poorly preserved ash, it is interbedded with sand and silt and is likely at the contact between Units D and G. This ash is probably correlatable with one of the White River ashes emanating from the southwest corner of the Yukon Territory which have been dated at 1890 and 1250 years old (Lerbekmo et al. 1975).

A radiocarbon date of 8870 ± 200 years on wood in Stewart River sediments by Burn et al. (1986) provides a minimum date for glaciation in the Mayo region (Table 1).

Dates obtained from other regions of the Yukon have been correlated into the Mayo region by comparison of soil characteristics, moraine morphology, glaciofluvial surface elevations, and permafrost feature development. The age of the soil on the McConnell end moraine has been estimated to be around 14 000 years in development (Tarnocai et al. 1985). The moraine is fresh and can be followed upstream into the study region (Hughes 1983c).

VII QUATERNARY HISTORY

Interglacial

During Mid Wisconsinan time (38.1 to 35.4 ka) a large wandering gravel-bed river flowed south through Mayo River valley and into the Stewart River valley (Figures 7 and 26). At this time the Stewart River upstream of Mayo was a small tributary of the Mayo River. Upstream of Fraser Falls the interglacial Stewart River drained through Nogold, Ethel and North Crooked Creeks into the Tintina Trench before joining the Mayo River near Stewart Crossing. The interglacial Mayo River was similar in nature to the present Stewart River, a broad wandering river with the competence to move clasts of cobble size as bedload. As the river left the confined Mayo River valley and entered the wider Stewart River valley it formed a braidplain with low relief bars and broad channels. Paleoflow measurements in the gravel are consistent with southward flow out of the Mayo valley curving to the southwest into the Stewart valley. The oldest visible sediments of the interglacial Mayo River are laterally continuous, coarse grained, gravelly channel and bar deposits. Successive layers of gravel kept the form of the channel as vertical accretion was faster than lateral channel migration. Abundant organic debris and a tree stump in growth position suggest that this river was relatively stable allowing vegetative growth on banks and bars. Ice wedge casts in this gravel indicates that temperatures were below freezing for an extended period.

During the late Mid Wisconsinan (35.4 to 29.6 ka) the river migrated laterally and built its main channel between the Mayo and MIV Sections. Decreasing clast size from the base to the top of Unit A in the Mayo Section indicates a general decrease in flow velocity. The deposits became better sorted and more characteristic of a braided river. Gradually the channels that existed in the Mayo Section were infilled by more ephemeral braided stream flow, only moving pebbles during flood events and for the most part being a relatively shallow stream. Synchronous with this is a decrease in occurrence and preservation of organic detritus indicating a change from the stable vegetated braidplain of a wandering gravel-bed river to a sparsely vegetated, rapidly migrating braidplain. Vegetation growth may also have decreased in response to cooling as ice advanced into the region. In the MIV Section the last deposits of the preglacial braided river are of quiet water tractional and suspension sedimentation. They are overbank or small side channel fill deposits of sand and silt with associated detrital organics. From pollen and macrofossil reconstruction a dry, low arctic tundra environment is suggested.

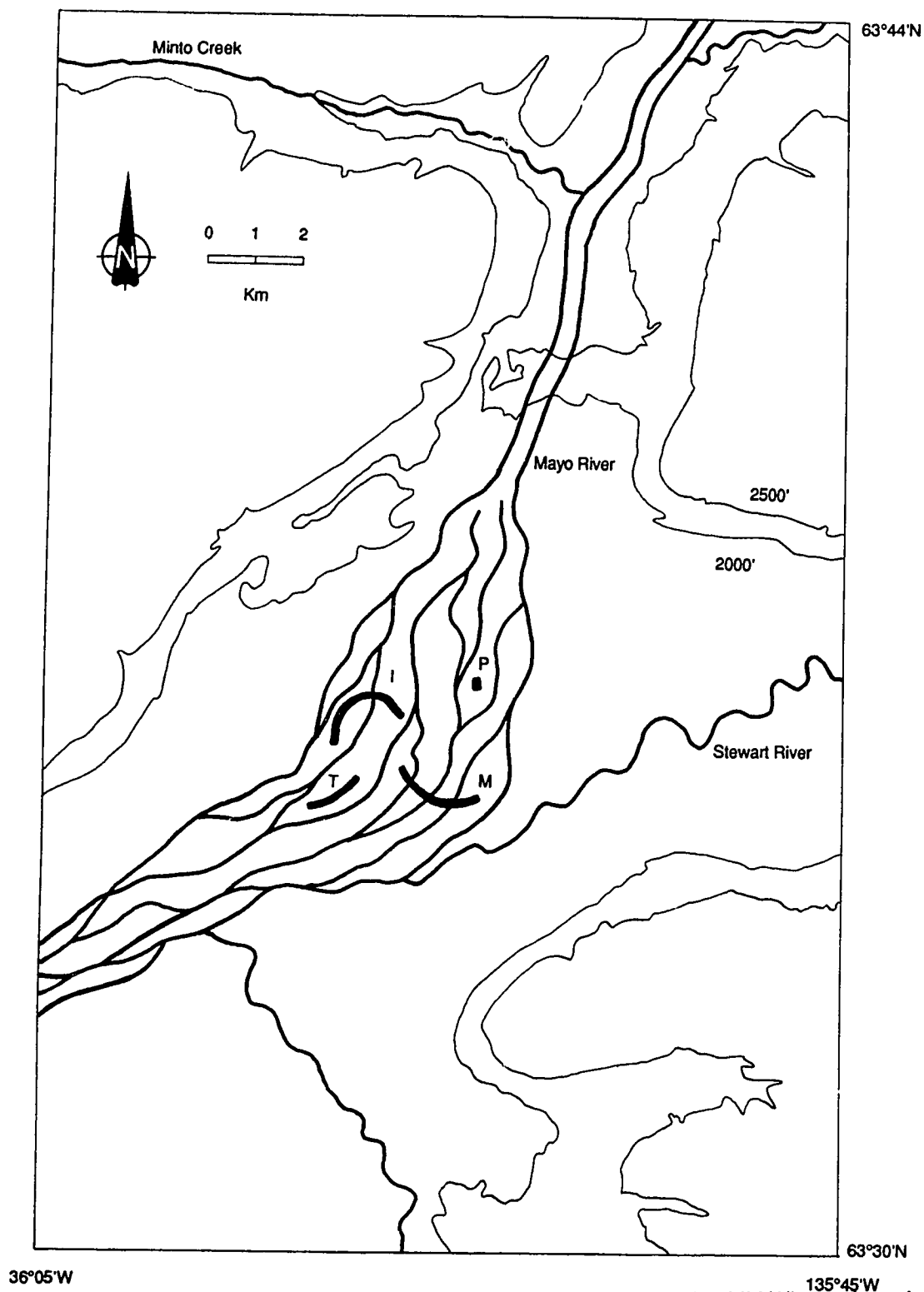


Figure 26: Paleogeographic reconstruction of the Mayo Region during Mid Wisconsinan time. In Figures 26 through 29 I, M, P and T represent the MIV, Mayo, McIntyre Park and Third Sections respectively. Present day 2000 and 2500 foot contours are also shown.

Proglacial

To the north and east of Mayo the Cordilleran McConnell age ice advanced along the Stewart River valley, Janet Lake valley, Mayo Lake valley, and South McQuesten River valley (Figures 7 and 27). The Mayo Lake lobe did not extend into the lower Mayo valley but appears to have been terminated about 10 kilometres west of Mayo Lake. The Janet Lake lobe probably entered the lower Mayo valley and coalesced with an arm of the Stewart valley ice which spilled northwards into the Mayo valley. On the whole however, the Mayo Lake valley from Wareham Lake to the McQuesten River valley was mostly ice free. Drainage from the ice masses was dominantly south through the Mayo valley into the Stewart valley or west through the South McQuesten valley. In the Mayo Section, elevated side channel deposits of the proglacial Mayo River are typical braided stream sediments. At the MIV Section the Stewart valley curves southwest and forms an oblique wall to ice flow and a thick sequence of ice-marginal sediments was deposited at the confluence of the Mayo River and the advancing ice. The glacier bulldozed gravel from the Mayo Section along the Stewart valley and up onto the valley wall. Initially the Mayo River drained along the side of the Stewart glacier (Figure 27) but was gradually deflected westwards and pushed higher along the margins of the valley. Sediment laden meltwater from the glacier and water and sediment of the Mayo River combined to deposit diamicton, gravel, sand and silt in highly disrupted beds. Rapid lateral and vertical changes in these sediments are characteristic of a proglacial environment.

A lake was dammed in the Mayo River valley by the Stewart valley ice to the south and the McQuesten valley ice to the north (Figure 7). This lake was fed by melting ice in the Janet and Mayo Lake valleys and the McQuesten River valley and had an outlet along the margin of the Stewart valley glacier. Broad channel forms scoured into the proglacial sediments are evidence of this initial ice-marginal channel of the Mayo River. As the Stewart glacier advanced and eventually blocked the Mayo valley at approximately 760 metres (2500 feet) water was forced to outlet through Minto Creek valley at an elevation of 670 metres (2200 feet; Figure 28).

Glacial

The different glacial sediments preserved in each section reflect the varying topographic positions of each section and the different depositional environments. As the glacier moved across the Mayo Section it was dominantly erosional at the base as evidenced by flutings, a clean sharp continuous contact, and cross-cutting of underlying beds and faults. Lodgement till, formed by advancing ice, is deposited on this contact for much of the section. Small pockets

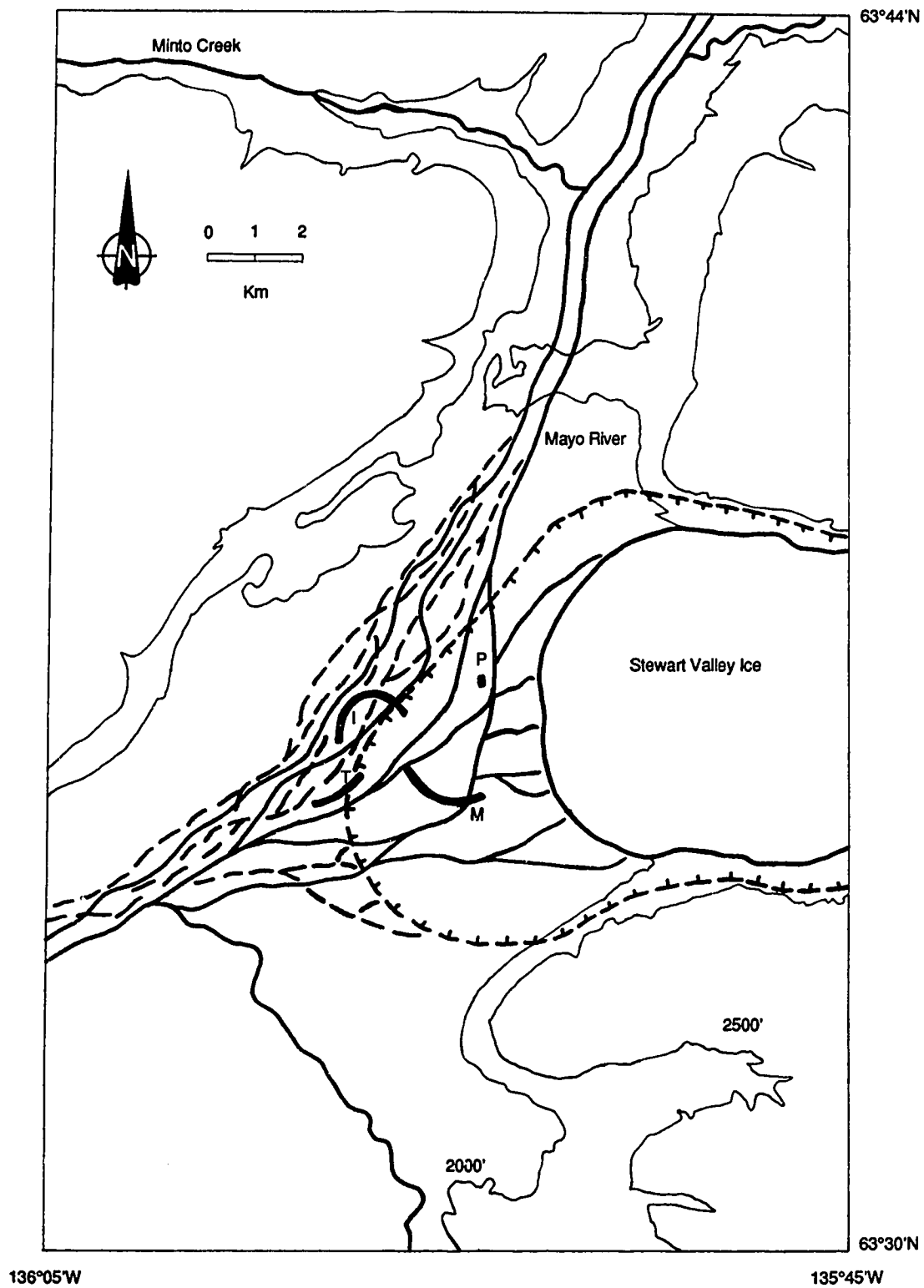


Figure 27: Paleogeographic reconstruction as Late Wisconsin Cordilleran McConnell ice advanced into the Mayo Region.

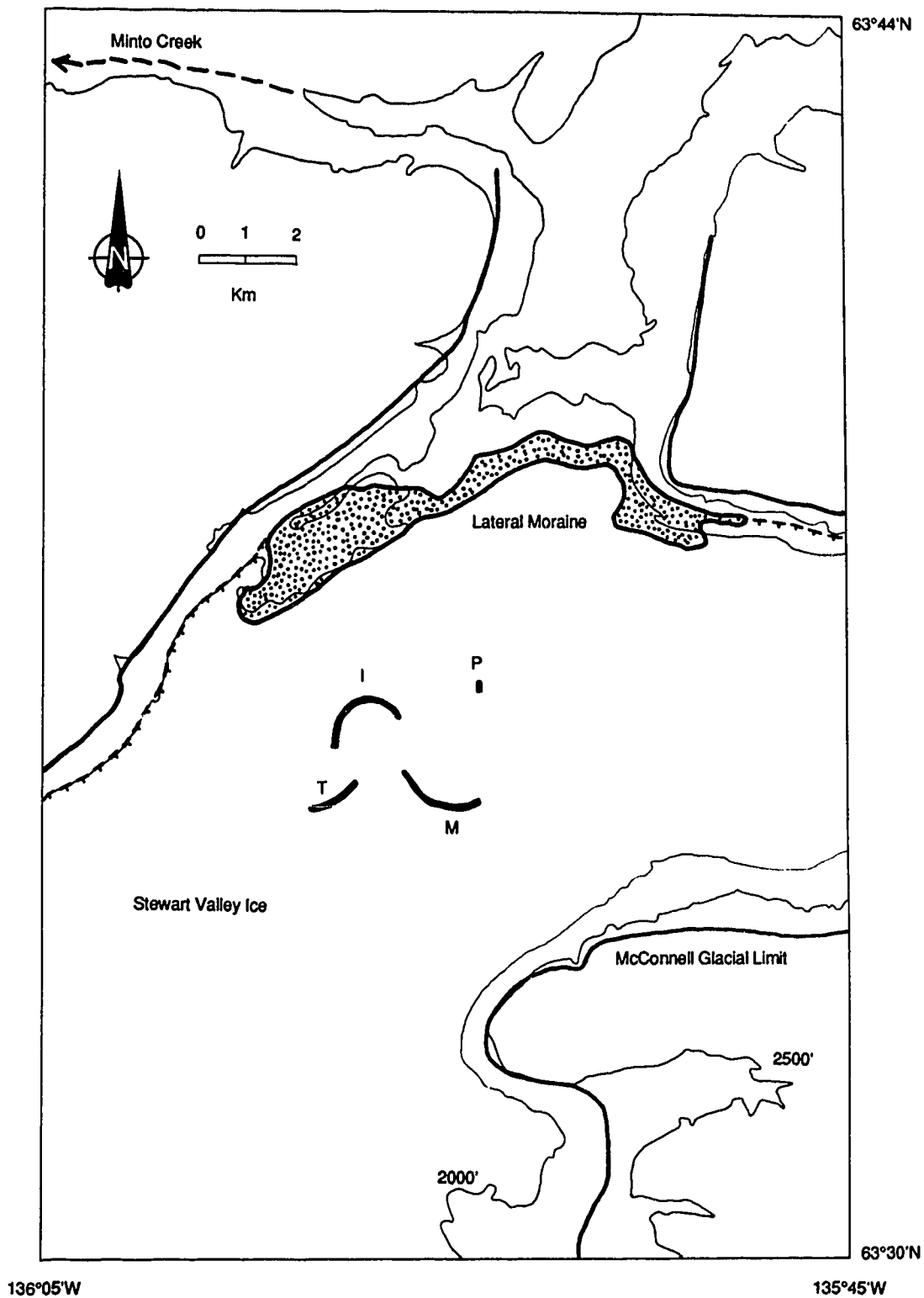


Figure 28: Paleogeographic reconstruction during full glacial times.

and lenses of mass-movement diamicton are found along the basal contact indicating that some subglacial cavities existed. During ice retreat active advance of ice could still form lodgement till, but dominantly meltout tills were being deposited. Meltout tills formed during active ice advance as indicated by stringers of gravel and sand stretching from the gravel up into the meltout till. Most of the meltout till was deposited as ice stagnated in situ and sediment settled vertically. Supraglacial and ice marginal mass-movement diamictons occur as a blanket on top of the meltout till. They extend along most of the section and, following the topography, cap the diamicton unit.

The glacier was deflected by the valley wall at the MIV Section and mass-movement sediments were deposited ice-marginally. At the downstream end of the section the proglacial sediment has a channel eroded into it which has been infilled by ice-marginal sediment gravity flows. Eventually the glacier flowed over the MIV Section, eroding a sharp contact and depositing a compact lodgement till with well developed horizontal partings. This till is only 20 to 50 centimetres thick and 200 to 300 metres wide as a result of decreased debris held higher in ice and lower compressive forces. Meltout till formed by basal ice ablation was deposited on top of lodgement till is up to 2 metres thick but not much more laterally extensive than the lodgement till. Towards either end, and on top of the meltout till, mass-movement diamictons are present. They are characterized by stratification and in one case foresets. Upstream there are large lobes of stratified diamicton with erosional bases that are isolated from each other in the section.

At the Third Section the diamicton unconformably overlies sand and small pebble gravel of Unit A. The exposure is assumed to have been close to the base of the valley and ice would preferentially follow the thalweg. As the glacier passed over this section it eroded and produced a flat surface, but did not deposit any till. The diamictons are interpreted to be mass-movement sediments deposited during ice retreat and stagnation. They are massive to crudely stratified and beds vary from 1 to 3 metres thick and may be traced laterally for up to 100 metres. They appear as lenses of diamicton separated vertically and laterally by sand, silt and clay.

The McConnell terminal moraine located downstream of Mayo can be traced upstream along the valley sides. The end moraine is at an elevation of 565 metres (1850 feet) and gradually rises upvalley to over 850 metres (2800 feet) on the western side of the Mayo River Valley (Figure 28). During full glacial times the Stewart valley ice spilled into the Mayo valley and moraines can be seen on the sides of the lower Mayo valley. The lateral moraine across the

Mayo River valley is a late-glacial limit of the Stewart valley glacier when ice may have briefly re-advanced.

Postglacial

Initially the retreating glacier may have been active but it eventually stagnated. A large ice mass became isolated near the downstream end of the Third Section and dammed drainage to approximately 550 metres (1800 feet) in the Stewart Valley (Figure 29). This dam blocked the lowest existing route for drainage of the meltwaters from the Stewart valley (Figure 7).

Meltwaters from the upper Stewart River were dammed from passing through the Ethel Lake valley which has a moraine at 760 metres (2500 feet), from North Crooked Creek which has a moraine ~730 metres (2400 feet), and from Talbot-Francis Creek which has a moraine at 610 metres (2000 feet). These moraines caused ponding of water and diversion of flow from the old pass of the Stewart River, through Nogold, Ethel and North Crooked Creeks, and into the lake in the Stewart River valley. This created a lake in the Stewart River valley extending as far as 35 kilometres upstream to Fraser Falls (Figure 7). The lake may have been very short lived as the rate of accumulation of water from ablating ice would be relatively high. Sediment was released from the ice dam and produced a 30 metre thick sequence of well bedded sand with occasional diamicton beds in the Third Section.

When the Stewart valley ice retreated below the level of the Minto Creek outlet (670 metres, 2200 feet) the Mayo Lake waters started to drain along the side of the glacier. A late-glacial readvance of the glacier formed a lateral moraine across the Mayo River valley (Figure 29), ponding water in the Wareham Lake region to an elevation of 610 metres (2000 feet). When this lake broke through the moraine it entrained a large volume of sediment and redeposited it as a delta prograding out of the Mayo valley into the Stewart valley (Figure 29). The main delta channel followed the course of the interglacial Mayo River between the Mayo and MIV Sections. Coarser gravel was largely deposited on the delta plain as the meltwaters entered the lake. Distributary channels may have a gravel lag but are dominantly infilled with a sequence of massive and rippled sand to laminated silt and clay. Sand was carried further into the lake than gravel and formed continuous horizontal beds in relatively shallow water on the delta plain and front. The sequence of deposits formed in the MIV Section is typical of sedimentation in a distributary channel delta.

Immediately postglacially the Mayo Section may have been covered by a stagnating ice mass. This accounts for the relative thickness of the meltout till in this section and the lack of

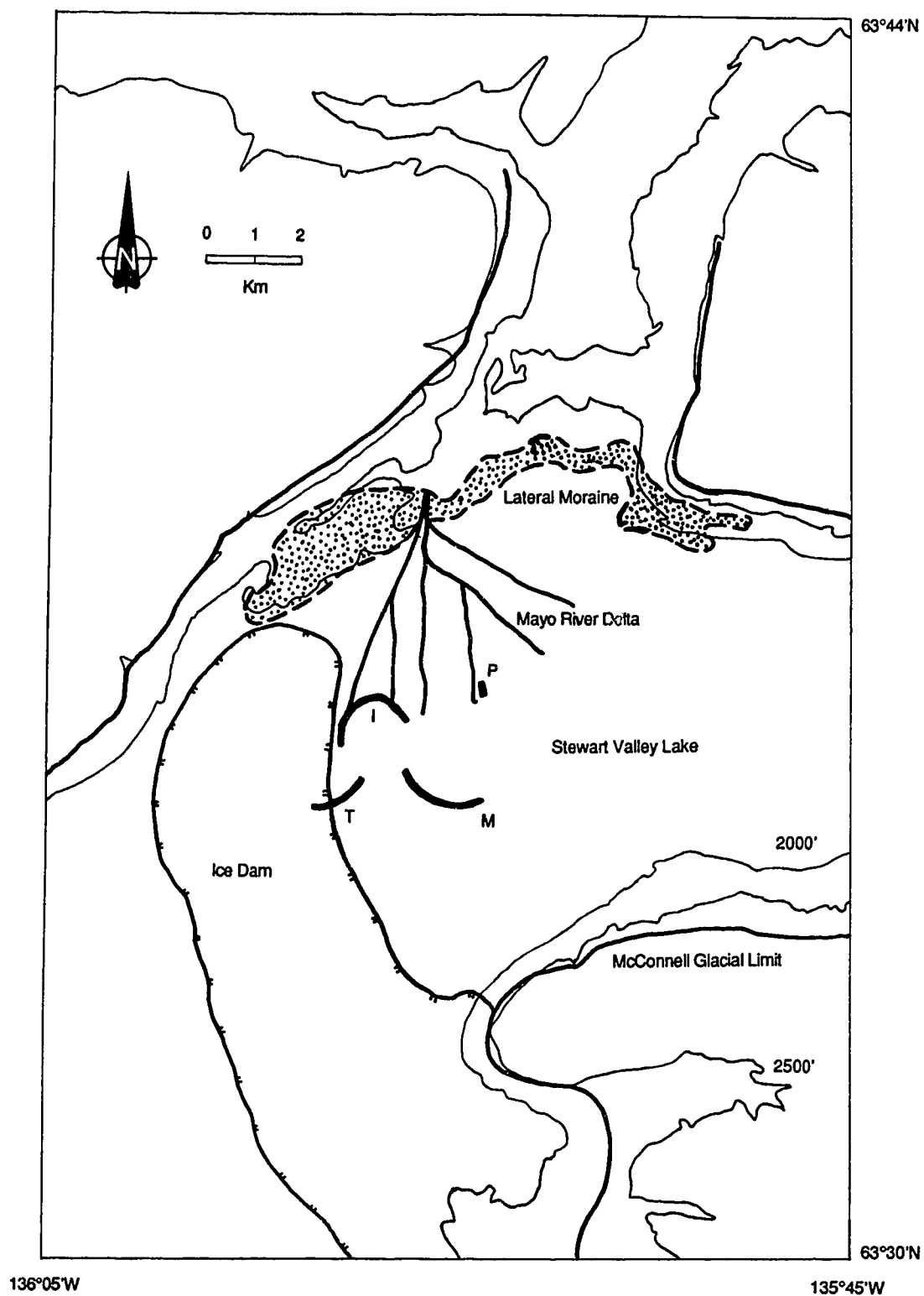


Figure 29: Immediate postglacial paleogeographic reconstruction of the Mayo region.

deltaic sediments. Later the ice melted and lacustrine depositional processes were active. The lake was deepest in the area of the Mayo Section and the sediments deposited are much thinner than in the other sections and are representative of distal deltaic and deep water lacustrine sedimentation. The thin diamicton lenses are evidence of higher energy subaqueous sediment gravity flows from the delta or topographic highs in the lake basin. Most of the deposition was tractional sand deposits of the inflowing Mayo and Stewart Rivers and suspension settling of silts and clays.

Capping the Third Section are broad trough shaped, stratified diamicton bodies that are up to 200 metres wide and 10 metres thick. These are large subaqueous sediment gravity flows formed as the Stewart Valley Lake drained. Catastrophic release of meltwater in the valley created instability along the valley walls and saturated sediments flowed downslope. Pebble fabrics of these sediments indicate a weakly preferred orientation to the northwest towards the valley base. The origin of these flows is likely the slopes to the east of Talbot Creek. The diamicton bodies consist of several individual flows, each with a different texture and flow direction. Sand lenses occurring between the diamictons are deposits of fluvial processes active between flow events.

Holocene

The present day topography of the region has been modified greatly by the action of the Mayo and Stewart Rivers (Figures 9 and 30). The MIV Section is capped by a discontinuous gravel and sand unit which represents a braidplain developed on the delta surface after the lake drained. Coarse gravel and sand from the apex region of the delta was reworked by fluvial action across the braided surface in broad shallow channels. This braidplain was abandoned as the stream rapidly incised a channel into the unconsolidated deltaic sediments forming the valley of the present day Mayo River. The Mayo River has reworked the eastern half of the delta leaving a relatively flat braidplain adjoining the glacial lake sediments upstream (Figures 9 and 30). The distal southerly portions of the delta have been eroded by the meandering action of the Stewart River.

The erosion of the deltaic sediments has provided most of the fine sediment required for the loess developed on top of the Third and MIV Sections. Winds blowing up the Stewart valley have moved the fine sediment from the talus cones and sections up onto the bluffs above the sections. Continued vegetative growth during loess deposition has built up a sequence of organic and loess deposits which cap the sections. On top of the Mayo Section a thin soil

Explanation of Map Unit Designations

A simple map unit designation consists of a genetic symbol (upper case letter) followed by the morphological descriptor(s) (lower case letter). The textural modifier(s) is applied as a prefix where texture is known from field observations. Compound map units, consisting of two simple designations separated by an oblique (/), are used where mixtures cannot be separated because of either limitations of map scale or inability to differentiate the units by airphoto interpretation. In the case of combinations of morainic (M) or colluvial (C) deposits, the combination is shown by use of the two genetic symbols, separated by a comma.

Textural Modifiers

f	fen
si	silt

Genetic Categories

A	Alluvial deposits
C	Colluvial deposits
E	Eolian deposits
G	Glaciofluvial deposits
L	Glaciolacustrine deposits
M	Morainic deposits
O	Organic deposits

Morphologic Modifiers

b	blanket
f	fan
k	thermokarst
p	plain
r	ridged
t	terrace
v	veneer (generally <2 metres thick)
x	complex (combinations of modifiers)

Figure 30: Surficial geology map of the Mayo region (modified from Hughes 1983c). The morainal ridge (stippled) is the lateral moraine deposited on the north side of the Stewart valley glacial lobe. The glacial limit of the McConnell glaciation can be seen on the north and south sides of the Stewart valley. The letters I, M, P and T are located at the Mayo Indian Village, Mayo, McIntyre Park and Third Sections respectively.

horizon has had time to develop. There is very little fine sediment in the Mayo Section and very little sediment has been carried up and deposited on top of the section. The soil develops on top of the postglacial lacustrine sediments which cap the section.

The Stewart River only became established postglacially in the present valley because its previous drainage had been cut off by terminal moraines. Bostock (1966) noted that the McConnell moraine can be followed from its terminal moraine as far southeast as Nogold Creek valley. The anomalous loop in the Stewart River at the mouth of Nogold Creek is the result of damming of the Ethel Lake and North Crooked Creek valleys by moraines (Figure 7). From Fraser Falls to Mayo the Stewart River has formed a wide, meandering alluvial plain (Figure 30) in fine lacustrine sediments. Downstream of Mayo this plain is confined or non-existent as the Stewart River cuts through coarser grained fluvial and morainal deposits. The drainage of the Mayo River has also changed, previously water flowed from as far north as the McQuesten River valley into the Stewart valley. Now, much of this water flows north and west into the McQuesten River valley. Only water coming out of Duncan Creek, Minto Creek and Mayo Lake flowed into the Mayo River.

The glacial lake sediments, located east of the Third Section and upstream of Mayo in the Stewart valley, are uniformly fine grained sands and silts. Numerous permafrost features are evident; thermokarst lakes, ice wedges, thaw slumps (retrogressive thaw flow slides) and ground ice are all present on the floodplain of the Stewart River. Wood pieces have been recovered from these sediments and provide a maximum age of 8870 ± 200 (Burn et al. 1986) for deglaciation.

VIII CONCLUSIONS

The objectives of this study are to determine the sedimentology of the exposed sequences, to interpret the environments of deposition and, combined with stratigraphic data, reconstruct the Quaternary history of the Mayo region central Yukon Territory. Detailed field and laboratory analyses focused on the examination of three sections exposed along the Stewart River. A lithostratigraphic framework was constructed on the basis of structure, grain size and lithology of the unconsolidated sediments. Thirteen sedimentary facies are recognized based on properties observable in the field. Sedimentary facies are used to infer depositional environments and to reconstruct the Quaternary history.

The sequence of sediments exposed in the Mayo region can be explained on the basis of a Mid-Wisconsinan interglacial followed by a Late Wisconsinan glacial advance and retreat. During the Mid Wisconsinan the Mayo River was a wandering gravel-bed river which flowed southwest through the Mayo and Stewart valleys. This river carried a coarse pebble-cobble bedload in broad aggradational channels. Pollen and macrofossil analyses indicate a low arctic tundra environment dominated by willow, with July temperatures depressed as much as 5°C. In the Mayo region the only glacial sediments present are those associated with the Late Wisconsinan glaciation, deposits of earlier glaciations having either been buried or eroded. As Late Wisconsinan ice advanced into the region the nature of sedimentation in the Mayo River shifted towards that more typical of a braided stream. Sediments became finer and the beds less laterally extensive as migration of the bars and channels increased in response to higher flow and sediment content.

Ice advanced into the study area from the east and deflected the Mayo River westwards. The river moved gradually higher along the margin of the advancing ice until it was dammed in the Mayo valley. Sedimentation at the ice margin resulted from proglacial sediment gravity flow diamictos and glaciofluvial activity in ice-marginal streams. Rapid sedimentation and high water content resulted in disrupted sediments with rapid vertical and lateral variations. During full glacial times the Mayo region was inundated by ice to approximately 850 metres and lodgement till and meltout till were deposited. The lower Mayo valley was virtually ice free and filled with meltwaters from the Stewart, Janet Lake, Mayo Lake, and McQuesten valley ice lobes. Water was able to outlet through Minto Creek at an elevation around 670 metres.

During deglaciation, when ice in the lower Stewart valley melted down to below the level of the Minto outlet, the Mayo valley lake drained to the southwest through an ice-marginal

meltwater channel. A late-glacial readvance formed a lateral moraine across the mouth of the Mayo valley blocking drainage from the north. Ice finally stagnated as blocks in the Stewart valley below Mayo, damming meltwater and forming a lake which extended upstream from Mayo to Fraser Falls. Meltwaters in the Mayo valley breached the lateral moraine and flowed into the Stewart valley lake forming a large distributary channel delta. Fine grained lacustrine sediments were deposited throughout much of the rest of the Stewart valley by suspension settling and underflows.

When the Stewart valley lake breached its ice dam, instability along the dam and adjacent valley walls resulted in deposition of sediment gravity flow deposits in that area. Lowered lake levels allowed the Mayo River to rapidly incise a channel into the unconsolidated deltaic sediments and eventually form the present day valley of the Mayo River. Diversion of the Stewart River occurred postglacially as the former channel of the Stewart in the Ethel Lake and North Crooked Creek valleys was blocked by morainic debris; water was diverted at Fraser Falls into the present Stewart valley east of Mayo. Incision and cutbank erosion by the Stewart and Mayo Rivers has created steep sided, unvegetated valleys allowing for thick loess deposits with buried paleosols to form on the cliff tops.

The facies scheme proposed here provides a rapid and efficient method for analysis of complex sedimentologic and stratigraphic sections and will aid in regional correlations. The application of the the facies approach to glacial, fluvial, deltaic and lacustrine sediments in other parts of central Yukon may aid in correlation of glacial and non-glacial units. Further study in the region is also needed to better bracket the onset and retreat of Late Wisconsinan ice.

BIBLIOGRAPHY

- Agriculture Canada Expert Committee on Soil Survey. 1987. Canadian System of Soil Classification, Second Edition, Agriculture Canada Publication 1646, 164p.
- American Society for Testing Materials. 1990. Standard method for particle size analysis of soils. D422-63 (Reapproved 1972) *In* Annual Book of Standards, 04-08: 91-97.
- Arnott, R.W.C. and Hand, B.M. 1989. Bedforms, primary structures and grain fabric in the presence of suspended sediment rain. *Journal of Sedimentary Petrology*, **59**: 1062-1069.
- Ashley, G.M., Southard, J.B. and Boothroyd, J.C. 1982. Deposition of climbing-ripple beds: a flume simulation. *Sedimentology*, **29**: 67-79.
- Berger, G.W. 1987 Thermoluminescence dating of the Pleistocene Old Crow tephra and adjacent loess, near Fairbanks, Alaska. *Canadian Journal of Earth Science*, **24**: 1975-1984.
- Bhattacharya, J.P. and Walker, R.G. 1992. Deltas. *In* Facies Models, Response to Sea Level Change. *Edited by* R.G. Walker and N.P. James. Geological Association of Canada, pp. 157-177.
- Bluck, B.J. 1974. Structure and directional properties of some valley sandur deposits in southern Iceland. *Sedimentology*, **21**: 533-554.
- Bluck, B.J. 1976. Sedimentation in some Scottish rivers of low sinuosity. *Transactions of the Royal Society of Edinburgh*, **69**: 425-456.
- Boothroyd, J.C., and Ashley, G.M. 1975. Process, Bar Morphology, and Sedimentary Structures on Braided Outwash Fans, Northeastern Gulf of Alaska. *In* Glaciofluvial and Glaciolacustrine Sedimentation. *Edited by* A.V. Jopling and B.C. McDonald. Society of Economic Paleontologists and Mineralogists, Special Publication 23, pp. 193-222.
- Bostock, H.S. 1943. Mayo, Yukon Territory, Map 890A. Department of Mines and Resources, Canada. Mines and Geology Branch.
- Bostock, H.S. 1948. Physiography of the Canadian cordillera, with special reference to the area North of the Fifty-Fifth Parallel. *Geological Survey of Canada Memoir* 247, 106p.
- Bostock, H.S. 1957. Yukon Territory. Selected Field Reports of the Geological Survey of Canada, 1898-1933. *Geological Survey of Canada Memoir* 284, 650p.
- Bostock, H.S. 1964. McQuesten. *Geological Survey of Canada, Map* 1143A. Department of Energy and Mines.
- Bostock, H.S. 1966. Notes on glaciation in central Yukon Territory. *Geological Survey of Canada Paper* 65-36, 18p.
- Bostock, H.S. 1970. Physiographic subdivisions of Canada. *In* Geology and Economic Minerals of Canada. *Edited by* R.J.W. Douglas. Canada Energy Mines and Resources, *Geological Survey of Canada, Economic Geology Report* Number 1, pp. 10-30.
- Boulton, G.S. 1968. Flow tills and related deposits on some Vestspitsbergen glaciers. *Journal of Glaciology*, **7**: 391-412.

- Boulton, G.S. 1970a. On the deposition of subglacial and meltout tills of the margin of certain Svalbard glaciers. *Journal of Glaciology*, 9: 231-245.
- Boulton, G.S. 1970b. On the origin and transport of englacial debris in Svalbard glaciers. *Journal of Glaciology*, 9: 217-231.
- Boulton, G.S. 1971. Till genesis and Fabric in Svalbard, Spitsbergen. *In Till: A symposium. Edited by R.P. Goldthwait.* Columbus, Ohio State University Press. pp.41-72.
- Boulton, G.S. 1972. Modern arctic glaciers as depositional models for former ice sheets. *Journal of the Geological Society of London*, 128: 361-393.
- Boulton, G.S. 1974. Processes and patterns of glacial erosion. *In Glacial Geomorphology. Edited by D.R. Coates.* Binghamton, N.Y., State University New York, pp. 41-88.
- Boulton, G.S. 1975. Processes and patterns of subglacial sedimentation: A theoretical approach. *In Ice Ages: Ancient and Modern. Edited by A.E. Wright and F. Moseley.* Geological Journal Special Issue 6, pp.7-42.
- Boulton, G.S. 1976. A genetic classification of tills and criteria for distinguishing tills of different origin. *In Till, its genesis and diagenesis. Edited by W. Stankowski.* Univ. A. Mickiewicza w Poznaniu. Ser. Geogr. 12, pp. 65-80.
- Boulton, G.S. 1978. Boulder shapes and grain-size distributions of debris as indicators of transport paths through a glacier and till genesis. *Sedimentology* 25: 773-799.
- Boulton, G.S. 1979. Processes of glacier erosion on different substrata. *Journal of Glaciology*, 23: 15-38.
- Boulton, G.S., and Eyles, N. 1979. Sedimentation by valley glaciers: A model and genetic classification. *In Moraines and Varves. Edited by Ch. Schluchter.* Rotterdam, Balkema, pp. 11-23.
- Boyle, R.W., Pekar, E.L. and Patterson, P.R. 1956. Geochemical investigation of heavy mineral content of streams and springs in the Galena Hill-Mount Haldane area, Yukon Territory. *Geological Survey of Canada Bulletin* 36.
- Boyle, R.W. and Cragg, C.B. 1957. Soil analysis as a method of geochemical prospecting in Keno Hill-Galena Hill area, Yukon Territory. *Geological Survey of Canada Bulletin* 39.
- Brayshaw, A.C. 1984. Characteristics and origin of cluster bedforms in coarse-grained alluvial channels. *In Sedimentology of Gravels and Conglomerates. Edited by E.M. Koster and R.J. Steel.* Canadian Society of Petroleum Geologists, Memoir 10, pp. 77-86.
- Brayshaw, A.C. 1985. Bed microtopography and entrainment thresholds in gravel-bed rivers. *Geological Society of America Bulletin*, 96: 218-223.
- Brayshaw, A.C., Frostick, L.E., and Reid, I. 1983. The hydrodynamics of particle clusters and sediment entrainment in coarse alluvial channels. *Sedimentology*, 30: 137-143.
- Bridge, J.S. 1978. Origin of horizontal lamination under turbulent boundary conditions. *Sedimentary Geology*, 20: 1-16.
- Bridge, J.S., and Best, J.L. 1988. Flow, sediment transport and bedform dynamics over the transition from dunes to upper-stage plane beds: implications for the formation of planar laminae. *Sedimentology*, 35: 753-763.

- Brown, R.J.E. 1978. Permafrost: Plate 32. In Hydrological Atlas of Canada, Ottawa, Fisheries and Environment Canada.
- Burn, C.R. 1987. Notes on features visible from the highway between Stewart Crossing and Mayo. In Guidebook to Quaternary Research in Yukon. Edited by S.R. Morison and C.A.S. Smith. XII INQUA Congress, Ottawa, Canada. National Research Council of Canada, Ottawa, pp.40.
- Burn, C.R. 1990. Implications for Palaeoenvironmental Reconstruction of Recent Ice-wedge development at Mayo, Yukon Territory. Permafrost and Periglacial Processes, 1: 3-14.
- Burn, C.R. and Friele, P.A. 1989. Geomorphology, vegetative succession, soil characteristics and permafrost in retrogressive thaw slumps near Mayo, Yukon Territory. Arctic, 42: 31-40.
- Burn, C.R. and Michel, F.A. 1988. Evidence for recent temperature-induced water migration into permafrost from the tritium content of ground ice near Mayo, Yukon Territory, Canada. Canadian Journal of Earth Sciences, 25: 909-915.
- Burn, C.R., Michel, F.A., and Smith, M.W. 1986. Stratigraphic, isotopic and mineralogic evidence for an early Holocene thaw unconformity at Mayo, Yukon Territory. Canadian Journal of Earth Sciences, 23: 794-803.
- Cairnes, D.D. 1916. Mayo Area. Sum. Rept. for 1915. In Yukon Territory, Selected Field Reports of the Geological Survey of Canada 1898 to 1933. Edited by H.S. Bostock. Geological Survey of Canada, Memoir 284, pp. 381-407.
- Campbell, R.B. 1967. Geology of the Glenlyon map-area, Yukon Territory. Geological Survey of Canada Memoir 352, 92p.
- Cant, D.J., and Walker, R.G. 1978. Fluvial processes and facies sequences in the sandy braided South Saskatchewan River, Canada. Sedimentology, 25: 625-648.
- Cheel, R.J. 1990. Horizontal lamination and the sequence of bed phases and stratification under upper-flow-regime conditions. Sedimentology, 37: 517-529.
- Cheel, R.J., and Middleton, G.V. 1986. Horizontal laminae formed under upper flow regime plane bed conditions. Journal of Geology, 94: 489-504.
- Church, M. 1983. Pattern of instability in a wandering gravel bed channel. In Modern and Ancient Fluvial Systems. Edited by J.D. Collinson and J. Lewin. Special Publication of the International Association of Sedimentologists, 6: 169-180.
- Cockfield, W.E. 1919. Mayo Area. Sum.Rept. for 1918. In Yukon Territory, Selected Field Reports of the Geological Survey of Canada 1898 to 1933. Edited by H.S. Bostock. Geological Survey of Canada, Memoir 284, pp. 461-477.
- Cockfield, W.E. 1920. Mayo Area. Sum. Rept for 1919. In Yukon Territory, Selected Field Reports of the Geological Survey of Canada 1898 to 1933. Edited by H.S. Bostock. Geological Survey of Canada, Memoir 284, pp. 483-487.
- Cockfield, W.E. 1921. Silver-lead deposits of the Keno Hill Area, Mayo District. Sum. Rept. for 1920. In Yukon Territory, Selected Field Reports of the Geological Survey of Canada 1898 to 1933. Edited by H.S. Bostock. Geological Survey of Canada, Memoir 284, pp. 488-493.

- Cockfield, W.E. 1924. Geology and Ore Deposits of Keno Hill, Mayo District. Sum. Rept. for 1923. *In* Yukon Territory, Selected Field Reports of the Geological Survey of Canada 1898 to 1933. *Edited by* H.S. Bostock. Geological Survey of Canada, Memoir 284, pp. 508-527.
- Collinson, J.D. 1970. Bedforms of the Tana River, Norway. *Geografiska Annaler*, **52A**: 31-56.
- Cwynar, L.C., Schweger, C.E. and Matthews, J.V. Jr. 1987. Quaternary Flora and Fauna of Yukon. *In* Guidebook to Quaternary Research in Yukon. *Edited by* S.R. Morison and C.A.S. Smith. XII INQUA Congress, Ottawa, Canada. National Research Council of Canada, Ottawa, pp. 29-30.
- Denton, G.H. and Stuiver, M. 1967. Late Pleistocene glacial stratigraphy and chronology, northeastern St. Elias Mountains, Yukon Territory, Canada. *Geological Society of America Bulletin*, **78**: 485-510.
- Desloges, J.R. and Church, M. 1987. Channel and floodplain facies in a wandering gravel-bed river. *In* Recent Developments in Fluvial Sedimentology. *Edited by* F.G. Ethridge, R.M. Flores and M.D. Harvey. Society of Economic Paleontologists and Mineralogists, Special Publication 39, pp.99-109.
- Domack, E.W., and Lawson, D.E. 1985. Pebble fabric in an ice-rafted diamict. *Journal of Geology*, **93**: 577-591.
- Drake, L.D. 1974. Till fabric control by clast shape. *Geological Society of America Bulletin*, **85**: 247-250.
- Dreimanis, A. 1976. Tills: their origin and properties. *In* Glacial Till. *Edited by* R.F. Legget. Royal Society of Canada Special Publication 12, pp. 11-49.
- Dreimanis, A. 1982. Work Group (1) - Genetic classification of tills and criteria for their differentiation: Progress report on activities 1977-1982, and definitions of glaciogenic terms. *In* INQUA Commission and lithology of Quaternary deposits, Report on activities 1977-1982, *Edited by* Ch. Schluchter. ETH-Zurich, pp. 12-31.
- Dreimanis, A. 1988. Tills: their genetic terminology and classification. *In* Genetic Classification of Glaciogenic Deposits, *Edited by* R.P. Goldthwait and C.L. Matsch, pp. 17-83.
- Dyck, W., Lowden, J.A., Fyles, J.G., and Blake, W., Jr. 1966. Geological Survey of Canada, Radiocarbon dates V, Paper 66-48, pp. 19.
- Edwards, M.B. 1986. Glacial Environments. *In* Sedimentary Environments and Facies, Second Edition. *Edited by* H.G. Reading. Blackwell Scientific Publications, Oxford, pp. 445-470.
- Elson, J.A. 1961. The geology of tills. *In* Proceedings of 14th Canadian Soil Mechanics Conference. *Edited by* E. Penner and J. Butler. N.R.C. Canada, Assoc. Comm. and Snow Mechanics. Techn. Memor., **69**, pp. 5-36.
- Elson, J.A. 1988. Comments on glacioteconite, deformation till, and comminution till. *In* Genetic Classification of Glaciogenic Deposits, *Edited by* R.P. Goldthwait and C.L. Matsch, pp. 85-88.
- Environment Canada. 1982. Canadian Climate Normals. Temperature and Precipitation, The North - Y.T. and N.W.T. Atmospheric Environment Service, Ottawa, Ontario, 55p.
- Eyles, N. 1979. Facies of supraglacial sedimentation on Icelandic and Alpine temperate glaciers. *Canadian Journal of Earth Sciences*, **16**: 1341-1362.

- Eyles, N., Eyles, C.H., and Miall, A.D. 1983. Lithofacies types and vertical profile models; an alternative approach to the description and environmental interpretation of glacial diamict and diamictite sequences. *Sedimentology*, 30: 393-410.
- Eyles, N., and Miall, A.D. 1984. Glacial Facies. *In* *Facies Models*, second edition. *Edited by* R.G. Walker. Geoscience Canada, Reprint Series 1, pp. 15-38.
- Eynon, G. and Walker, R.G. 1974. Facies relationships in Pleistocene outwash gravels, southern Ontario: a model for bar growth in braided rivers. *Sedimentology*, 21: 43-70.
- Fecht, K.R. and Tallman, A.M. 1977. Bergmounds along the western margin of the channeled scablands, south central Washington; Abstract with Program, Geological Society of America, 10: p 400.
- Ferguson, R. and Werritty, A. 1983. Bar development and channel changes in gravelly River Feshie, Scotland. *In* *Modern and Ancient Fluvial Systems*. *Edited by* J.D. Collinson and J. Lewin. Special Publication of the International Association of Sedimentologists, 6: 181-193.
- Foscolos, A.E., Rutter, N.W. and Hughes, O.L. 1977. The use of pedological studies in interpreting the Quaternary history of central Yukon Territory. *Geological Survey of Canada Bulletin* 271, 48p.
- Frostick, L.E., Lucas, P.M. and Reid, I. 1984. The infiltration of fine matrices into coarse grained alluvial sediments and its implication for stratigraphic interpretation. *Journal of the Geological Society of London*, 141: 955-965.
- Gabrielse, H., Tempelman-Kluit, D.J., Blusson, S.L. and Campbell, R.B. 1977. Macmillan River, Yukon-District of MacKenzie-Alaska, Map 1398A. Geological Survey of Canada, Department of Energy Mines and Resources.
- Goldthwait, R.P. 1971. Till: a symposium. Ohio State University Press, Columbus, Ohio.
- Green, L.H. 1958. McQuesten Lake and Scougale Creek map-areas, Yukon Territory (106 D/3 and 106 D/2). Geological Survey of Canada, Paper 58-4, 5p.
- Green, L.H., and McTaggart, K.C. 1960. Structural studies in the Mayo District, Yukon Territory. *Proceedings of the Geological Association of Canada*, 12: 119-134.
- Green, L.H. and Roddick, J.A. 1962. Dawson, Larsen Creek, and Nash Creek map-areas, Yukon Territory. Geological Survey of Canada, Paper 62-7, 20p.
- Gustavson, T.C. 1978. Bedforms and stratification of modern gravel meander lobes, Nueces River, Texas. *Sedimentology*, 25: 401-426.
- Haldorsen, S. 1981. Grain-size distribution of subglacial till and its relation to glacial crushing and abrasion. *Boreas*, 10: 91-105.
- Haldorsen, S. 1982. The genesis of tills from Astadalen, southeastern Norway. *Norsk Geol. Tidsskr.*, 62: 11-32.
- Haldorsen, S. and Shaw, J. 1982. The problem of recognizing meltout till. *Boreas*, 11: 261-269.
- Hallet, B. 1981. Glacial abrasion and sliding: their dependence on the debris concentration in basal ice. *Annals of Glaciology*, 2: 23-28.

- Hamilton, D. and Bischoff, J.C. 1984. Uranium series dating of fossil bones from the Canyon Creek vertebrate locality in Central Alaska. *United States Geological Survey, Circular* 939, pp. 26-29.
- Harms, J.C, Southard, J.B., and Walker, R.G. 1982. Structures and sequences in clastic rocks. *Society of Economic Paleontologists and Mineralogists. Short Course No.9*, 239p.
- Harms, J.C., and Fahnestock, R.K. 1965. Stratification, Bed Forms, and Flow Phenomena (with an example from the Rio Grande). *In Primary Sedimentary Structures and their Hydrodynamic Interpretations. Edited by G.V. Middleton. Society of Economic Paleontologists and Mineralogists, Special Publication 12*, pp. 84-115.
- Harrison, P.W. 1957. A clay-till fabric; its character and origin. *Journal of Geology*, **65**: 275-303
- Hein, F.J. 1984. Deep sea and fluvial braided channel conglomerates: a comparison of two case studies. *In Sedimentology of Gravels and Conglomerates. Edited by E.H. Koster and R.J.Steel. Canadian Society of Petroleum Geologists, Memoir 10*, pp. 33-49.
- Hein, F.J., and Walker, R.G. 1977. Bar evolution and development of stratification in the gravelly, braided Kicking Horse River, British Columbia. *Canadian Journal of Earth Sciences*, **14**: 562-570.
- Hughes, O.L. 1983a. Surficial geology and geomorphology, Big Kaizas Lake Yukon Territory. *Geological Survey of Canada, Department of Energy Mines and Resources, Map 2-1982*.
- Hughes, O.L. 1983b. Surficial geology and geomorphology, Grey Hunter Peak, Yukon Territory. *Geological Survey of Canada, Department of Energy Mines and Resources, Map 3-1982*.
- Hughes, O.L. 1983c. Surficial geology and geomorphology, Janet Lake, Yukon Territory. *Geological Survey of Canada, Department of Energy Mines and Resources, Map 4-1982*.
- Hughes, O.L. 1983d. Surficial geology and geomorphology, Mount Edwards, Yukon Territory. *Geological Survey of Canada, Department of Energy Mines and Resources, Map 5-1982*.
- Hughes, O.L., Campbell, R.B., Muller, J.E. and Wheeler, J.O. 1969. Glacial limits and flow patterns, Yukon Territory, south of 65 degrees North latitude. *Geological Survey of Canada, Paper 68-34*, 9p.
- Hughes, O.L., Harrington, C.R., Janssens, J.A., Matthews, J.V. Jr., Morlan, R.E., Rutter, N.W., and Schweger, C.E. 1981. Upper Pleistocene stratigraphy, paleoecology, and archaeology of the Northern Yukon Interior, Eastern Beringia. 1. Bonnet Plume Basin. *Arctic*, **34**: 329-365.
- Hughes, O.L., Matthews, J.V. Jr., and Schweger, C.E. 1987. Stop 11: Mayo Indian Village Section. *In Guidebook to Quaternary Research in Yukon. Edited by S.R. Morison and C.A.S. Smith. XII INQUA Congress, Ottawa, Canada. National Research Council of Canada, Ottawa*, pp.42-44.
- Hughes, O.L., Rutter, N.W. and Clague, J.J. 1989. Yukon Territory (Quaternary stratigraphy and history, Cordilleran Ice Sheet). *In Quaternary Geology of Canada and Greenland. Edited by R.J. Fulton. Geological Survey of Canada, Geology of Canada, No. 1*.

- Jackson, L.E., Jr., Barendregt, R., Irving, E., and Ward, B. 1990. Magnetostratigraphy of early to middle Pleistocene basalts and sediments, Fort Selkirk area, Yukon Territory. *In* Current Research, part E, Geological Survey of Canada, Paper 90-1E, pp. 277-286.
- Jopling, A.V. 1965. Laboratory Study of the Distribution of Grain Sizes in Cross-Bedded Deposits. *In* Primary Sedimentary Structures and their Hydrodynamic Interpretations. *Edited by* G.V. Middleton. Society of Economic Paleontologists and Mineralogists, Special Publication 12, pp. 53-65.
- Jopling, A.V., and Walker, R.G. 1968. Morphology and origin of ripple-drift cross-laminations, with examples from the Pleistocene of Massachusetts. *Journal of Sedimentary Petrology*, **38**: 971-984.
- Keele, J. 1906. Upper Stewart River Region. Ann. Rept., vol XVI, pt. C (1905). *In* Yukon Territory, Selected Field Reports of the Geological Survey of Canada 1898 to 1933. *Edited by* H.S. Bostock. Geological Survey of Canada, Memoir 284, pp. 160-172.
- Keele, J. 1905. The Duncan Creek Mining District. Sum. Rept. for 1904. *In* Yukon Territory, Selected Field Reports of the Geological Survey of Canada 1898 to 1933. *Edited by* H.S. Bostock. Geological Survey of Canada, Memoir 284, pp. 127-143.
- Klassen, R.W. 1978. A unique stratigraphic record of late Tertiary-Quaternary events in Southeastern Yukon. *Canadian Journal of Earth Sciences*, **15**: 1884-1886.
- Klassen, R.W. 1987. The Tertiary-Pleistocene stratigraphy of the Liard Plain, southeastern Yukon Territory. Geological Survey of Canada, Paper 86-17, 16p.
- Kruger, J. 1984. Clasts with stoss-lee form in lodgement tills: A discussion. *Journal of Glaciology*, **30**: 241-243.
- Kruger, J. 1979. Structures and textures in till indicating subglacial deposition. *Boreas*, **8**: 323-340.
- Langford, R., and Bracken, B. 1987. Medano Creek, Colorado, as a model for upper-flow-regime fluvial deposition. *Journal of Sedimentary Petrology*, **57**: 863-870.
- Lawson, D.E. 1979a. Sedimentological analysis of the western terminus region of the Matanuska Glacier, Alaska. Cold Regions Research and Engineering Laboratory. Report. 79-9.
- Lawson, D.E. 1979b. A comparison of the pebble orientations in ice and deposits of the Matanuska Glacier, Alaska. *Journal of Geology*, **87**: 629-645.
- Lawson, D.E. 1981a. Sedimentologic characteristics and classification of depositional processes and deposits in the glacial environment. Cold Regions Research and Engineering Laboratory. Report. 81-27.
- Lawson, D.E. 1981b. Distinguishing characteristics of diamictons at the margin of the Matanuska Glacier, Alaska. *Annals of Glaciology*, **2**: 78-84.
- Lawson, D.E. 1982. Mobilization, movement and deposition of active subaerial sediment flows, Matanuska Glacier, Alaska. *Journal of Geology*, **90**: 279-300.
- Lawson, D.E. 1988. Glacigenic resedimentation: classification concepts and application to mass-movement processes and deposits. *In* Genetic Classification of Glacigenic Deposits, *Edited by* R.P. Goldthwait and C.L. Matsch. Rotterdam, Balkema, pp. 147-169.

- Leopold, L.B., and Wolman, M.G. 1957. River channel patterns: braided, meandering and straight. U.S.G.S. Professional Paper 282B, 39-85.
- Lerbekmo, J.R., Westgate, J.A., Smith, D.G.W. and Denton, G. 1975. New data on the character and history of the White River volcanic eruption. *In Quaternary Studies. Edited by R.P. Suggate and M.M. Creswell. The Royal Society of New Zealand Bull., 13, pp. 203-209.*
- Levson, V.M., and Rutter, N.W. 1986. A facies approach to the stratigraphic analysis of late Wisconsinan sediments in the Portal Creek area, Jasper National Park, Alberta. *Geographie physique et Quaternaire, 40: 129-144.*
- Levson, V.M., and Rutter, N.W. 1988. A lithofacies analysis and interpretation of depositional environments of montane glacial diamictites, Jasper, Alberta, Canada. *In Genetic Classification of Glacigenic Deposits. Edited by R. P. Goldthwait and C. L. Matsch. Rotterdam, Balkema, pp. 117-140.*
- Lowe, D.R. 1979. Sediment gravity flows: Their classification and some problems of application to natural flows and deposits. *SEPM Special Publication 27, pp. 75-82.*
- Lowe, D.R. 1982. Sediment gravity flows: II. Depositional models with special reference to the deposits of high density turbidity currents. *Journal of Sedimentary Petrology, 52: 279-297.*
- Marcussen, I. 1975. Distinguishing between lodgement till and flow till in Weichsalian deposits. *Boreas, 4: 113-123.*
- Mark, D.M. 1973. Analysis of axial orientation data, including till fabrics. *Geological Society of America Bulletin, 84: 1369-1374.*
- Mark, D.M. 1974. On the interpretation of till fabrics. *Geology, 2: 101-104.*
- Matthews, J.V. Jr., Schweger, C.E., and Hughes, O.L. 1990. Plant and Insect Fossils from the Mayo Indian Village Section (Central Yukon): New Data on Middle Wisconsinan Environments and Glaciations. *Geographie physique et Quaternaire, 44: 15-26.*
- McConnell, R.G. 1901. Exploration of Tintina Valley from the Klondike to Stewart River. Sum. Rept. for 1900. *In Yukon Territory, Selected Field Reports of the Geological Survey of Canada 1898 to 1933. Edited by H. S. Bostock. Geological Survey of Canada, Memoir 284, pp. 26-29.*
- McKee, E.D. 1965. Experiments on Ripple Lamination. *In Primary Sedimentary Structures and their Hydrodynamic Interpretations. Edited by G. V. Middleton. Society of Economic Paleontologists and Mineralogists, Special Publication 12, pp. 66-83.*
- McTaggart, K.C. 1950. Keno and Galena Hills, Yukon Territory. *Geological Survey of Canada Preliminary Maps 50-20A and 50-20B.*
- McTaggart, K.C. 1960. The geology of Keno and Galena Hills, Yukon Territory. *Geological Survey of Canada Bulletin 58, 37p.*
- Miall, A.D. 1987. Recent developments in the study of fluvial facies models. *In Recent Developments in Fluvial Sedimentology. Edited by F.G. Ethridge, R.M. Flores and M.D. Harvey. Society of Economic Paleontologists and Mineralogists, Special Publication 39, pp. 2-9.*
- Miall, A.D. 1985. Architectural-element analysis: A new method of facies analysis applied to fluvial deposits. *Earth Science Reviews, 22: 261-308.*

- Miall, A.D. 1978. Lithofacies types and vertical profile models in braided river deposits: a summary. *In* *Fluvial Sedimentology*. Edited by A. D. Miall. Canadian Society of Petroleum Geologists, Memoir 5, pp. 597-604.
- Morison, S.M. and Hein, F.J. 1987. Sedimentology of the White Channel gravels, Klondike area, Yukon Territory: fluvial deposits of a confined valley. *In* *Recent Developments in Fluvial Sedimentology*. Edited by F.G. Ethridge, R.M. Flores and M.D. Harvey. Society of Economic Paleontologists and Mineralogists, Special Publication 39, pp.205-216.
- Morlan, R.E. 1980. Taphonomy and archaeology in the Upper Pleistocene of the northern Yukon Territory: a glimpse of the peopling of the New World. National Museums of Canada, National Museum of Canada, Mercury Series, Archaeological Survey of Canada, Paper 94, 398p.
- Muller, E.H. 1983a. Dewatering during lodgement of till. *In* *Tills and Related Deposits*. Edited by E. B. Evenson, Ch. Schluchter, and J. Rabassa. Rotterdam, Balkema, pp. 13-18.
- Muller, E.H. 1983b. Till genesis and the glacier sole. *In* *Tills and Related Deposits*. Edited by E. B. Evenson, Ch. Schluchter, and J. Rabassa. Rotterdam, Balkema, pp. 19-22.
- Nardin, T.R., Hein, F.J., Gorsline, D.S. and Edwards, B.D. 1979. A review of mass-movement processes, sediment and acoustic characteristics, and contrasts in slope and base-of-slope systems versus canyon-fan-basin floor systems. SEPM Special Publication 27, pp. 61-73.
- Neill C.R. 1973. Hydraulic and morphologic characteristics of Athabasca River near Fort Assiniboine. Alberta Research Council, Edmonton. Highway River Engineering Division Report REH/73/3, 23p.
- Oswald, E.T. and Senyk, J.P. 1977. Ecoregions of Yukon Territory. Fisheries and Environment Canada, 115p.
- Ovenshine, A.T. 1970. Observations of iceberg rafting in Glacier Bay, Alaska, and the identification of ancient ice-rafted deposits. *Geological Society of America Bulletin*, **81**: 891-894.
- Paola, C., Wiele, S.M., and Reinhart, M.A. 1989. Upper-regime parallel lamination as the result of turbulent sediment transport and low amplitude bedforms. *Sedimentology*, **36**: 47-60.
- Rampton, V.N. 1971. Late Pleistocene glaciations in the Snag-Klutlan area, Yukon Territory. *Arctic*, **24**: 277-300.
- Reid, I., Brayshaw, A.C., and Frostick, L.E. 1984. An electromagnetic device for automatic detection of bedload motion and its field applications. *Sedimentology*, **31**: 269-276.
- Roddick, J.R. 1967. Tintina Trench. *Journal of Geology*, **75**: 23-33.
- Rubin, D.M. 1987. Cross-bedding, bedforms and paleocurrents. SEPM, Concepts in Sedimentology and Paleontology, Volume 1, 187p.
- Rust, B.R. 1972a. Structure and process in a braided river. *Sedimentology*, **18**: 221-245.
- Rust, B.R. 1975. Fabric and Structure in glaciofluvial gravels. *In* *Glaciofluvial and Glaciolacustrine Sedimentation*. Edited by A. V. Jopling and B. C. McDonald. Society of Economic Paleontologists and Mineralogists, Special Publication 23, pp. 238-248.

- Rust, B.R. 1984. Proximal braidplain deposits in the Middle Devonian Malbaie Formation of Eastern Gaspé, Quebec, Canada. *Sedimentology*, **31**: 675-695.
- Rust, B.R., and Koster, E.H. 1984. Coarse Alluvial Deposits. *In* *Facies Models*, second edition. Edited by R.G. Walker. Geoscience Canada, Reprint Series 1, pp. 53-70.
- Rutter, N.W., Foscolos, A.E., and Hughes, O.L. 1978. Climatic trends during the Quaternary in central Yukon based upon pedological and geomorphological evidence. *In* *Quaternary Soils*, Edited by Mahaney, W.C., Geo Abstracts, Norwich, U.K. pp.309-359.
- Shaw, J. 1977. Till body morphology and structure related to glacier flow. *Boreas*, **6**: 189-201.
- Shaw, J. 1979. Genesis of the Sveg tills and Rogen moraines of central Sweden: A model of basal melt out. *Boreas*, **8**: 409-426.
- Shaw, J. 1982. Melt-out till in the Edmonton area, Alberta, Canada. *Canadian Journal of Earth Sciences*, **19**: 1548-1569.
- Shaw, J. 1983. Forms associated with boulders in melt-out till. *In* *Tills and Related Deposits*. Edited by E. B. Evenson, C. Schluchter, and J. Rabassa. Rotterdam, Balkema, pp. 3-12.
- Shaw, J. 1985. Subglacial and ice marginal environments. *In* *Glacial Sedimentary Environments*. Edited by G. M. Ashley, J. Shaw and N. D. Smith. Society of Economic Paleontologists and Mineralogists, Short Course 16, pp. 7-84.
- Shaw, J. 1987. Glacial sedimentary processes and environmental reconstruction based on lithofacies. *Sedimentology*, **34**: 103-116.
- Shaw, J. 1988. Sublimation till. *In* *Genetic Classification of Glacigenic Deposits*, Edited by R.P. Goldthwait and C.L. Madsch, pp. 141-142.
- Smith, C.A.S., Tarnocai, C. and Hughes, O.L. 1986. Pedological investigations of Pleistocene glacial drift sequences in the central Yukon. *Geographie physique et Quaternaire*, **40**: 129-137.
- Smith, N.D. 1971. Pseudo-planar stratification produced by very low amplitude sand waves. *Journal of Sedimentary Petrology*, **41**: 903-915.
- Smith, N.D. 1974. Sedimentology and bar formation in the Upper Kicking Horse River, a braided outwash stream. *Journal of Geology*, **81**: 205-223.
- Smith, N.D. 1985. Proglacial Fluvial Environment. *In* *Glacial Sedimentary Environments*. Edited by G.M. Ashley, J. Shaw and N.D. Smith. Society of Economic Paleontologists and Mineralogists, Short Course 16, pp. 84-134.
- Smith, S.A. 1989. Sedimentation in a meandering gravel-bed river: the River Tywi, South Wales. *Geological Journal*, **24**: 193-204.
- Smith, S.A. 1990. The sedimentology and accretionary styles of an ancient gravel-bed stream: the Budleigh Salterton Pebble Beds (Lower Triassic), southwest England. *Sedimentary Geology*, **67**: 199-219.
- Tarnocai, C. 1987. Stop 13: Stewart Neosol on Terminal McConnell Moraine. *In* *Guidebook to Quaternary Research in Yukon*. Edited by S.R. Morison and C.A.S. Smith. XII INQUA Congress, Ottawa, Canada. National Research Council of Canada, Ottawa, pp. 45.

- Tarnocai, C., Smith, C.A.S., and Hughes, O.L. 1985. Soil development on Quaternary deposits of various ages in central Yukon Territory. *In* Current Research, Part A. Geological Survey of Canada Paper 85-1A: 229-238.
- Tarnocai, C. and Schweger, C.E. 1991. Late Tertiary and early Pleistocene paleosols in northwestern Canada. *Arctic*, **44**: 1-11.
- Tempelman-Kluit, D. 1980. Evolution of Physiography and Drainage in Southern Yukon. *Canadian Journal of Earth Sciences*, **17**: 1189-1203.
- Teichert, C. 1958. Concepts of facies. *Bulletin of the American Association of Petroleum Geologists*, **42**: 2718-2744.
- Thomas, G.S.P., and Connell, R.J. 1984. Iceberg drop, dump and grounding structures from Pleistocene glacio-lacustrine sediments, Scotland. *Journal of Sedimentary Petrology*, **55**: 243-249.
- Trautman, M.A., and Walton, A. 1962. Isotopes, Inc. Radiocarbon Measurements II. *Radiocarbon*, **4**: 35-42.
- Varnes, D.J. 1978. Slope movement types and processes. *In* Landslides, analysis and control. *Edited by* Schuster, R.L. and Krizek, R.J. Washington, D.C. National Academy of Science, pp.11-33.
- Vernon, P. and Hughes, O.L. 1966. Surficial geology, Dawson, Larsen Creek, and Nash Creek map-areas, Yukon Territory (116B and 116C east half, 116A and 106D). Geological Survey of Canada, Bulletin 136, 25p.
- Wahl, H.E., Fraser, D.B., Harvey, R.C., and Maxwell, J.B. 1987. Climate of Yukon. Climatological Studies, Number 40. Environment Canada, Atmospheric Environment Service, 323p.
- Walker, R.G., and Cant, D.J. 1984. Sandy Fluvial Systems. *In* Facies Models, second edition. *Edited by* R.G. Walker. Geoscience Canada, Reprint Series 1, pp. 71-90.
- Walker, R.G. 1984. Turbidites and Associated Coarse Clastic Deposits. *In* Facies Models, second edition. *Edited by* R.G. Walker. Geoscience Canada, Reprint Series 1, pp 15-38.
- Ward, B.C. 1993. Quaternary Geology of Glenlyon map area (105L), Yukon Territory. Unpublished Ph.D. Thesis, University of Alberta, 232p.
- Westgate, J.A. 1989. Isothermal plateau fission-track ages of hydrated glass shards from silicic tephra beds. *Earth and Planetary Science Letters*, **95**:226-234.
- Westgate, J.A., Stemper, B.A. and Pewe, T.L. 1990. A 3 m.y. record of Pliocene-Pleistocene loess in interior Alaska. *Geology*, **18**: 858-861.
- Whiting, P.J., Dietrich, W.E., Leopold, L.B., Drake, T.G., and Shreve, R.L. 1988. Bedload sheets in heterogeneous sediment, *Geology*, **16**: 105-108.
- Wintle, A.G. and Westgate, J.A. 1986. Thermoluminescence age of Old Crow tephra in Alaska. *Geology* **14**: 594-597.
- Zingg, T. 1935. Beitrage zur Schatteranalyse. *Schweizerische Mineralogische und Petrographische Mitteilungen*, **15**:39-40.

APPENDIX 1A : Three dimensional pebble fabric data listing the mean lineation, dip and eigenvectors for all samples in the Mayo region.

Fabric #	Mean Lineation	Dip	S1	S2	S3
Facies 1 : Lodgement till (13 Fabrics)					
M-01 (860m)	053°	15°	0.83	0.11	0.06
M-03 (900m)	061°	14°	0.69	0.25	0.06
M-04 (900m)	066°	24°	0.86	0.08	0.06
M-04A (905m)	066°	14°	0.88	0.11	0.01
M-05 (1040m)	058°	12°	0.82	0.15	0.03
M-07 (1265m)	073°	17°	0.76	0.14	0.10
M-09 (780m)	058°	11°	0.81	0.15	0.04
M-26 (830m)	067°	15°	0.74	0.20	0.06
M-28 (900m)	070°	10°	0.84	0.15	0.01
I-20 (750m)	080°	12°	0.76	0.22	0.02
I-22 (700m)	074°	8°	0.81	0.18	0.01
I-23 (920m)	072°	17°	0.74	0.21	0.05
I-41 (920m)	059°	16°	0.79	0.18	0.03
Average	066°	14°	0.79	0.16	0.04
Mayo Section (9)	064°	15°	0.80	0.15	0.04
MIV Section (4)	071°	13°	0.78	0.20	0.04
Facies 2 : Meltout till (14 fabrics)					
M-02 (860m)	063°	11°	0.83	0.14	0.04
M-06 (1030m)	053°	12°	0.79	0.19	0.02
M-08 (1260m)	054°	23°	0.86	0.10	0.04
M-10 (1460m)	064°	14°	0.68	0.27	0.05
M-11 (1460m)	049°	14°	0.66	0.29	0.05
M-12 (1460m)	052°	12°	0.73	0.22	0.06
M-13 (1250m)	048°	18°	0.73	0.22	0.06
M-14 (1250m)	067°	16°	0.76	0.19	0.06
M-16 (490m)	013°	11°	0.85	0.14	0.02
M-27 (830m)	053°	12°	0.79	0.20	0.02
M-29 (900m)	071°	17°	0.77	0.19	0.05
I-21 (750m)	095°	9°	0.90	0.08	0.02
I-42 (920m)	095°	15°	0.71	0.26	0.03
I-43 (1255m)	086°	14°	0.69	0.29	0.03
Average	062°	14°	0.77	0.20	0.04
Mayo Section (11)	054°	14°	0.77	0.19	0.04
MIV Section (3)	092°	12°	0.77	0.21	0.03

Fabric #	Mean Lineation	Dip	S1	S2	S3
Facies 3 : Mass-movement (15 Fabrics)					
M-15 (490m)	176°	27°	0.62	0.31	0.08
I-44 (1255m)	293°	16°	0.70	0.27	0.03
I-45 (320m)	265°	13°	0.85	0.12	0.03
I-46 (240m)	272°	17°	0.68	0.27	0.05
T-24 (50m) (Lower)	065°	16°	0.62	0.33	0.05
T-25 (60m)	106°	16°	0.69	0.26	0.05
T-32 (60m)	284°	18°	0.61	0.35	0.04
T-33 (60m)	233°	20°	0.71	0.24	0.05
T-34 (110m)	283°	13°	0.68	0.29	0.03
T-35 (130m)	258°	18°	0.55	0.33	0.12
T-36 (150m)	248°	14°	0.77	0.19	0.04
T-37 (150m)	258°	17°	0.58	0.31	0.11
T-38 (180m)	260°	13°	0.68	0.29	0.03
T-39 (220m)	116°	17°	0.49	0.41	0.10
T-40 (500m)	291°	14°	0.73	0.22	0.05
Average	227°	17°	0.65	0.29	0.06
Mayo Section (1)	176°	27°	0.62	0.31	0.08
MIV Section (3)	277°	17°	0.74	0.22	0.04
Third Section, Lower (1)	065°	16°	0.62	0.33	0.05
Third Section, Upper (10)	234°	16°	0.65	0.29	0.06
Facies 4 : Massive and stratified matrix-filled gravels					
M-30 (20m)	92°	8°	0.97	0.02	0.01
M-31 (20m)	92°	7°	0.97	0.03	0.00

APPENDIX 1B : Unidirectional rose diagrams representing two dimensional pebble orientations in diamictons in the Mayo region. Sample statistics are the mean lineation, average pebble dip, and the primary, secondary and tertiary eigenvalues of each sample. N is the number of pebbles measured in each sample.

Facies 1 : Lodgement till (13 Fabrics)

M-01
Mean Lineation 053°
Dip 15°
S1 0.83
S2 0.11
S3 0.06



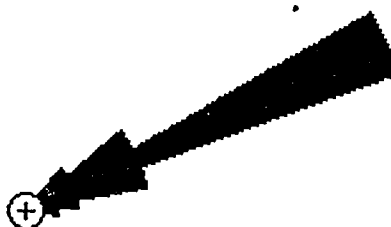
N = 50

M-03
Mean Lineation 061°
Dip 14°
S1 0.69
S2 0.25
S3 0.06



N = 50

M-04
Mean Lineation 066°
Dip 24°
S1 0.86
S2 0.08
S3 0.06



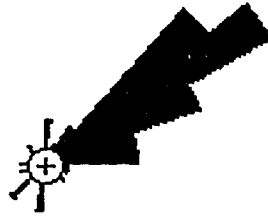
N = 25

M-04A
Mean Lineation 066°
Dip 14°
S1 0.88
S2 0.11
S3 0.01



N = 50

M-05
 Mean Lineation 058°
 Dip 12°
 S1 0.82
 S2 0.15
 S3 0.03



N = 50

M-07
 Mean Lineation 073°
 Dip 17°
 S1 0.76
 S2 0.14
 S3 0.10



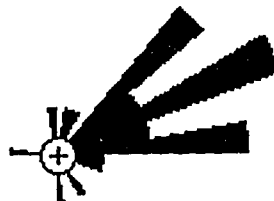
N = 50

M-09
 Mean Lineation 058°
 Dip 11°
 S1 0.81
 S2 0.15
 S3 0.04



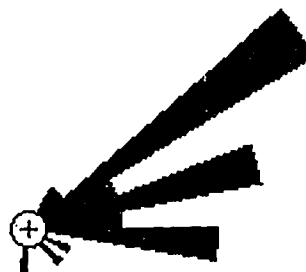
N = 50

M-26
 Mean Lineation 067°
 Dip 15°
 S1 0.74
 S2 0.20
 S3 0.06



N = 25

M-28
 Mean Lineation 070°
 Dip 10°
 S1 0.84
 S2 0.15
 S3 0.01



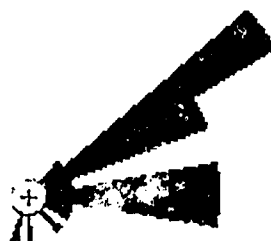
N = 25

I-20
Mean Lineation 080°
Dip 12°
S1 0.76
S2 0.22
S3 0.02



N = 25

I-22
Mean Lineation 074°
Dip 8°
S1 0.79
S2 0.18
S3 0.01



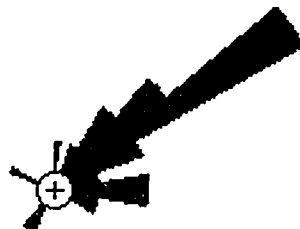
N = 25

I-23
Mean Lineation 072°
Dip 17°
S1 0.74
S2 0.21
S3 0.05



N = 25

I-41
Mean Lineation 059°
Dip 16°
S1 0.79
S2 0.18
S3 0.03



N = 25

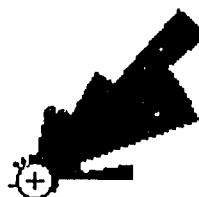
Facies 2 : Meltout till (14 fabrics)

M-02
 Mean Lineation 063°
 Dip 11°
 S1 0.83
 S2 0.14
 S3 0.04



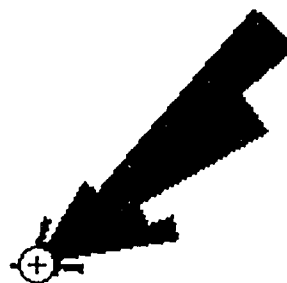
N = 50

M-06
 Mean Lineation 053°
 Dip 12°
 S1 0.79
 S2 0.19
 S3 0.02



N = 48

M-08
 Mean Lineation 054°
 Dip 23°
 S1 0.86
 S2 0.10
 S3 0.04



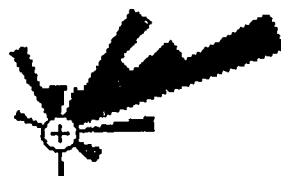
N = 50

M-10
 Mean Lineation 064°
 Dip 14°
 S1 0.68
 S2 0.27
 S3 0.05



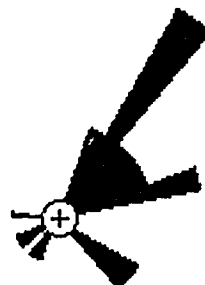
N = 50

M-11
Mean Lineation 049°
Dip 14°
S1 0.66
S2 0.29
S3 0.05



N = 25

M-12
Mean Lineation 052°
Dip 12°
S1 0.73
S2 0.22
S3 0.06



N = 25

M-13
Mean Lineation 048°
Dip 18°
S1 0.73
S2 0.22
S3 0.06



N = 25

M-14
Mean Lineation 067°
Dip 16°
S1 0.76
S2 0.19
S3 0.06



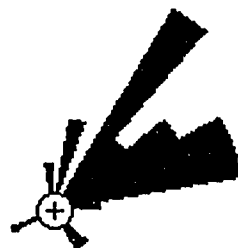
N = 25

M-16
Mean Lineation 013°
Dip 11°
S1 0.85
S2 0.14
S3 0.02



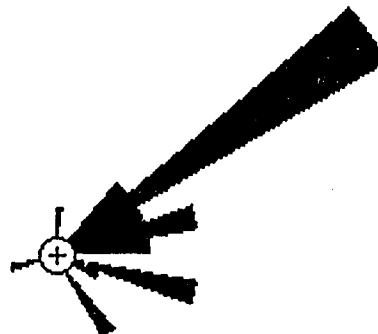
N = 25

M-27
 Mean Lineation 053°
 Dip 12°
 S1 0.79
 S2 0.20
 S3 0.02



N = 25

M-29
 Mean Lineation 071°
 Dip 17°
 S1 0.77
 S2 0.19
 S3 0.05



N = 25

I-21
 Mean Lineation 095°
 Dip 9°
 S1 0.90
 S2 0.08
 S3 0.02



N = 25

I-42
 Mean Lineation 095°
 Dip 15°
 S1 0.71
 S2 0.26
 S3 0.03



N = 25

I-43
 Mean Lineation 086°
 Dip 14°
 S1 0.69
 S2 0.29
 S3 0.03



N = 25

Facies 3 : Mass-movement (15 Fabrics)

M-15
 Mean Lineation 176°
 Dip 27°
 S1 0.62
 S2 0.31
 S3 0.08



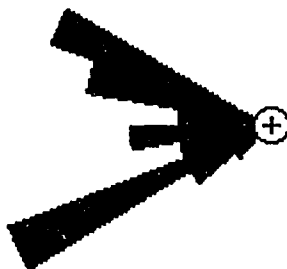
N = 25

I-44
 Mean Lineation 293°
 Dip 16°
 S1 0.70
 S2 0.27
 S3 0.03



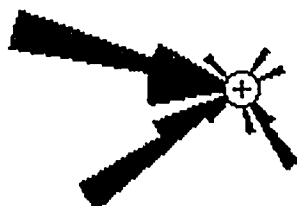
N = 25

I-45
 Mean Lineation 265°
 Dip 13°
 S1 0.85
 S2 0.12
 S3 0.03



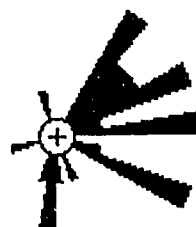
N = 25

I-46
 Mean Lineation 272°
 Dip 17°
 S1 0.68
 S2 0.27
 S3 0.05



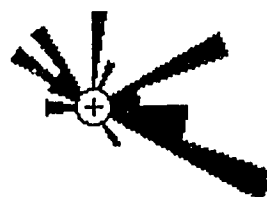
N = 25

T-24 (LOWER)
 Mean Lineation 065°
 Dip 16°
 S1 0.62
 S2 0.33
 S3 0.05



N = 25

T-25
 Mean Lineation 106°
 Dip 16°
 S1 0.69
 S2 0.26
 S3 0.05



N = 25

T-32
 Mean Lineation 284°
 Dip 18°
 S1 0.61
 S2 0.35
 S3 0.04



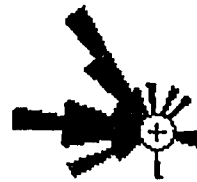
N = 25

T-33
 Mean Lineation 233°
 Dip 20°
 S1 0.71
 S2 0.24
 S3 0.05



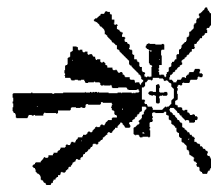
N = 25

T-34
 Mean Lineation 283°
 Dip 13°
 S1 0.68
 S2 0.29
 S3 0.03



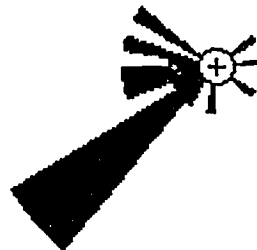
N = 25

T-35
 Mean Lineation 258°
 Dip 18°
 S1 0.55
 S2 0.33
 S3 0.12



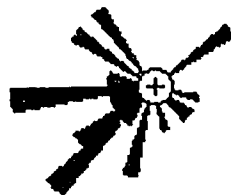
N = 25

T-36
 Mean Lineation 248°
 Dip 14°
 S1 0.77
 S2 0.19
 S3 0.04



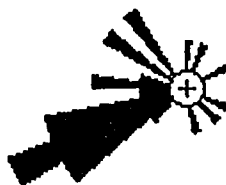
N = 25

T-37
 Mean Lineation 258°
 Dip 17°
 S1 0.58
 S2 0.31
 S3 0.11



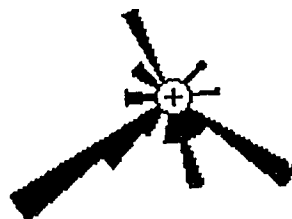
N = 25

T-38
 Mean Lineation 260°
 Dip 13°
 S1 0.68
 S2 0.29
 S3 0.03



N = 25

T-39
 Mean Lineation 116°
 Dip 17°
 S1 0.49
 S2 0.41
 S3 0.10



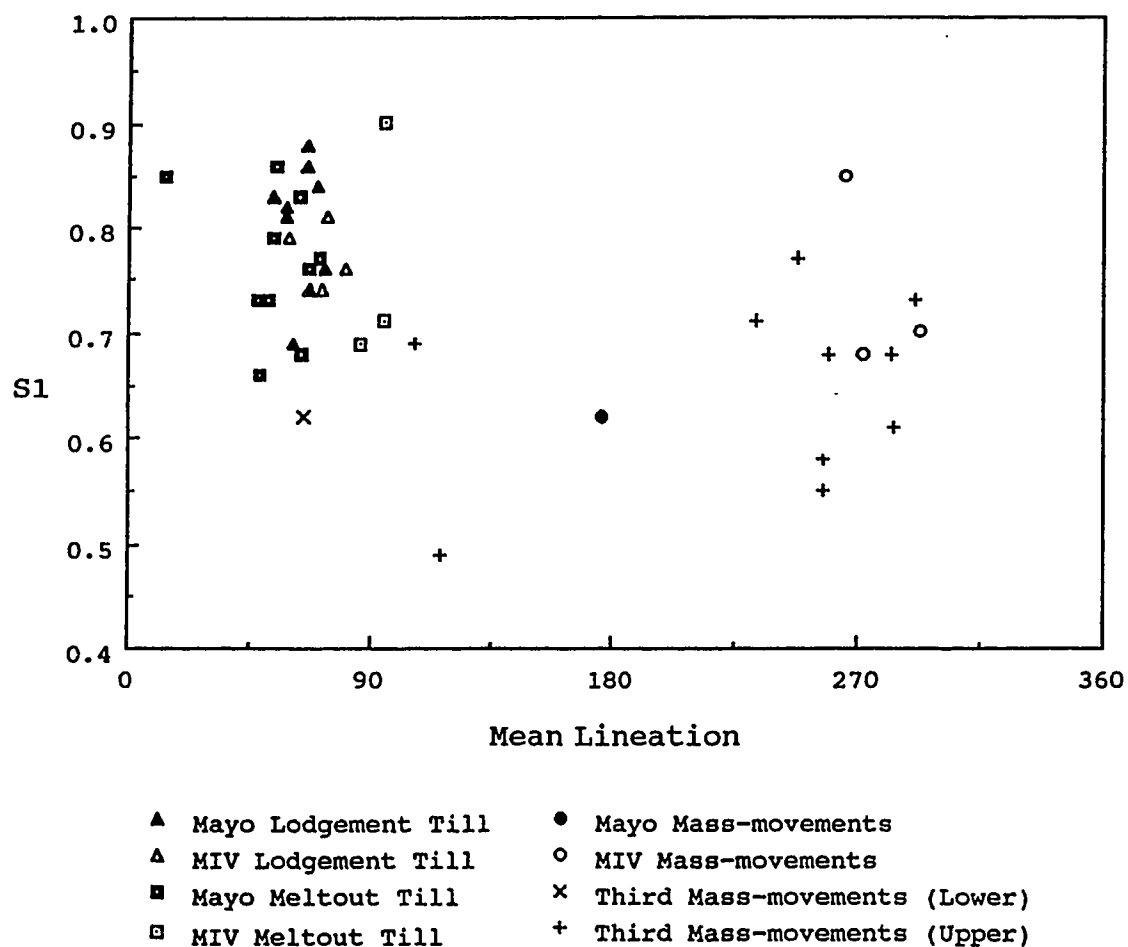
N = 25

T-40
 Mean Lineation 291°
 Dip 14°
 S1 0.73
 S2 0.22
 S3 0.05

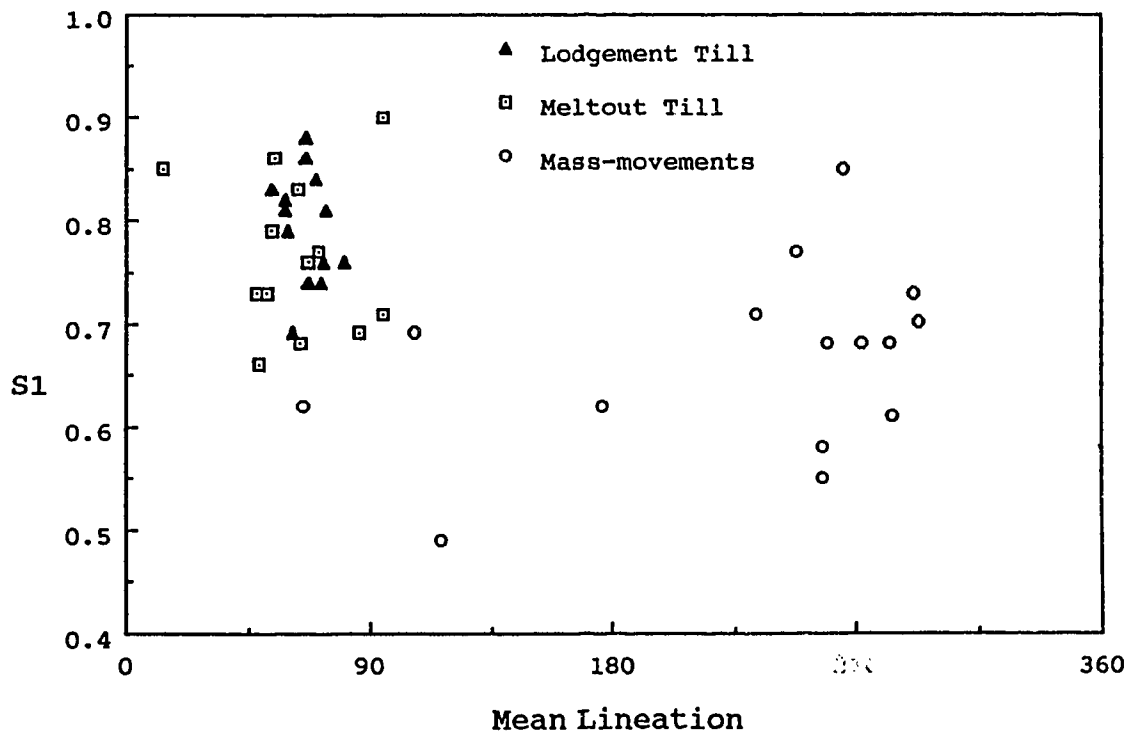


N = 25

APPENDIX 1C : Cumulative graphs of the primary eigenvalues plotted against the mean lineation of pebble fabrics in the Mayo region.



Graph illustrates the fabrics of each facies in the different sections.



This figure illustrates the fabrics of each facies in the Mayo Region.

**APPENDIX 2A : Grain size analysis, percentages of sand, silt and clay
from diamicton samples in the Mayo Region.**

Sample #	Sand	Silt	Clay
Facies 1 : Lodgement till (8 samples)			
HHT-88067, I, G	47.30	45.40	7.30
HHT-88157, M, G	47.00	41.30	11.80
HHT-88192, M	48.00	43.00	9.00
HHT-88205, M, G	38.00	51.50	10.50
HHT-88212, M, G	51.40	37.60	11.00
HHT-89305, I	56.20	33.90	9.90
HHT-89308, I	46.50	37.00	16.50
HHT-89318, I	47.50	40.40	12.20
Average	47.70	41.30	11.00
Facies 2 : Meltout till (25 samples)			
HHT-88068, I, G	47.10	45.90	7.00
HHT-88119, M, G	53.00	37.00	6.30
HHT-88121, M, G	59.00	33.50	7.50
HHT-88145, M	56.50	29.50	14.00
HHT-88147, M	54.50	34.50	11.00
HHT-88159, M, G	52.10	39.60	8.30
HHT-88180, M	31.50	55.00	13.50
HHT-88183, M	50.50	35.00	14.50
HHT-88184, M	63.00	35.50	11.50
HHT-88185, M	60.00	26.50	13.50
HHT-88189, M	50.50	33.30	16.20
HHT-88190, M	54.00	32.80	13.20
HHT-88193, M	51.50	38.50	12.00
HHT-88194, M	54.50	30.00	15.50
HHT-88206, M, G	49.70	41.40	8.90
HHT-88207, M, G	42.10	53.40	4.60
HHT-88208, M, G	57.80	30.40	11.80
HHT-88209, M, G	57.10	35.10	7.80
HHT-88219, M	57.50	30.50	12.00
HHT-88221, M	66.50	23.50	10.00
HHT-89306, I	48.00	43.50	8.50
HHT-89309, I	47.20	43.90	8.90
HHT-89311, I	46.50	43.00	10.50
HHT-89319, I	47.00	42.50	10.50
HHT-89320, I	45.50	44.80	9.70
Average	52.10	37.50	10.40

Sample #	Sand	Silt	Clay
Facies 3 : Mass-movement (38 samples)			
HHT-88012, I, G	43.20	51.40	5.40
HHT-88043, T, G	52.80	38.50	8.80
HHT-88044, T, G	37.80	51.30	11.00
HHT-88045, T, G	29.00	59.80	11.30
HHT-88046, T, G	27.50	61.00	11.60
HHT-88048, T, G	32.10	47.50	20.50
HHT-88049, T, G	50.00	43.60	6.40
HHT-88050, T, G	49.30	43.80	7.00
HHT-88051, T, G	47.70	44.00	8.30
HHT-88052, T, G	47.10	41.70	11.30
HHT-88063, I, G	39.40	54.90	5.70
HHT-88072, T	20.50	70.50	9.00
HHT-88073, T	33.50	50.00	16.50
HHT-88074, T	30.50	60.50	9.00
HHT-88075, T	30.00	61.80	8.20
HHT-88076, T	38.00	54.00	8.00
HHT-88077, T	49.50	40.50	10.00
HHT-88078, T	48.50	40.50	11.00
HHT-88079, T	45.00	46.00	9.00
HHT-88080, T	51.50	37.50	11.00
HHT-88081, T	42.00	46.00	12.00
HHT-88082, T	48.00	39.00	13.00
HHT-88083, T	44.50	41.50	14.00
HHT-88084, T	43.00	45.30	11.70
HHT-88085, T, G	21.20	65.60	13.30
HHT-88086, T, G	46.00	44.00	10.00
HHT-88087, T, G	48.70	42.60	8.70
HHT-88088, T, G	50.80	40.40	8.90
HHT-88116, M, G	63.00	32.20	4.80
HHT-88117, M, G	58.80	36.40	4.80
HHT-88118, M, G	57.70	37.00	5.30
HHT-88144, M	78.50	13.50	8.00
HHT-88156, M, G	59.60	33.10	7.40
HHT-88179, M	58.00	26.50	15.50
HHT-89307, I	57.00	35.80	7.30
HHT-89310, I	42.00	47.00	11.00
HHT-89313, I	46.00	46.00	8.00
HHT-89317, I	46.50	43.00	10.50
Average	42.90	43.90	13.20

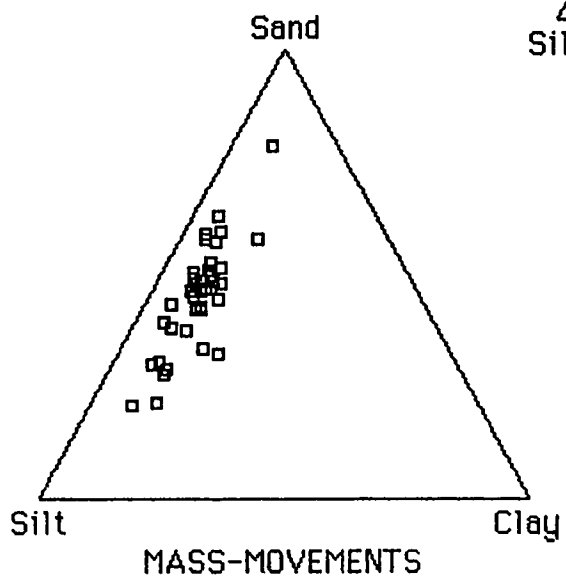
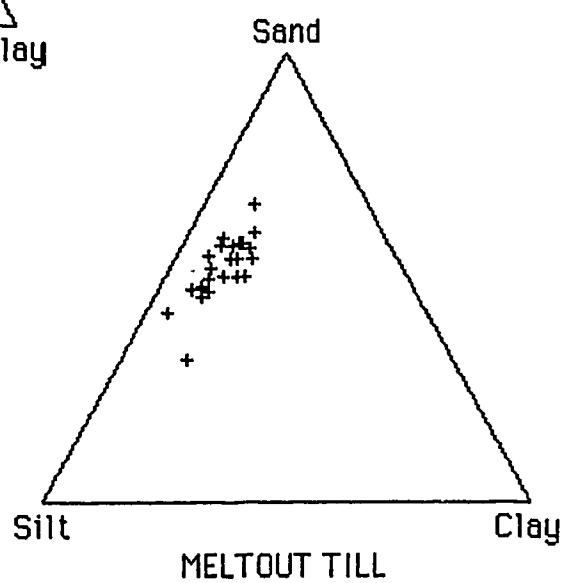
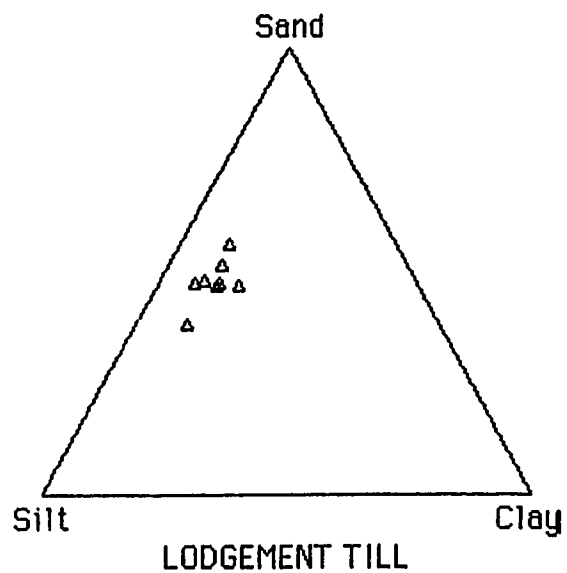
M = Mayo Section

I = Mayo Indian Village Section

T = Third Section

G = Samples analysed by the Geological Survey of Canada

APPENDIX 2B : Grain size ternary plots of diamicton facies in the Mayo region.



APPENDIX 3A : Raw pebble data for samples from the Mayo region.

Sample #	Quartzite	Gneiss	Schist	Chert	Sandstone	Vein qtz	Igneous	Total
----------	-----------	--------	--------	-------	-----------	----------	---------	-------

Unit A : Lower gravels and sands (22 samples)

HHT-88006	40	13	9	0	0	22	1	85
HHT-88089	34	5	6	21	1	12	1	80
HHT-88090	30	2	5	20	3	13	2	75
HHT-88091	47	8	6	9	1	22	2	95
HHT-88093	44	10	11	1	1	35	3	105
HHT-88095	30	12	12	10	1	34	6	105
HHT-88096	43	12	10	2	0	23	0	90
HHT-88097	45	9	14	1	0	31	0	100
HHT-88099	28	9	9	1	0	23	0	70
HHT-88100	33	5	9	1	1	14	2	65
HHT-88101	20	6	9	1	1	11	2	50
HHT-88102	59	4	16	4	2	32	3	120
HHT-88104	42	16	14	4	0	24	0	100
HHT-88105	27	9	19	2	2	30	1	90
HHT-88106	35	12	15	2	0	34	2	100
HHT-88107	34	9	10	1	0	29	2	85
HHT-88108	36	7	8	0	0	23	1	75
HHT-88109	47	14	13	1	2	48	0	110
HHT-88110	21	14	9	0	1	19	1	65
HHT-88154	39	2	9	5	0	17	1	75
HHT-88155	38	7	7	2	3	33	7	95
HHT-88216	32	7	1	1	0	26	3	70

Unit B : Lower sands and gravels (15 samples)

HHT-88004	20	13	12	1	6	13	1	65
HHT-88008	11	3	7	15	15	8	1	60
HHT-88009	35	7	2	21	8	7	0	80
HHT-88054	42	7	5	22	7	9	0	95
HHT-88055	58	3	3	23	4	6	1	110
HHT-88057	66	0	1	15	3	11	4	100
HHT-88062	57	7	2	23	2	12	2	105
HHT-88066	75	1	1	31	0	17	0	125
HHT-88176	12	0	8	34	1	10	0	65
HHT-88177	17	13	10	8	3	24	0	75
HHT-88178	31	24	14	5	4	26	1	105
HHT-88187	25	16	17	0	13	38	1	110
HHT-89301	31	11	2	16	3	12	0	75
HHT-89302	36	7	0	21	4	12	0	80
HHT-89303	69	17	0	28	4	10	2	130

Sample # Quartzite Gneiss Schist Chert Sandstone Vein qtz Igneous Total

Unit C : Diamicton (43 samples)

HHT-88013	34	12	0	19	2	17	1	85
HHT-88072	15	3	0	32	5	10	0	65
HHT-88073	13	2	1	33	3	10	0	65
HHT-88074	25	5	0	40	2	11	2	85
HHT-88075	14	5	0	33	6	7	0	65
HHT-88076	20	6	1	24	4	9	1	65
HHT-88077	17	14	0	23	5	11	5	75
HHT-88078	26	4	1	32	6	15	1	85
HHT-88079	33	11	0	7	3	19	2	75
HHT-88080	21	5	3	37	12	5	2	75
HHT-88081	22	8	2	26	6	23	3	90
HHT-88082	28	11	0	50	9	13	4	115
HHT-88083	17	2	0	29	2	19	1	70
HHT-88084	19	6	0	33	8	14	0	80
HHT-88112	31	25	7	5	3	43	1	115
HHT-88120	38	24	4	21	16	15	2	120
HHT-88144	29	16	7	30	10	26	2	120
HHT-88145	32	1	0	25	3	11	2	75
HHT-88146	5	9	2	17	11	4	2	50
HHT-88147	19	12	0	18	6	22	3	80
HHT-88148	14	23	7	37	15	31	3	130
HHT-88158	9	15	8	12	11	17	3	75
HHT-88160	40	21	4	26	16	16	2	125
HHT-88179	23	4	2	41	4	1	0	75
HHT-88180	37	8	0	44	6	8	2	105
HHT-88181	8	5	2	23	5	7	0	50
HHT-88182	33	5	1	50	14	9	0	115
HHT-88183	37	7	0	37	5	9	0	95
HHT-88184	27	8	0	58	3	9	0	103
HHT-88185	23	9	0	29	3	7	4	75
HHT-88189	27	4	0	22	2	5	0	60
HHT-88190	20	13	1	23	0	17	1	75
HHT-88192	18	11	0	29	3	8	1	70
HHT-88193	33	12	3	29	6	14	1	90
HHT-88194	27	11	0	28	6	12	0	85
HHT-88219	37	6	0	67	3	7	0	120
HHT-88221	27	5	0	41	5	7	0	85
HHT-89305	20	6	4	34	8	18	0	90
HHT-89308	19	8	0	32	3	7	1	70
HHT-89310	16	6	2	36	3	7	0	100
HHT-89311	9	5	0	36	5	5	0	60
HHT-89317	15	7	5	29	7	6	1	70
HHT-89319	28	12	1	51	10	8	0	110

Sample #	Quartzite	Gneiss	Schist	Chert	Sandstone	Vein qtz	Igneous	Total
----------	-----------	--------	--------	-------	-----------	----------	---------	-------

Unit D : Upper sands (4 samples)

HHT-88065	49	6	0	35	6	18	1	115
HHT-88071	72	10	10	19	17	40	2	170
HHT-89315	23	24	8	10	12	22	6	115
HHT-89322	33	22	1	5	4	10	0	75

Unit F : Upper gravels (5 samples)

HHT-88058	57	4	7	13	4	34	1	120
HHT-88069	62	2	8	9	1	16	3	110
HHT-89304	34	24	0	9	7	23	1	100
HHT-89316	47	18	4	11	4	26	5	105
HHT-89321	36	21	4	6	3	19	11	100

APPENDIX 3B : Pebble lithology percentages for samples from the Mayo region. Each sample is divided into three main categories based on the regional bedrock geology.

Sample #	Quartzite	Chert	Sandstone
Unit A : Lower gravels and sands (22 samples)			
HHT-88006	100	0	0
HHT-88089	68	31	1
HHT-88090	62	33	5
HHT-88091	86	12	1
HHT-88093	97	1	1
HHT-88095	82	16	2
HHT-88096	97	3	0
HHT-88097	99	1	0
HHT-88099	99	1	0
HHT-88100	97	1	1
HHT-88101	96	2	2
HHT-88102	93	4	3
HHT-88104	95	5	0
HHT-88105	94	3	3
HHT-88106	97	3	0
HHT-88107	98	2	0
HHT-88108	100	0	0
HHT-88109	98	1	3
HHT-88110	99	0	1
HHT-88154	91	9	0
HHT-88155	92	3	5
HHT-88216	98	2	0
Average	93	6	1

Unit B : Lower sands and gravels (15 samples)

HHT-88004	87	1	11
HHT-88008	41	29	29
HHT-88009	61	28	11
HHT-88054	62	30	9
HHT-88055	70	25	5
HHT-88057	79	18	3
HHT-88062	72	25	2
HHT-88066	71	29	0
HHT-88176	36	63	1
HHT-88177	81	14	5
HHT-88178	88	7	5
HHT-88187	81	0	19
HHT-89301	70	25	5
HHT-89302	64	31	5
HHT-89303	73	24	3
Average	69	23	8

Sample #	Quartzite	Chert	Sandstone
Unit C : Diamicton (43 samples)			
HHT-88013	69	28	3
HHT-88072	33	58	9
HHT-88073	30	64	6
HHT-88074	42	56	2
HHT-88075	33	57	10
HHT-88076	49	44	7
HHT-88077	53	39	9
HHT-88078	45	46	9
HHT-88079	82	13	5
HHT-88080	38	47	15
HHT-88081	49	41	10
HHT-88082	40	51	9
HHT-88083	38	58	4
HHT-88084	39	49	12
HHT-88112	89	6	5
HHT-88120	64	21	15
HHT-88144	57	33	10
HHT-88145	53	42	5
HHT-88146	36	39	25
HHT-88147	56	32	11
HHT-88148	46	38	16
HHT-88158	58	22	21
HHT-88160	62	24	15
HHT-88179	39	56	5
HHT-88180	48	46	6
HHT-88181	35	53	12
HHT-88182	38	48	13
HHT-88183	51	43	6
HHT-88184	37	60	3
HHT-88185	50	45	5
HHT-88189	57	40	3
HHT-88190	59	41	0
HHT-88192	48	47	5
HHT-88193	58	35	8
HHT-88194	53	39	8
HHT-88219	38	59	3
HHT-88221	41	52	7
HHT-89305	42	47	11
HHT-89308	43	52	5
HHT-89310	38	57	5
HHT-89311	26	65	9
HHT-89317	43	46	11
HHT-89319	40	50	10
Average	47	44	10

Sample #	Quartzite	Chert	Sandstone
Unit D : Upper sands (4 samples)			
HHT-88065	58	36	6
HHT-88071	72	15	13
HHT-89315	72	13	15
HHT-89322	86	8	6
Average	72	18	10

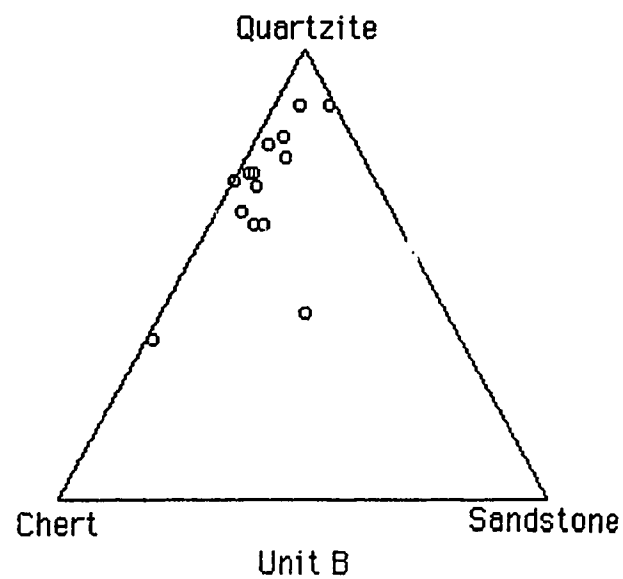
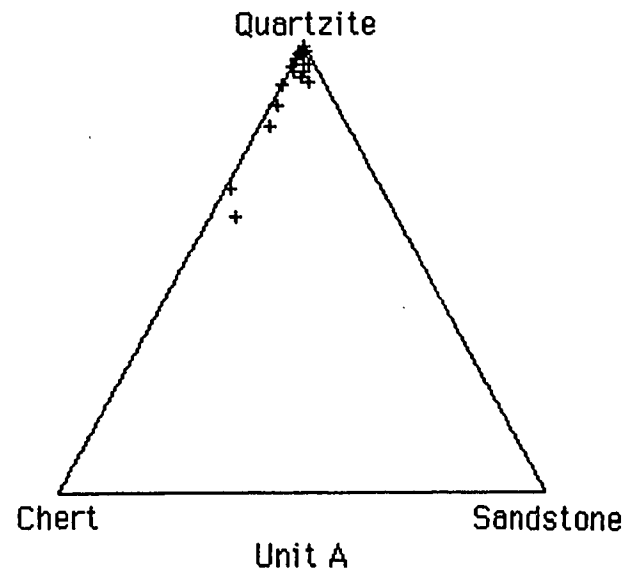
Unit F : Upper gravels (5 samples)

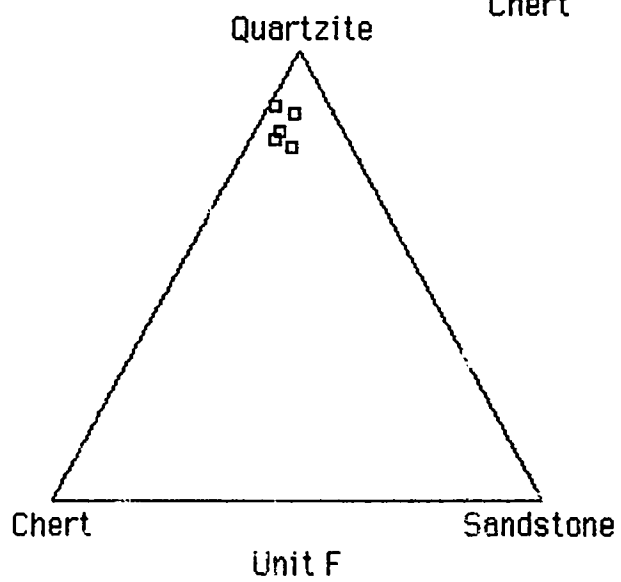
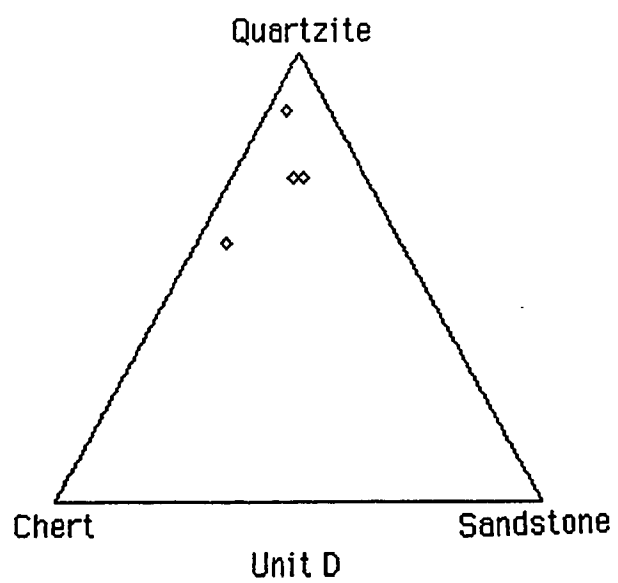
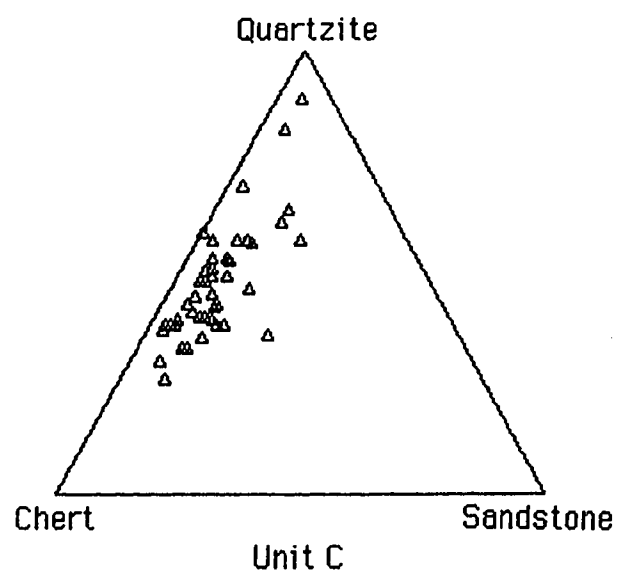
HHT-88058	80	15	5
HHT-88069	88	11	1
HHT-89304	78	12	9
HHT-89316	83	13	5
HHT-89321	8	9	4
Average	83	12	5

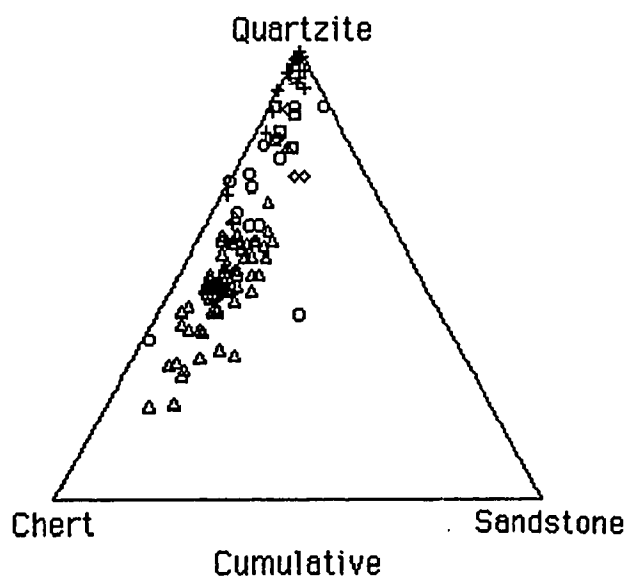
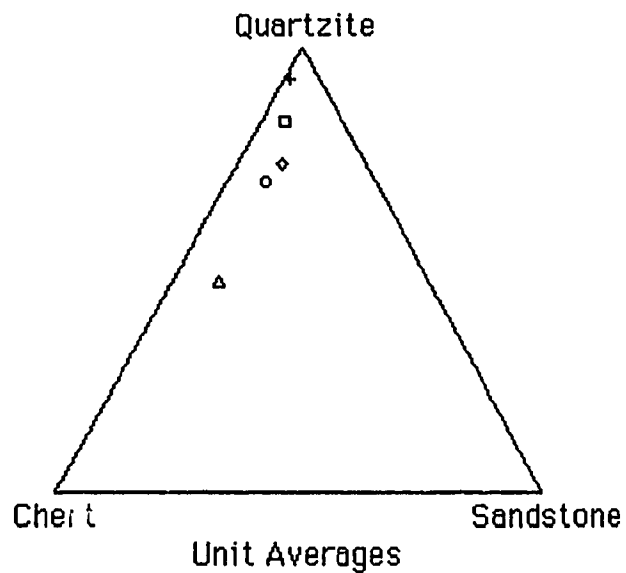
Averages

Unit A (22 samples)	95	6	1
Unit B (15 samples)	69	23	8
Unit C (43 samples)	48	44	10
Unit D (4 samples)	72	13	10
Unit F (5 samples)	83	12	5

APPENDIX 3C : Pebble lithology ternary diagrams of units from the Mayo region. Analysis plotted from data in Appendix 3B.



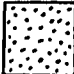


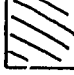
















- + Unit A Lower gravels and sands
- Unit B Lower sands and gravels
- Δ Unit C Diamicton
- ◊ Unit D Upper sands
- ◻ Unit F Upper gravels

APPENDIX 4A : Lithostratigraphic logs and detailed section diagrams of the Mayo section. Vertical logs are labelled according to the distance in metres from the upstream end of the section. Section diagrams have vertical logs, lithostratigraphic units, pebble fabrics, and radiocarbon dates indicated. Legend for the logs is below.

	Clays and silts		Planar stratification
	Sands		Trough cross-stratification
	Pebbly sands		Planar cross-stratification
	Matrix-filled gravels		Erosional stoss climbing ripples
	Openwork gravels		Depositional stoss climbing ripples
	Diamicton		Sediment gravity flow margin
	Lenses		Organics
	Frost wedge		Fault

x Radiocarbon date

M-01 Pebble fabric

Cl Clay

P Pebbles

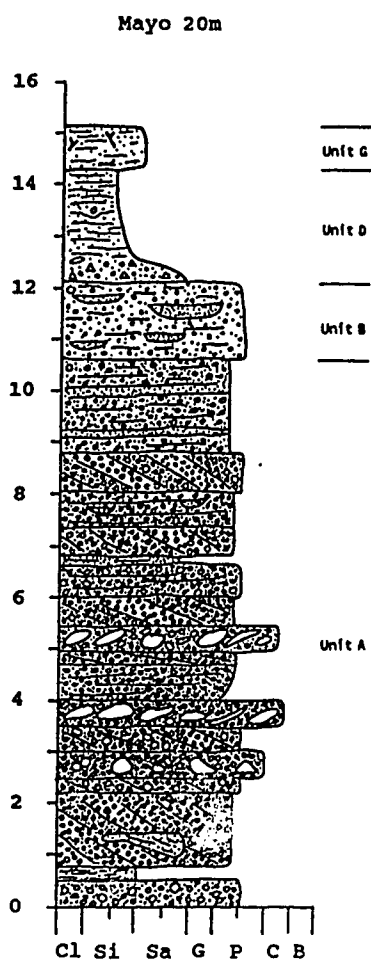
Si Silt

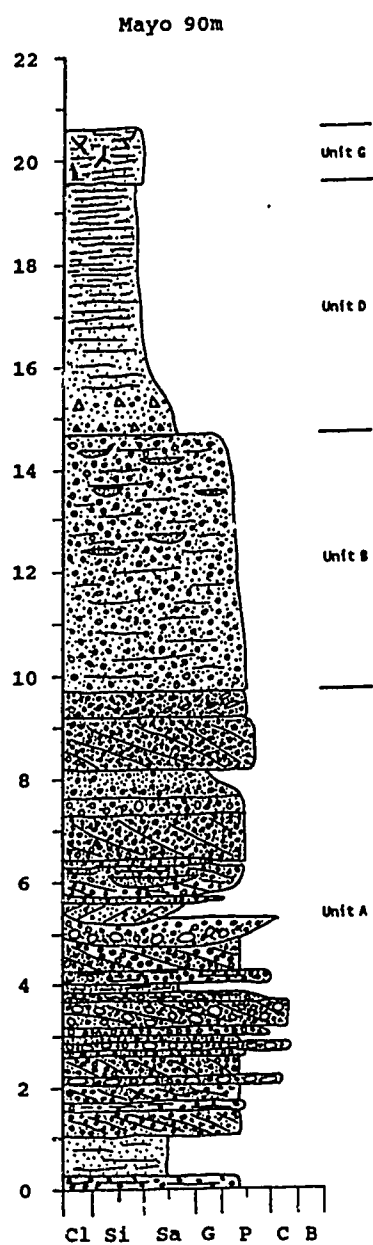
C Cobbles

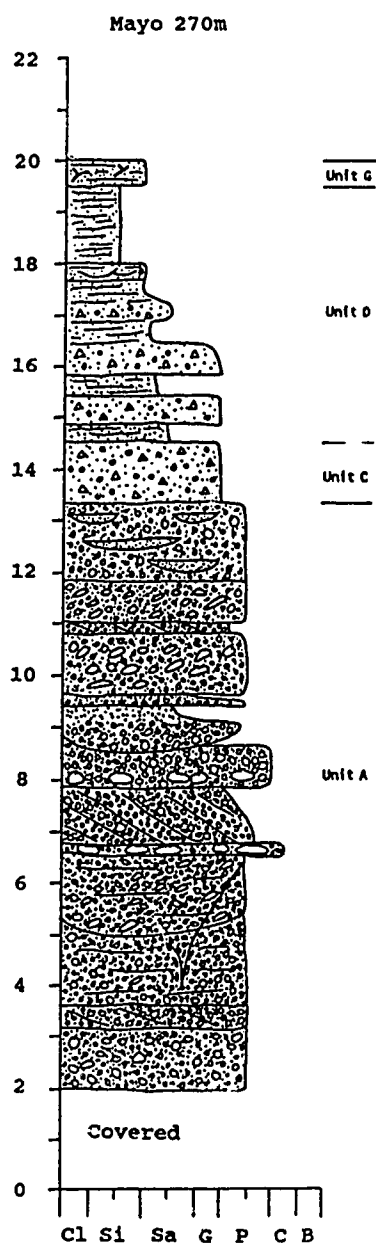
Sa Sand

B Boulders

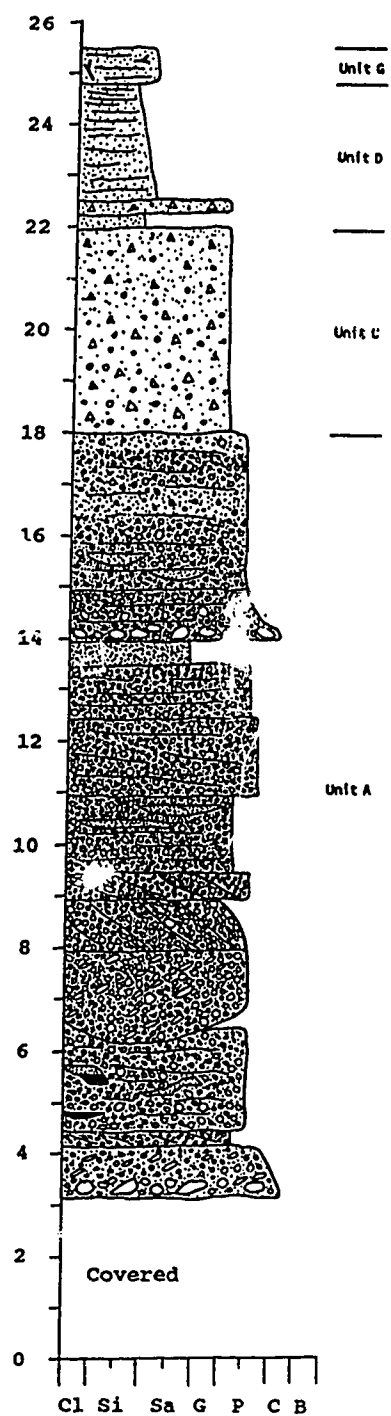
G Granules

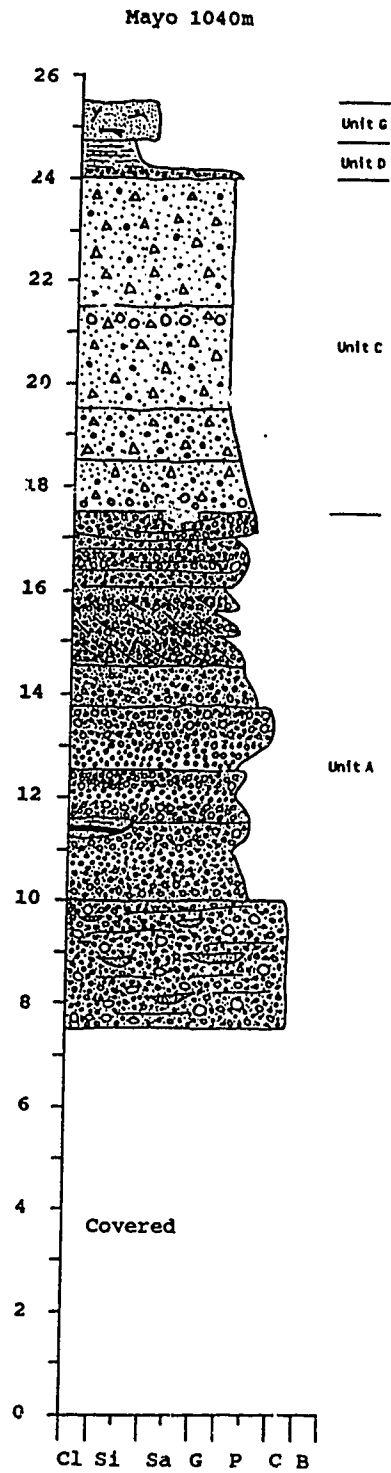


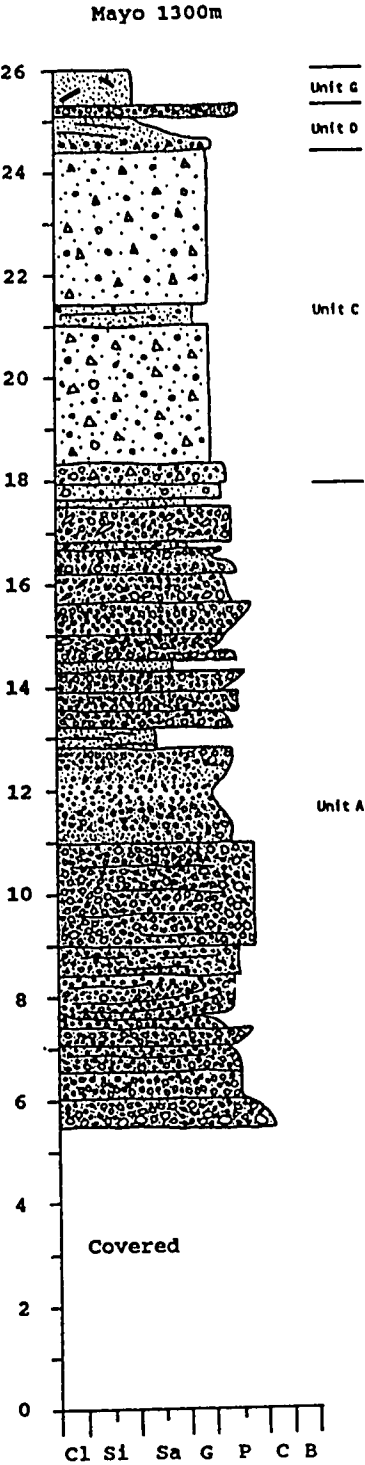




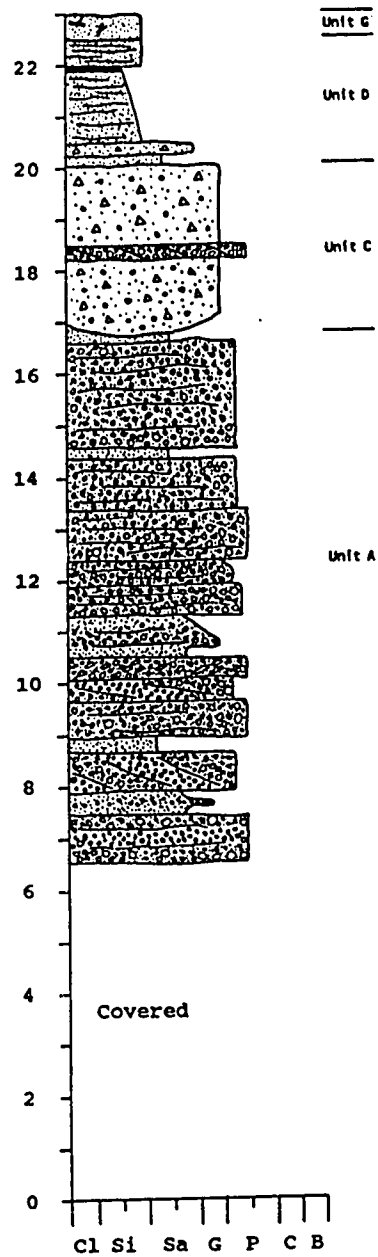
Mayo 860m





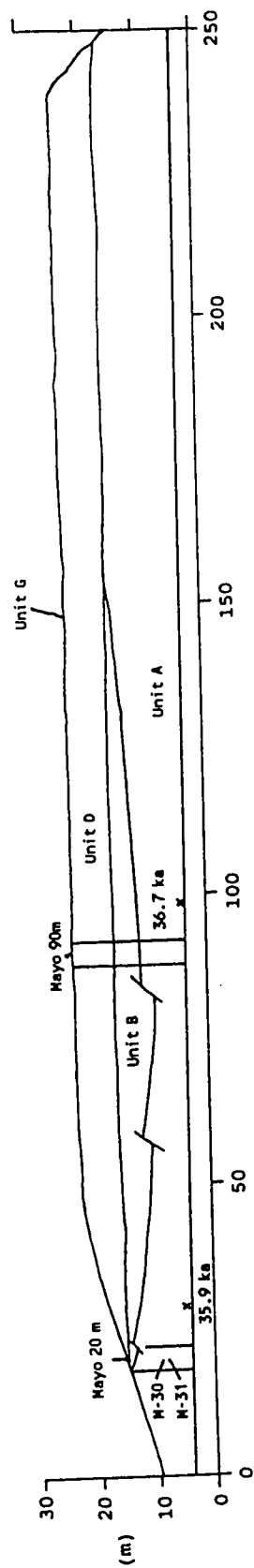


Mayo 1460m

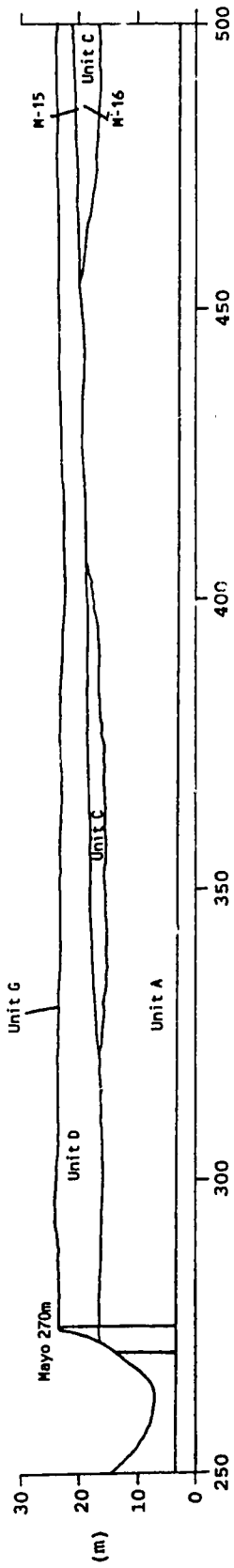


MAYO SECTION

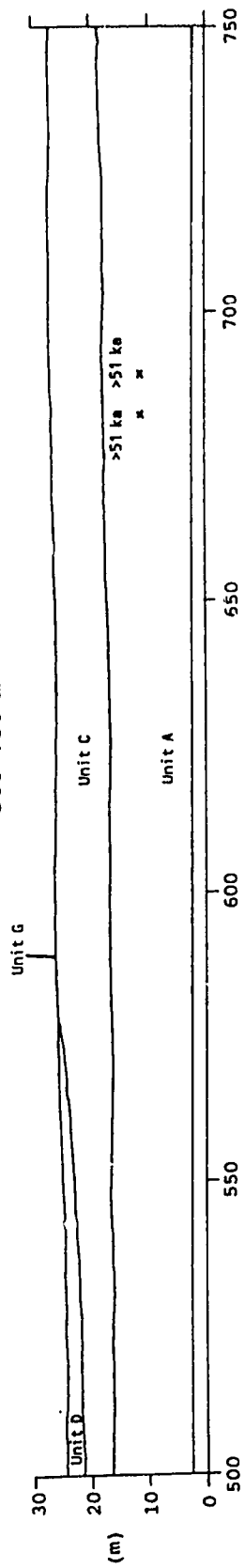
0-250 m

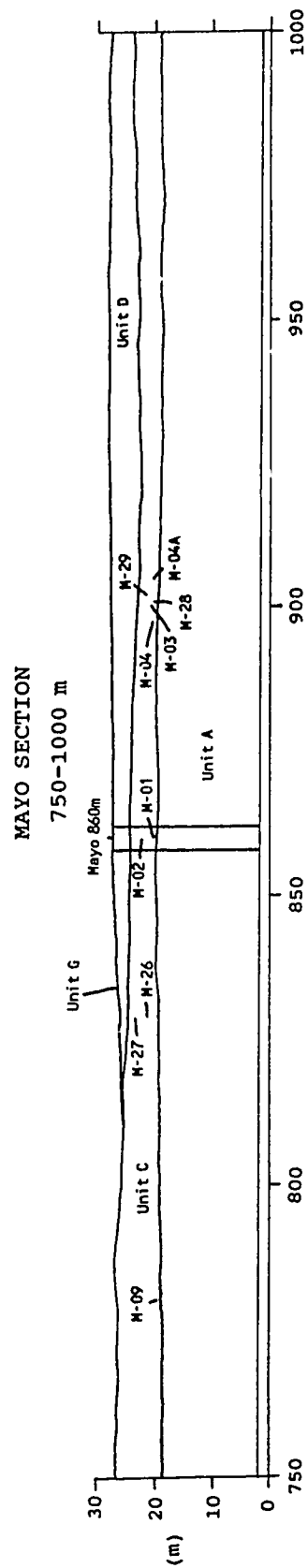


MAYO SECTION
250-500 m



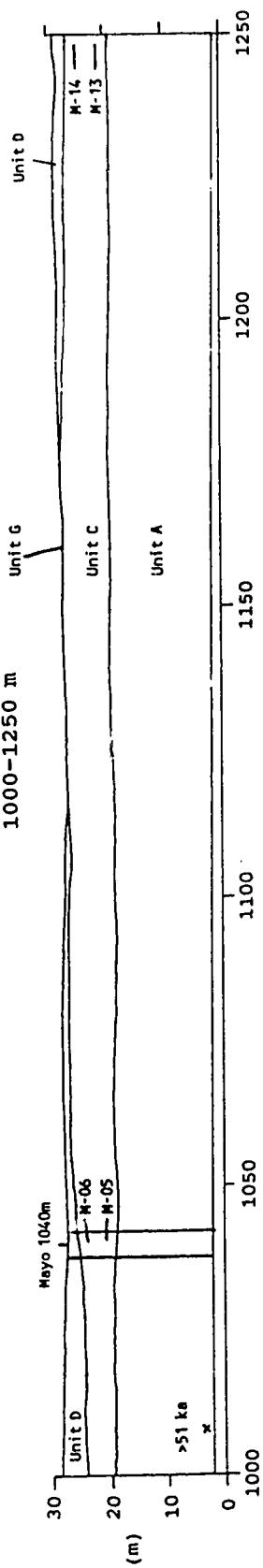
MAYO SECTION
500-750 m

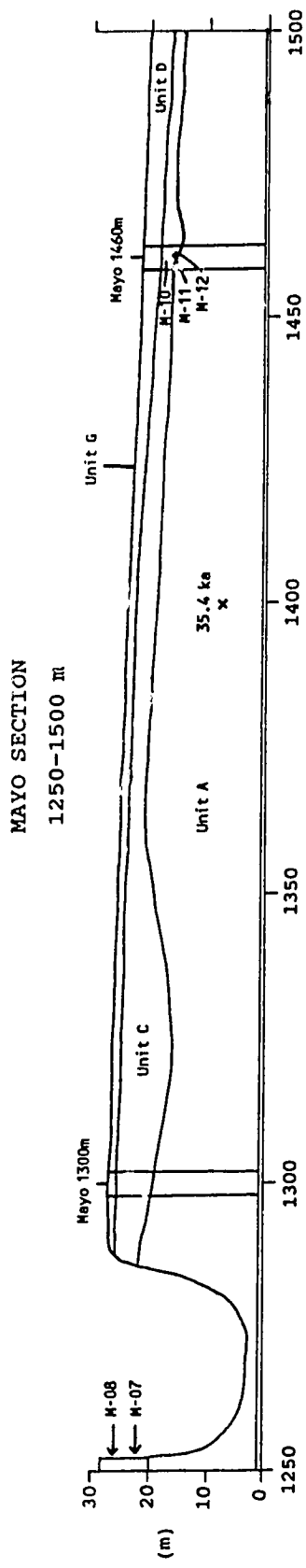




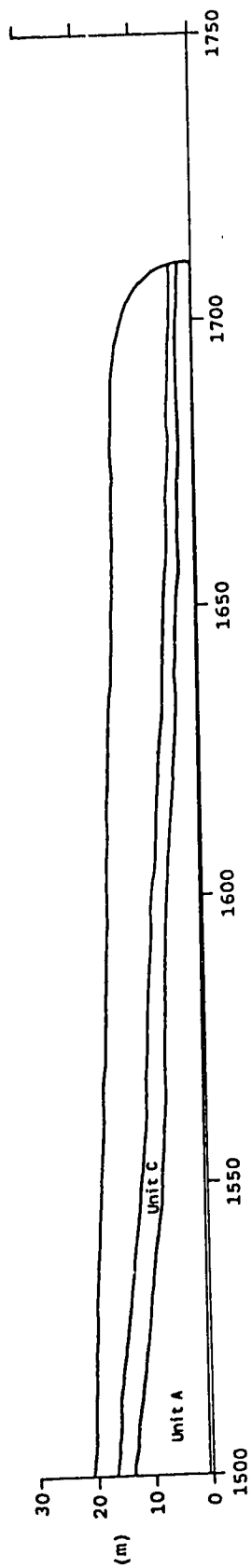
MAYO SECTION

1000-1250 m

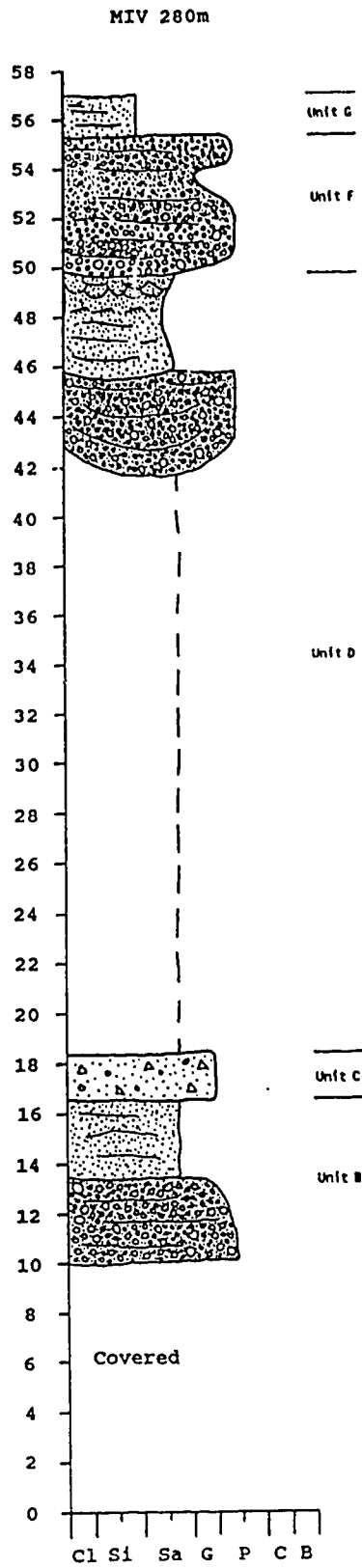


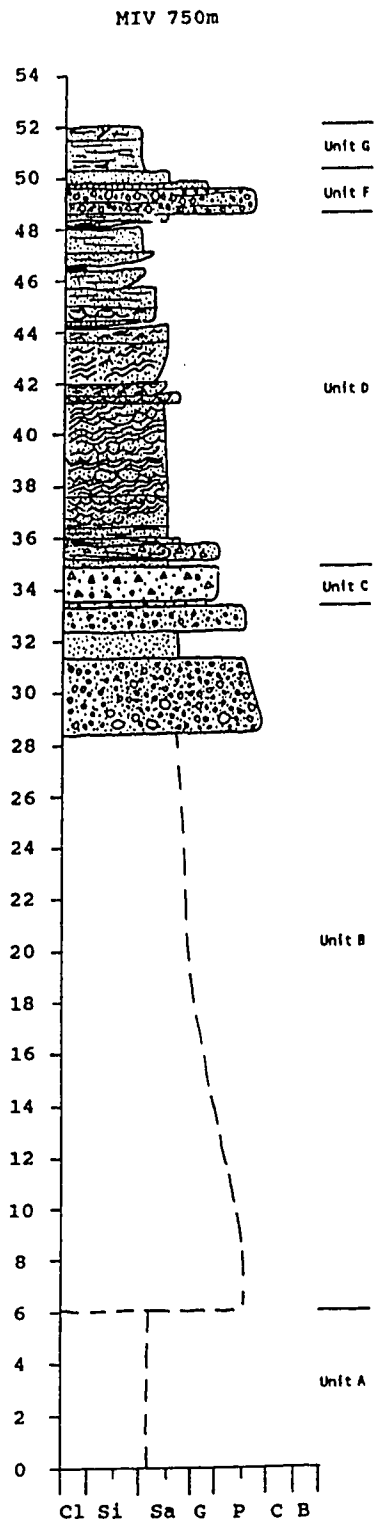


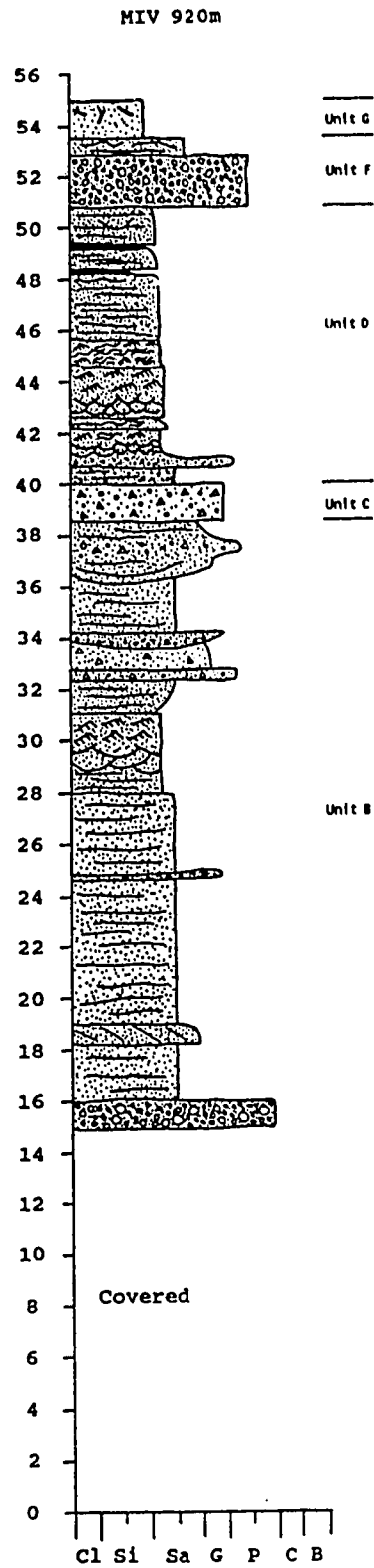
MAYO SECTION
1500-1750 m

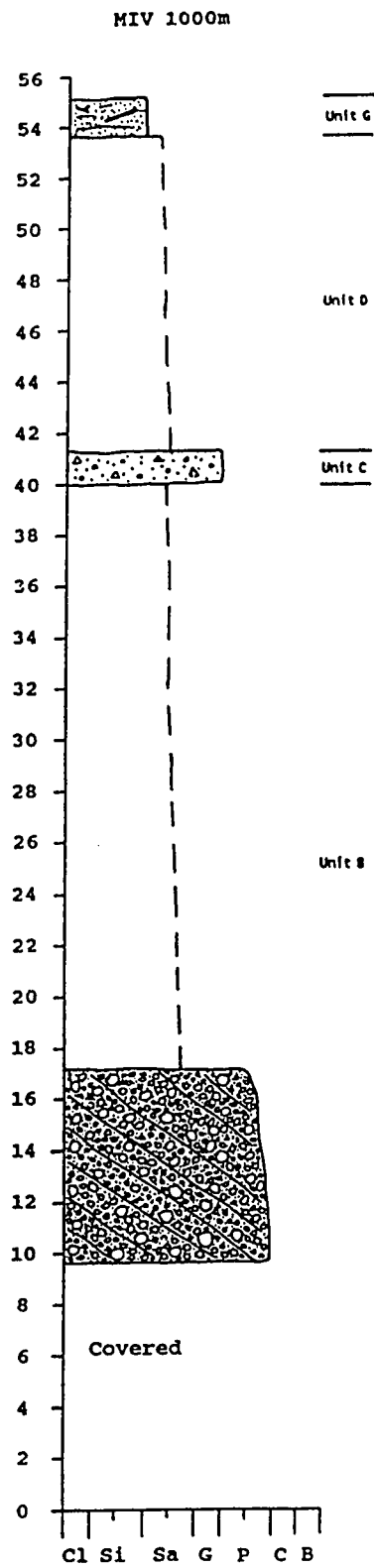


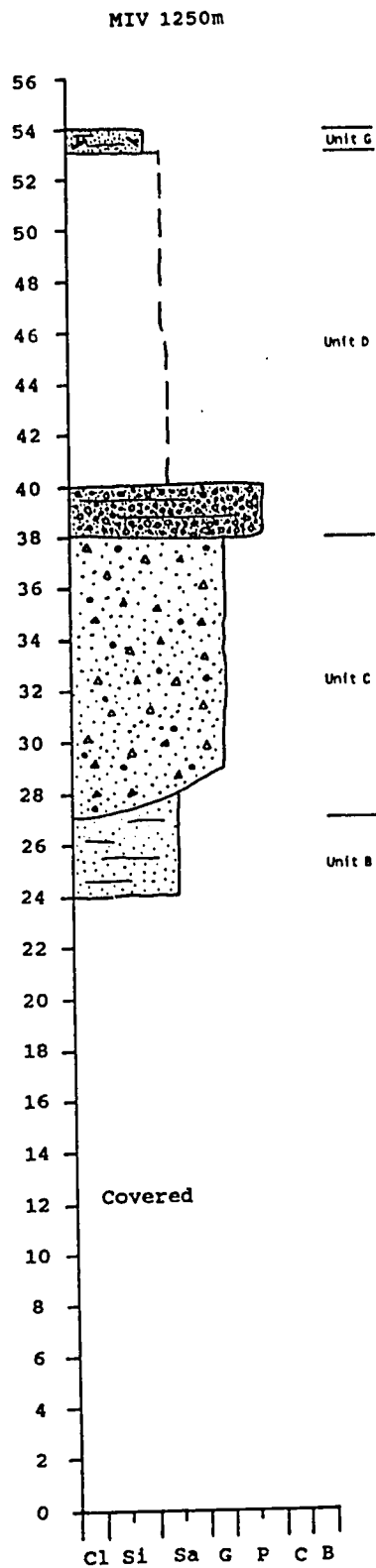
APPENDIX 4B : Lithostratigraphic logs and detailed section diagrams of the Mayo Indian Village section. Vertical logs are labelled according to the distance in metres from the upstream end of the section. Section diagrams have vertical logs, lithostratigraphic units, pebble fabrics, and radiocarbon dates indicated.



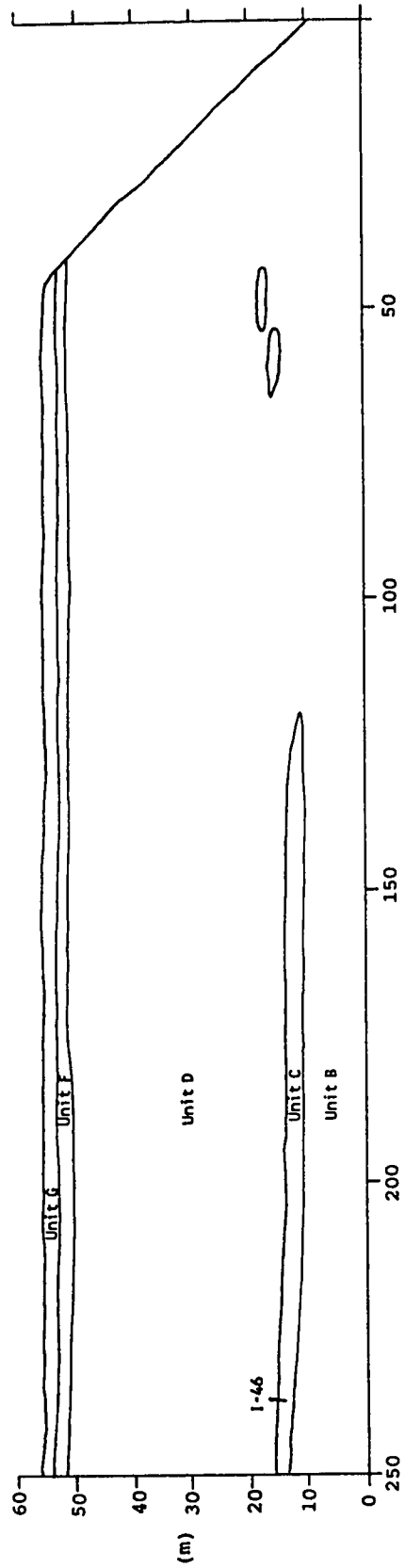






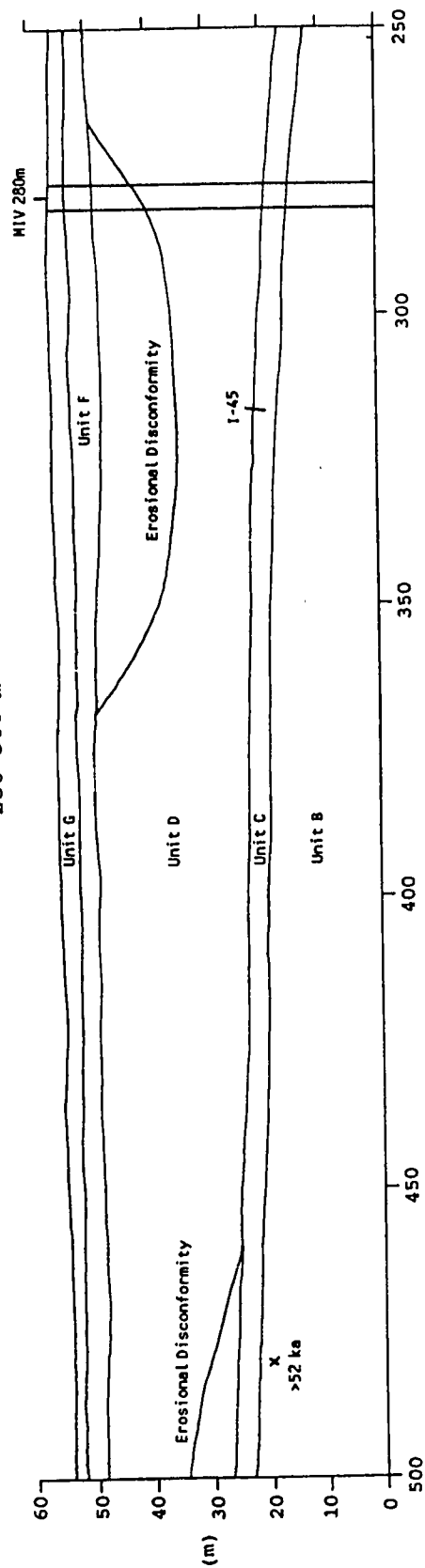


MAYO INDIAN VILLAGE SECTION
0-250 m

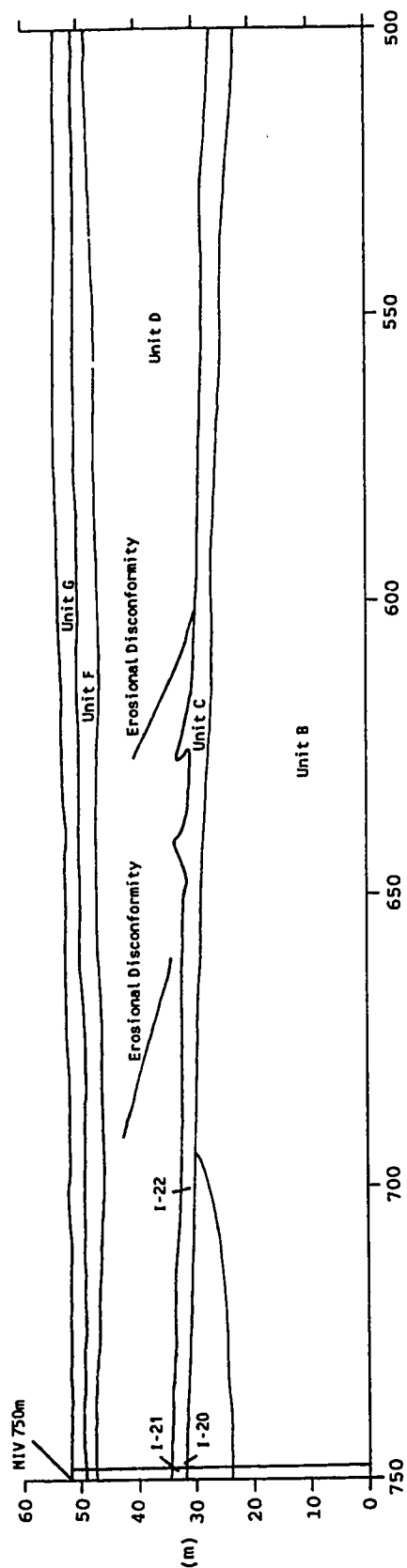


MAYO INDIAN VILLAGE SECTION

250-500 m

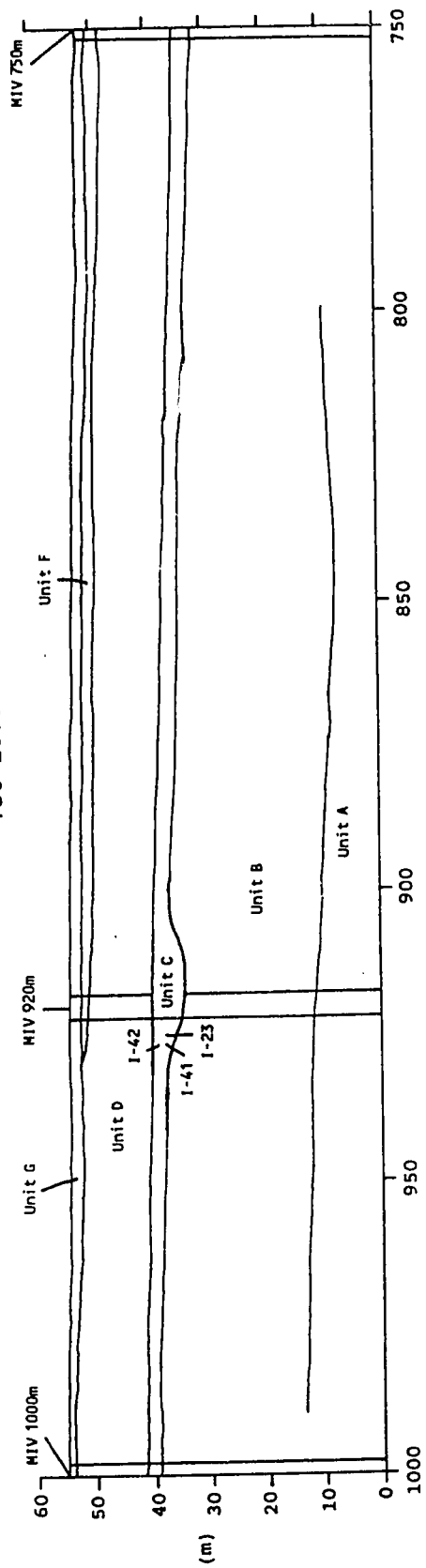


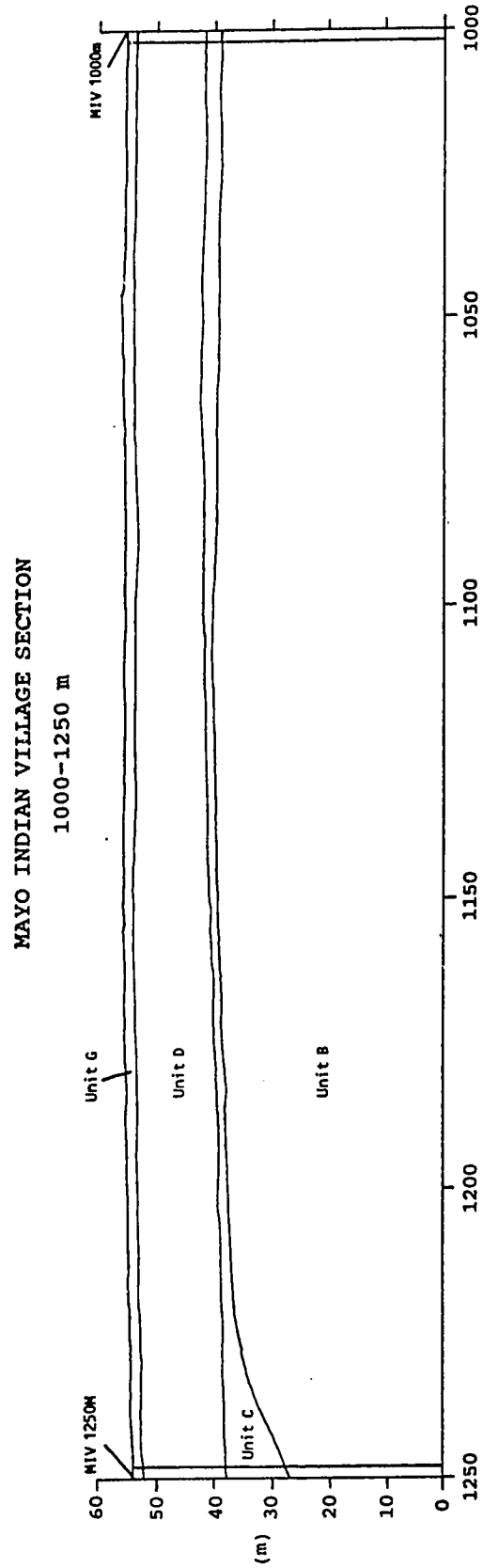
MAYO INDIAN VILLAGE SECTION 500-750 m



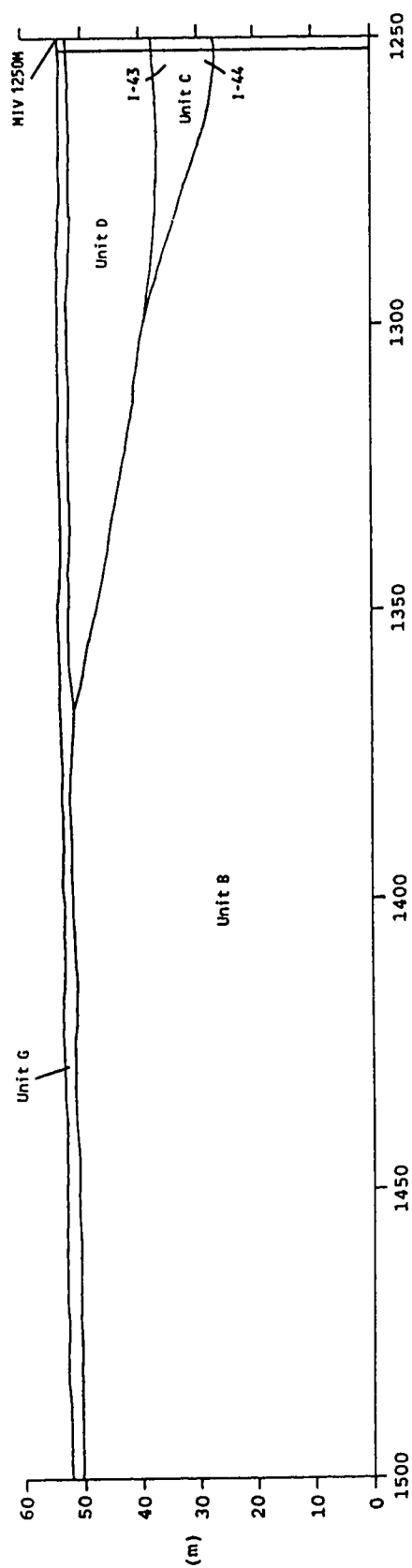
MAYO INDIAN VILLAGE SECTION

750-1000 m

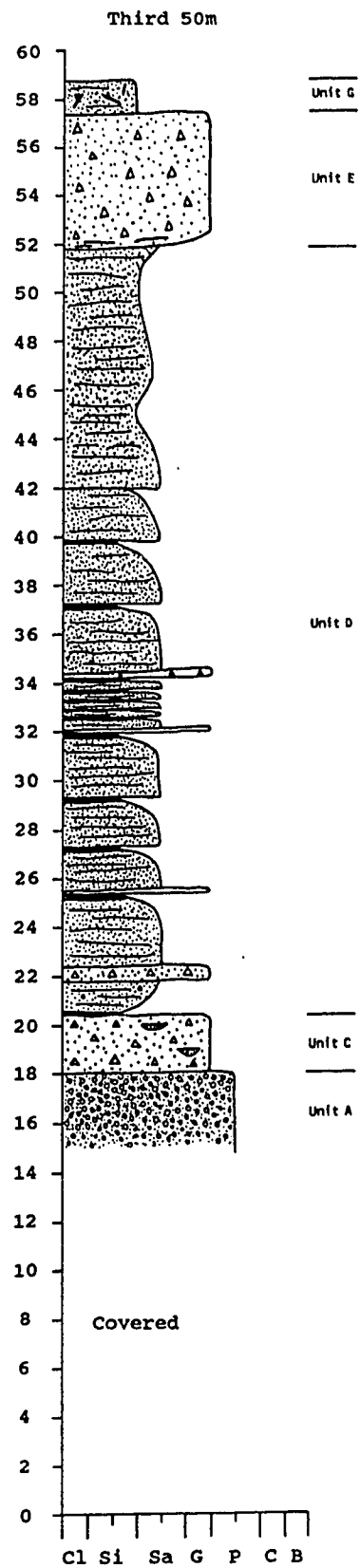




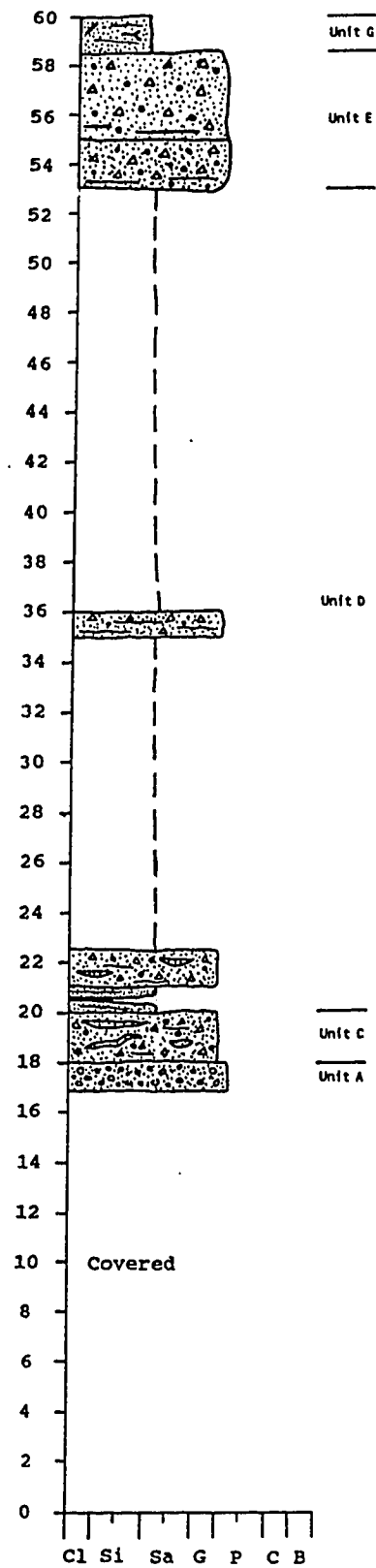
MAYO INDIAN VILLAGE SECTION
1250-1500 m

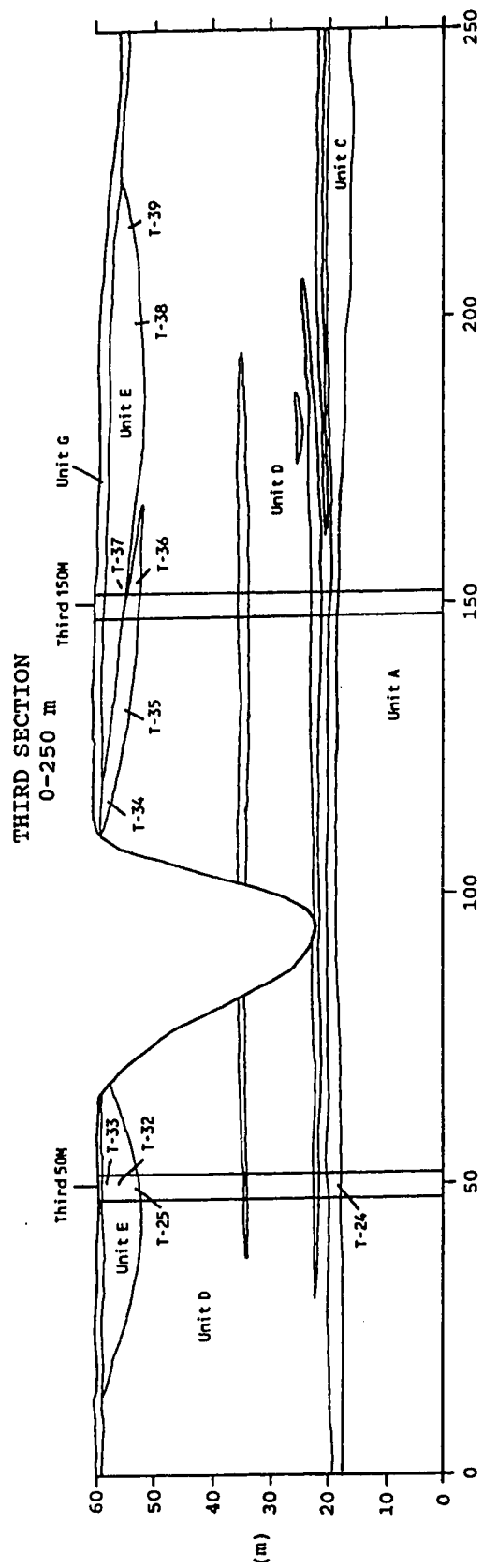


APPENDIX 4C : Lithostratigraphic logs and detailed section diagrams of the Third section. Vertical logs are labelled according to the distance in metres from the upstream end of the section. Section diagrams have vertical logs, lithostratigraphic units, and pebble fabrics indicated.

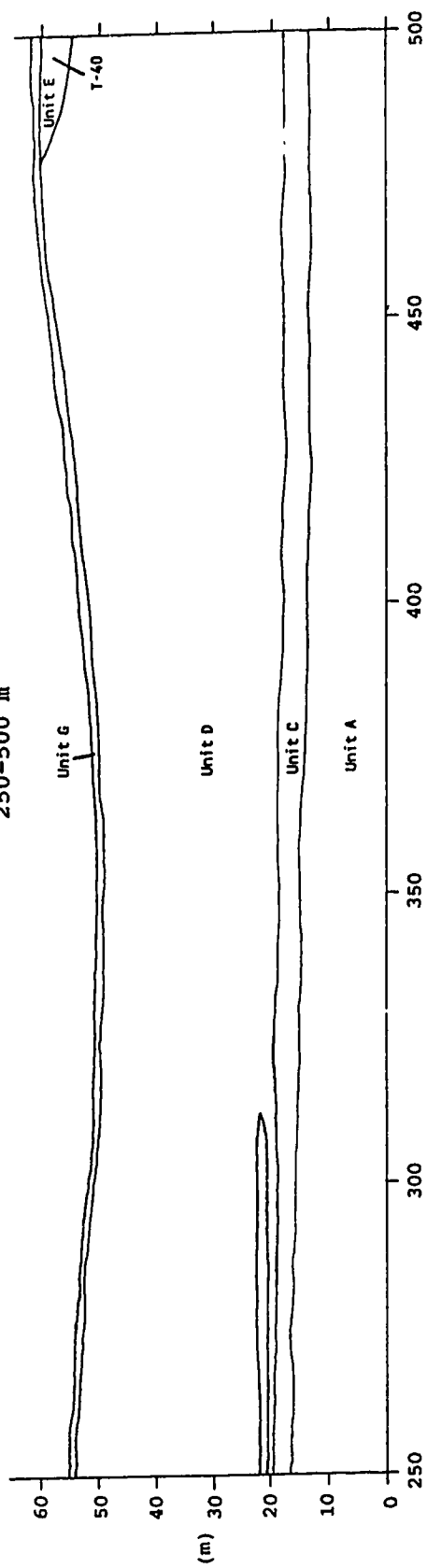


Third 150m





THIRD SECTION
250-500 m



APPENDIX 5 : Wood identification reports.

Wood identification report 88-42 : Mayo Indian Village Section

- HHT-88011 1 large disk from log. Picea sp. (spruce).
- HHT-88011B 2 large logs. Both Picea sp. (spruce).
- HHT-88053 A mixture of roots, twigs and larger fragments that include Picea/Larix (spruce/larch) and Salix sp. (willow). Picea is certainly present, but Larix is probably represented as well.

Wood identification report 88-43 : Mayo Section

- HHT-88016 Numerous small to medium sized twigs. Salix sp. (willow).
- HHT-88030 Numerous small to large twigs. Salix sp. (willow).
- HHT-88032 Four large twigs. Salix sp. (willow).
- HHT-88034 One large twig. Salix sp. (willow).
- HHT-88037 Several poorly preserved fragments. Salix sp. (willow).
- HHT-88038 One large fragemnt. Picea sp. (spruce).
- HHT-88040 Numerous large and small roots, twigs and fragments. Salix sp. (willow).
- HHT-88041 Numerous small to large twigs and fragments. Salix sp. (willow).
- HHT-88094 Numerous fairly large twigs and fragments. Salix sp. (willow).
- HHT-88098 Numerous large fragments. Salix sp. (willow).
- HHT-88201 Several poorly preserved fragments. Salix sp. (willow).
- HHT-88213 Numerous small to medium twigs. One Salix sp. (willow) and numerous Picea sp. (spruce) twigs.
- HHT-88214 Numerous medium sized twigs and fragments. Picea sp. (spruce) and Salix sp. (willow).
- HHT-88215 Numerous fragments of various sizes. Poorly preserved. Two pieces are Salix sp. (willow). Remainder are Picea sp. (spruce).
- HHT-88217 One large fragment. Picea sp. (spruce).
- HHT-88227 Four fragments. Salix sp. (willow).

Identification by R.J. Mott of the Geological Survey of Canada.

APPENDIX 6 : Radiocarbon dates.

The Geological Survey of Canada laboratory reference number, distance from the upstream terminus of the section, elevation, unit the sample was enclosed in, type of wood, and the radiocarbon date follow the field number.

HHT-88011 (GSC-5123(HP)) : Large log taken at 480 m in the MIV Section at 20 m elevation above river level (505 m.a.s.l.) in Unit B. Wood was identified as *Picea* sp. (spruce) and dated at $>52\ 000$.

HHT-88032 (GSC-5139(HP)) : Four large twigs taken at 98 m in the Mayo Section at 0.5 m elevation above river level (492.5 m.a.s.l.) in Unit A. Wood was identified as *Salix* sp. (willow) and dated at $36\ 700 \pm 400$.

HHT-88038 (GSC-5152(HP)) : Large log taken at 1007 m in the Mayo Section at 1 m elevation above river level (493 m.a.s.l.) in Unit A. Wood was identified as *Picea* sp. (spruce) and dated at $>51\ 000$.

HHT-88098 (GSC-4927(HP)) : Numerous large fragments taken at 1400 m in the Mayo Section at 8 m elevation above river level (500 m.a.s.l.) in Unit A. Wood was identified as *Salix* sp. (willow) and dated at $35\ 400 \pm 320$.

HHT-88214 (GSC-4920(HP)) : Sample taken at 689 m in the Mayo Section at 12 m elevation above river level (504 m.a.s.l.) in Unit A. Wood was identified as *Picea* sp. (spruce) and dated at $>51\ 000$.

HHT-88215 (GSC-4924(HP)) : Sample taken at 682 m in the Mayo Section at 12 m elevation above river level (504 m.a.s.l.) in Unit A. Wood was identified as *Picea* sp. (spruce) and dated at $>51\ 000$.

HHT-88227 (GSC-5142(HP)) : Four wood fragments taken at 30 m in the Mayo Section at 1.0 m elevation above river level (493 m.a.s.l.) in Unit A. Wood was identified as *Salix* sp. (willow) and dated at $35\ 900 \pm 380$.